VOLUME 07 / September 2019

detritus

Multidisciplinary Journal for Waste Resources & Residues

Editor in Chief:
RAFFAELLO COSSU

detritusjournal.com

an official journal of:
iwwg
international waste working group

CISA

ISSN 2611-4135 / ISBN 9788862650632
DETRITUS - Multidisciplinary Journal for Waste Resources & Residues

Detritus is indexed in the Emerging Sources Citation Index (ESCI), Clarivate Analytics, Web of Science.

© 2019 CISA Publisher. All rights Reserved
The journal contents are available on the official website: www.detritusjournal.com
Open access articles under CC BY-NC-ND license (http://creativecommons.org/licenses/by-nc-nd/4.0/)
Legal head office: Cisa Publisher - Eurowaste Srl, Via Beato Pellegrino 23, 35137 Padova - Italy / www.cisapublisher.com

Graphics and layout: Elena Cossu, Anna Artuso - Studio Arcoplan, Padova / studio@arcoplan.it
Printed by Cleup, Padova, Italy
Front page photo credits: 'Life in garbage' courtesy of Azim Khan Ronnie, Bangladesh

For subscription to printed version, advertising or other commercial opportunities please contact the Administration Office at administration@eurowaste.it

Papers should be submitted online at https://mc04.manuscriptcentral.com/detritusjournal
Instructions to authors may be found at https://detritusjournal.com/guide-for-authors/
For any enquiries and information please contact the Editorial Office at editorialoffice@detritusjournal.com

Registered at the Court of Padova on March 13, 2018 with No. 2457

www.detritusjournal.com

VOLUME 07 / September 2019

detritus

Multidisciplinary Journal for Waste Resources & Residues

Editor in Chief:
RAFFAELLO COSSU

detritusjournal.com

an official journal of:
iwwg
international waste working group

CISA

Detritus - Multidisciplinary Journal for Waste Resources and Residues - is aimed at extending the "waste" concept by opening up the field to other waste-related disciplines (e.g. earth science, applied microbiology, environmental science, architecture, art, law, etc.) welcoming strategic, review and opinion papers. **Detritus is indexed in the Emerging Sources Citation Index (ESCI)**, **Clarivate Analytics, Web of Science**. Detritus is an official journal of IWWG (International Waste Working Group), a non-profit organisation established in 2002 to serve as a forum for the scientific and professional community and to respond to a need for the international promotion and dissemination of new developments in the waste management industry.

EDITOR-IN-CHIEF:

Raffaello Cossu, University of Padova, Italy
E-mail: raffaello.cossu@unipd.it

ASSOCIATE EDITORS:

Israel Alba, Israel Alba Estudio, Spain
E-mail: israel@israelalba.com

Damià Barcelo, ICRA Catalan Institute for Water Research, Spain
E-mail: damia.barcelo@idaea.csic.es

Pierre Hennebert, INERIS, France
E-mail: pierre.hennebert@ineris.fr

Anders Lagerkvist, Lulea University of Technology, Sweden
E-mail: anders.lagerkvist@ltu.se

Michael Nelles, University of Rostock, Germany
E-mail: michael.nelles@uni-rostock.de

Abdul-Sattar Nizami, King Abdulaziz University, Saudi Arabia
E-mail: nizami_pk@yahoo.com

Mohamed Osmani, Loughborough University, UK
E-mail: m.osmani@lboro.ac.uk

Roland Pomberger, Montanuniversitaet Leoben, Austria
E-mail: Roland.Pomberger@unileoben.ac.at

Alessandra Polettini, University of Rome "La Sapienza", Italy
E-mail: alessandra.polettini@uniroma1.it

Marco Ritzkowski, TuTech Innovation GmbH, Germany
E-mail: m.ritzkowski@tuhh.de

Howard Robinson, Phoenix Engineering, UK
E-mail: howardrRobinson@phoenix-engineers.co.uk

Rainer Stegmann, TuTech Innovation GmbH, Germany
E-mail: stegmann@tuhh.de

Timothy Townsend, University of Florida, USA
E-mail: ttown@ufl.edu

Hans van der Sloot, Hans Van der Sloot Consultancy, The Netherlands
E-mail: hans@vanderslootconsultancy.nl

Ian Williams, University of Southampton, UK
E-mail: i.d.Williams@soton.ac.uk

Jonathan Wong, Hong Kong Baptist University, Hong Kong
E-mail: jwcwong@hkbu.edu.hk

Hideki Yoshida, Muroran Institute of Technology, Japan
E-mail: gomigomi@mmm.muroran-it.ac.jp

Aoran Yuan, University of Birmingham, United Kingdom
E-mail: Yuanhr@ms.giec.ac.cn

Liangtong Tony Zhan, Zheijangu University, China
E-mail: zhanlt@zju.edu.cn

Christian Zurbruegg, Eawag/Sandec, Switzerland
E-mail: christian.zurbruegg@eawag.ch

EDITORIAL OFFICE:

Gioia Burgello, Eurowaste Srl, Italy
E-mail: editorialoffice@detritusjournal.com

MANAGING EDITORS:

Werner Bidlingmeier, Bauhaus-University Weimar
Portraits
werner.bidlingmaier@uni-weimar.de

Elena Cossu, Studio Arcoplan, Italy
Waste Architecture
E-mail: studio@arcoplan.it

Anders Lagerkvist, Lulea University of Technology, Sweden
Forum Moderator
E-mail: anders.lagerkvist@ltu.se

Maria Cristina Lavagnolo, University of Padova, Italy
Developing Countries Corner
E-mail: mariacristina.lavagnolo@unipd.it

Alberto Pivato, University of Padova, Italy
Research to industry and industry to research
E-mail: alberto.pivato@unipd.it

Elena Cristina Rada, University of Insubria, Italy
Info from the World
E-mail: elena.rada@uninsubria.it

Roberto Raga, University of Padova, Italy
Books Review
E-mail: roberto.raga@unipd.it

Marco Ritzkowski, TuTech Innovation GmbH, Germany
New projects
E-mail: m.ritzkowski@tuhh.de

Rainer Stegmann, TuTech Innovations GmbH, Germany
Waste and Art
E-mail: stegmann@tuhh.de

EDITORIAL ADVISORY BOARD:

Mohammad Alamgir, Khulna University of Engineering & Technology, Bangladesh

Luca Alibardi, Cranfield University, UK

Andreas Bartl, Vienna University of Technology, Austria

Luciano Butti, B&P Avvocati, Italy

Dezhen Chen, Tongji University, China

Christophe Cord'Homme, CNIM Group, France

Hervé Corvellec, Lund University, Sweden

Frederic Coulon, Cranfield University, UK

Francesco Di Maria, University of Perugia, Italy

Lisa Doeland, Radboud University Nijmegen, The Netherlands

George Ekama, University of Capetown, South Africa

Marco Frey, Sant'Anna School of Advance Studies, Italy

Dieter Gerten, Potsdam Institute for Climate Impact Research and Humboldt University of Berlin, Germany

Apostolos Giannis, Nanyang Technological University, Singapore

Ketil Haarstad, Norwegian Institute for Bioeconomy, Norway

Uta Krogmann, Rutgers University, USA

Jianguo Liu, Tsinghua University, China

Wenjing Lu, Tsinghua University, China

Claudio Fernando Mahler, COPPE/UFRJ, Brazil

Marco Ragazzi, University of Trento, Italy

Jörg Römbke, ECT GmbH, Germany

Natalia Sliusar, Perm National Reseach Polytechnic University, Russia

Evangelos Voudrias, Democritus University of Thrace, Greece

Casta Zecena, Universidad de San Carlos de Guatemala, Guatemala

detritus | Multidisciplinary Journal for Waste Resources & Residues

CISA

Editorial

LETTING REMAINDERS GET STUCK IN OUR THROATS

What is waste? To my eyes the carton in the middle of a roll of toilet-paper is something to put in the paper recycling bin, whereas my handicraft-minded daughter takes it for the upper-part of the pillar of a castle and my rats use it as construction material for their nest. Apparently, waste is a subjective term. In all three cases one might say it is not waste – really – but a resource. This neatly fits the current social narrative about waste, that takes waste not so much as a problem, but as a resource (Corvellec and Hultman 2012).

In late-capitalism we dream dreams of zero waste and remainder-less recycling, in which everything is put to use and becomes a resource once again in an ongoing circular movement. Things are to be endlessly transformed into new things, that can be exchanged again and again (O'Brien 1999). This discourse frames waste as always already managed and manageable (Corvellec 2014), underpins the logic of sustainable growth and helps to frame waste as "an object of manageable sustainability" (Valenzuela and Böhm 2017, 29). As a problem, waste was a stark reminder of the dark side of capitalist consumerism. As a resource, however, all "traces of wastefulness" (Valenzuala and Böhm 2017) disappear and waste loses its critical edge. In short: the resourcification of waste strips it of its power as a doomsayer urging us to curb our consumption.

Instead of framing waste as easily manageable and digestible, I suggest we let it get stuck in our throats. A lozenge offered by the World Bank (2018) last year in the face of the expectation that global waste generation will increase by 70% by 2050, puts the (Western) mantra of "reduce, re-use, recycle" very much in perspective. The focus on consumer waste is also very much misleading. Although the often-quoted statistic of 3% municipal waste to 97% industrial waste is shady (Liboiron 2016), municipal waste sure isn't our biggest problem. Waste messes with our dreams of (economic) growth without residues and remainders and invites us to reflect on its (in)digestibility. French philosopher Jacques Derrida can help us out here, whose thought on the biodegradable and on "eating well" offers a 'revised metabolic imagery' (Gabrys 2013, 219) which allows us to get a grip on the digestibility of waste.

'What is a thing? What remains? What, after all, of the remains?' (Derrida 1989, 812). With these questions Derrida launches into 'Biodegradables. Seven Diary Fragments' (1989), a text in which he reflects on things degrading and on what remains of them. The "biodegradable thing" has a strange status among things, as it is 'hardly a thing, destined to pass away, to lose its identity as a thing and become a non-thing' (Derrida 1989, 813). When we ask about the biodegradability of things, we ask how things that once were something lose their identity and become nothing, non-things. Although Derrida is not concerned specifically with (material) waste-things (he inquires mostly what remains of texts, if one idea, story or view is more degradable than another and wherein does this degradability lie) his thoughts on the biodegradable are also of interest to those concerned with material remainders, that is, with waste. In this I follow Michael Peterson, who argues that Derrida's 'engagement with the survival of texts is at once a thinking through of waste' (Peterson 2018, 253).

Derrida gives us the following definition of the biodegradable: 'to be (bio)degradable means at least two things: on the one hand, the annihilation of identity; on the other hand, the chance to pass into the general milieu of culture, into the "life" of "culture" while enriching it with anonymous nourishing substances.' (838) Biodegradability is, then, all about the ability to lose identity, to fall apart and in so doing become (nourishment for) something else. Derrida relates this process to the function of great works of art in cultures and remarks that they should be both biodegradable (as otherwise they would not be able to enrich and nourish a culture) and 'resist erosion' (845) or, differently put, should be able to be 'assimilated as inassimilable' (845).

What about the word "biodegradable" itself? Derrida calls it an artificial word, made up of both Greek (bios, life) and Latin (degradere, stepping down) and is generally used to refer to products that are artificial and synthetic, 'from plastic bags to nuclear waste' (Derrida 1989, 815). When we speak about biodegradability, we mostly refer to things that resist the process of decay and are non¬-biodegradable, not so much living [bios] (or dead), but undead. Things get stuck in time and for a certain period are unable to become something else. Biodegradation is always a matter of time. As Michael Naas points out, when we speak of the biodegradable, we usually don't refer to organic things, that is, to things that are and always were able to decompose without technical aid. Nor do we refer to rocks or mineral as nonbiodegradable. The biodegradable thing is, then, 'the name given to a certain category of artificial, industrial, often mass-produced "thing"' (Naas 2015, 193).

Derrida's analysis of biodegradability is, then, all about dealing with the (unwelcome) inheritance of things living-on [sur-vie] after we are done with them. Whereas in works of art we admire that they keep their form, that they remain, we'd rather our waste did not. The biodegradable is, as Der-

Editor in chief:
Raffaello Cossu
email: raffaello.cossu@unipd.it

Detritus / Volume 07 - 2019 / pages 1-3
https://doi.org/10.31025/2611-4135/2019.13851
© 2019 Cisa Publisher. Open access article under CC BY-NC-ND license

rida puts it, 'on the side of life' (824). That is, in order to give life, to enrich and to nourish, things must be able to lose their identity, their form. This does not mean, however, that the nonbiodegradable – waste – is on the side of death. For the problem of the nonbiodegradable is not that it doesn't "die" – nuclear waste, suggested by Derrida as an example of the 'absolute nonbiodegradable' (863), is finite too – but that it takes a long time to do so. The nonbiodegradable does not so much refer to the dead, but the undead, to things that are in-between life and death. Just like zombies, who refuse to die and continue to haunt us. The nonbiodegradable, then, seems to refer to things getting stuck, things not losing form, things being (in places) we don't want (them) to be and, although undead, continuing to act and demand our care.

How to deal with these remainders? Derrida's concept of "eating well" is of interest here. In an interview in 1991 Derrida reflects on what it would mean to "eat well", referring both to the literal ingestion of substances, of food, and of the figural ingestion of values and ideas and asks how we can learn to do that well. Derrida: 'The moral question is thus not, nor has it ever been: should one eat or not eat, eat this and not that, the living or the nonliving, man or animal, but since one must eat in any case and since it is and tastes good (bien) to eat, and since there's no other definition of the good (du bien), how for goodness sake should one eat well (bien manger)?' (Derrida 1991, 114) Eating well is a social thing. It is not only about what we eat ourselves, but also about what we give to eat. What do we give to eat to future generations? What will they inherit from us? It appears we are offering them a lot of things that are not easily digestible, like plastic and nuclear waste. Just like eating, digesting is a joined event. Digesting is something you do together – without the bacteria that inhabit my microbiome I would not be able to digest a thing. Digestion is about taking in, taking out nutrients for energy, growth, repair and then giving back what remains, that is to become a nutrient for something else.

Waste management should, then, be concerned with the digestibility of waste, that is, the degree in which a material is able to lose its specific form or shape and become something else. Or put differently (and with waste as the "undead" in mind), to deal with remainders and to provide "end-of-life care". Dutch-based Italian researcher and designer Maurizio Montalti explores what this end-of-life care could look like in his art-design project The Ephemeral Icon (2010). This project centers around the monobloc, the classic one-piece plastic chair that we have all sat in at one point in our lives, and asks how this "eternal icon" – the monobloc itself can break down of course, but the plastic it's made of will take a long time to degrade – can be turned into an "ephemeral icon". How to 'infuse life to trigger a process of final dissolution', Montalti asks, and 'dress it up for death'? (Montalti 2010, 48) Montalti experiments with fungi that, as it turns out (in lab conditions), can be tricked into taking plastic for something edible and digesting it (Figure 1).

Since the completion of Montatlti's project in 2010, plastic eating bacteria have been found in the wild (Yoshida et al. 2016) which has even led to the creation of a

FIGURE 1: Officina Corpuscoli – The Ephemeral Icon - Decomposition Steps ©Corpuscoli_Montalti.

"mutant enzyme" that appears to be very skilled in eating PET (Austin et al. 2018). Have we entered the era of eating well? And if bacteria are starting to eat plastics, don't they help us close the loop, similar to what a resource-approach to waste does? Biodegradability does seem to present 'an ideal vision of matter, lapsing back into "nature" without leaving a visible residue' (Gabrys 2013, 216) and in so doing naturalize plastic and construe it as non-problematic matter. The 'recalcitrance of plastic' (Gabrys 2013, 216), however, ensures that this does not run smoothly. As Jennifer Gabrys point out, reflection on biodegradability points to a 'more collective understanding of material processes' (218). These plastic eating bacteria are unruly, they evolved without our help in the garbage dump in which they were found and will probably evolve and live on to do unexpected things. There is no closing the loop in such an ongoing and collective process. We could also ask if letting other organisms deal with our waste is yet another way of dumping our waste in a vulnerable, less powerful community and avoid taking responsibility for it. Instead, we should try and learn to live with it.

Derrida's notion of "eating well" is about recognizing the way in which we are connected to and interdependent with processes that fall outside our control and learn to eat and give to eat as best we can within these interdependencies.

And let's not forget that eating well is about what comes out at the back end – too. We can wipe our asses, flush the toilet and put the remaining carton in the recycling bin and convince ourselves all will be re-assimilated, or we could take another look back and really deal with our shit.

Lisa Doeland *
Radboud Universiteit Faculteit der Filosofie Theologie en Religiewetenschappen, Radboud Reflects, The Netherlands
* l.doeland@reflects.ru.nl

REFERENCES

Austin, H.P, D.M. Allen, B. S. Donohue et al. (2018) 'Characterization and engineering of a plastic-degrading aromatic polyesterase', PNAS, 115(19): E4350-E4357.

Corvellec, H and J. Hultman (2012) 'From "less landfilling" to "wasting less": Societal narratives, socio-materiality, and organizations', Journal of Organizational Change Management, 25(2): 297-314.

Corvellec, H. (2014) 'Recycling food waste into biogas, or how management transforms overflows into flows', in C. Barbara and L. Orvar (eds.), Coping with excess. How organizations, communities and individuals manage overflows, 154-172. Cheltenham: Edward Elgar Publishing.

Derrida, J. (1989) 'Biodegradables. Seven Diary Fragments', Critical Inquiry, 15(4): 812-873.

Derrida, J. (1991) '"Eating well", or the calculation of the subject: an interview with Jacques Derrida', in E. Cadava, P. Conner and J-.L. Nancy (eds.), Who comes after the subject?, 96-119. London: Routledge.

Gabrys, J. (2013) 'Plastic and the work of the biodegradable', in J. Gabrys, G. Hawkins and M. Michael, Accumulation. The material politics of plastic, 208-227. London and New York: Routledge.

Kaza, S., L. Yao, P. Bhada-Tata and F. van Woerden. (2018) What a Waste 2.0. A Global Snapshot of Solid Waste Management to 2015. Washington, DC: World Bank.

detritus | Multidisciplinary Journal for Waste Resources & Residues

CISA

ENERGY POTENTIAL OF SOLID WASTE GENERATED AT A TERTIARY INSTITUTION: ESTIMATIONS AND CHALLENGES

Adelere E. Adeniran [1], AbdulGaniyu O. Adelopo [2,*], Adetinuke T. Aina [2], Afolasade T. Nubi [2] and Oluwatobi O. Apena [3]

[1] *Department of Civil & Environmental Engineering, University of Lagos, Nigeria*
[2] *Works & Physical Planning Department, University of Lagos, Nigeria*
[3] *Department of Electrical and Electronic Engineering, University of Lagos, Nigeria*

Article Info:
Received:
10 April 2019
Revised:
10 June 2019
Accepted:
02 July 2019
Available online:
01 August 2019

Keywords:
Waste to energy
Residual waste
Calorific value
Moisture content
Municipal solid waste

ABSTRACT

Waste to energy (WtE) refers to any treatment process that creates energy in the form of electricity or heat from a waste source. This research reviews the potential uses of municipal solid waste generated at the University of Lagos, Akoka campus as a sustainable energy source for the tertiary institution. Waste characterization study of the residual waste at the University's sorting centre was conducted to determine the amount, composition and physical properties of the waste. A novel compositional trending ratio (CTR) was used to evaluate the possible calorific variation in samples using ASTMD3286-77 method. A validation of the experimental results was carried out using energy estimation model described by Smith and Scott (2005) and World Bank (1999). The major components of the residual waste were mainly polythene materials (24%), inert (30%), organic waste (15%), and paper (15%). The average calorific value of 17.23 MJ/kg and moisture content of 41.3% could potentially generate 34, 787 kWh daily (about 48.32% of the 72,000 kWh energy demand of the University). There was no significant statistical difference between experimental energy estimation of samples and model energy values ($p < 0.001$) and a Relative Percent Difference (RPD) < 3% (experimental energy 1112.1MJ/Kg, model value 1108.3 MJ/Kg). The major challenge to adopting WtE technology is the gap in daily tonnage of waste generated which can be overcome through collaborative solid waste management program with closed neighborhood and tertiary institution. The findings provide resourceful information on sustainable management of waste generated for a typical tertiary institution.

1. INTRODUCTION

Energy generation is pivotal to economic, social and intellectual development of any nation. The drive towards meeting the global energy demand has created immense challenges with 90% of energy generated from fossil fuels having attendant risks to human health and the environment (Cheng and Hu, 2010). One of the ways of sustainable energy generation is through Waste to energy (WtE). White refers to any treatment process that creates energy in the form of electricity or heat from waste (Pour et al., 2018). The creation of energy from waste in the form of gas, liquid or solid have the potential of reducing over dependent on fossil fuels, hence viable alternative method to managing most municipal solid waste (MSW) and residual waste. What technologies have the potential to reduce the volume of the original waste by 90 per cent, depending on the waste composition of waste used and the advancement in the technology deployed (Cheng and Hu, 2010). There are over 2000 conventional WtE facilities worldwide using more than 130 million tons MSW each year to produce energy. 64% of world's WtE is achieved through waste incineration plant while other forms of renewable energy from waste are generated from landfill gas (LFG) and anaerobic digestion of organic waste (Pour et al., 2018). Waste incinerators have been successfully deployed in many developed countries in Europe, Asia and the UK. The US generates about 14,000 GWh annually from about 29 million tonnes of MSW through WtE incineration facilities (Stocker, 2013).

Most developing countries have huge challenges in the use of white incinerator plants due to the large investments and operating costs, but more importantly is the absence of profound knowledge on waste generation and composition which form the bedrock in the choice and design of WtE plant. According to World bank technical guideline for

* Corresponding author:
AbdulGaniyu O. Adelopo
email: aadelopo@unilag.edu.ng

https://doi.org/10.31025/2611-4135/2019.13842
© 2019 Cisa Publisher. Open access article under CC BY-NC-ND license

WtE plant, 1999, the major preconditions factors to WtE plant before the financial implication assessment are: i) A mature and well-functioning waste management facility operated for a number of years, ii) disposal of solid waste at a controlled and well operated landfill iii) The supply of combustible waste at a stable volume which at least 90% of daily capacity of the WtE facilities iv) The average lower calorific value must not fall below 6 MJ/kg.

Although, Nigeria is richly endowed with various energy resources: crude oil, natural gas, coal, biomass, solar, wind, hydro resources, yet her development has been negatively impacted by the gap of energy demand and supply to both formal and informal sectors of the country (Oyedepo, 2012). The nation currently generates about 3,920 MW with per capita power capacity of 28.57 W which is not enough to meet even the domestic consumption demand (Oyedepo, 2012, Ibikunle et al., 2019). Most tertiary institution's energy demands are higher than the normal municipal settlement with huge energy needed to carry-out continuous research.

An energy deficit in these institutions from the national grid is often supplemented through the independent generation of electricity by heavy generators which increase the environmental pollution and the use of fossil fuel. Sustainable means of alternative energy generation for tertiary institution could help reduce these negative environmental impacts.

University communities as model mini cities with a known potential population, activities and lifestyle provide an opportunity for structural evaluation of the WtE associated conditions. Cultural differences, climate, and socioeconomic conditions are expected to have a limiting influence on waste composition variation within a campus.

For a successful outcome of what project accurate data on the future trends in waste quantities and characteristics will inform the basis for the design of the plant. Most university community's growth rate is strategically monitored by local and international standard for effective running (Alshuwaikhat and Abubakar, 2008).

University community can therefore represent a model community suitable for the evaluation of WtE potential especially in developing countries having challenges with solid waste data and record keeping.

The heating values of MSW largely depend on the lower calorific value which is the heat required to vaporize any free water in the waste and while providing for any dilution effect of non-combustible ash in the waste (cooper et al., 1999). Estimated calorific values of MSW can be determined using established predictive mathematical models for each waste sample type or by experimental procedures (Menikpura et al., 2007). Data on the Higher Heating Value of MSW have been widely published, but with concern over the disparity range between experimental determination and predictive model (Kathiravale et al., 2003a).

Kalantarifard et al., 2011 had observed that experimental determination of calorific energy with a bomb calorimeter using 0.5 to 1 g of waste sample may not adequately account for the possible variance in MSW composition. While Menikpura et al., 2007 had successfully validated experimental determination of energy variation in MSW composition of Kandy, Sri Lanka using Modified Dulong and Shafizadeh model energy values.

A good estimation of the impact of variation in waste composition and volume is critical values for the determination of waste energy estimation and the operation of what plant. An extreme waste composition of predominantly sand and plastics could adversely affect the operation of WtE despite relatively high average lower calorific value. Establishment of an evaluation scheme to determine the variation trends in waste composition and generation are often challenging in proposing WtE plant.

This research proposed a novel compositional trending ratio (CTR) to evaluate the possible calorific variation in waste generated on a university campus. An experimental and model predictions energy evaluation system was used with the view to determine energy potential inherent in the wastes.

2. MATERIALS AND METHODS

2.1 Sampling area

University of Lagos, Akoka campus is located in the Western part of Lagos, Nigeria. It is one of the major University campuses in Nigeria with an estimated 561 hectares of land area hosting 10 faculties, 330 staff housing units, 15 students' hostels and several administrative and academic buildings. Detailed demography of the University is as presented by Adeniran et al. (2017). In order to provide a sustainable environment suitable for teaching, research and social life, the University of Lagos, Akoka campus, embarked on reformation of its environmental and waste management system by dividing the campus into zones and employing private waste managers to ensure effective waste collection.

Two private waste managers were employed to collect waste for zone A, B, C and D which were mainly academic and residential areas respectively (Figure 1). The waste is disposed at the University Sorting Centre where each waste manager sorts the recyclable wastes and packages it for onward transfer to recycling company. The recycling program has made available real-time data on solid waste generation trends in the University as reported by the characterization studied carried-out to determine the compositional trend in the fresh waste disposed (Adeniran et al., 2017). This study showed that waste recovery will be needed for the University to achieve a zero waste goal.

Wastes not having local recycling market or not effectively separated (about 98% of total waste generated) are left on the sorting field (about 3189 m^2) as residual waste. The residual waste is finally disposed onto the landfill.

2.2 Sampling procedure

Sampling of the residual waste was carried out using systematic gridding procedures as described by Resource Conservation Reservation Authority Waste Sampling Draft Technical Guideline, (USEPA, 2002). The site was gridded into ten sampling cells with each cell of approximately 318.9 m^2. Each cell was located using the Global Position System (GPS) device and an average of 5 kg sample collected from each sampling point. Samples were collected

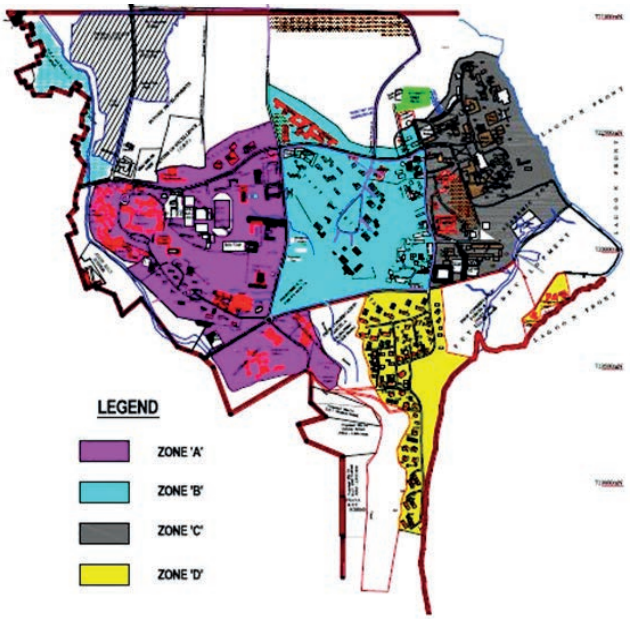

FIGURE 1: Map of University of Lagos, Akoka campus showing solid waste management zones.

using decontaminated hand shovel and placed in labeled polythene bags for onward transfer to the laboratory for analysis. Samples were collected between April and August 2017 at the sorting centre.

2.3 Moisture Content of sample

The moisture content of samples was evaluated using ASTM D3173 procedure (ASTM, 1988). Samples were dried in the oven at 105°C till constant weight was attained and the % moisture content of samples determined as thus:

$$\%\ moisture\ content\ (MC) = \frac{WW\text{-}DW}{WW}\ X\ 100 \quad (1)$$

Where WW is the weight of wet sample and DW is the dried sample weight.

The dried samples were separated into classes based on physical identification of the types of waste. Waste classifications were in line with IPPC, 2009 and Adelopo et al., 2017 municipal waste grouping.

2.4 Calorific value determination

The Calorific Value (CV) of the residual waste is expressed as energy content (E), or heat value, released when burnt in air (García et al., 2012). The Net Calorific value (NCV), or Lower Heating Value (LHV) was used in the evaluations of sample. The NCV was measured in terms of the energy content per unit mass (García et al., 2012).

$$E\ (MJ) = M \times NCV \quad (2)$$

Where NCV is net calorific value and M is the sample mass.

The net calorific energy content of each sample was determined using ASTM E711-87- Standard Test Method for Calorific Value of Refuse-Derived Fuel by Bomb Calorimeter (ASTM, 2004), using oxygen bomb calorimeter (CAL2K model). The calorimeter was calibrated using 0.5 g of benzoic acid before sample analysis. 0.5 g sample was weighed using analytical weighing balance and placed in the combustion chamber of the calorific analyser. The calorific values of samples were determined by burning the weighed sample in oxygen bomb calorimeter under controlled pressure of 3 MPa. The energy values of samples were determined in triplicate and the average value taken after proper allowance for thermometer and thermochemical corrections. Accounting for possible variation in waste components is critical to the determination of MSW calorific value (World bank, 1999). Kalantarifard et al., 2011 had observed that experimental determination of calorific energy with a bomb calorimeter using 0.5 g -1 g of sample may not adequately account for the possible variance in MSW composition. To this end, the average % compositional ratio of the residual waste was determine and the major constituents of the residual waste were varied at definite % compositional ratio (0:0% content, PC: present % composition, 50:50% > PC) refers to as Compositional Trending Ratio (CTR) to determine the energy content trend for various waste components. The variation in the waste components was designed to accommodate different possible waste generation pattern in the institution which may be influenced by occasion on campus-graduation and matriculation ceremonies (February/March) that could increase plastic bottles and organic components of waste. Also, during vacation (September-November) which could reduce paper component in the generated waste. A total of 12 composite representative samples of defined % compositional ratios were homogenized before analyzed.

The total estimated potential energy per day for each composite sample was determined as thus:

$$E = NCVi * M_{pd} \quad (3)$$

Where M_{pd} is the mass of average residual waste generated on campus per day.

Energy in term of kWh per day (Eeq) was determined using equation 4.

$$Eeq = \frac{1}{3.6\times10^{1}} * E \quad (4)$$

Annually waste generation projection was determined according to the World Bank's 1999, model:

$$Generated\ waste = PP\ (1+\ GRpp)^{\ n}\ X\ wc\ (1+GR_{KF})^{\ n} \quad (5)$$

Where PP is the present population, GR the growth rate and wc, waste generation per capita KF, is the actual key figure, and n the forecast year.

The energy potential of residual waste determined through oxygen bomb calorimeter was compared with energy potential estimation model described by Smith and Scott (2005), and World Bank (1999). The models determined average energy content for each type of waste which is cumulated per composite waste sample.

2.5 Data analysis

A correlation study using Statistical Package for Social Sciences 21 (SPSS) was deployed to determine the relationship between the components of samples, moisture content and the calorific values of samples.

3. RESULTS AND DISCUSSION

3.1 Residual composition

Fresh wastes are wastes evaluated on the first day of disposal at the sorting centre while residual waste are wastes left at the sorting centre for a period of 8-12 weeks after disposal and sorting of needed recyclable waste. The major components of the residual waste were mainly polythene materials (24%), inert (30%), organic waste (15%), and paper (15%) representing 74% of total waste composition. Figure 2 compares the compositional trend between the fresh waste disposed and residual waste intended for energy recovery. Major non-biodegradable component remain constant in both cases (polythene bags 24%, e-waste 0%, and glass 2%) despite the difference in the sample-Fresh waste and residual waste. This could indicate the regular generation trend of these wastes on campus and also that the recycling programme had not adequately cater for these set of waste. Conversely, increment in inert waste (8% in fresh waste to 30% in residual waste) may be due to the decomposition of other degradable waste like paper, food and textile which could mix up with the soil component of waste. Degraded waste were observed to influence the increase in the % composition of fine/soil component of disposed municipal waste by Sormunen et al. (2008) Jain et al. (2014) and Quaghebeur et al. (2013). An independent sample t- test was used to evaluate similarity between the compositional properties of the fresh disposed waste and the residual waste. Of the 12 constituents evaluated, 4 classes (inert, organic matter, plastic and textiles) showed a significant statistical difference ($p<0.05$).

3.2 Percentage Moisture content

The % moisture content (MC) of samples is presented in Figure 3. The MC of samples varied (within 21% and 69%) with 60% of the samples having MC below 50%. The moisture content of sample could be attributed to the effect of constituent wastes in each of the samples as presented in the supplementary data. This was investigated using a correlation studies between % moisture content and waste component (Table 1). The study shows that plastic, polythene and inert components had a strong negative statistical correlation of - 0.611, -0.561, -0.644 with the P value at 0.01, 0.01 and 0.05 respectively. This indicates that moisture content decreases with increased content of these sets of waste. Researchers have attributed the non- porous nature of polythene and plastic material as a major compositional factor affecting the moisture content of composite municipal waste (Quaghebeur et al., 2013 and Adelopo et al., 2017). Cheng et al. (2007) had identified high moisture content of waste as having significantly effect on its combustibility. The average % moisture content of samples (41.3%) is within viable condition for waste to energy. This meets the basic moisture content criteria of less than 45% as reported by Cheng and Hu (2010) and central pollution control, (2016). It is also lower than moisture content of municipal waste incinerated in China and Malaysia (55%) and Philippines (48%) (Kathirvale et al., 2003, Cheng and Hu, 2010, World bank, 1999).

3.3 Calorific value

Table 2 presents the variations in the waste components of each composite samples and the energy obtainable from the samples. The highest calorific values (23 MJ/kg) was recorded with polythene component at the highest possible % composition ratio (50 % above the present composition) while the lowest calorific values (11 MJ/kg) was obtained when inert constituent was varied at 50% above the present % composition of residual waste. All the possible variations evaluated (0% to 50% of polythene, organic waste, paper and inert components) were above the minimum energy level of 6 MJ/Kg for viable WtE feed (World bank, 1999).

Figure 4 compares the experimental energy values of residual waste determined using Oxygen bomb calorime-

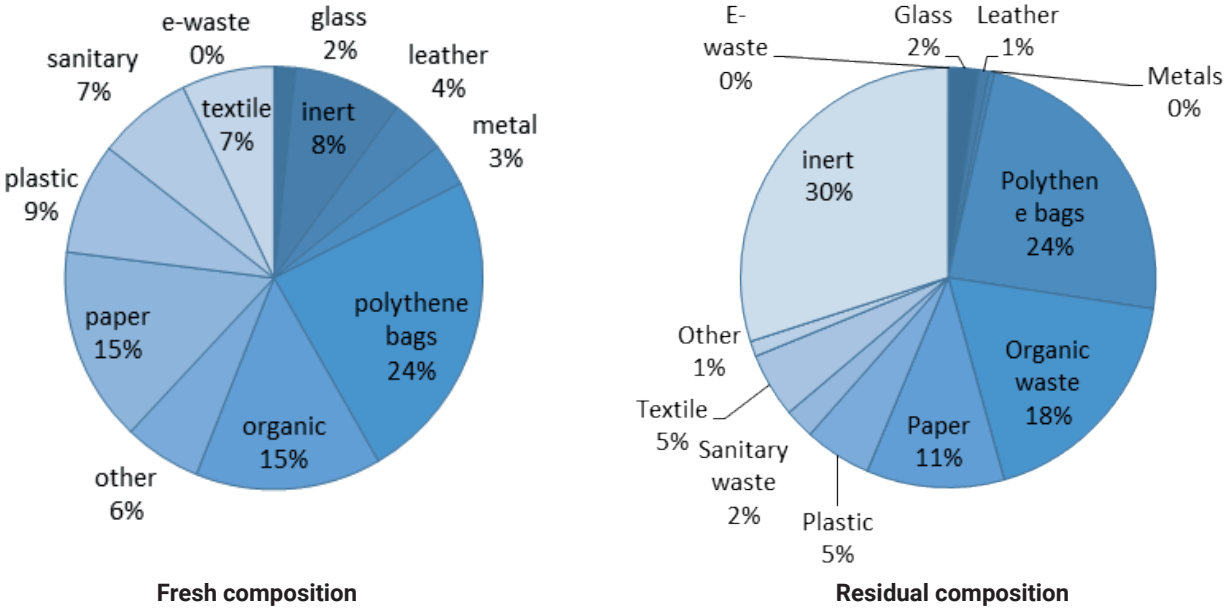

Fresh composition **Residual composition**

FIGURE 2: Comparing the compositional trends in the fresh and residual waste of the University.

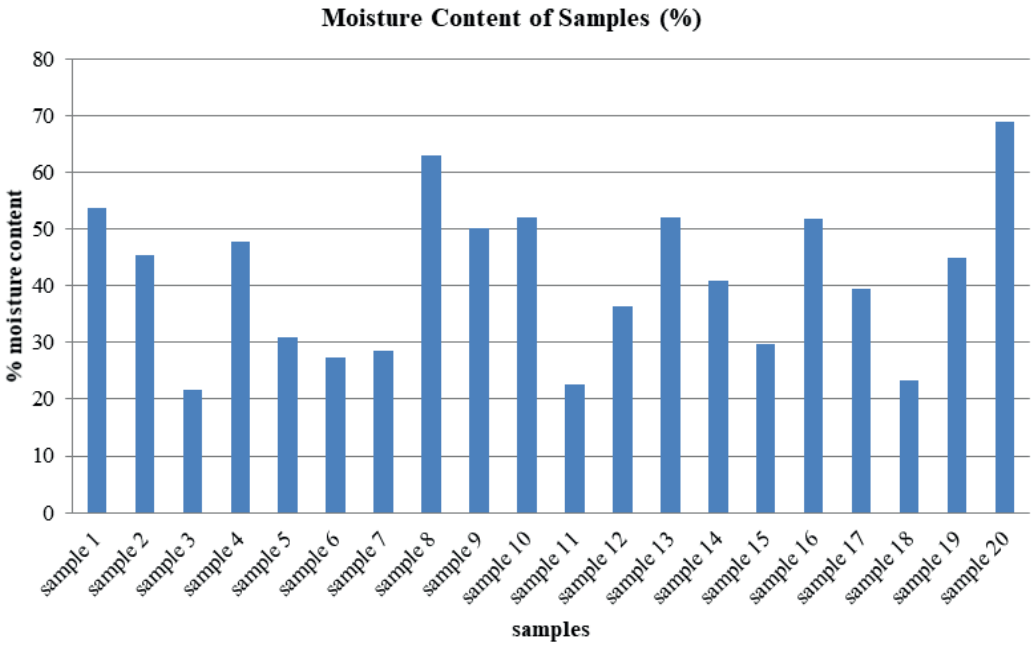

FIGURE 3: Moisture content of samples.

ter with energy estimation model described by Smith and Scott (2005) and World bank (1999). Both methods indicated strong agreement in the energy potential of the residual waste evaluated (experimental energy 1112.1 MJ/Kg, model value 1108.3 MJ/Kg) with a low relative percent difference of 3%. This further reinforces the energy potential in the residual waste samples. It also implies that the applied composite formation method using % composition of waste can reduce the possible variation associated with experiment determination of energy content of waste sample. No significant statistical difference between experimental energy values and the values of energy obtained via model energy estimate with P< 0.001.

Table 3 presents the correlation studies between % compositional ratio in waste component and calorific value. The result shows that polythene and inert components have significant effects on the calorific value of the samples. While there is a strong positive statistical correlation between increasing % composition of Polythene component and calorific value (0.646 with P value of 0.05), inert component had a negative statistical correlation (-0.586 with P value of 0.01) with the calorific value of samples. This implies that increase in polythene increase the calorific value of the waste and increase in inert waste decreases calorific energy potential of the waste.

The energy recovery model further confirms the effect of polythene and inert materials on the energy value of residual waste being responsible for 61% (39% from poly-

TABLE 1: Correlation studies of waste components and moisture content.

	E-waste	Glass	Leather	Metal	Polythene	Organic	Paper	Plastic	Sanitary	Textile	Other	Inert	Moisture
E-waste	1.000	-.090	.075	.020	-.138	-.058	-.189	.063	.195	-.114	.120	.170	.019
Glass		1.000	-.413	-.128	.089	-.029	-.364	-.151	.217	.091	.164	.165	-.093
Leather			1.000	-.202	-.095	-.055	.329	-.106	-.039	.091	-.486 *	-.468*	.273
Metal				1.000	-.138	.193	-.462*	.172	.244	.207	.379	.420	-.126
Polythene					1.000	-.224	-.111	.630 **	-.165	-.187	.188	.337	-.611**
Organic						1.000	-.020	-.347	.059	.021	.304	-.167	.192
Paper							1.000	-.035	-.453*	-.043	-.443	-.520*	.146
Plastic								1.000	-.139	.132	.248	.542*	-.561*
Sanitary									1.000	.104	.290	.248	.009
Textile										1.000	.079	.056	.101
Other											1.000	.405	-.094
Inert												1.000	-.664 **
Moisture													1.000

*** Correlation is significant at the 0.01 level (2-tailed)*
** Correlation is significant at the 0.05 level (2-tailed)*

TABLE 2: Variation in the waste components of each composite samples and energy obtainable.

sample code based on varied component	% composition of sample					Energy content (MJ/Kg)
	Polythene	Organic waste	Paper	Inert	Others	
PE_0	0%	24%	14%	39%	22%	13.28
Pe_{pc}	24%	18%	11%	30%	17%	18.25
PE_{50}	32%	16%	10%	27%	15%	20.36
OW_0	29%	0%	13%	37%	21%	16.07
OW_{pc}	24%	18%	11%	30%	17%	17.95
OW_{50}	22%	25%	10%	28%	16%	15.94
PP_0	27%	20%	0%	34%	19%	13.66
PP_{pc}	24%	18%	11%	30%	17%	18.02
PP_{50}	23%	17%	16%	28%	16%	15.14
IN_0	34%	26%	16%	0%	24%	20.12
IN_{pc}	24%	18%	11%	30%	17%	17.95
IN_{50}	21%	16%	10%	39%	15%	11.62

PE: polythene / OW :Organic waste / PP: paper / IN: inert / 0 :0% content / PC: present % / composition, 50: 50% > PC

thene and 22% from inert) of the potential energy from the residual waste (Table 4). Managing the variation in these components of waste would affect the energy potential of waste recoverable from the residual waste. Cheng et al., 2007 had observed that low energy content waste (4-6.7 MJ/Kg) from food waste reduced the energy generation in some WtE plant in China while higher energy generation were obtained from WtE in Europe and USA due to relative higher energy content waste like polythene materials.

Sources of waste variation in a modelled community like the University campus are often limited to the activities on campus which can be evaluated. The degrees in waste variation are also minimal compared to the variation expected in MSW (Okeniyi et al., 2012). Level of education, income statute, life style are majors factors influencing the type of waste generated (Hoornweg and Bhada-Tata, 2012). Irwan et al. (2011) had attribute generation of large quantity non-biodegraded waste to life style of people having tertiary education and are above average income earners which conform to most population within the University community. Major events on campus that could induce waste variation are expected to increase energy potential of waste due to possible generation of more non-biodegraded waste (paper, plastic and polythene). Report of some tertiary institutions waste characterization studies as presented by Armijo de Vega et al. (2008), Smyth et al. (2010) and Okeniyi et al. (2012) strongly confirm the availability of higher quantities of non bio-gradable waste.

The energy potential of residual waste generated daily on campus is estimated as 139,146 kWh as presented in Table 4. According to Kathiravale et al., 2003 and World

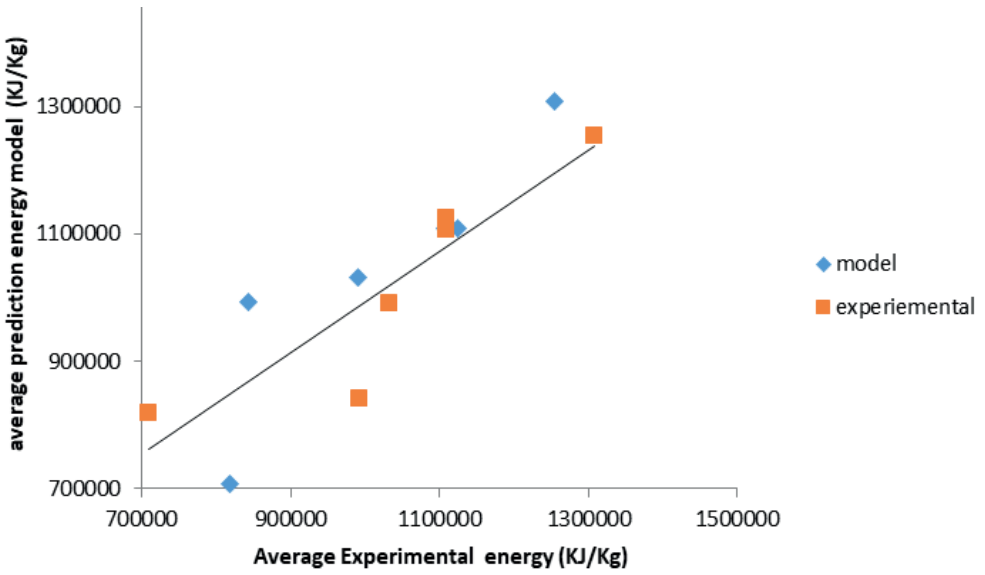

FIGURE 4: Variation in the waste components of each composite samples and energy obtainable.

TABLE 3: Correlation studies of major components of the samples and calorific values.

	Polythene	Organic	Paper	Inert	Calorific
Polythene	1.000	-.194	-.246	-.194	.646 **
Organic		1.000	-.194	-.153	-.133
Paper			1.000	-.194	-.148
Inert				1.000	-.586 *
Calorific					1.000

*** Correlation is significant at the 0.01 level (2-tailed)*
** Correlation is significant at the 0.05 level (2-tailed)*

bank, 1999, only 50% to 25% of the total energy potential is recoverable depending on conversion techniques. The residual waste could potentially generate 34, 787 kWh (at 25% recovery potential) which will be able to power 7000 electric cooker (1000 W rating) of resident member of the institution for 3 hours. It has the potential of reducing the diesel consumption for 2hours daily. The average diesel consumption for the University's 2250 KVA Cummins generators is at 200 litre per hour. If WtE is harnessed for a month this could cut the carbon print of the university via diesel consumption by 10%. A higher energy potential could have been achieved from the fresh waste disposed (50,148 KWh per daily using model method) if used directly for WtE. This is due to increase in the % composition of waste component having high calorific values (plastic, paper textile) compared to the residual waste (Figure 1). The use of fresh disposed waste may, however, undermine the present recycling effort of the University and reduce communal participation in waste management via waste sorting.

The energy content of waste may be adversely affected if the University's construction demolition waste (C&D waste) is mixed with present composition of waste. Inert waste content tends to lower the calorific energy content of the generated waste. The University will need to ensure an effect controlled measure to prevent disposal of its C&D along with other waste.

3.4 Volume of Generation Projection

Waste forecast over the life span of a WtE plant (15 to 20 years) is essential in assessing energy generation feasibility. During this period, apart from change in government policy on waste management which may influence waste management on campus, population growth of the institution is assumed to be the major factor that could influence waste generation and composition. Annually waste generation was determined in accordance with University's population growth rate as content in the University Master Plan. The trends in the data of waste generated and characterized on campus for the past three years were used as the key factors in projection analysis(per capita generation at 0.58 kg/person/day).

Table 5 presents the estimated waste generations projection for fifteen years. The data shows a possible growth in the power recoverable from waste by 16% (34,787 kWh per day to 41,302 kWh per day) within fifteen years at 25% efficiency. This provides a good incentive that increase in waste generation as a result of increase in population can be sustainably utilize for the community benefit.

However, the daily waste generated at the University of Lagos campus (32.2 tons to 38.4 tons) for the entire duration fall short of the minimum requirement of 250 t/day for eco-friendly WtE plants (Cheng and Hu, 2010 and 2007). This major challenge can however be managed with collaboration with four other major tertiary institutions which are in close proximity to the University. These tertiary institutions pay tipping charges to dispose their waste at the municipal landfill. Presentation of a cost-analysis benefit could attract the interest of these tertiary institutions having potentially similar waste generation pattern. Waste generation and characterization of each tertiary will be needed to ascertain their compatibility for the program.

More Universities in developed countries are leveraging on the waste generated on campus and within their immediate community to generate renewable energy for the campuses' sustainability programs. University of Iowa, US, had set 2025 to end the present use of coal plant and

TABLE 4: Caloric value of waste determined from model calorific value and % energy contribution of each waste type.

Waste type	Quantity of waste (g)	Model Calorific Value(MJ/Kg)	Calorific value per waste type (MJ/Kg)	% Energy contribution per waste type
E- waste	44.1	0	0	0
Glass	1425.3	0	0	0
Leather	491.8	22.5	11.066	1%
Metals	263.3	0	0	0%
Polythene bags	14655.7	27.3	400.1	36%
Organic waste	11248	6.7	75.4	7%
Paper	6618.9	17.5	115.8	10%
Plastic	3214.2	45	144.6	13%
Sanitary waste	1430.7	15	21.5	2%
Textile	3070.8	19	58.3	5%
Other	734	6.7	4.9	0%
inert	18439.8	15	276.6	25%
Total	61636.6		1108.3	100%

TABLE 5: Waste generation projection and potential energy contente.

Year	Population	Generation per day (Kg)	Quantity of residual waste for recovery # (Kg)	Calorific value per day (MJ/Kg)	Equivalent in kWh per day	Recoverable energy at 25% efficiency(KWh
2017	55695	32303	29073	500927	139146	34787
2018	56363	32690	29421	506930	140814	35203
2019	57045	33086	29777	513062	142517	35629
2020	57739	33489	30140	519306	144252	36063
2021	58437	33894	30504	525587	145997	36499
2022	59150	34307	30876	531998	147777	36944
2023	59867	34723	31250	538446	149568	37392
2024	60613	35155	31640	545153	151431	37858
2025	61354	35585	32027	551823	153284	38321
2026	62123	36031	32428	558734	155204	38801
2027	62897	36480	32832	565701	157139	39285
2028	63690	36940	33246	572834	159121	39780
2029	64479	37398	33658	579930	161092	40273
2030	65301	37875	34087	587323	163145	40786
2031	66127	38354	34518	594753	165209	41302

 # 90% of daily generation

completely switch to combined heat and power plant (CHPP) which depends on the biomass waste generated on campus and the wood chip waste from closed factories (Iowa, 2014). UC Davis college of Engineering uses renewable energy from anaerobic digester to generate 12,000 kWh daily from 50 tons of organic waste generated from within the university campus and cleaned segregated organic waste collected from its neighbourhood (Davis UC, 2014).

WtE can be effectively used to stimulate most University's sustainability programmes in developing countries and drive the larger community participation in sustainable energy activities.

4. CONCLUSIONS

The findings have indicated that the waste composition in the University has huge potential energy (11 MJ/Kg -23 MJ/Kg) with low variations in waste. Polythene and inert are major components which could significantly affect energy values of the waste representing 61% of recoverable energy potential. The average calorific value of 17.23 MJ/kg and moisture content of 41.3% could potentially generate potentially generate 34,787 kWh energy per day. This could cut the carbon print of the university via diesel consumption by 10%. The daily waste generated at the university of Lagos campus (32.2 t) fall short of the minimum requirement of 250 t/day for eco-friendly WtE plants but could be managed by collaboration with the neighborhood and the other four (4) tertiary institutions around since tertiary community has the potential of generating more non-biodegraded waste. These findings present a systematic procedure to evaluating waste parameters towards a WtE for a model institution. In making a final step to WtE, a further study is necessary to evaluate the economics and environmental impact of the types and location of WtE plants to be deployed.

5. SUMMARY AND RECOMMENDATION

The characterization of residual waste in the University campus was carried out in order to determine the energy potential and possible effect of waste composition variation on energy content. A compositional Trending Ratio (CTR) was introduced to evaluate the possible calorific variation in samples using both experimental and predictive models. Our findings indicated that:

- The University waste composition has huge energy potential estimated at 34,787 kWh energy per day with daily waste average calorific value of 17.23 MJ/kg and moisture content of 41.3%;
- Polythene and inert wastes are major components affecting energy values of the waste representing 61% of recoverable energy potential;
- The experimental and predictive model energy values showed significant agreement with a low relative percent difference of 3% for each CTR sample evaluated;
- The daily waste generation capacity of the university campus (32.2t) fall short of the minimum requirement of 250t per day for WtE.

These findings underpin the need for a policy that encourages collaborative waste management among institutions with similarity in waste composition for sustainable waste management.

REFERENCES

Adeniran A.E. Nubi A.T. Adelopo A.O. 2017. Solid Waste Generation and characterization in the University of Lagos for a sustainable waste management.Waste Management 67, 3-10.

Adelopo, A.O., Haris, P.I., Alo, B., Huddersman, K., Jenkins, R.O. 2017. Seasonal variations in moisture content and the distribution of total organic carbon in landfill composites: case of active and closed landfills in Lagos, Nigeria. Int. J.Environ. Waste Manage. 20(2), 171-185.

Alshuwaikhat, H.M., Abubakar, I. 2008. An integrated approach to achieving campus sustainability: assessment of the current campus environmental management practices. Journal of Cleaner Production 16, 1777–1785.

Armijo de Vega, C., Ojeda Benitez, S., Ramirez Barreto, M.E. 2008. Solid waste characterization and recycling potential for a university campus. Waste Manage. 2(Suppl. 1), S21–S26.

ASTM .1988. Standard Test Method for Determination of the Composition of Unprocessed Municipal Solid Waste, ASTMA standard d 5231-5292 (Reapproved 1998), American Society for Testing and Materials, USA.

ASTM E711-87 .2004. Standard Test Method for Gross Values of Refuse-Derived Fuel by the Bomb Calorimeter (Re-approved), American Society for Testing and Materials, West Conshohocken, PA.

Cheng, H., Zhang, Y., Meng, A., Li, Q .2007. Municipal solid waste fuelled power generation in China: a case study of waste-to-energy in Changchun city. Environ. Sci. Technol. 41, 7509–7515

Cheng, H., Hu Y. 2010. Municipal solid waste (MSW) as a renewable source of energy: Current and future practices in China. Bioresource Technology 101, 3816–3824.

Cooper, C.D.,Kim B., MacDonald J. 1999. Estimating the Lower Heating Values of Hazardous and Solid Wastes, Journal of the Air & Waste Management Association, 49:4, 471-476, DOI: 10.1080/10473289.1999.10463816.

Jain, P., Powell, J.T., Smith, J.L., Townsend, T.G., Tolaymat, T. 2014. Life-cycle inventory and impact evaluation of mining municipal solid waste landfills. Environmental Science andTechnology. 48(5), 2920–2927.

Central Pollution Control Board. 2016. Selection Criteria for Waste Processing Technologies. Ministry of Environment, Forests and Climate Change. PariveshBhawqan, East Arjun Nagar, Shahdara: Ministry of Environment, Forests and Climate Change.

García, R., Pizarro C., Lavín, A. G., Bueno, J.L.2012. Characterization of Spanish biomass wastes for energy use, Bioresource Technology, 103, 249-258.

Hoornweg, D. and Bhada-Tata, P. 2012. What a waste: a global review of solid waste management, World Bank, Washington DC, USA.

Ibikunle R.A, Titiladunayo I.F., Akinnuli B.O., Dahunsi S.O., Olayanju T.M.A. 2019. Estimation of power generation from municipal solid wastes: A case Study of Ilorin metropolis, Nigeria. Energy Reports 5, 126–135.

IPCC – International Panel on Climate Change .2006. Guidelines for National Greenhouse Gas Inventories, Vol. 5-Waste [online] http://www.ipccnggip.iges.or.jp/public/2006gl/vol5.html(accessed August 2017).

Irwan, D., Basri, E. A., Watanabe, K. 2011. Interrelationship between affluence and household size on municipal solid waste arising: evidence from selected Residential areas of putrajaya. Journal of Asian Scientific Research 2,747-758

Iowa 2014.University of Iowa timeline path to zero coal,https://www.facilities.uiowa.edu/uem/renewable-energy/ (accessed on November 2017)

Kalantarifard A., Yang, G. S.2011.Energy potential from municipal solid waste IntanjungLangsat Landfill, Johor, Malaysia. International Journal of Engineering Science and Technology 3(12), 8560 – 8568.

Kathiravale, S., Muhd Yunu,M., Sopian, K., Samsuddin, A.H. 2003a. Modeling the heating value of Municipal Solid Waste. Fuel 82, 1119–1125.

Kathiravale, S., MuhdYunus, M., Sopian, K., Samsuddin, A.2003. Energy potential from municipal solid waste in Malaysia. Renewable Energy 29, 559–567.

Menikpura, S.N.M., Basnayake, B.F.A., Boyagoda, P.B., Kularathne I.W. 2007. Estimations and Mathematical Model Predictions of Energy Contents of Municipal Solid Waste (MSW) in Kandy. Tropical Agricultural Research19, 389 – 400.

Okeniyi, J.O. Anwan, E.U., Okeniyi, E.U. 2012. Waste Characterization and Recoverable Energy potential Using waste generated in model community in Nigeria. Journal of Environmental Science and Technology 5(4), 232-240.

Oyedepo, S. O. 2012. On energy for sustainable development in Nigeria. Renewable and Sustainable. Energy Reviews 16, 2583– 2598.

Pour, N., Webley, P. A., Cook, P. J.2018. Potential for using municipal solid waste as a resource for bioenergy with carbon capture and storage (BECCS). International Journal of Greenhouse Gas Control 68, 1–15.

Quaghebeur, M., Laenen, B., Geysen, D., Nielsen, P., Pontikes, Y.2013. Characterization of landfilled materials: screening of the enhanced landfill mining potential. J. Clean. Prod. 55, 72–83.

Sormunen, K., Ettala, M. and Rintala, J. 2008. Detailed internal characterisation of two Finnish landfills by waste sampling. Waste Management 28(1), 151-163.

Stocker, T.F.2013. Climate change – the physical science basis. Working Group I Contribution to the Fifth Assessment Report of the Intergovernmental Panel on Climate Change. pp. 2013

Smyth, D.P., Fredeen, A.L., Booth, A.L.2010. Reducing solid waste in higher education: the first step towards 'greening' a university campus. Resource Conservation Recycling 54, 1007–1016.

Davis, U.C. 2014- UC Davis College of engineering biodigester turn campus waste into campusenergy.http://engineering.ucdavis.edu/blog/uc-davis-biodigester-turns-campus-waste-campus-energy/ (accessed December, 2017).

USEPA .2002. RCRA Waste Sampling Draft Technical Guidance. Planning, Implementation and Assessment. EPA530-D-02-002. Office of Solid Waste, Washington, DC.

World Bank.1999. Technical Guidance Report on Municipal Solid Waste Incineration, The International Bank for Reconstruction and Development ,Washington, D.C. 20433, U.S.A.

Zhang X., Cheng, X. 2009. Energy consumption, carbon emissions, and economic growth in China. Ecological Economics 68, 2706-2712.

detritus | Multidisciplinary Journal for Waste Resources & Residues

CISA

HAZARD CLASSIFICATION OF WASTE: REVIEW OF AVAILABLE PRACTICAL METHODS AND TOOLS

Pierre Hennebert *

INERIS (French National Institute for Industrial Environment and Risks), BP 2, F-60550 Verneuil-en-Halatte, France

Article Info:
Received:
22 March 2019
Revised:
01 August 2019
Accepted:
22 August 2019
Available online:
26 September 2019

Keywords:
Hazardous properties
HP 1 to HP 15
POP

ABSTRACT

The different steps for the classification of waste as hazardous are the collection of information, the use of the European list of waste, the sampling, the analysis, the tests, the hypothesis of speciation of elements into mineral substances, the collection of hazard statement codes of substances, and finally, the comparison of weighted sum or maxima of concentrations or tests results with given concentration limits for each hazard property, or possible use of now available internet sites. Practical methods are suggested: tables for generic classification of elements, for "worst case with information" speciation hypothesis of elements into mineral substances, tests for hazardous property HP 1, HP 2, HP 3, HP 12, HP 14, methods for HP 9 and HP 15.

1. INTRODUCTION

The hazard classification of waste is useful for the sound management and the recycling of potential resources. According to the EU, the chemicals and waste policy areas are now converging, since the aim is to minimize the adverse effects on human health and the environment, by phasing out hazardous chemicals or reducing their release into the air, water and soil. An exhaustive analysis of elements and substances as well as some tests are required to prove that a waste is non-hazardous. This process can help to identify substances of concern not clearly evidenced by the waste management community. Many of these substances were legally used when the products were manufactured, but when those products become waste and are recovered, the now banned or restricted substances may still be contained in the recovered material. This classification can be used to improve the recycling of resources and to avoid dispersion of hazardous elements or substances during uncontrolled uses (avoiding loops of hazardous substances). Some notable examples are plastic products with low concentration of antimony and brominated flame retardants from recycled plastics, concrete blocks with granulate of lead activated glass from cathode ray tubes, or dike reinforcement by sand and gravel from copper and lead slags.

This paper will introduce practical methods and tests for waste classification. A novel approach for speciation of elements into substances based on "worst case with information" of the physico-chemical characteristics of the waste, as a first step for classification, will be proposed. This method makes it possible to immediately identify the elements that cannot classify the waste as hazardous and thus to concentrate the classifier's efforts on the elements that can be classified as hazardous. A special attention to HP 14 'Ecotoxic' will be paid, the most frequent hazard property (when the multiplying factors of the concentration are used for the most hazardous substances, as in products).

To fine-tune the classification of waste is not a routine job. Interactive sites like HazWasteOnline (https://www.hazwasteonline.com/ of OneTouch Data, UK) or ClassifyMyWaste (https://www.ecn.nl/classifymywaste/ of Energy Centre of the Netherlands, NL) are helpful in the speciation options, and provide reliable and up-to-date hazard statement codes, classification rules and classification reports. The first site mentioned, HazWasteOnline, has nice interfaces for uploading the data of composition. The speciation options are proposed to the user. The website documents all the choices in a very complete report. The ClassifyMyWaste website offers worst-case calculations for all the elements mentioned in the CLP. This first approach is useful to identify elements of concern.

The structure of this document follows the logical reasoning of waste classification: (i) Legal background, technical guidance, general assessment, (ii) Sampling, analyses and tests, (iii) Hazard statement codes of substances, (iv) Speciation of elements into mineral substances, (v) Hazard properties of waste (mixtures of substances).

The purpose of this paper is to help waste producers, waste managers and public authorities to use the classification of hazardous waste. In addition to the legal obliga-

* Corresponding author:
Pierre Hennebert
email: pierre.hennebert@ineris.fr

Detritus / Volume 07 - 2019 / pages 13-28
https://doi.org/10.31025/2611-4135/2019.13846
© 2019 Cisa Publisher. Open access article under CC BY-NC-ND license

tions, this classification allows the management of hazardous waste by controlling the risk of their reuse or recycling for people, infrastructures, and the environment.

2. LEGAL BACKGROUND, TECHNICAL GUIDANCE, GENERAL ASSESSMENT

The 15 hazard properties of waste plus the POP rendering waste hazardous are presented in Table 1, that will be used all along the paper. They cover physical, health and environmental hazard. They can be assessed by expertise, by (bio)test, or by chemical composition and calculations (last column of Table 1).

Legal background can be found in the EU (2014a, b), the EU (2017a), and in national regulations. A European notice of technical guidance is available (EU 2018). UK and Nordic countries have proposed guidance documents (NRW et al. 2018, Norden 2015). To assess whether a waste is hazardous or not, the available data about the waste composition and properties must first be gathered, data such as:

- Knowledge of the waste and the process originating the waste;
- Literature data;
- Statistics of composition;
- Waste analysis (fractional composition analysis, physical and chemical characterization, bioassay, etc…).

The existing information on the waste can at best be enough to classify without performing complementary (analytical) work. Otherwise, it can guide the choices on the order and verification of the 15 hazard properties and the persistent organic pollutant (POP) content.

A tiered assessment is recommended:

- 1st tier: The classification by origin of the waste according to the European List of Waste (LoW) as "hazardous", "non-hazardous", or as "mirror entry". In this latter case:
- 2nd tier: Some HP can be assessed as "hazardous" or "non-hazardous" by expert judgment;
- 3rd tier: The remaining HP can be assessed as "hazardous" or "non-hazardous" from organic substances content and simple "worst case with information" hypothesis (using the tables of this document) from total elemental content. If the "worst case with information" approach is unsatisfactory (unrealistic, not in accordance with what is known of the waste), perform 4th tier;
- 4th tier: For some HP, perform specialized total analysis, leachate analysis or speciation of mineral content (from elements to mineral substances), or tests.

If the waste exhibits at least one hazard property among the 15 HP or exceed some POP specific concentration, it is classified as hazardous. Conversely, to demonstrate that a waste is not hazardous, the 15 properties and POPs concentration must be checked as non-hazardous. For suspected hazardous waste, cascading work is typically performed in an order depending of the waste and is stopped as soon as one property is verified as hazardous. For suspected non-hazardous waste, a comprehensive study of the entire HP set is performed. It is important to remember that landfill acceptance criteria cannot replace the waste hazardousness assessment.

The European list of Waste (EU 2014a) has been refined with a more precise definition of "absolute" entries (hazardous or not) and "mirror" entries (waste that can be hazardous or not depending on the concentration of hazardous substances) in (EU 2018). If the waste fits in an "absolute entry", the classification is done. Otherwise, further analyses (calculations or testing) are required.

3. SAMPLING, ANALYSES AND TESTS

The first step is the representative sampling. A precise sampling plan requires the previous knowledge of the elements or substances' distribution, ideally for each range of particle size. Standards for sampling plan calculations and sampling techniques are available (EN 14899, CEN/TR 15310-1 to -5, EN 15002). Regarding waste of electrical and electronic equipment (WEEE), sampling plans are suggested for some fractions (CENELEC 2015). For solid waste, the key concept (from the binomial law) is the number of particles that must be in a portion of matter to be representative of a larger portion of matter. This number depends on the analytical precision achievable for the analyses of the smallest possible test portion, and the frequency of particles having the studied property. From data of analytical variability and experimental data, the resulting recommended number of particles that should constitute a sample at any scale from the waste stream (thousands of tons) to the test portion (frequently less than one gram) is estimated being 100 000 if some particles are rare (1 of 1000) (CEN TR/15310-1 to -5, EN 15002, Hennebert 2019). Sampling delivers one or more laboratory samples.

The second step is the analysis. The laboratory samples must be pre-treated according to EN 15002. A standard method to determine the elements and organic substances contained in waste (with an analytical mass balance > 90% for solid waste and > 70% for liquid waste - not considering water) is practiced in France (AFNOR XP X30-489, Hennebert et al. 2013) and discussed at the CEN level (TC 444 'Environmental analyses of solid matrices'). Specific laboratory methods are needed for some peculiar analyses:

- Petroleum cuts (gasoline – i.e. CAS No 8006-61-9, gas oils/diesel – i.e. CAS No 68334-30-5, mineral lubricating oil – i.e. CAS No 64742-54-7) and creosote (CAS No 90640-85-0) should be identified and quantified as such (and not molecule by molecule) by the laboratory, additionally to total petroleum hydrocarbons (C10-C40), since they have harmonized classification (i.e. diesel HP 7 'Carcinogenic' H351 concentration limit of 1%). The concentration of the cut is, of course, much higher (and hence classifying) than the concentration of individual hydrocarbon molecule. The precise CAS No of the petroleum cut(s) should be attributed by the laboratory, by comparing the chromatographic response of the sample with standards. These specialized analyses should be performed by skilled laboratories;
- The transformation of congeners analysis to the con-

TABLE 1: The 15 hazard properties and POP property of waste and classification methods.

Category and HP	Hazard	Hazard Class and Category codes Hazard Statement Codes	Cut-off values	Methods, classification rules and Concentration Limits
Physical				
HP 1	Explosive	H200, H201, H202, H203, H204, H240, H241	/	Presence or tests (mainly EC A14) or expertise
HP 2	Oxidising	H270, H271, H272	/	Presence or tests (mainly UN 01) or expertise
HP 3	Flammable	H220 à H226, H228, H242, H251, H252, H260, H260	/	Presence or tests (mainly UN N1) or expertise
Health				
HP 4	Irritant (Skin irritation and eye damage)	H314 Skin corr. 1A H318 Eye dam. 1 H315 Skin irrit. 2, H319 Eye irrit. 2	1%	A: ∑ H314 1A ≥ 1% B: ∑ H318 ≥ 10% C: ∑ (H315 et H319) ≥ 20%
HP 5	Specific target organ toxicity/Aspiration Toxicity	H370 STOT SE 1 H371 STOT SE 2 H335 STOT SE 3 H372 STOT RE 1 H373 STOT RE 2 H304 Asp. Tox. 1	/	A: max (H370) ≥ 1% B: max (H371) ≥ 10% C: max (H335) ≥ 20% D: max (H372) ≥ 1% E: max (H373) ≥ 10% F: max (H304) ≥ 10% G: ∑ H304 ≥ 10% and global cinematic viscosity of the waste at 40°C < 20.5 mm²/s
HP 6	Acute Toxicity	H300 Acute Tox.1 (Oral) H300 Acute Tox. 2 (Oral H301 Acute Tox. 3 (Oral) H302 Acute Tox 4 (Oral) H310 Acute Tox.1 (Dermal) H310 Acute Tox.2 (Dermal) H311 Acute Tox. 3 (Dermal) H312 Acute Tox 4 (Dermal) H330 Acute Tox 1 (Inhal.) H330 Acute Tox.2 (Inhal.) H331 Acute Tox. 3 (Inhal.) H332 Acute Tox. 4 (Inhal.)	Cat. 1, 2 or 3: 0.1% Cat. 4: 1%	A: ∑ H300 1 ≥ 0.1% B: ∑ H300 2 ≥ 0.25% C: ∑ H301 ≥ 5% D: ∑ H302 ≥ 25% E: ∑ H310 1 ≥ 0.25% F: ∑ H310 2 ≥ 2.5% G: ∑ H311 ≥ 15% H: ∑ H312 ≥ 55% I: ∑ H330 1 ≥ 0.1% J: ∑ H330 2 ≥ 0.5% K: ∑ H331 ≥ 3.5% L: ∑ H332 ≥ 22.5%
HP 7	Carcinogenic	H350 Carc. 1A et 1B H351 Carc. 2	/	A: max (H350) ≥ 0.1% B: max (H351) ≥ 1%
HP 8	Corrosive	H314 Skin Corr. 1A, 1B et 1C	1%	A: ∑ H314 ≥ 5%
HP 9	Infectious	/	/	Presence of infectious germs code UN 2814 or 2900 or by origin or by expertise
HP 10	Toxic for reproduction	H360 Repr. 1A et 1B H361 Repr. 2	/	A: max (H360) ≥ 0.3% B: max (H361) ≥ 3%
HP 11	Mutagenic	H340 Muta. 1A et 1B H341 Muta. 2	/	A: max (H340) ≥ 0.1% B: max (H341) ≥ 1%
HP 12	Toxic gas	Presence of substances with HSC EUH029, EUH031, EUH032	/	Presence of these substances by detection of specific gases PH_3, HCN, HF, H_2S, SO_2, HCl et Cl_2 emitted during a test
HP 13	Sensitizing	H317 Skin Sens. 1 H334 Resp. Sens. 1	/	A: max (H317) ≥ 10% B: max (H334) ≥ 10%
Environment				
HP 14	Ecotoxic	H400 Aquatic Acute 1 H410 Aquatic Chronic 1 H411 Aquatic Chronic 2 H412 Aquatic Chronic 3 H413 Aquatic Chronic 4 H420	H400, H410: 0.1% H411, H412, H413: 1%	A: ∑ H400 ≥ 25% B: ∑ [(100*H410) + (10*H411) + (H412)] ≥ 25% C: ∑ (H410 + H411 + H412 + H413) ≥ 25% D: max (H420) ≥ 0.1% Or tests
Physical, Health and Environment (Evolutive)				
HP 15	Capable of exhibiting a hazardous property not displayed by the original waste	Presence of substances with HSC H205, EUH001, EUH019, EUH044 (explodes if heated or dried or confined)		A property HP 1 to HP 14 may appears by evolution of the waste Or presence of substances with HSC in the third column Or expertise
Health and Environment				
POP	Waste containing one or more POP substances with a concentration > CL	Polychlorinated dibenzo-p-dioxins et dibenzofurans (PCDD/PCDF), DDT, chlordane, hexachlorocyclohexanes (including lindane), dieldrin, endrin, heptachlor, hexachlorobenzene, chlordecone, aldrin, pentachlorobenzene, PCB, mirex, toxaphene, hexabromobiphenyl.		PCDD/PCDF: ≥ 15 µg TEQ/kg Others: ≥ 50 mg/kg

centration of (total) polychlorobiphenyls (PCB) should be done according to EN 12766-1 and EN 12766-2 (petroleum products and used oils) as explained in (EU 2018): the total PCB content is calculated as five times the sum of the concentrations of 6 selected congeners 28, 52, 101, 138, 153 and 180 (method B). These congeners represent in fact about 20% of the mass of all the congeners in the commercial mixtures (with variations according to the rate of chlorination thereof);
- Some POP substances require specific laboratory methods;
- The extraction yield of additives in plastics (brominated flame retardants in fire-protected plastics, pesticides in packaging), must be checked with reference material. The analysis of brominated flame retardants in plastics should be done according to EN 62321-6, and in the other waste material according to EN 16377. These analyses are best conducted in industrial (product control) laboratories rather than environmental laboratories.

For HP 1 'Explosive', HP 2 'Oxidising', HP 3 'Flammable', HP 12 'Release of an acute toxic gas' and HP 14 'Ecotoxic', laboratory tests complement the laboratory analyses, or are the preferred methods. These tests will be presented with these HPs.

4. HAZARD STATEMENT CODES OF SUBSTANCES

A third step is to gather the hazard statement codes of substances (HSC) found or assessed in the waste. The EU "harmonized" classification of Table 3.1 of Annex VI of the CLP Regulation (CLP 2008) and its different adaptations to technical progress (ATP) should first be used (spreadsheet file: https://echa.europa.eu/information-on-chemicals/annex-vi-to-clp). The ECHA's Classification and Labeling (C & L Inventory) database (with the information of Table 3.1 (blue-headed tables), and the classification by the notifiers (yellow-headed tables)) (http://echa.europa.eu/web/guest/information-on-chemicals/cl-inventory-database) are not validated by ECHA but can be used in the absence of harmonized classification. In France, the portal of chemicals of INERIS (http://www.ineris.fr/substances/fr/) is also taken as a reference (bilingual English/French).

5. SPECIATION OF ELEMENTS INTO MINERAL SUBSTANCES

The laboratory delivers a total elemental concentration for each element, and a substance concentration for organic substances. The elements have no hazard statement codes (HSC), except for 11 elements with "generic" classification (Table 2). So, the fourth step is speciation of elemental concentrations into mineral substances concentrations.

Some forms or substances have specific methods:

- Calcium oxide or hydroxide (important for HP 4/ HP 8 in thermal process residues like slags, bottom ashes, ashes) and limed waste (sludges from WWTP) or containing lime (concretes and mortars and construction and demolition waste) should be measured according to EN 1744-1 (aggregates, not suitable for low concentrations) or EN 451-1 (fly ash). The EN 459-2 (building lime) and the EN 196-2 (cement) should not be used for another waste/material. Quicklime CaO and hydrated lime $Ca(OH)_2$ can be differentiated by thermogravimetry (quantification of the loss of water during heating). These analyses are carried out by laboratories specialized in studies and research on building materials;
- Chromium (VI), also called chromate, is measured by EN 15192.

Specialized laboratory methods are available for speciation: X-ray diffraction (limit of quantification 5%-1%), thermogravimetry (0.5%), specific extraction and analysis (as calcium oxide and chromate), and extraction at different pH with geomodelling (10 mg/kg). These methods are not practiced in routine characterization of waste, excepted Cr (VI). A synthesis can be found in AFNOR FD X30-494:2015.

A first simple approach is to calculate "worst case with information" substances concentrations (Table 3), using among other information of leaching concentrations. If the waste is calculated not hazardous, the assessment can be stopped. In Table 3, the elements are presented in the following order: major elements (of the earth's crust), major anions, 12 "heavy metals", and various minor, rare or little sought-after elements. A summary for teh 12 "hevy metals" is presented in Table 4.

5.1 Choice of substances "worst case with information" of Tables 3 and 4

1. Generic hazard statements are used primarily because they avoid hypotheses of speciation in substances. It is necessary to check in the Harmonized Table the hazard statements for substances (Annex VI of CLP) that the "other substances" of the same element (most often chemical industry intermediates, or highly reactive substances not found in common waste) are not in the waste. Substances with only one hazardous element are preferred (i.e. lead sulfate rather than lead arsenate);
2. Soluble forms if they have the relevant hazard statement codes (mainly sulphate - higher molar mass - for most properties, and chloride in some cases) are then used because they are often biologically more active, and their presence and concentration may be verified by leachable concentrations (EN 12457-2);
3. The most hydrated forms of substances are chosen because the concentration of element is lower for a given substance concentration;
4. In the absence of soluble forms, simple oxides (and among families of oxides, the most present form in the natural environment) have been chosen;
5. Of the major elements, only those forming acids and strong bases with hazard statements were used. Elementary forms (metal, oxidation stage 0) and very reactive forms, especially with water (hydrides, ...) were not retained, with one exception: elemental lithium, present in some rechargeable cells and batteries at a concentration of about 2%. The case of glass wool (index No.

650-016-00-2, H351), refractory ceramic fibers (index No. 650-017-00-8, H350), glass microfibers (fiber optic index No.° 014-046-00-4 H350 and glass fiber index no. 014-047-00-X H351) (see file Annex VI of the CLP mentioned above) has not been considered here. If the presence of such fibers is suspected (for instance in the ceramic of some models of catalytic converters), specialized laboratory analyses have to be performed;

6. Finally, when only one substance in the element has the relevant hazard statement, it is chosen, even if it is rare. For example: the only lead substance with the hazard statement H350 for the property HP 7 'Carcinogenic' is a sulfo-chromic pigment, with a lead concentration limit of 0.1%.

The conversion of the substance concentration into the elemental concentration is obtained by multiplying the mass percentage of the element in the substance (ratio of the atomic mass of the element multiplied by its stoichiometric coefficient, and the molar mass of the substance).

5.2 Indications of presence of these forms "worst case with information" in the waste

The presence and concentration of the chosen soluble forms (sulfate for most properties and chloride in some cases) can be verified by leachable concentrations (EN 12457-2). The pH and buffering capacity indicate whether acids (Cl, F, S, P, N) or bases (Na, Ca) are present and at which concentration (XP CEN/TS 15364). The redox potential and the redox capacity indicate whether oxidants [Cr (VI), Mn (VII), Cl_2] or reductants [Fe (II), sulphide, sulphite] are present and at which concentration (XP CEN/TS 16660). Calcium oxide and total chromate have specific analytical methods (see Analysis section).

5.3 Using the table

For properties defined by concentration maxima (denoted Max HP 5, Max HP 7, Max HP 10, Max HP 11, Max HP 13), if the total concentration of the element in the waste is less than the concentration limit of the "worst case with information" expressed in the element, the waste is not hazardous for this property by this element.

For the properties defined by sums of concentration (denoted Σ HP 4, Σ HP 6, Σ HP 8, Σ HP 14), the concentrations of the substances of all the elements plus the concentrations of relevant organic substances must be added according to the hazard statements in accordance with the rules of the Table 1. CLP "Note 1" of generic entries means that the concentration limit applies to the element and not to the substances. These cases are reported in Table 3.

The HP 14 property is presented for the three hazard statements codes (HSC) H400, H410 and H411, given that 50% of the hazardous waste is, in addition to the other properties, ecotoxic (according to our observations with the M factor system, explained below). Virtually all acute ecotoxic substances H400 are also ecotoxic chronic H410. Manganese and selenium may have one form with HSC H410 and another with HSC H411, which justifies two different lines for chronic HP14. Substances with hazard statements H412 and H413 are less numerous. Mineral substances ("worst case with information" approach) with the hazard statement H412 are SnCl4 (CAS No. 7646-78-8) and powdered nickel <1 mm (CAS No. 7440-02-0). Mineral substances ("worst case with information" approach) with the hazard statement H413 are cadmium sulphide (CAS No. 1306-23-6), various nickel oxides (i.e. CAS No. 11099-02-8), and the elements Co, Se, Th and U (at the zero-oxidation stage), but the concentration limit is 25% (Table 3). Waste with concentrations of 25% of these elements are resources.

6. HAZARD PROPERTIES OF WASTE (MIXTURE OF SUBSTANCE)

During the fifth step, the hazard properties can be assessed by applying classification rules (Table 1). Concentrations of substances lower than the cut-off values must not be considered. Waste can also be hazardous by some POP substances (EU 2014a) with specific concentration limits. The full list of these POPs and their specific concentration limits are presented in Table 5. Note that there are other POP substances that do not classify the waste as hazardous by their POP characteristics but can classify waste as hazardous for some HPs by their specific hazard statement codes and concentrations, like non-POP substances. These substances and their HSC are included in the spreadsheet file presented in Chapter 4 and are presented in the second part of Table 5 (without “x” in the 4th column).

Most POP substances also have hazard statement codes (not shown in Table 5), and hence concentration limits for HP, but they are always higher than by their POP content. Only short chain chlorinated paraffins (SCCPs) have a CL by HP lower than CL by POP regulation.

6.1 Physical hazard

6.1.1 By tests: HP 1 ‘explosive’, HP 2 ‘Oxidising’, HP 3 ‘Flammable’

These HPs are defined by the presence of substances with relevant HSC. They are in practice assessed by expert judgment and the origin of the waste, or by tests (Table 6). It has been recently suggested to calculate them if the chemical composition is known in detail (EU 2018). The website HazWasteOnline (see below) assesses HP 3 with total petroleum hydrocarbon analysis. The most commonly used methods are EC A9 (flash point for liquid waste) and UN N1 (speed of flame progression in a row of solid waste).

6.2 (Human) Toxicity

6.2.1 By analysis and calculation: HP 4 ‘Irritant — skin irritation and eye damage’, HP 6 ‘Acute Toxicity”, HP 8 ‘Corrosive’ (sums of concentrations for these HPs); HP 5 ‘Specific target organ toxicity (STOT)/Aspiration Toxicity’, HP 7 ‘Carcinogenic’, HP 10 ‘Toxic for reproduction, HP 11 ‘Mutagenic’, HP 13 ‘Sensitising’, HP ‘POP’ (maxima of concentrations for these HPs)

These HPs are typically calculated from chemical composition (Table 1). Biological tests have been evoked (EU 2018), without further clarification.

TABLE 2: Generic entry classification (hazard class and category, and hazard statement code) of 11 elements (CLP, 2008).

Element	Index number	Chemical international identification	Number of substances with a specific entry (« specified elsewhere »)	Hazard class and category	Hazard Statement Code
As	033-002-00-5	arsenic compounds, with the exception of those specified elsewhere in this Annex. Note 1	4	Acute Tox. 3 * Acute Tox. 3 * Aquatic Acute 1 Aquatic Chronic 1	H331 H301 H400 H410
	033-005-00-1	arsenic acid and its salts with the exception of those specified elsewhere in this Annex.	6	Carc. 1A Acute Tox. 3 * Acute Tox. 3 * Aquatic Acute 1 Aquatic Chronic 1	H350 H331 H301 H400 H410
Ba	056-002-00-7	barium salts, with the exception of barium sulphate, salts of 1-azo-2-hydroxynaphthalenyl aryl sulphonic acid, and of salts specified elsewhere in this Annex	9	Acute Tox. 4 * Acute Tox. 4 *	H332 H302
Be	004-002-00-2	beryllium compounds with the exception of aluminium beryllium silicates, and with those specified elsewhere in this Annex	2	Carc. 1B Acute Tox. 2 * Acute Tox. 3 * STOT RE 1 Eye Irrit. 2 STOT SE 3 Skin Irrit. 2 Skin Sens. 1 Aquatic Chronic 2	H350i H330 Cat2 H301 H372 ** H319 H335 H315 H317 H411
Cd	048-001-00-5	cadmium compounds, with the exception of cadmium sulphoselenide (xCdS.yCdSe), reaction mass of cadmium sulphide with zinc sulphide (xCdS.yZnS), reaction mass of cadmium sulphide with mercury sulphide (xCdS.yHgS), and those specified elsewhere in this Annex. Note 1	15	Acute Tox. 4 * Acute Tox. 4 * Acute Tox. 4 * Aquatic Acute 1 Aquatic Chronic 1	H332 H312 H302 H400 H410
Cr(VI)	024-017-00-8	chromium (VI) compounds, with the exception of barium chromate and of compounds specified elsewhere in this Annex	19	Carc. 1B Skin Sens. 1 Aquatic Acute 1 Aquatic Chronic 1	H350i H317 H400 H410
Hg	080-002-00-6	inorganic compounds of mercury with the exception of mercuric sulphide and those specified elsewhere in this Annex. Note 1	6	Acute Tox. 2 * Acute Tox. 1 Acute Tox. 2 * STOT RE 2 * Aquatic Acute 1 Aquatic Chronic 1	H330 Cat2 H310 H300 Cat2 H373 ** H400 H410
	080-004-00-7	organic compounds of mercury with the exception of those specified elsewhere in this Annex. Note 1	7		
Pb	082-001-00-6	lead compounds with the exception of those specified elsewhere in this Annex. Note 1	17	Repr. 1A Acute Tox. 4 * Acute Tox. 4 * STOT RE 2 * Aquatic Acute 1 Aquatic Chronic 1	H360Df H332 H302 H373 ** H400 H410
Sb	051-003-00-9	antimony compounds, with the exception of the tetroxide (Sb_2O_4), pentoxide (Sb_2O_5), trisulphide (Sb_2S_3), pentasulphide (Sb_2S_5) and those specified elsewhere in this Annex. Note 1	7	Acute Tox. 4 * Acute Tox. 4 * Aquatic Chronic 2	H332 H302 H411
Se	034-002-00-8	selenium compounds with the exception of cadmium sulphoselenide and those specified elsewhere in this Annex	5	Acute Tox. 3 * Acute Tox. 3 * STOT RE 2 Aquatic Acute 1 Aquatic Chronic 1	H331 H301 H373** H400 H410
Tl	081-002-00-9	thallium compounds, with the exception of those specified elsewhere in this Annex	3	Acute Tox. 2 * Acute Tox. 2 * STOT RE 2 * Aquatic Chronic 2	H330 Cat2 H300 Cat2 H373 ** H411
U	092-002-00-3	uranium compounds with the exception of those specified elsewhere in this Annex	2	Acute Tox. 2 * Acute Tox. 2 * STOT RE 2 Aquatic Chronic 2	H330 Cat2 H300 Cat2 H373** H411

HP 4/HP 8

A European document (EU 2018) proposes, in line with the CLP, for classification according to HP 4 and HP 8 to consider the pH (≤ 2 and ≥ 11.5) and the buffer capacity (neutralization capacity of acids and bases, expressed in H^+ or OH^- equivalent per kg of material), especially in the case where not all substances in the composition of the waste are known. There is no buffer value indicated

TABLE 3: Concentration limits (CL) expressed in substance and in element concentrations by "worst case with information" approach for 36 elements and 9 hazard properties by calculation (NH: not hazardous for these 9 HP; "Note 1": the concentration limit applies to the element; CL by element percentage with four digits to have direct conversion to mg/kg; the lowest CL by element is colored).

Element	HP	Hazard Statement Code	CL by substance	«worst case with information» substance	Formula	CAS No	CL by element
Majors elements (cations)							
Si	NH						
Al	NH						
Fe	HP 4 (sum)	H315 H319	20%	Ferrous sulfate heptahydrate	$FeSO_4.7H_2O$	7782-63-0	4.0176
Mn	HP 5 (max)	H373	10%	Manganese sulphate	$MnSO_4$	7785-87-7	3.6384%
	HP 6 (sum)	H302	25%	Potassium permanganate	$KMnO_4$	7722-64-7	8.6910%
	HP 14 (sum) H400	H400	25.00%	Potassium permanganate	$KMnO_4$	7722-64-7	8.6910%
	HP 14 (sum) H410 H411 H412	H410	0.25%	Potassium permanganate	$KMnO_4$	7722-64-7	0.0896%
	HP 14 (sum) H410 H411 H412	H411	2.50%	Si pas KMnO4 (H400, H410) : MnSO4	$MnSO_4$	7785-87-7	0.9096%
Ca	HP 4 (sum)	H319	20%	Calcium chloride	$CaCl_2$	10043-52-4	7.2232%
	HP 4 (sum)	H315 H318	10%	Calcium oxide	CaO	1305-78-8	7.1470%
	HP 5 (max)	H335	20%	Calcium oxide	CaO	1305-78-8	14.2939%
Mg	NH						
Na	HP 4 (sum)	H314 1A	1%	Sodium hydroxide; caustic soda	NaOH	1310-73-2	0.5748%
	HP 8 (sum)	H314 1A	5%	Sodium hydroxide; caustic soda	NaOH	1310-73-2	2.8740%
K	HP 4 (sum)	H315 H319	20%	Potassium chromate	$K2CrO_4$	7789-00-6	8.0537%
	HP 8 (sum)	H314 1B	5%	potassium hydrogensulphate	$KHSO_4$	7646-93-7	1.4357%
Cr III	NH						
V	HP 5 (max)	H372	1%	Divanadium pentaoxide; vanadium pentoxide	V_2O_5	1314-62-1	0.5602%
	HP 6 (sum)	H302	25%	Divanadium pentaoxide; vanadium pentoxide	V_2O_5	1314-62-1	14.0044%
	HP 10 (max)	H361	3.00%	Divanadium pentaoxide; vanadium pentoxide	V_2O_5	1314-62-1	1.6805%
	HP 11 (max)	H341	1.00%	Divanadium pentaoxide; vanadium pentoxide	V_2O_5	1314-62-1	0.5602%
	HP 14 (sum) H410 H411 H412	H411	2.50%	Divanadium pentaoxide; vanadium pentoxide	V_2O_5	1314-62-1	1.4004%
Major elements (anions)							
B	HP 4 (sum)	H318	10%	Perboric acid, sodium salt, tetrahydrate = sodium perborate tetrahydrate	$NaBO_3.4H_2O$	10486-00-7	0.7024%
	HP 10 (max)	H360	0.30%	Disodium tetraborate decahydrate; borax decahydrate	$Na-2B_4O7.10H_2O$	1303-96-4	0.0340%
Cl	HP 8 (sum)	H314 1B	5%	Hydrochloric acid ... % (concentration >5%)	HCl	7647-01-0	4.8619%
F	HP 4 (sum)	H314 1A	1%	Hydrofluoric acid ... % (concentration > 1%)	HF	7664-39-3	0.9497%
	HP 6 (sum)	H300 Cat 2	0.25%	Hydrofluoric acid ... % (concentration > 0.25%)	HF	7664-39-3	0.2374%
	HP 8 (sum)	H314 1A	5%	Hydrofluoric acid ... % (concentration >5%)	HF	7664-39-3	4.7483%
N	HP 4 (sum)	H314 1A	1%	Nitric acid ... % (concentration > 1%)	HNO_3	7697-37-2	0.2223%
	HP 8 (sum)	H314 1A	5%	Nitric acid ... % (concentration > 5%)	HNO_3	7697-37-2	1.1114%

P	HP 8 (sum)	H314 1B	5.00%	Phosphoric acid ... %, orthophosphoric acid ... %	H_3PO_4	7664-38-2	1.5804%
S	HP 4 (sum)	H314 1A	1%	Sulphuric acid ... % (concentration > 1%)	H_2SO_4	7664-93-9	0.2543%
	HP 8 (sum)	H314 1A	5%	Sulphuric acid ... % (concentration > 5%)	H_2SO_4	7664-93-9	1.2714%
« Heavy metals »							
As	HP 6 (sum)	H300 Cat 2	0.25%	Diarsenic trioxide; arsenic trioxide	As_2O_3	1327-53-3	0.1893%
	HP 7 (max)	H350	0.10%	Arsenic acid and its salts with the exception of those specified elsewhere in this Annex	$H3AsO_4$	7778-39-4	0.0528%
	HP 8 (sum)	H314	5%	Diarsenic trioxide; arsenic trioxide	As_2O_3	1327-53-3	3.7870%
	HP 10 (max)	H360	0.30%	Lead hydrogen arsenate	$PbHAsO_4$	7784-40-9	0.0648%
	HP 14 (sum) H400	H400	25.00%	Generic classification (substance not defined). Note 1	As		25.00%
	HP 14 (sum) H410 H411 H412	H410	0.25%	Generic classification (substance not defined). Note 1	As		0.25%
Ba	HP 6 (sum)	H301 H332	5.00%	Barium chloride	$BaCl_2$	10361-37-2	3.2975%
Cd	HP 5 (max)	H372	1%	Cadmium sulfate	$CdSO_4$	10124-36-4	0.5392%
	HP 6 (sum)	H301 H330 Cat 2	0.50%	Cadmium sulfate	$CdSO_4$	10124-36-4	0.2696%
	HP 7 (max)	H350	0.10%	Cadmium sulfate	$CdSO_4$	10124-36-4	0.0539%
	HP 10 (max)	H360	0.30%	Cadmium sulfate	$CdSO_4$	10124-36-4	0.1618%
	HP 11 (max)	H340	0.10%	Cadmium sulfate	$CdSO_4$	10124-36-4	0.05%
	HP 14 (sum) H400	H400	25.00%	Generic classification (substance not defined). Note 1	Cd	10124-36-4	25.00%
	HP 14 (sum) H410 H411 H412	H410	0.25%	Generic classification (substance not defined). Note 1	Cd	10124-36-4	0.25%
Cr VI	HP 5 (max)	H372	1%	Sodium chromate	Na_2CrO_4	10588-01-9	0.3210%
	HP 6 (sum)	H301 H312 H330 Cat 2	0.50%	Sodium chromate	Na_2CrO_4	10588-01-9	0.1606%
	HP 7 (max)	H350	0.10%	Sodium chromate or Generic classification	Na_2CrO_4	10588-01-9	0.0321%
	HP 8 (sum)	H314	5%	Sodium chromate	Na_2CrO_4	10588-01-9	1.6051%
	HP 10 (max)	H360	0.30%	Sodium chromate	Na_2CrO_4	10588-01-9	0.0963%
	HP 11 (max)	H340	0.10%	Sodium chromate	Na_2CrO_4	10588-01-9	0.0321%
	Max HP 13	H317 H334	10%	Sodium chromate	Na_2CrO_4	10588-01-9	3.2102%
	HP 14 (sum) H400	H400	25.00%	Sodium chromate or Generic classification	Na_2CrO_4	10588-01-9	8.0250%
	HP 14 (sum) H410 H411 H412	H410	0.25%	Sodium chromate or Generic classification	Na_2CrO_4	10588-01-9	0.0803%
Cu	HP 4 (sum)	H315 H319	20%	Copper sulfate	$CuSO_4.5H_20$	7758-98-7	5.0905%
	HP 6 (sum)	H302	25%	Copper sulfate	$CuSO_4.5H_20$	7758-98-7	6.3631%
	HP 14 (sum) H400	H400	25.00%	Copper sulfate	$CuSO_4.5H_20$	7758-98-7	6.3631%
	HP 14 (sum) H410 H411 H412	H410	0.25%	Copper sulfate	$CuSO_4.5H_20$	7758-98-7	0.0636%
Hg	HP 4 (sum)	H315 H319	20%	Mercury (I) chloride	Hg_2Cl_2	10112-91-1	17.2440%
	HP 5 (max)	H372	1%	Mercuric chloride	$HgCl_2$	7487-94-7	0.7578%
	HP 6 (sum)	H300 Cat 2	0.25%	Generic classification (substance not defined). Note 1	Hg	7783-35-9	0.2500%
	HP 8 (sum)	H314	5%	Mercuric chloride	$HgCl_2$	7487-94-7	3.7889%

	HP 10 (max)	H360	0.30%	Mercury	Hg	7439-97-6	0.3000%
	HP 11 (max)	H341	1.00%	Mercuric chloride	$HgCl_2$	7487-94-7	0.7578%
	HP 14 (sum) H400	H400	25.00%	Generic classification (substance not defined). Note 1	Hg	7783-35-9	25.0000%
	HP 14 (sum) H410 H411 H412	H410	0.25%	Generic classification (substance not defined). Note 1	Hg	7783-35-9	0.2500%
Mo	HP 7 (max)	H351	1.00%	Molybdenum trioxide	MoO_3	1313-27-5	0.6665%
Ni	HP 4 (sum)	H318	10%	Nickel dinitrate	$Ni(NO_3)_2$	13138-45-9	3.2126%
	HP 5 (max)	H372	1%	Nickelous sulfate	$NiSO_4$	7786-81-4	0.3793%
	HP 6 (sum)	H331	3.50%	Nickel dichloride	$NiCl_2$	7718-54-9	1.5853%
	HP 7 (max)	H350	0.10%	Nickelous sulfate	$NiSO_4$	7786-81-4	0.0379%
	HP 10 (max)	H360	0.30%	Nickelous sulfate	$NiSO_4$	7786-81-4	0.1137%
	HP 11 (max)	H341	1.00%	Nickelous sulfate	$NiSO_4$	7786-81-4	0.3793%
	Max HP 13	H317 H334	10%	Nickelous sulfate	$NiSO_4$	7786-81-4	3.7934%
	HP 14 (sum) H400	H400	25.00%	Nickelous sulfate	$NiSO_4$	7786-81-4	9.4807%
	HP 14 (sum) H410 H411 H412	H410	0.25%	Nickelous sulfate	$NiSO_4$	7786-81-4	0.0948%
Pb	HP 5 (max)	H373	10%	Generic classification (substance not defined). Note 1	Pb		10.0000%
	HP 6 (sum)	H332	22.50%	Generic classification (substance not defined). Note 1	Pb		22.5000%
	HP 7 (max)	H350	0.10%	Only: Lead sulfochromate yellow; C.I. Pigment Yellow 34; [This substance is identified in the Colour Index by Colour Index Constitution Number, C.I. 77603.]. Note 1	Pb	1344-37-2	0.1000%
	HP 10 (max)	H360	0.30%	Generic classification (substance not defined). Note 1	Pb		0.3000%
	HP 14 (sum) H400	H400	25.00%	Generic classification (substance not defined). Note 1	Pb		25.0000%
	HP 14 (sum) H410 H411 H412	H410	0.25%	Generic classification (substance not defined). Note 1	Pb		0.2500%
Sb	HP 6 (sum)	H301	5.00%	Antimony trifluoride	SbF_3	7783-56-4	3.4058%
	HP 7 (max)	H351	1.00%	Antimony trioxide	Sb_2O_3	1309-64-4	0.8354%
	HP 8 (sum)	H314	5%	Antimony pentachloride	$SbCl_5$	7647-18-9	2.0360%
	HP 14 (sum) H410 H411 H412	H411	2.50%	Generic classification (substance not defined). Note 1	Sb	-	25.0000%
Se	HP 5 (max)	H373	10%	Generic classification (substance not defined) / Hyp. selenium dioxide	SeO_2	7446-08-4	7.1165%
	HP 6 (sum)	H300 Cat 2	0.25%	Sodium selenite	Na_2SeO_3	10102-18-8	0.1142%
	Max HP 13	H317	10%	Sodium selenite	Na_2SeO_3	10102-18-8	4.5662%
	SeO2	H400	25.00%	Generic classification (substance not defined) / Hyp. selenium dioxide	SeO_2	7446-08-4	17.7912%
	HP 14 (sum) H410 H411 H412	H410	0.25%	Generic classification (substance not defined) / Hyp. selenium dioxide	SeO_2	7446-08-4	0.1779%
	HP 14 (sum) H410 H411 H412	H411	2.50%	Sodium selenite	Na_2SeO_3	10102-18-8	1.1416%

Zn	HP 4 (sum)	H318	10%	Zinc sulphate (hydrous) (mono-, hexa- and hepta hydrate)	$ZnSO_4:7H_2O$	7446-19-7	2.2741%
	HP 6 (sum)	H302	25%	Zinc sulphate (hydrous) (mono-, hexa- and hepta hydrate)	$ZnSO_4:7H_2O$	7446-19-7	5.6851%
	HP 8 (sum)	H314	5%	Zinc chloride	$ZnCl_2$	7646-85-7	2.43986%
	HP 14 (sum) H400	H400	25.00%	Zinc sulphate (hydrous) (mono-, hexa- and hepta hydrate)	$ZnSO_4:7H_2O$	7446-19-7	5.6851%
	HP 14 (sum) H410 H411 H412	H410	0.25%	Zinc sulphate (hydrous) (mono-, hexa- and hepta hydrate)	$ZnSO_4:7H_2O$	7446-19-7	0.0569%
Minor and rare elements							
Ag	HP 8 (sum)	H314	5%	Silver nitrate	$AgNO_3$	7761-88-8	3.1750%
	HP 14 (sum) H400	H400	25.00%	Silver nitrate	$AgNO_3$	7761-88-8	15.8750%
	HP 14 (sum) H410 H411 H412	H410	0.25%	Silver nitrate	$AgNO_3$	7761-88-8	0.1588%
Be	HP 4 (sum)	H315 H319	10%	Generic classification (substance not defined) / Hyp. beryllium hydroxide	$Be(OH)_2$	13327-32-7	2.0946%
	HP 5 (max)	H372	1%	Generic classification (substance not defined) / Hyp. beryllium hydroxide	$Be(OH)_2$	13327-32-7	0.2095%
	HP 6 (sum)	H301	5.00%	Generic classification (substance not defined) / Hyp. beryllium hydroxide	$Be(OH)_2$	13327-32-7	1.0473%
	HP 7 (max)	H350	0.10%	Generic classification (substance not defined) / Hyp. beryllium hydroxide	$Be(OH)_2$	13327-32-7	0.0209%
	Max HP 13	H317	10%	Generic classification (substance not defined) / Hyp. beryllium hydroxide	$Be(OH)_2$	13327-32-7	2.0946%
	HP 14 (sum) H410 H411 H412	H411	2.50%	Generic classification (substance not defined) / Hyp. beryllium hydroxide	$Be(OH)_2$	13327-32-7	0.5237%
	HP 6 (sum)	H302	25.00%	Cobalt sulfate. Note 1	$CoSO_4$	10124-43-3	25.0000%
Co	HP 7 (max)	H350	0.10%	Cobalt sulfate. Note 1	$CoSO_4$	10124-43-3	0.1000%
	HP 10 (max)	H360	0.30%	Cobalt sulfate. Note 1	$CoSO_4$	10124-43-3	0.3000%
	HP 11 (max)	H341	1.00%	Cobalt sulfate. Note 1	$CoSO_4$	10124-43-3	1.0000%
	Max HP 13	H317 H334	10%	Cobalt sulfate. Note 1	$CoSO_4$	10124-43-3	10.0000%
	HP 14 (sum) H400	H400	25.00%	Cobalt sulfate. Note 1	$CoSO_4$	10124-43-3	25.0000%
	HP 14 (sum) H410 H411 H412	H410	0.25%	Cobalt sulfate. Note 1	$CoSO_4$	10124-43-3	0.2500%
Li	HP 8 (sum)	H314	5%	Lithium (element)	Li	7439-93-2	5.0000%
Sn	HP 8 (sum)	H314	5%	Tin tetrachloride; stannic chloride	$SnCl_4$	7646-78-8	2.2781%
	HP 14 (sum) H410 H411 H412	H412	25%	Tin tetrachloride; stannic chloride	$SnCl_4$	7646-78-8	11.39%
Tl	HP 4 (sum)	H315	20%	Dithallium sulphate; thallic sulphate	Tl_2SO_4	7446-18-6	16.1944%
	HP 5 (max)	H372	1%	Dithallium sulphate; thallic sulphate	Tl_2SO_4	7446-18-6	0.8097%
	HP 5 (max)	H373	10%	Generic classification (substance not defined) / Hyp. thallium(III) oxide	Tl_2O_3	7446-18-6	8.9492%
	HP 6 (sum)	H300 Cat2	0.25%	Dithallium sulphate; thallic sulphate	Tl_2SO_4	7446-18-6	0.2024%
	HP 14 (sum) H410 H411 H412	H411	2.50%	Generic classification (substance not defined) / Hyp. thallium(III) oxide	Tl_2O_3	-	2.2373%

U	HP 5 (max)	H373	10%	Generic classification (substance not defined) / Hyp. uranium oxide	UO_2		8.8150%
	HP 6 (sum)	H300 Cat2	0.25%	Generic classification (substance not defined) / Hyp. uranium oxide	UO_2		0.2204%
	HP 14 (sum) H410 H411 H412	H411	2.50%	Generic classification (substance not defined) / Hyp. uranium oxide	UO_2	-	2.2038%

TABLE 4: Synthesis of Concentration limits (CL) expressed in element for 12 heavy metals and metalloids by "worst case with information" approach (blank : not hazardous for this HP; "Note 1": the concentration limit applies to the element; the lowest CL by element is colored): if the total concentration of the element is lower than CL min (penultimate column), the waste is not hazardous by that element.

CL min (%) / Elts	HP 4	HP 5	HP 6	HP 7	HP 8	HP 10	HP 11	HP 13	HP 14 ΣH400	HP 14 Σ100*H410+ 10*411+ 412	HP 14 Σ100*H410+ 10*411+ 412	CL min (%)	Corresponding substance
	Sum	Max	Sum	Max	Sum	Max	Max	Max	Sum	Sum	Sum		
Cut-off value (%)	1		0.1/1		1				0.1	0.1 (H410)	1 (H411)		
As			0.1893	0.0528	3.7870	0.0648			25.0000	0.2500		0.0528	Generic. Note 1
Ba			3.2975									3.2975	$BaCl_2$
Cd		0.5392	0.2696	0.0539		0.1618	0.0539		25.0000	0.2500		0.0539	$CdSO_4$
Cr VI	5.3552	0.3970	0.1985	0.0268	1.9848	0.1191	0.0268	2.6776	6.6940	0.0669		0.0268	Na_2CrO_4
Cu	5.0905		6.3631						6.3631	0.0636 → 0.1		→ 0.1000	$CuSO_4.5H_20$
Hg	17.2440	0.7578	0.2500		3.7889	0.3000	0.7578		25.0000	0.2500		0.2500	Generic. Note 1
Mo				0.6665								0.6665	MoO_3
Ni	3.2126	0.3793	1.5853	0.0379		0.1138	0.3793	3.7934	9.4807	0.0948 → 0.1		0.0379	$NiSO_4$
Pb		10.0000	22.5000	0.3000		0.3000			25.0000	0.2500		0.3000	Generic. Note 1
Sb			3.4058	0.8354	2.0360						2.5000	0.8354	Sb_2O_3
Se		7.1165	0.1142					4.5662	17.7912	0.1779	1.1416	0.1142	Na_2SeO_3
Zn	2.2741		5.6851		2.3986				5.6851	0.0569 → 0.1		→ 0.1000	$ZnSO_4.7H_2O$

in the European document. For alkaline waste, the most frequently relevant substances are NaOH (H314-1A in the CLP, cut-off value 1%, HP 4 if sum ≥ 1% and HP 8 if sum ≥ 5%) and $CaO/Ca(OH)_2$ (H315 in the ECHA declaration system, cut-off value 1%, HP 4 if sum ≥ 20%). Practically, the concentration of (totally soluble) NaOH in the waste can be assessed by the concentration of leachable Na and the pH of the leachate. The concentration of $CaO/Ca(OH)_2$ must be measured by a dedicated analysis (see Chapter 5 Speciation). If the pH of the leachate is ≥ 11.5, these analyses should be used to correctly assess HP 4. Speciation of Ni and Zn in substances should also be performed for HP 4 and HP 8. If either Ni or Zn is the only element with HSC H314 1A, 1B and 1C, H315, H318 and H319 in the waste, concentration of Table 3 can be used. Otherwise, the sum of concentrations of substances must be used (Table 1).

6.2.2 By list: HP 9 'Infectious'

It is suggested to use the UN ADR list of infectious organisms, or the origin of the waste, or an expert judgment (ADR 2014). A technical report is available (Hennebert 2017).

6.2.3 By test: HP 12 'Release of an acute toxic gas"

The definition of HP 12 is that waste contains substances with HSC EUH029, EUH031 and EUH032. These (very) reactive substances are not analyzed in routine environmental laboratories. Therefrom, the following method is proposed (Hennebert et al. 2016a):

1. Measure the volume of gases emitted into contact with water or an acid (automated calcimeter in 5 min, solid/liquid ratio of 10 l/kg, acid 2.5 M HNO_3). The limit of quantification has been found at INERIS to be 0.1 liter of gas per kg of raw waste in 5 minutes;
2. If gas is emitted beyond that limit, check if one of the following gases is emitted: HCN, HF, PH_3, H_2S, SO_2, HCl and Cl_2 with detection probes or simple qualitative colorimetric methods;
3. If one of these gases is detected, specify the emitting substances (either by direct method if they are in high concentration or by calculation by the "worst case" method if they are in low concentrations, or by specific methods) and check whether they have a hazard statement code EUH029, EUH031 or EUH032, or alternatively check if the waste is likely to contain substances with these HSC (list in the publication).

6.3 Ecotoxicity

6.3.1 By calculation: HP 14 'Ecotoxic'

The calculation formulas are presented in Table 1.

TABLE 5: Hazard property by POP substances (EC 2008 and updates).

Substance	CAS No	EC No	Waste hazardous if concentration > CL (2014/ 955/ UE)	Concentration limit of the POP regulation
Polychlorinated dibenzo-p-dioxins and dibenzofurans (PCDD/PCDF)			X	15 µg/kg (= 0.0000015%) (Toxicity Equivalent Factors for congeners in the POP regulation)
DDT (1,1,1-trichloro-2-2-bis(4-chloro-phenyl)ethane)	50-29-3	200-024-3	X	50 mg/kg (= 0.005%)
Chlordane	57-74-9	200-349-0	X	50 mg/kg (= 0.005%)
Hexachlorocyclohexanes, including lindane	58-89-9 319-84-6 319-85-7 608-73-1	210-168-9 200-401-2 206-270-8 206-271-3	X	50 mg/kg (= 0.005%)
Dieldrine	60-57-1	200-484-5	X	50 mg/kg (= 0.005%)
Endrine	72-20-8	200-775-7	X	50 mg/kg (= 0.005%)
Heptachlore	76-44-8	200-962-3	X	50 mg/kg (= 0.005%)
Hexachlorobenzene	118-74-1	200-273-9	X	50 mg/kg (= 0.005%)
Chlordecone	143-50-0	205-601-3	X	50 mg/kg (= 0.005%)
Aldrine	309-00-2	206-215-8	X	50 mg/kg (= 0.005%)
Pentachlorobenzene	608-93-5	210-172-5	X	50 mg/kg (= 0.005%)
Polychlorobiphenyles (PCB)	1336-36-3 and others	215-648-1	X	50 mg/kg (= 0.005%)
Mirex	2385-85-5	219-196-6	X	50 mg/kg (= 0.005%)
Toxaphene	8001-35-2	232-283-3	X	50 mg/kg (= 0.005%)
Hexabromobiphenyle	36355-01-8	252-994-2	X	50 mg/kg (= 0.005%)
Endosulfan	115-29-7 959-98-8 33213-65-9	204-079-4		50 mg/kg (= 0.005%)
Hexachlorobutadiene	87-68-3	201-765-5		100 mg/kg (= 0.01%)
Naphtalenes polychlores				10 mg/kg (= 0.001%)
Alkanes C10-C13, chloro (short-chain chlorinated paraffins) (SCCPs)	85535-84-8	287-476-5	Lower CL by HP14 H410: 0.25%	10 000 mg/kg (= 1%)
Tetrabromodiphenylether $C_{12}H_6Br_4O$				Σ tetra-. penta-. hexa- et hepta-BDE: 1 000 mg/kg (= 0.1%)
Pentabromodiphenylether $C_{12}H_5Br_5O$				
Hexabromodiphenylether $C_{12}H_4Br_6O$				
Heptabromodiphenylether $C_{12}H_3Br_7O$				
Decabromodiphenylether - Bis(penta-bromophenyl) ether	1163-19-5	214-604-9	Decision in 2019	1 000 mg/kg for products (EU 2017b)
Perfluorooctane sulfonic acid and its derivatives (PFOS) $C_8F_{17}SO_2X$ (X = OH, Metal salt (O-M +), halide, amide, and other derivatives including polymers)	1763-23-1 [1] 2795-39-3 [2] 70225-14-8 [3] 29081-56-9 [4] 29457-72-5 [5]	217-179-8 [1] 220-527-1 [2] 274-460-8 [3] 249-415-0 [4] 249-644-6 [5]		50 mg/kg (= 0.005%)
Hexabromocyclododecane (HBCDD) 'Hexabromocyclododecane' means: HBCDD, 1,2,5,6,9,10-HBCDD and its main diastereoisomers: alpha- HBCDD; beta-HBCDD; and gamma- HBCDD	25637-99-4 3194-55-6 134237-50-6 134237-51-7 134237-52-8	247-148-4 221-695-9		1 000 mg/kg (= 0.1%). Subject to review by the Commission by 20.4.2019
Candidate POP: Dicofol	115-32-2	204-082-0		
Candidate POP: Pentadecafluoroctano-ic acid (perfluorooctanoic) (PFOA), its salts and derivatives	335-67-1	206-397-9		
Candidate POP: Perfluorohexane sulfonic acid (PFHxS), its salts and derivatives	355-46-4	206-587-1		

TABLE 6: Tests for HP 1, HP 2, HP 3.

H properties	Definition of "product"	Methods
H1 Explosive	Substances and preparations which may explode under the effect of flame or which are more sensitive to shocks or friction than dinitrobenzene	EC Method A14: thermal and mechanical sensitivities (impact and friction)
H2 Oxidizing	Substances and preparations which, in contact with other substances, particularly flammable substances, present a highly exothermic reaction	Gas: Method ISO 10156 (paragraph 5) Liquids: UN O2 test (liquid oxidizers) Solids: UN test O1 (oxidizing solids)
H3-A Highly flammable	Substances and preparations: in liquid form, with a flash point below 21°C, or	EC method A9
	which may become hot and finally catch fire in air at ambient temperature without any input of energy, or	Test UN N2 (pyrophoric solids) or UN N3 (pyrophoric liquids) and UN N4 (solid, self-heating)
	In the solid state, which may readily catch fire after brief contact with a source of ignition and which continue to burn or to be consumed after removal of the source of ignition, or	Test UN N1 (flammable solids)
	in the gaseous state, which are flammable in air at normal pressure, or	A11 EC method or a method of ISO 10156 (paragraph 4) standard
	which, in contact with water or damp air, evolve highly flammable gases in hazardous quantities.	Test UN N5 (substances which, in contact with water, emit flammable gases)
H3-B Flammable	Liquid substances and preparations having a flash point equal to or greater than 21°C and less than or equal to 55°C	EC method A9

Discussion on calculation methods

The method does not include the multiplier of concentration of substances with H400 and H410 hazard statement codes of the CLP (M factors), developed by classificators of products to fine tune the calculated ecotoxicity of mixtures with the most ecotoxic substances (CLP 2008). This multiplier (10, 100, 1000…) depends on the ecotoxicological effects of pure substances observed in ecotoxicological laboratory tests for substance classification. The method with M factors (CLP method limited to the level 1 and 2 of chronic ecotoxicity) has the best correspondence (80%) with the European List of Waste (Hennebert et al. 2014, 2016b, MEEM 2015). The list of harmonized M-factors is continuously completed (for instance 10 M-factors for copper in ATP9 of CLP (EU 2016)). Some classification of waste with the two methods are presented in Table 7. This point is raised because discrepancies occur when some waste become products in the circular economy and vice-versa (examples in Table 7). Without M factors, the sum of acute ecotoxic substances H400 must reach 25% of the waste, and the waste will almost never be ecotoxic acute. The rule that classifies waste is that of chronic ecotoxicity.

Attribution of an ecotoxicity hazard statement code H400 and H410 to H413 to an element

To avoid speciation hypothesis and to attribute an HSC to an element in a waste (whatever is/are the substance(s) of the element), a simple method is to compare the leachable fraction of this element to the lowest published EC_{50} (concentration producing 50% of biological effect in acute/short term tests) or NOEC (no-observed effect concentration in chronic/longer term tests) of that element. The ECHA Guidance document states that: "IV.2.3 Comparison of aquatic toxicity data and solubility data - A decision on whether or not the substance is classified will be made by comparing aquatic toxicity data and solubility data." (page 586 of ECHA 2017). The measured solubility of an element from a substance is compared with published ecotoxicological data of the same (dissolved) element (USEPA data base, INERIS portal, list for common elements and corresponding HSC in Hennebert et al. 2014). If the soluble concentration of the element from the unknown substance(s) is lower than the classifying EC_{50} or NOEC of that dissolved element, that substance is not ecotoxic. If it is higher, the element is ecotoxic, and an HSC can be attributed to the unknown substance(s) of this element, according to the CLP rules (see Table 4.1.0 of the CLP, not presented here). The total concentration of the element (and not only the leachable concentration! See for instance CEWEP 2017) must be used in the HP 14 calculation. This approach has been proven to be consistent for a large set of waste with the European List of Waste classification and the calculation method with M-factors (Hennebert et al. 2016b). Tables of lowest EC_{50} and NOEC are supplied in this later paper.

Bioavailability

The assessment of waste should consider the bioavailability of the substances (EU 2017, 2018). According to ECHA guideline: "In general, there are no specific environmental test methods developed to measure biological availability of substances or mixtures." (ECHA 2017). Bioavailability of elements and substances of waste is not limited to the leachable fraction: ingestion, inhalation, dermal contact are significant routes of exposure. The bioavailable fraction is not measurable. It seems today that the best method to assess bioavailability is to use a battery of biotests (Table 8).

Classification by calculation with leachable concentrations instead of total concentrations

The principle is to calculate the sum of ecotoxic substances using leachable concentrations, rather than total concentrations. Leachable concentrations of metals are

TABLE 7: Waste less severely and more severely classified without multiplying factors of concentration of substances with H400 and H410 hazard statement codes for HP 14 'Ecotoxic' chronic by calculation.

Chronic ecotoxicity	Concentration limits		Hazard HP14 vs CLP	Example of elements (« worst case with information ») or substance
M-factor	HP14: hazardous if ∑ [(100 * H410) + (10 * H411) + (H412)] ≥ 25%	CLP chronic 2: hazardous if ∑ [(10 * M * H410) + (H411)] ≥ 25%		
1 or no M	0.25% = 2 500 mg/kg	2.5% = 25 000 mg/kg	Overestimated by factor 10	Waste with Ag, Mn, Ni Plastics with brominated flame retardants
10	0.25% = 2 500 mg/kg	0.25% = 2 500 mg/kg	Equal	Waste with As, Co, Cr(VI), Cu, Pb, Se, Zn Waste with some PAH: anthracene, benzo(k) fluoranthene, fluoranthene, pyrene
100	0.25% = 2 500 mg/kg	0.025% = 250 mg/kg	Underestimated by factor 10	Waste with Cd, Hg Waste with PAH benzo(g,h,i)perylene Packaging and plastics with pesticide
1000 - 1000000	0.25% = 2 500 mg/kg	0.0025% = 25 mg/kg	Underestimated by factor 100…100000	Packaging and plastic with pesticide (i.e. chlorpyrifos M = 1 000 000)

TABLE 8: Proposed Biotest battery for HP 14 with validated concentration limits (CL) based on a set of non-hazardous and hazardous waste according to the European List of Waste (sample preparation EN 15002, EN 14735 without pH neutralization of the leachate).

Test	Standard	Expression of results of the test: Concentration of waste generating 50% effect (EC_{50})	Duration	CL (in fraction of waste in the respective dilution medium): The waste is hazardous if measured EC_{50} < CL
Aquatic tests (liquid waste or leachate of solid waste)				
Inhibition of the light emission of *Vibrio fischeri* (Luminescent bacteria test)	EN ISO 11348-3 (2007)	Eluate concentration which results in 50% inhibition of light emission (EC_{50})	30 min	EC_{50} < 15.8% rounded 15%
Freshwater algal growth inhibition test with *Pseudokirchneriella subcapitata*	EN ISO 8692 (2012)	Eluate concentration which results in 50% inhibition of population growth (EC_{50})	72 hours	EC_{50} < 7.03% rounded 10%
Inhibition of the mobility of *Daphnia magna*	EN ISO 6341 (2012)	Eluate concentration which results in 50% inhibition of mobility (EC_{50})	48 hours	EC_{50} < 7.95% rounded 10%
Terrestrial tests (solid waste)				
Soil contact test with *Arthrobacter globiformis*	ISO 18187 (2014)	Waste concentration which results in 50% inhibition of enzyme activity (EC_{50})	6 hours	EC_{50} < 2.25% rounded 5%
Effects of chemicals on the emergence and growth of higher plants (*Brassica rapa*)	EN ISO 11269-2 (2012)	Waste concentration which results in 50% inhibition of growth (EC_{50})	14 days	EC_{50} < 13.7% rounded 15%
Avoidance test with earthworms (*Eisenia fetida*)	ISO 17512-1 (2007)	Waste concentration which affects behavior by 50% (EC_{50})	48 hours	EC_{50} < 3.75% rounded 5%

typically 1/100 to 1/1000 of the total concentrations. This method classified 0 sample hazardous from 19 different waste, while the method with M factors classified 12 samples hazardous (Hennebert et al. 2014). A similar result has been found by ECN for incinerator bottom ashes (CEWEP 2017): the 95th percentile of a set of bottom ashes was found not ecotoxic based on the leaching concentration, and ecotoxic based on the total content. Furthermore, the leaching concentrations were lower than the cut-off values (CEWEP 2017).

6.3.2 By tests: HP 14 'Ecotoxic'

It is recognized that test results prevail on calculation results (EU 2017a, EU 2018), due to not-enough-detailed chemical analysis, unknown antagonist or synergic effects, unknown speciation, unknown bioavailability, and so on. An additional reason is that the current calculation formula for waste do not use the M factors. No harmonized test battery is available at EU level. Building on a very large inter-laboratory trial in 2006 (Moser and Römbke 2009, Moser and Kessler 2009, Moser et al. 2010), French and German experts have suggested a test battery (Pandard and Römbke 2013), now without options and with validated concentration limits (Hennebert 2018) (Table 8). Concentration limits are based on a reference: it is not possible to assess "ex nihilo" the hazardousness or not of a given biological effect. Educated guess by experts has not produced a consensus on that topic since the '90s (Hennebert 2018). The proposed concentrations limits are simply the highest ecotoxic effect observed in a set of 10 waste non-hazardous by the European list of waste (taken as the reference) and well-studied from Belgium, France and Germany. They have correctly classified 13 hazardous waste by list as ecotoxic. Hence, these limits are validated by 23 waste from 3 countries. They can be improved, as more data of H or non-H by list (in particular from the Member States of the EU) are available.

Discussion on neutralization of leachate of acid or alkaline waste before dilution and testing, or for some dilutions

EN 14735:2006 "Characterization of waste - Preparation of waste samples for ecotoxicity tests" states at section 10.5 pH: "Tests shall be carried out without pH adjustment of the test portion. pH of all test mixtures is measured at the beginning and at the end of the test and reported." And in a note (non-normative): "If toxic effects are observed in the dilutions where pH is not compatible with the survival of the organisms, the test(s) can be repeated with pH adjustment of the test portion." As most elements (in particular in equilibrium with a solid phase) are more soluble in acid and alkaline pH domains (for instance CEWEP 2017), the pH neutralization (for some dilutions of the test portion or for the whole test portion) precipitates a significant part of the elements (for instance Nilsson et al. 2016) and reduce ecotoxicity beyond the effect of $[H^+]$ or $[OH^-]$ concentrations. The classification of waste for the hazard property HP 14 'Ecotoxic' is weakened: experimental data show that neutralization of the leachate before dilution deletes ecotoxicity, even when the final pH of the different mixtures of culture medium and waste leachate is the same. The effects are less if only the ecotoxic dilutions are neutralized (and not the original leachate). Additional neutralization of leachates removes ecotoxicity, beyond the ecotoxicity of H^+ and OH^-. It should be noted that the culture media that is mixed with the waste leachate at different dilutions for the test (the result of the test is a dose/response relationship) is buffered for acid/base concentrations. The test battery has been developed since 2006 without pH neutralization of the leachate.

To reduce ecotoxicity for beneficial use, prior to reuse or storage in contact with natural environment, the waste flow (and not the laboratory waste leachate) should be pre-treated. For acidic waste (like waste containing sulphide that oxidize to sulfuric acid in contact with air), input of alkalinity (eventually with waste like concrete) is necessary. For alkaline waste, a simple solution is to let them freely evolve by natural carbonation with atmospheric CO_2, to reach the desired pH, like the "maturation" of the municipal solid waste incinerator bottom ashes. If the soluble alkalinity in the waste is sodic or potassic, soluble calcium (like synthetic gypsum from desulfurization of fumes of coal power plants) must be added. The soluble alkalinity will precipitate as calcium carbonate, and the pH of the liquid phase will be about 8.5 when the reaction is completed.

6.4 Capable of exhibiting a hazardous property not displayed by the original waste

Aside the presence of some very specific heating or explosive substances in confined environments with specific HSC (EU 2018), this HP needs a specific study. Waste with reduced substances that can oxidize with detrimental environmental effects (sulphidic ores unbalanced by alkalinity, producing sulfuric acid and dissolving mined elements, acid mine drainage), substances that can be liberated by anaerobic biodegradation of organic matter (decay of marine algae producing toxic H_2S) or on the long term by weathering of minerals, should be considered. The presence of sulphide and alkalinity can be assessed by EN 15875. It should be noted that "acid-generating tailings from processing of sulphide ore" are a hazardous entry in the European List of Waste (01 03 04*; "*" means hazardous in the list).

7. CONCLUSIONS

A complete set of practical methods is now available for a proper classification of waste, becoming more important as loops of material are increasingly created in the circular economy. Experience has shown that unexpected substances can be detected by the methods expounded here, allowing a better management of matters and materials.

A novel approach for speciation of elements into substances based on "worst case with information" of the physico-chemical characteristics of the waste, as a first step for classification, has been suggested. This method makes it possible to immediately identify the elements that cannot classify the waste as hazardous and thus to concentrate the classifier's efforts on the elements that can classify as hazardous.

Finally, the identification of the hazard helps waste producers, waste managers and public authorities to manage hazardous waste by controlling the risk of their reuse or recycling for people, infrastructures, and the environment.

REFERENCES

ADR 2014. United Nations - The European Agreement on the International Transport of Dangerous Goods. The European Agreement on the International Transport of Dangerous Goods, Volume I. 1254 p. http://www.unece.org/fileadmin/DAM/trans/danger/publi/adr/adr2015/ADR2015e_WEB.pdf

AFNOR FD X30-494:2015. Abdelghafour M, David F, Domas J, Gemise-Fareau C, Hennebert P, Humez N, Laborde E, Louchez G, Piantone P, Rebischung F, Vernus E. 2015. Caracterization of waste – Speciation of elements in waste (in French). 19 p.

AFNOR X30-489:2013. Characterization of waste – Determination of the content of elements and substances in waste. AFNOR, France.

CEN/TR 15310-1 to -5:2007. Characterization of waste – Sampling of waste material. CEN, Brussels, Belgium.

CENELEC CLC/TS 50625-3-1:201.5 Requirements for collection, logistics and processing for Waste Electrical and Electronic Equipment (WEEE) - Part 3-1: Specifications for depollution – Overview. CENELEC, Brussels, Belgium.

CENELEC CLC/TS 50625-3-1:2015 Requirements for the collection, logistics and treatment of WEEE - Part 3-1: Specification relating to depollution - General. CENELEC, Brussels, Belgium.

CEWEP 2017. Guidance document on hazard classification of MSWI bottom ash. ECN May 2017 ECN-E–17-024. Klymko T, Dijkstra JJ, van Zomeren A. 37 p. http://www.cewep.eu/wp-content/uploads/2017/09/ecn-e-17-024_guidance_document_on_eu_mswi_ba_hazard_classification.pdf

CLP 2008. Regulation (EC) n° 1272/2008 of the European parliament and of the Council of 16 December 2008 on classification, labelling and packaging of substances and mixtures, amending and repealing Directives 67/548/EEC and 1999/45/EC, and amending Regulation (EC) No 1907/2006. 31.12.2008. Official Journal of the European Union L 353/1. Last update https://echa.europa.eu/fr/regulations/clp/legislation

EC 2008. Regulation (EC) No 850/2004 of the European parliament and of the Council of 29 April 2004 on persistent organic pollutants and amending Directive 79/117/EEC. Official Journal of the European Union, L 158, p. 7, 30.4.2004, last amended Commission Regulation (EU) 2016/460 of 30 March 2016, Official Journal of the European Union, L 80, p. 17, 31.3.2016. https://eur-lex.europa.eu/legal-content/EN/TXT/PDF/?uri=CELEX:32004R0850&rid=1

ECHA 2017. Guidance on the Application of the CLP Criteria Guidance to Regulation (EC) No 1272/2008 on classification, labelling and packaging (CLP) of substances and mixtures Version 5.0 July 2017. 647 p. https://echa.europa.eu/guidance-documents/guidance-on-clp

EN 12457-2:2002. Characterization of waste – Compliance test for leaching of granular waste materials and sludges – Part 2: One stage batch test at a liquid to solid ratio of 10 l/kg for materials with particle size below 4 mm (without or with size reduction). CEN, Belgium.

EN 12766-1: Petroleum products and waste oils - Determination of PCBs and related products - Part 1: Separation and determination of a selection of PCB congeners by gas chromatography (GC) with use of a capture detector Electrons (ECD). CEN, Belgium.

EN 12766-2: Petroleum products and waste oils - Determination of PCBs and related products - Part 2: Calculation of polychlorinated biphenyls (PCBs) content. CEN, Belgium.

EN 14735:2006. Characterization of waste - Preparation of waste samples for ecotoxicity tests. CEN, Belgium.

EN 14899:2015. Characterization of Waste — Sampling of waste materials — Framework for the preparation and application of a Sampling Plan. CEN, Belgium.

EN 15002:2015. Characterization of waste — Preparation of test portions from the laboratory sample. CEN, Belgium.

EN 15192:2007. Characterization of waste and soil - Determination of chromium (VI) in solid materials by alkaline digestion and ion chromatography with spectrophotometric detection. CEN, Belgium.

EN 15875:2011. Characterization of waste - Static test for the determination of the acid generation potential and the neutralization potential of sulphide waste. CEN, Belgium.

EN 16377: 2013. Characterization of waste — Determination of brominated flame retardants (BFR) in solid waste. CEN, Brussels, Belgium.

EN 62321-6: 2015. Determination of certain substances in electrotechnical products – Part 6: Polybrominated biphenyls and polybrominated diphenyl ethers in polymers by gas chromatography-mass spectrometry (GC-MS). CEN, Brussels, Belgium.

EU 2014a. Commission Decision 2014/955/EU of 18 December 2014 amending Decision 2000/532/EC on the list of waste pursuant to Directive 2008/98/EC of the European Parliament and of the Council. Official Journal of the European Union. 30.12.2014. L 370/44. https://eur-lex.europa.eu/legal-content/EN/TXT/PDF/?uri=CELEX:32014D0955&rid=1

EU 2014b. Commission Regulation (EU) No 1357/2014 of 18 December 2014 replacing Annex III to Directive 2008/98/EC of the European Parliament and of the Council on waste and repealing certain Directives. Official Journal of the European Union. 19.12.2014. L 365/89. https://eur-lex.europa.eu/legal-content/EN/TXT/PDF/?uri=CELEX:32014R1357&rid=1

EU 2016. ATP 9: Commission Regulation (EU) 2016/1179 of 19 July 2016 amending, for the purposes of its adaptation to technical and scientific progress, Regulation (EC) No 1272/2008 of the European Parliament and of the Council on classification, labelling and packaging of substances and mixtures. http://eur-lex.europa.eu/legal-content/EN/TXT/?uri=uriserv:OJ.L_.2016.195.01.0011.01.ENG&toc=OJ:L:2016:195:TOC

EU 2017a. Council Regulation (EU) 2017/997 of 8 June 2017 amending Annex III to Directive 2008/98/EC of the European Parliament and of the Council as regards the hazardous property HP 14 'Ecotoxic'. Official Journal of the European Union. 14.6.2017. L 150/1. https://eur-lex.europa.eu/legal-content/EN/TXT/PDF/?uri=CELEX:32017R0997&rid=1

EU 2017b. Commission Regulation (EU) 2017/227 of 9 February 2017 amending Annex XVII to Regulation (EC) No 1907/2006 of the European Parliament and of the Council concerning the Registration, Evaluation, Authorisation and Restriction of Chemicals (REACH) as regards bis(pentabromophenyl)ether. Official Journal of the European Union. 10.2.2017. L35/6. https://eur-lex.europa.eu/legal-content/EN/TXT/PDF/?uri=CELEX:32017R0227&rid=1

EU 2018. European Commission. Commission notice on technical guidance on the classification of waste (2018/C 124/01). OJEU 9.4.2018. 134 p.https://eur-lex.europa.eu/legal-content/EN/TXT/PDF/?uri=CELEX:52018XC0409(01)&qid=1530609217830&from=EN

Hennebert P, Humez N, Conche I, Bishop I, Rebischung F. 2016b. Assessment of four calculation methods proposed by the EC for waste hazard property HP 14 'Ecotoxic'. Waste Management 48 (2016) 24–33.

Hennebert P, Papin A, Padox J-M. 2013. The evaluation of an analytical protocol for the determination of substances in waste for hazard classification. Waste Management 33 (2013) 1577–1588

Hennebert P, Samaali I, Molina P. 2016a. A proposal for a test method for assessment of hazard property HP 12 ("Release of an acute toxic gas") in hazardous waste classification – Experience from 49 waste. Waste Management 58, 25–33. 2016

Hennebert P, van der Sloot H, Rebischung F, Weltens R, Geert L, Hjelmar O. 2014. Classification of waste for hazard properties according to the recent propositions of the EC using different methods. Waste Management 34 (2014) 1739–1751.

Hennebert P. 2017. Evaluation de la propriété de danger des déchets HP 9 'Infectieux' : Etat sommaire des méthodes existantes et propositions de méthode. Rapport INERIS DRC-16-159393-07763A. 15/06/2017. 50 p. Available upon request.

Hennebert P. 2018. Proposal of concentration limits for determining the hazard property HP 14 for waste using ecotoxicological tests. Waste Management 74, April 2018, Pages 74-85.

Hennebert P. 2019. Sorting of waste for circular economy: sampling when (very) few particles have (very) high concentrations of contaminant or valuable element (with bi- or multi-modal distribution). 17th International Waste Management and Landfill Symposium (Sardinia 2019), 30/09 – 04/10/2019, Cagliari, Italy

MEEM 2015. (French Ministry for Environment). Contribution of France to the « Study to assess the impacts of different classification approaches for hazard property « H14 » on selected waste streams ». Van Heeswyck E, Hennebert P, Rebischung F, Pandard P. http://ec.europa.eu/environment/waste/studies/pdf/hazard%20property%20annex%206.pdf

Moser, H., Kessler, H., 2009. Ecotoxicological characterization of waste as an instrument in waste classification and risk assessment. Chap 29 of In: Moser, H., Römbke, J. (Eds.), 2009. Ecotoxicological characterization of waste – results and experiences from an international ring test. Springer, New York, USA, pp. 281– 290.

Moser, H., and Römbke, J. (Eds), 2009. Ecotoxicological characterization of waste - Results and experiences of a European ring test. Springer Ltd.,NewYork, USA. 308 pp. All results and raw data at http://ecotoxwasteringtest.uba.de/h14/index.jsp

Moser, H., Römbke, J., Donnevert, G., Becker, R., 2010. Evaluation of biological methods for a future methodological implementation of the Hazard criterion H14 'ecotoxic' in the European waste list (2000/532/EC). Waste Manage. Res. 29 (2), 180–187.

Nilsson, M., L. Andreas, A. Lagerkvist. Effect of accelerated carbonation and zero valent iron on metal leaching from bottom ash. Waste Management 51 (2016) 97–104.

Norden 2015. Nordic Council of Ministers 2015. Hazardous waste classification - Amendments to the European Waste Classification regulation -what do they mean and what are the consequences? Wahlström W, Laine-Ylijoki J, Wik O, Oberender A, Hjelmar O. TemaNord 2016:519, ISSN 0908-6692, 123 p.

NRW et al 2018. Natural Resources Wales, Scottish Environment Protection Agency, Northern Ireland Environment Agency, Environment Agency 2018. Technical Guidance WM3. Waste Classification - Guidance on the classification and assessment. 181 p. https://www.gov.uk/government/publications/waste-classification-technical-guidance

Pandard P, Römbke J. 2013. Proposal for a "Harmonized" Strategy for the Assessment of the HP 14 Property, Integrated Environmental Assessment and Management — Volume 9, Number 4—pp. 665–672.

XP CEN/TS 15364:2006. Characterization of waste - Acid and basic neutralization capacity test. CEN, Belgium.

XP CEN/TS 16660:2015. Characterization of waste - Determination of reducing properties and reducing capacity. CEN, Belgium.

detritus | Multidisciplinary Journal for Waste Resources & Residues

CISA

THE SOCIAL, ENVIRONMENTAL AND ECONOMIC BENEFITS OF REUSE BY CHARITY SHOPS

Robin Osterley [1] and Ian Williams [2,*]

[1] *Charity Retail Association, 4th Floor, 356 Holloway Road, N7 6PA, London, United Kingdom*
[2] *University of Southampton, Faculty of Engineering and Physical Sciences, SO17 1BJ, Southampton, United Kingdom*

Article Info:
Received:
18 July 2018
Revised:
31 May 2019
Accepted:
16 July 2019
Available online:
26 September 2019

Keywords:
Charity shops
Reuse
Social
Environmental
Economic
Circular economy

ABSTRACT

Charity shops are retail outlets selling mainly second-hand donated goods to raise funds for their parent charities. The charity retail sector is becoming an increasingly significant player in terms of demonstrating the benefits of reuse and how it can be practically realised. This paper provides an overview of the UK's charity retail sector and considers the social, environmental and economic benefits of charity shops. We estimate there are 11,200 charity shops in the UK that employ 23,000 staff and have a volunteer workforce of 230,000. Approximately 95% of the clothes charity shops receive are either recycled or reused, diverting 331,000 tonnes of textiles from landfill and reducing CO_2 emissions by 6.9 million tonnes in 2015/16. A key factor in understanding how charity shops contribute to social good includes understanding and quantifying how they might contribute to the development of the circular economy via the encouragement and practical realisation of reuse. We see this paper as a step in this process, flagging the social, environmental and economic benefits of charity shops and highlighting the need for additional research into the contribution of the charity retail sector to reuse and resource preservation/recovery.

1. INTRODUCTION

The circular economy is a relatively new concept that has been attracting a lot of recent attention. It is becoming fashionable for industrialists, businesses and politicians to talk about "closing the loop", ensuring "resource security" and "resource efficiency", and "joining the circular economy." Reuse is an important waste prevention measure as it extends product life, deferring or even eliminating the need to extract virgin raw materials to manufacture new products. In poorer countries, repair and reuse is a way of life; they contribute significantly to poverty reduction by providing an income for substantial numbers of poor and marginalized workers (Williams and Shaw, 2017). The fact that they facilitate greater material recovery is a bonus in such societies. In developed countries, reuse via buying "second hand" or "reconditioned" was traditionally the domain of the relatively poor or young people trying to look fashionable on a miserly budget. Indeed, within the European Union (EU), there has been an increasing focus on reuse, as stated under Article 11 of the EC Directive 2008/98/EC, detailing the requirement of all member states to "take measures, as appropriate, to promote the re-use of products… by encouraging the establishment and support of reuse and repair networks" (European Parliament and the Council of the European Union, 2008). However, reuse of products has come into fashion again; people are buying items that are "pre-loved" or "pre-owned" in order to make their money go further or to get more for their money (Williams and Shaw, 2017) or to make a quasi-political statement. As an example of a relevant social trend, rising numbers of people are purchasing second hand 'vintage items' of clothing partially because brands are now weaving in inspirations from past trends - essentially reviving them or introducing them to those who have yet to experience them (Cassidy and Bennett 2012) - and partially because of increasing interest by consumers in purchasing ethically sourced items (Pookulangara and Shepard, 2013).

There are various strategies for the preservation of value of products and components upon their end of use, including: direct resale, repair, upgrade, refurbishment, remanufacturing and repurposing. Reuse via direct resale in today's society takes many different forms. Large and small scale car boot sales and flea markets have been running for many years and are still very popular today (Gregson and Crewe, 1997; Gregson et al, 2013). The UK high street is home to various stores that sell second hand items, including charity shops, large multinational companies such as Cash Converters and CEX and smaller chains or independent second-hand stores. Additionally, the Internet has served as a place to sell used items ever since its

* Corresponding author:
Ian Williams
email: idw@soton.ac.uk

Detritus / Volume 07 - 2019 / pages 29-35
https://doi.org/10.31025/2611-4135/2019.13849
© 2018 Cisa Publisher. Open access article under CC BY-NC-ND license

conception, on both a local and international scale. Amazon and eBay allow second-hand items to be sold globally, whilst Gumtree, Facebook Marketplace, Freecycle and Depop allow consumers to search their local area for used products at a lower cost. Consequently, the charity retail sector is becoming an increasingly significant player in terms of demonstrating the benefits of reuse and how it can be practically realised.

Charity shops are largely a British institution. They are retail outlets selling mainly second-hand donated goods to raise funds for their parent charities. They also function as a way of raising awareness of the parent charity. The charity shop in its contemporary form stems from efforts by charities after the Second World War to raise donations for the war effort in the United Kingdom (UK). One of the first shops was established in 1947 in Oxford, when Oxfam was overwhelmed by donations from the public in response to an appeal for aid to alleviate the post war famine in Greece. Post-1985 saw a much more rapid expansion in the number of charities with shops and the number of charity shops in the UK, as charities began to realise the significant amount of money that could be made (Horne, 2000). There is still a high level of dependence of charities upon aid from the public for survival (Gaskin, 1999). Nevertheless, the Oxfam shop on Broad Street in Oxford is still in operation today (Grimsey et al, 2013).

From its origins, the UK charity retail sector has evolved and expanded considerably. Faced with increased demand driven by the economic downturn, the rising cost of living, and a shrinking public sector, charities depend more than ever on their stores as a stable source of funding (especially unrestricted funding) for the services they provide. Yet charity shops have a value beyond fundraising for parent charities. Charity shops provide valuable reuse and recycling services and inexpensive goods to an increasingly large section of the population; six in every ten of the UK's population have purchased from a charity shop in the past year, and nearly eight in every ten have donated goods (Bartlett, 2012). Charity shops are highly prevalent and established across the UK (Hyndman and McConville, 2018).

Charity shops also provide a number of important social and economic benefits to individuals – including customers, donors or volunteers – and local communities across the UK, and are increasingly vital to Britain's struggling high streets. Long before the recent recession, the effects of rising online sales and out-of-town retail growth was adversely impacting on high streets, precipitating the disappearance of 15,000 stores from town centres between 2000 and 2009 (Portas, 2011). The state of Britain's high streets would be even worse if it were not for the presence of charity shops.

In this paper, we provide an overview of the UK's charity retail sector and consider the social, environmental and economic benefits of charity shops. We would like to acknowledge that some of the paper is drawn from reports commissioned by the Charity Retail Association from Demos (www.demos.co.uk) and published Open Access (Paget and Birdwell, 2013; Harrison-Evans, 2016).

2. THE UK'S CHARITY RETAIL SECTOR

2.1 Overview

Estimates of the numbers of charity shops in the UK are a bit unreliable since surveys are carried out infrequently. Our current estimate is around 11,200 shops in the UK: 83% in England, 9% in Scotland, 5% in Wales and 3% in Northern Ireland. There are over 400 shops in the Republic of Ireland. They are represented by the Irish Charity Shops Association (www.icsa.ie). We estimate that charity shops raise around £270 million for a range of causes each year.

There has been an increase in the number of paid staff in recent years, although the majority of people working in charity shops are volunteers. There are over a quarter of a million retail volunteers nationwide, and some shops are run entirely by volunteers.

Many people shop in charity shops because they want to support the activities of the parent charity. A growing number of people use charity shops because of the environmental and ethical benefits of the reuse of goods, rather than buying completely new goods, or dumping used goods. Indeed, sales of items brought in to charity shops have increased recently (CRA, 2018a). Other people shop in charity shops because they like the range of goods available. Many charity shops stock clothes, furnishings, crockery, CDs and DVDs that are no longer available in other stores. Many people visit charity shops to pick up retro and vintage clothing in particular. This reuse of textiles provides many positive benefits in terms of sustainability:

- The lifecycle of products is extended. This means that labour already input into producing existing goods is not wasted (Castellani et al. 2015);
- Less environmental damage results from collection and transport of second-hand clothing than is created by extracting virgin raw materials (Farrant et al, 2010). Approximately 95% of clothes donated to charity shops are either reused or recycled (Harrison-Evans, 2017). It was estimated that, in 2016/17, 323,000 tonnes of textiles were diverted from landfill after being donated to charity shops, which reduced CO_2 emissions by around 6.8 million tonnes and saved councils £27 million in landfill tax (CRA, 2018b);
- Relatively deprived members of society benefit from redistribution of resources (Horne, 1998, 2000; Parsons, 2002; Broadbridge and Parsons, 2003; Lovatt, 2015; Harrison-Evans, 2017; Castellani et al, 2015);
- The economy is stimulated by the provision of new job opportunities and in some cases there is a specific effort to employ disadvantaged people (Castellani et al, 2015; ReDo, n.d).

Charity shops are also popular because the prices are often lower than other shops, even commercial second-hand shops. Over 90% of goods sold in charity shops are from donations. Some shops also sell 'bought-in' goods. These are new goods which are sold for profit. The average charity shop sells around 6% new goods. Many shops sell only donated goods, but others sell both bought-in and ethically produced 'fair trade' goods. A shop must sell wholly or mainly donated goods in order to retain its

status as serving a "charitable purpose"; this is crucial in terms of charitable tax relief on business rates (see below).

Most charity shops sell ladies', men's and children's clothing, books, toys, ornaments, kitchenware, dvds, music, computer games, furnishings and bric-a-brac. Some charity shops also sell furniture and electrical appliances, and some are specialist shops, such as bookshops, bridal or music.

Charity shops benefit from tax concessions under UK tax law because all the profits from a charity shop go to fund the work of the charity, which provides public benefit. Charity shops, therefore, serve a "charitable purpose". Charity shops benefit from exemption from corporation tax on profits, a zero VAT rating on the sale of donated goods and 80% mandatory non-domestic rate relief, on property taxes. This 80% relief is funded by central Government. A further 20% rate relief is available at the discretion of local authorities. Other types of business are eligible for different sorts of relief from full business rates liability; these include small business rate relief, and relief for small shops in rural settlements.

Money that has been raised goes to the parent charity, to further their charitable work. Charity shops in the UK raise money that funds medical research, overseas aid, environmental initiatives, supporting sick and deprived children, homeless people, mentally and physically disabled people, for animal welfare and for many other causes.

At their best, charity shops can provide a highly rewarding consumer experience, giving people the satisfaction of having found a desirable item, at an attractive price, while benefiting charity and the environment in the process. Of course, the quality of charity shops can vary significantly. Some still conform to the persistent stereotype of selling damp and disordered stock, but increasingly this is becoming an outdated stereotype. Charity retail today is highly professionalised: goods are clean, shops are well stocked and displays are expertly laid out, with high quality donated brand name items at affordable prices. This shift has been driven by changing consumer expectations, an increasing trend of recruiting ex-commercial retailers to work in charity retail and increased competition – with the likes of eBay, Gumtree and cash-for-clothes shops - for donations, and low-cost high street retailers for sales. There is also a general realisation that charity retail is a significant contributor to the work of charities across Britain and - indirectly - to resource preservation.

2.2 The Charity Retail Association

The Charity Retail Association has its origins in the Charities Advisory Trust (CAT) in the early 1990s. The CAT was, and still is, a group dedicated to improving the effectiveness of charities, especially in their trading and income generation dimensions, and was started in 1979 by Dame Hilary Blume. Dame Hilary responded to the large increase of charity shops in the 1980s and early 1990s by offering training sessions and advice, and it soon became clear that there was an appetite for a forum dedicated to discussing the issue of retail in the charitable environment.

Thus was born the Charity Shops Group, formed at an inaugural meeting at the National Council for Voluntary Organisations in 1992. CAT acted as the secretariat for the Group, which offered networking, lectures and seminars, working lunches and other ways of exchanging information. This proved so successful that it was decided to formalise the Group with a steering committee, whose first chair was Colin Sandford of the British Heart Foundation (BHF). At this point the Group was also starting to attract smaller charities as well as the established large retail chains such as Marie Curie, Shelter, Oxfam, British Red Cross, Help the Aged, BHF and others.

In the later 1990s, a national voice for the sector became increasingly sought after, especially to deal with issues such as business rates relief and value added tax (VAT). It was felt by the steering group that a more formal approach was now needed, and the members of the group co-funded a consultancy project whose conclusion was that, given the right business model, a formal association was sustainable and desirable and that there was considerable support within the sector to fund such an organisation. This led, in 1999, to a separation from CAT, and the formation of the new Association – the Association of Charity Shops (ACS). Its first conference, held in 2000 at Church House in Westminster, attracted around 200 delegates, and rapidly became a highly successful annual affair with a very successful trade exhibition attached. In the same year were launched the first website and the first special interest group, and the first corporate members joined. Subsequent years saw the introduction of a number of additional member services including a legal advice line, the members' area of the website, further special interest groups, and more emphasis on lobbying and advocacy work. In 2002, the prestigious Charity Retail Awards were started.

In 2004 ACS moved to share premises with the Association of Charitable Foundations in Bloomsbury in central London. The following years saw a gradual increase in the profile of ACS within government against a background of considerable growth within the association's membership, both charitable and corporate. The ACS changed its name to the Charity Retail Association (CRA) in 2013.

The CRA is now the leader of the charity retail sector in the UK, with over 75 % of the shops in the UK under its umbrella, including the 9 of the 10 largest by income generation: British Heart Foundation; Oxfam GB; Cancer Research UK; Barnardo's; Sue Ryder; Salvation Army; British Red Cross; Scope; and Marie Curie. Examples of member services that promote reuse include:

- The "Style Me in Seconds" Toolkit; this aims to create a positive image of charity shops as fun and interesting places to shop for the younger generation;
- The "Social Value" toolkit; this aims to allow the CRA to aggregate the social value created by the charity shop movement as a whole, to build a stronger evidence base to advocate on behalf of its members and to help CRA members to make this case for themselves.

3. METHODOLOGY

In 2013 (and again in 2017; see below), Demos undertook a range of quantitative and qualitative research to ex-

plore the benefits that charity shops provide, including:

- Three focus groups with experts from the charity and retail sectors, town planners and economists, and members of the public, in London and Rochdale;
- A representative survey of 2,200 members of the public - a survey of 300 charity shop managers and volunteers;
- Semi-structured interviews with charity shop managers and volunteers, independent retailers and local authority staff in six areas of the UK: Birmingham, Margate and Morpeth (England); Newport (Wales); Paisley (Scotland), Newry (Northern Ireland);
- A comprehensive review of all the available quantitative evidence from our case study areas – both local economic health indicators (including footfall, change in rental values, and vacancy rates) and trends relating to charity retail over a five year period.

During 2015 the third sector faced an unprecedented amount of criticism from a range of sources on issues such as unsolicited fundraising approaches, charity efficiency and executive pay. It was against this background that the CRA decided, in early 2016, to commission an update report from Demos, supported by the Carnegie UK Trust. This study, which provided an updated analysis of the social value created by charity shops, also employed a variety of quantitative and qualitative techniques, including:

- A survey of 650 charity shop managers and volunteers (484 managers, 192 volunteers).
- A nationally representative survey of 2,000 British citizens.
- Semi-structured interviews with senior charity retail staff, shop managers and volunteers
- An analysis of updated local economic data on the same study locations as in the 2013 report with the exception of Newry.

The work outlined in Section 4 is largely derived from Demos's studies. Details of the methods employed and the results secured are in Paget and Birdwell (2013) and Harrison-Evans (2017).

4. BENEFITS OF CHARITY SHOPS

4.1 Economic benefits

Charity retail is vital to charities' incomes and the health of the high street. While they account for only 0.39 % of UK retail sales (2013), charity shops generate as much as 18.7% of UK charities' total income. They are an important lifeline for recession-hit charities, through their fundraising and by boosting their public profile; 59% of people believed that charity shops' presence on the high street encourages people to give to charity (2013). In this respect, charity retail has taken on particular importance as a source of charitable funding. At the peak of the recession the total amount given to charity declined by 13% (NVCO, 2012) and 59% of charities reported having been affected by the downturn (NVCO, 2012).

A majority of the British public shop or donate to a charity shop every year. Polling in 2017 shows that 74% of UK adults donated to charity shops in the past 12 months, and 61% purchased at least one item from a charity shop over that same period. Although many people do so only a handful of times a year (roughly 60% of donors and shoppers donate or purchase up to five times a year), for some visiting a charity shop to drop off clothes or pick up a bargain is a regular pastime. Roughly 1 in 20 people are 'super-donors' or 'super-shoppers', doing so over 20 times a year. These donors and shoppers provide the stock and sales revenue that charity shops need. In 2015/16 charity shops generated over £270 million in profits to support the work and impact of their parent charities, equating to roughly 3% of the voluntary sector's total income. While total income generated by charity retail rose to £1.3 billion in 2015/16, because of rising costs profits fell by 9% on the previous financial year.

The charity retail sector has not been immune to the recession; it has faced the challenge of meeting increased demand with a reduced supply of donated stock, as people have been more inclined to hold on to old clothes for longer or used them to generate cash. However, in a weak economic climate charities stand only to benefit from having more income streams, and retail has proved a robust and reliable one. It is also likely that the growth and continued presence of charity shops may have maintained footfall to high streets, which are suffering from the downturn as well as the longer-term effects of seismic changes in the retail landscape. Despite improvements in the wider economy since 2013, there has been little wholesale improvement in the fortunes of the high street, with some downward pressures (particularly that from online competition) intensifying. For struggling town centres, charity shops therefore continue to play a vital role in filling otherwise vacant lots, and generating footfall to at least partially offset the departure of other businesses.

Charity shops are increasingly important for members of the public due to the increased cost of living. They provide affordable goods to people on a low income. Two-thirds of the public and over 90% of shop managers and volunteers thought their shops supplied affordable goods to people on a low income. The minimum cost of living in the UK rose by as much as 25% during the recent recession (Joseph Rowntree Foundation, 2016), and prices continue to rise at a much faster rate than wages. The impact is being felt at all levels of society, including the poorest and the so-called 'squeezed middle'. This is reflected in the steady broadening of charity shops' customer base. The A, B and C2 groups are the most likely to buy and to donate goods, challenging the view that charity shops are the preserve of any one socioeconomic group. A total of 38% of all social groups said they would be 'likely' or 'very likely' to buy second hand from charity shops as a way of saving money.

There is no evidence that charity shops are having an adverse economic impact on the high street. Specifically, an economic analysis of available data found that charity shops do not increase rents for other shops on the high street and do not prevent small and medium-sized businesses from opening on the high street. There is no evidence to suggest that the growth of charity shops is causing or facilitating high street decline.

Indeed, charity shops are stabilising the high street in a difficult economic climate and will be increasingly important to the evolution of British high streets. The town of Margate provides a clear example of the role that charity shops can play in supporting high street recovery. During the recession that started in 2008, Margate's high street suffered badly, with the town recording the worst rate of shop closures in Britain in 2009, and vacancy rates jumping to nearly 40% 2012. As vacancy rates began to spike, charity shops played a role in filling the gap, and the proportion of empty lots gradually decreased. Vacancy rates have now (2017) fallen to nearly half of their recessionary peak, and this improvement has accompanied a dramatic change in fortunes for the town, which has become an arts and culture hub, thanks in part to the opening of the gallery Turner Contemporary in 2011. Margate's cultural revival led it winning Pearlshare's award for being the best seaside town in Britain (2016) with judges praising the town's 'retro buzz'. Charity shops form a key part of this retro identity; some of the town's charity retailers have redesigned stores to emphasise a boutique or specialist offer. For example, the Pilgrim's Hospice retail chain has set up Frocks 'n' Socks, a shop stocking only vintage clothing and homeware, and Oasis, a local domestic violence charity, set up its first charity shop in 2014, designed to create a 'boutique feel', stocking 'retro-chic' clothing.

Thus, contrary to the view that they are having a negative impact locally, charity shops appear to be exerting a stabilising influence on ailing high streets as they have ensured that footfall remains steady, they cater to specific local needs, and they fill shops that would otherwise be empty. They are also preventing increases in crime and antisocial behaviour by occupying vacant premises. As the sector becomes more professional (e.g. using visual merchandising skills) and more specialised (e.g. setting up vintage boutiques or specialist music stores), charity shops are contributing to a more vibrant and eclectic retail mix on certain high streets. With charity shops increasingly providing access to services, they can potentially be leaders of the 'evolution' of the high street.

4.2 Social benefits

Charity shops provide significant benefits to individuals through opportunities for volunteering and employment. Charity shops employ an estimated 23,000 staff across the UK, and have a volunteer workforce of some 230,000. This level of employment assists the economy as well as benefiting individuals. Approximately 6% of adults (18+) have worked or volunteered in a charity shop at some point in their lives, equating to nearly 3 million people across Great Britain. Volunteers generally report being overwhelmingly happy with their role, with 93% of those surveyed (in 2017) saying that they were satisfied, and 90% saying they would recommend their organisation as a 'great place to work'. Volunteers of different ages and backgrounds get notably different benefits from their work. For example, when asked about the most significant benefit of their volunteering role, older people most commonly cite contribution to charity or the social aspects of the role, and most younger people mention work experience, and developing skills and confidence. In addition, volunteers say that they value the chance to gain retail experience as a path to paid employment or back into employment after a period of illness or injury. Charity shops provide a place for those with poor physical or mental health to interact socially and build self-esteem and are increasingly providing opportunities for people within or leaving the criminal justice system. Job seeking volunteers most commonly cite improved confidence and self-esteem as the primary benefit of their work, and significant majorities said that they had improved their communication, team-working, problem-solving, organisational and numeracy skills. Several charity retailers, particularly the larger chains, provide volunteers with an opportunity to formally recognise their new skills through a qualification. This enables volunteers to gain a National Vocational Qualification (NVQ) in retail, customer service, visual merchandising and other related areas.

Charity shops provide a space for social interaction for volunteers and members of the public, facilitating local cohesion. Charity shops combat social isolation in their local communities among volunteers and customers. Respondents to the public survey and large numbers of volunteers and staff report that older and other vulnerable people use shops to 'drop in' for a chat. One in five members of the public said they had met or talked to someone new in a charity shop, while 30% said they provided a space for social interaction, 29% said they provided a sense of community and 28% said that charity shops encouraged different generations to meet. The employees and volunteers in charity shops are overwhelmingly from the local area, and value charity shops for social interaction. Over 90% of volunteers cited 'socialising and meeting new people' as a benefit of volunteering, while one in ten cited this as the most important benefit they received from volunteering.

Charity shops are well placed to cater to the specific needs of their local community through local partnerships and access to services. Social value is most effective where it has the flexibility to be responsive to local needs. Innovative examples of effective local partnerships include South Bucks Hospice's four-way partnership with the local council, a nearby prison and a waste management company, and a charity shop in Wales which set up a mobile sale stall in a local care home. Demos' research found that some charity shops are used as 'gateways' and signposts to charities' services and even to deliver services directly (as with housing advice at some Shelter stores). More generally, charity shops have a potential for showcasing, promoting and hosting services, which is often underexploited.

Members of the public and retailers are generally positive about charity shops on British high streets. For example, three out of four (74%) respondents were supportive of charity shops receiving 80% business rate relief. Similarly, interviews with charity shop managers, volunteers and independent retailers highlighted the benefits of charity shops to the community and the high street. Those independent retailers who had negative attitudes towards charity shops tended to perceive them as a source of competition in an already difficult economic environment. Positive attitudes among the public were linked to transparency about how

the money raised from charity retail is spent.

4.3 Environmental benefits

Charity shops provide significant environmental benefits through the reuse and recycling of goods, which saves landfill space and helps the UK reduce its CO_2 output. Goods that are not directly sold in the UK are either sold on to textile remanufacturing plants, or sold in developing countries abroad.

The opportunity for reusing and recycling materials is the most widely recognised benefit provided by charity shops. Approximately 95% of the clothes charity shops receive are either recycled or reused. This has a significant environmental impact, diverting 331,000 tonnes of textiles from landfill in 2015/16, and in doing so reducing carbon dioxide emissions by an estimated 6.9 million tonnes per annum. Diverting clothing and other goods from landfill also has economic benefits for local councils by reducing costs of landfill tax (the tax paid by local councils for disposing of waste in landfill sites). In 2015/16 this saved UK councils an estimated £27 million.

The significant fall in the rag price in recent years (dropping from on average 45 pence to 37 pence per kilo between 2014 and 2016) has reduced the incentive for charity retailers to sell on unwanted goods to textile recyclers. This may have a positive environmental impact by encouraging charity shops to increase the reuse of donated stock. Although recycling goods is clearly preferable to sending them to landfill, it still carries with it some environmental costs, predominantly in the energy and chemicals required for the industrial recycling process. In contrast, reusing goods has none of these environmental downsides. There is emerging evidence that charity shops wish to promote greater reuse of stock in response to the fall in rag price; some retail chains have introduced discount stores as a way to sell stock that is in good condition, but was previously unwanted.

An example of a charity shop providing environmental benefits can be seen in Box 1. Recognising the environmental benefits and current fiscal incentives around reuse, some charities (including large national chains, such as Sue Ryder) have set up dedicated 'reuse' shops often located at, or near, local recycling centres. These shops have generally been developed through pioneering partnerships between charity retailers, local councils, and waste management companies, brought together by the mutual environmental and economic benefits that reuse can bring. For example, Wrexham Borough Council entered into one such partnership with waste management contractor FCC Environment and local hospice Nightingale House, launching a new store at a recycling centre in 2016. Under the partnership, staff from FCC Environment retrieve useable items from the recycling centre where the shop is located, and from two other household waste sites in the city. They clean and safety test these items before placing them in the reuse shop, run by Nightingale House. By innovating in this way charity retailers are helping to increase the proportion of goods that are reused and in doing so maximising environmental and cost saving benefits.

BOX 1: Example of the environmental benefits of charity shops.

South Bucks Hospice (SBH) has seven shops in total. In 2012, the charity teamed up with Buckinghamshire County Council and FCC Environmental, an international waste management company, to run two of FCC's ten recycling centres. At each of these, designated 'reuse champions' identify resaleable items, which are sold at SBH's onsite reuse shops. In the first seven months of the scheme 33,512 items were sold. Over time, a very strong relationship has built up between the recycling centre and local residents. This has driven up recycling behaviour in the community, and raised awareness of the hospice.

SBH also has another, four-way, partnership with the council, FCC Environmental and Her Majesty's Prison (HMP) Bovingdon. Once a week, bicycles deposited at the recycling centre are sent to the prison to be repaired. SBH pays for the spare parts needed for the repairs, and sells the bikes through the reuse shops, which have sold 2,200 bicycles since July 2012. Not only does the scheme provide an opportunity for prisoners to improve their social skills and work readiness, it also leads to a National Vocational Qualification (NVQ) in bicycle repair – a route into employment on release. All four stakeholders gained from the partnership: the county council reduced the amount of waste sent to landfill; FCC reduced its costs; local residents benefit from bargain goods; and funds are raised for the hospice.

5. CONCLUSIONS

Until recently, charity retail was a social good that was generally taken for granted. Charity shops encourage recycling and reuse and provide goods to people at affordable prices all the while raising income for parent charities. However, the charity retail sector – as well as the British high street and economy as a whole – is undergoing significant changes. The number of charity shops on British high streets has been rising since the early 2000s, with particular growth since the 2008 recession. Many are also becoming increasingly professionalised in their appearance and sales strategy, and are thus providing greater competition with other high street retailers and countering negative perceptions of charity shops as dusty and disorganised. A consequence of this resurgence is that the charity retail sector is becoming an increasingly significant player in terms of demonstrating the benefits of reuse (and recycling) and how it can be practically realised.

The social value of charity shops includes:

- The amount of money raised for each charity;
- Services provided by those charities with the money raised;
- The number of people employed in charity shops and resulting benefits;
- The number of people volunteering in charity shops and resulting benefits;
- Environmental impacts of reusing and recycling goods; and
- Benefits to social interaction, cohesion and offender rehabilitation.

The community benefits provided by charity retail include:

- providing direct local services in local areas;
- promoting access to charity and other local services;
- providing opportunities for social interaction and cohesion;

- forging local partnerships with local institutions;
- reusing and recycling goods;
- providing affordable goods; and
- maintenance of footfall on local high streets that are otherwise struggling to compete with out-of-town shopping centres and the rise of internet shopping.

There is no doubt that the total value of charity shops goes far beyond the amount of money they raise for their parent charities. Calculating a social return on investment (SROI) figure for the entire charity retail sector is incredibly difficult because of the wide range of charities that operate charity shops, as well as the range of specific activities that those charities undertake. To work towards a calculation of social value for the entire sector, each individual charity should begin to understand and quantify its own social value. A key factor in understanding how charity shops contribute to social good includes understanding and quantifying how they might contribute to the development of the circular economy via the encouragement and practical realisation of reuse. We see this paper as a step in this process, flagging the social, environmental and economic benefits of charity shops and highlighting the need for further research into the contribution of the charity retail sector to reuse and resource preservation/recovery.

ACKNOWLEDGEMENTS

The authors would particularly like to acknowledge the work of Peter Harrison-Evans, Alexandra Paget and Jonathan Birdwell from Demos.

REFERENCES

Bartlett, J. (2012). The Data Dialogue, London: Demos.

Broadbridge, A. and Parsons, L. (2003). Still serving the community? The professionalisation of the UK charity retail sector. International Journal of Retail & Distribution Management, 31(8), 418-427.

Cassidy and Bennett (2012), The rise of vintage fashion and the vintage consumer, Fashion Practice, 4(2), 239-261.

Castellani, V., Sala, S., and Mirabella, N. (2015), Beyond The Throwaway Society: A Life-Cycle Based Assessment Of The Environmental Benefit Of Reuse. Integrated Environmental Assessment and Management, 11(3), 373-382.

Charity Retail Association (2018a), The definitive annual survey of the charity retail market: The Charity Shops Survey 2018, England: CSA, Available from: https://outlook.office.com/mail/search/id/AAQkADU1NTFhYWExLTFiZmQtNGZlMS1iNjBmLWUyOTIwZDgyYzY0ZgAQAFKcwrg4pkB9iKbcX4lGd5k%3D/sxs/AQMkADU1ATFhYQExLTFiZmQtNGZlMS1iNjBmLWUyOTIwZDgyYzY0ZgBGAAAD3KDOU4GYCEuXUJRamDjq5gcAN4OYuVK%2Bf0i6BurUr3Q2YQAAAgEMAAAAN4OYuVK%2Bf0i6BurUr3Q2YQACGsA5pwAAAESABAAv5rljFeX1kOQ%2Fed3KPp%2BJQ%3D%3D, [Accessed: 15/04/19].

Charity Retail Association (2018b). Charity Retail Association's key findings from 2017's research programme. London: Charity Retail Association.

European Parliament and the Council of the European Union (2008), Directive 2008/98/EC of The European Parliament and of the Council of 19 November 2008 on waste and repealing certain Directives.

Farrant, L., Olsen, S. T and Wangel, A (2010). Environmental benefits from reusing clothes. The International Journal of Life Cycle Assessment, 15(7), 726-736.

Gaskin, K (1999). Blurred vision: Public trust in charities. International Journal of Non-Profit and Voluntary Sector Marketing, 4(2), 163-178.

Gregson, N. and Crewe, L. (1997). The Bargain, the Knowledge, and the Spectacle: Making Sense of Consumption in the Space of the Car-Boot Sale. Environment and Planning D: Society and Space, 15(1), pp.87-112.

Gregson, N. and Crewe, L. (2003). Second-hand cultures. Oxford: Berg.

Grimsey, B. et al (2013). The Grimsey Review: An alternative future for the high street. Available at: http://www.vanishinghighstreet.com/wp-content/uploads/2016/03/GrimseyReview04.092.pdf (accessed 4 Nov 2013).

Harrison-Evans, P. (2017). Shopping for good: the social benefits of charity retail. Available at: https://www.demos.co.uk/project/shopping-for-good/ (accessed 26 Feb 2018).

Horne, S. (1998). Charity shops in the UK. International Journal of Retail & Distribution Management, 26(4), 155-161.

Horne, S. (2000). The charity shop: purpose and change. International Journal of Nonprofit and Voluntary Sector Marketing, 5(2), 113-124.

Hyndman, N and McConville (2018). Trust and accountability in UK charities: Exploring the virtuous circle. The British Accounting Review, 50(2), 227-237.

Joseph Rowntree Foundation (2016). Households below a minimum income standard: 2008/09-2013/14. Available at: https://www.jrf.org.uk/report/households-below-minimum-income-standard-200809-201314 (accessed Oct 2013).

Lovatt, M. (2015). Charity Shops and the Imagined Futures of Objects: How Second-Hand Markets Influence Disposal Decisions when Emptying a Parent's House. Culture Unbound: Journal of Current Cultural Research, 7(1), 13-29.

National Council for Voluntary Organisations (NVCO) Civil Society Almanac (2012). What impact did the recession have upon the voluntary sector? Available at: https://data.ncvovol.org.uk/a/almanac12/almanac/voluntary-sector/finance-thebig-picture/what-impact-did-the-recession-have-upon-thevoluntary-sector/ (accessed Oct 2013).

Paget, A. and Birdwell, J. (2013). Measuring the social value of charity shops. Available at: https://www.demos.co.uk/files/DEMOS_givingsomethingbackREPORT.pdf?1385343669 (accessed 20 Feb 2018).

Parsons, E. (2002). Charity retail: past, present and future. International Journal of Retail & Distribution Management, 30(12), 586-594.

Pookulangara, S. and Shepard, A. (2013), Slow fashion movement: Understanding consumer perceptions- An exploratory study, Journal of Retailing and Consumer Services, 20(2), 200-206.

Portas, M. (2011). The Portas Review: An independent review into the future of our high streets. Available at: https://www.gov.uk/government/uploads/system/uploads/attachment_data/file/6292/2081646.pdf (accessed 4 Nov 2013).

ReDo (n.d). ReDO's Mission, Available from: http://loadingdock.org/redo/index.htm, [Accessed: 28/03/19].

Williams, I.D. and Shaw, P.J. (2017). Editorial: Reuse: Fashion or future? Waste Management, 60, 1-2.

detritus | Multidisciplinary Journal for Waste Resources & Residues

CISA

UTILIZATION OF RECYCLED POLYPROPYLENE, CELLULOSE AND NEWSPRINT FIBRES FOR PRODUCTION OF GREEN COMPOSITES

Vesna Ž. Bogataj [1,*], Peter Fajs [1], Carolina Peñalva [2], Marko Omahen [3], Matjaž Čop [4] and Ari Henttonen [5]

[1] *TECOS, Slovenian Tool and Die Development Centre, Kidričeva 25, 3000, Celje, Slovenia*
[2] *AITIIP Centro Tecnológico, Romero 12, 50720, Zaragoza, Spain*
[3] *OMAPLAST, Kosovelova cesta 3, 1230, Grosuplje, Slovenia*
[4] *ADRIA Mobil, Straška cesta 50, 8000, Novo Mesto, Slovenia*
[5] *ECOPULP Finland Oy, Suviojantie 9, 45610, Koria, Finland*

Article Info:
Received:
01 July 2019
Revised:
18 September 2019
Accepted:
20 September 2019
Available online:
26 September 2019

Keywords:
Waste plastics
Recycled polypropylene
Newspaper fibre
Reclaimed cellulose fibre
Mechanical properties
Thermal properties
Fibre reinforced composites
Recycling

ABSTRACT

This work investigates the feasibility of using the recycled polypropylene (rPP), cellulose (CF) and newsprint (NP) fibres in polyolefin reinforced composites. Recycled PP filled with 40 wt.% of cellulose (rPP/CF) or newsprint (rPP/NP), with the addition of impact modifier (IM) and compatibilizing agent (CA), have been prepared with extrusion melting and injection moulding. Melting and crystallization behaviour of plain matrix and composites were measured by differential scanning calorimetry (DSC). Morphological and mechanical properties were also studied using scanning electron microscope (SEM) and tensile testing, respectively. Thermal stability of composites was similar to neat rPP for both types of the filler used. Though, the crystallinity was progressively decreased with the addition of CF or NP. The DSC further revealed an occurrence of the two distinct melting transitions, meaning that the examined materials were not based on pure polypropylene (PP), but are rather blends of high-density polyethylene (HDPE) and PP, what has been confirmed also by the Fourier transform infrared spectroscopy (FTIR). The largest single source of contaminations in recycled PP comes from HDPE since both polymers are identified by a similar density and can be accidentally mixed during the conventional physical separation process. Composites reinforced with CF have shown better mechanical performances than those based on reclaimed NP fibres, what can be attributed to the initial fibre quality. Tensile strength of the composites filled with CF and NP fibres was 36 MPa and 29 MPa, respectively, in disparity to 23 MPa measured for neat rPP. The fibre addition further resulted in substantial increase in Young modulus of the composites. The addition of CF and NP fibres lead to an improved modulus of elasticity by 16 and 47%, respectively. Waste paper in the form of recovered cellulose or reclaimed newsprint fibre can thus meet all the technical requirements to become an alternative to inorganic fillers in thermoplastic composites.

1. INTRODUCTION

One of the key priorities of the EU Strategy for Circular Economy is an accelerated shift to a more resource efficient economic model in Europe, providing a pragmatic and effective solution to the gradual and limited depletion of virgin resources. By closing the material cycles in production sectors, this modern economy allows Europe to increase the resource productivity by up to 3 percent annually. This would generate a primary resource benefit of as much as 0.6 trillion EURO per year by 2030 (EMF and McKinsey, 2015) to the Europe's economies. In addition to the ecological and economical awareness, the legislative actions adopted along the EU member states likewise strongly encourage the development of reusability and recycling modelling for discarded materials, including waste paper and plastics.

Paper is the most recycled product in the world and Europe is the global champion in paper recycling, exceeding the rate of 72% (EPRC, 2017). On the other hand, scarcely around 26% of all plastics streams are recycled in Europe (Shen and Worrell, 2014). In 2016, 27.1 million tonnes of plastic waste were collected through official schemes in the EU28+NO/CH in order to be reintegrated back into the production cycles. Out of this volume, 31.1% of plastic waste was recycled, 41.6% was incinerated, and 27.3% has been

* Corresponding author:
Vesna Ž. Bogataj
email: vesna.zepic.bogataj@tecos.si

https://doi.org/10.31025/2611-4135/2019.13857
© 2019 Cisa Publisher. Open access article under CC BY-NC-ND license

committed to the landfills. This year represents an important milestone, since for the first time, more plastic waste was recycled than landfilled (PlasticsEurope, 2018). In addition, the recent Chinese "Green Fence" policy has limited the export of waste plastics to China and this has caused a build-up of waste materials in Europe. The implications of Europe's substantial exports of plastics waste are now becoming clearer as the issues arise from the Green Fence blockade. Europe now needs to find a resolution in order to allow new investments in plastic waste recycling and to deal with the plastic waste that was in past exported. The challenge to recycle more and to fully implement the waste hierarchy model, with prevention, reuse, recycling, recovery and disposal as the least preferable option, continues and remains as one of the most important shift tags in implementation of the EU Circular Economy Package (EC, 2015). There are many product types that are currently not widely collected but could be in future. For example, advanced sorting technologies for PP are now available but not yet fully implemented as an operative collection system is not yet in place.

The possibility of using the municipal solid wastes in the development of new value-added products is an attractive venture, especially with respect to the large quantity of paper and plastic waste generated daily. The throwaway era is behind us, and these days we need to focus on end-of-service life and recycling issues for these materials. Since the composites are naturally mixtures of different materials, it is reasonable to expect that it would be easier and less expensive to utilize the mixed waste plastics in them.

If we look further, the recycled paper fibre can meet all the requirements for replacing the inorganic fillers in thermoplastic composites, what has been thoroughly reviewed in the literature (Mochane et al. 2019; Jariwala and Jain, 2019). Although waste paper recycling maintains an important role in a sustainable environment, the use of recycled/secondary fibre for making the paper requires special treatments for deinking, cleaning and refinement. Subsequent wastewater and sludge treatments significantly increase the production costs. On the contrary, the utilization of recycled and recovered paper fibres as reinforcers in a composite does not require extensive pre-treatments, but decreases the demand for natural resources, saves energy and water, and reduces pollution. The added advantage of these composites results from maintaining trees by reducing the use of virgin natural fibres, making the products cheaper on a price per weight basis, since fillers are often less expensive than the polymer, while at the same time increasing their end performances. A continuous upgrade of such materials in terms of mechanical, thermal and dimensional performances has demonstrated the industrial applicability to various fields of applications, specifically for load-bearing applications. Thanks to their genuine technical, cost-efficient and environmental advantages, natural fibre reinforced composites (Sydow & Bieńczak, 2018; Holbery & Houston, 2006; Kowaluk, 2017) are flourishing and can no longer be considered merely as an example of "greenwashing".

The ultimate goal of this research is to study the properties of the produced composites, prepared for maximised fractional utilisation of the waste paper fillers, balanced against the deleterious effects on the material properties, while remaining potentially an economically viable process. All the input materials for new composites were derived from municipal solid waste, i.e. recovered newsprint fibres, reclaimed cellulose fibres, and recycled waste plastic polyolefines (rPP). The effects of various filler types, impact modifier and compatibilizing agent on the mechanical and thermal properties of the resulting composites were evaluated and compared with the properties of plain rPP.

This study is a part of the LIFE CEPLAFIB project (LIFE17 ENV/SI/000119) in which eco-composites based on recycled polyolefines reinforced with different natural fibres and fillers, obtained as byproducts from industrial production plants, are being developed and investigated for its industrial use as a sandwich acoustic barrier panels in construction/building sector, rigid packaging insertions for industrial packaging and interior RV equipment for the caravanning sector.

2. EXPERIMENTAL

2.1 Materials

Recycled polypropylene (rPP) was supplied by the recycling company OMAPLAST (Slovenia) with a melt flow index (MFI) between 7.0 and 10.0 g/10min, and the density of 0.910 g/cm³. Virgin PP (BormedTM RF830-MO), supplied by Borealis (Vienna, Austria) and virgin HDPE (HDI2061 Natural), supplied by Braskem IDESA, Mexico), were used in FTIR comparative analysis, serving as the reference spectra. Cellulose (CF) and newsprint (NP) fibres were provided by Ecopulp Oy (Koria, Finland) after chemical bleaching and mechanical recovering, respectively, of the received waste residues from pulp & paper industry. NP and CF were shredded into smaller fraction particulates and dried in a vacuum oven at 60°C over-night to ensure that the moisture content was minimal. The measured aspect ratio (defined as the ratio of fibre length to diameter) was 38 for NP and 58 for CF. The percentage of fibre additivation was in all cases 40 wt. %. Liococene PP-MA 7452 TP (CA), grafted with 7 wt.% of maleic anhydride, supplied from Clariant Produkte (Deutschland) GmbH, Germany, was used as compatibilizer, and propylene-based elastomer Vistamaxx™ 6202, supplied by HSH Chemie Group, Slovenia, served as an impact modifier (IM). The blend composition and sample designations used in this study are presented in Table 1. The composition of the composite materials has been selected on the basis of the preliminary results obtained, where 26 different formulations has been studied and tested, varying the type of fillers (i.e. newsprint fibres with two different size reductions: NP sieved to final fraction of 2 mm and milled NP fibres, cellulose fibres and barely husk fibres), filler contents (0, 20, 30 and 40 wt. %) and the contents of CA (0, 3 and 5 wt. %) and IM (0, 3 and 5 wt. %) in the final formulation.

2.2 Processing

All the raw components were premixed in sealed containers and shaken manually. The blends were com-

pounded by simultaneous addition of all components into the Labtech LTE 20-44 twin screw extruder with a barrel temperature of 170°C at the feed section and 180°C at the die head. The screw rotation speed was fixed at 200 rpm. The extruded strands were quenched in water and pelletized. The extruded blends were injection moulded into standard tensile specimens. Prior to injection moulding, pellets were dried in a dryer (60°C for 24 hours). A Krauss Maffei 80/380 CX injection moulding machine was used with barrel temperatures of 150-180°C. The injection-moulded specimens were then stored in desiccators prior to testing.

2.3 Characterization Analyses

2.3.1 Tensile Testing

Tensile tests using a Zwick/Roell Z005 (Zwick GmbH & Co. KG, Ulm, Germany) were carried out in compliance with ISO 527-1-2 under the ambient conditions with a crosshead speed of 5 mm min^{-1}. The distance between the grips was set to 60 mm. The presented values of elasticity modulus (E_t), tensile strength (σ_M), and elongation at break (ε_b) are an average from at least six replicates from each final material.

2.3.2 Differential Scanning Calorimetry

The melting and crystallization behavior of neat rPP and composites were studied using a Mettler-Toledo HP DSC-1 with a temperature range of 25-180°C, under the nitrogen purge and heating rate of 10°C/min. Crystallization temperature (Tc), melting temperature (Tm), enthalpy of crystallization (ΔHc), and enthalpy of melting (ΔHm) of samples were calculated. The percent of crystallinity (% Xc) was calculated from the Equation (1), where is the fusion heat of 100% crystalline PP (equal to 207 J g^{-1}; TA Instruments) or (HD)PE (equal to 293 J g^{-1}; Wunderlich, 1990) and Wv represents the mass fraction of the polymer component within the final composites formulation.

$$\mathrm{Xc}\ (\%) = \frac{\Delta H_m}{W_v \cdot \Delta H_m^0} \times 100 \qquad (1)$$

2.3.3 Fourier-transform infrared spectroscopy

The chemical structure of recycled PP was analysed with Fourier transform infrared spectroscopy. For the identification of recyclate composition, the spectra of virgin PP and HDPE were also recorded to enable the comparative analysis based on their specific absorption bands. All the samples were prepared in the form of thin films. The instrument used was a Spectrum One FTIR spectrometer (Perkin Elmer, USA), working in the attenuated total reflection (ATR) mode on a ZnSe crystal. The spectra were collected at a resolution of 4 cm^{-1} over the range from 650 to 4000 cm^{-1}. In total, 64 scans were averaged for each spectrum.

2.3.4 Scanning Electron Microscopy

Morphology of the composite fractured surfaces were examinated after tensile test using low vacuum JEOL 5500 LV scanning electron microscope (SEM), equipped with Oxford Inca (EDX) energy dispersive spectroscopy. An operating voltage of 20 kV and magnifications of 100x and 500x were used.

3. RESULTS AND DISCUSSION

3.1 Mechanical properties

Results of the tensile modulus (E_t), tensile strength (σ_M) and elongation at break (ε_b) of plain rPP and composites with two different reinforcing components, i.e. CF and NP, as a function of CA and IM additivation are presented in Table 2. The representative stress-strain curves are illustrated in Figure 1. In general, the addition of the reinforcing elements, independly of their origin (CF or NP), has proven to be a successful technique for improving the mechanical properties of the basic polymer matrix. The values of the tensile modulus and strength obtained for the resulting composites were substantially higher than that of plain recycled PP. Compared to the neat rPP the addition of CF or NP fibres lead to an improved modulus of elasticity by 16% and 47%, respectively, and the values of the tensile strength for samples filled with CF and NP fibres was 36 MPa and 29 MPa, respectively, in contrast to the 23 MPa measured for recycled neat PP. The elongation at break on the other hand was decreased with the addition of fibres. This is governed by the fact that composites become more brittle with the addition of flaky fillers, however higher strength means a harder thus less deformable material. Since polypropylene has a hydrophobic nature and the cellulose based fibres has a hydrophilic surface charge, the usage of maleic anhydride grafted coupling agent has certainly contributed

TABLE 1: Sample composition of rPP/CF and rPP/NP Composite.

Sample formulation	rPP [wt. %]	CF [wt. %]	NP [wt. %]	CA [wt. %]	IM [wt. %]
rPP	100	0	0	0	0
rPP/CF	52	40	0	3	5
rPP/NP	52	0	40	3	5

TABLE 2: Mechanical properties of rPP and composites with respect to the type of the reinforcing filler.

Sample	Young Modulus E_t [MPa]	Tensile Strength σ_T [MPa]	Elongation at Break ε_b [%]
rPP	384 ± 18	23 ± 0.05	49 ± 6.00
rPP/CF	447 ± 14	36 ± 0.44	11 ± 0.22
rPP/NP	564 ± 68	29 ± 0.46	09 ± 1.96

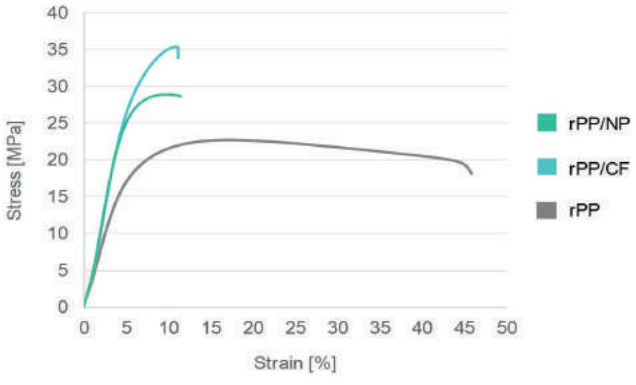

FIGURE 1: Comparison of tensile stress versus strain curve for rPP and composites filled with CF and NP fibres.

to the amplified inter-phase compatibility, as evidenced also by the SEM results, and hence the adhesion between the components of the composite (Yang et al. 2007; Žepič et al. 2016).

In addition to the tolerable interphase compatibility, various supplementary parameters are also influencing the mechanical performances of fibre reinforced composites, including the fibre aspect ratio, filler dispersion, particle dimension, stress transfer at the interface and mixing temperatures (Ashori and Nourbakhsh, 2008). To achieve a proper trade off between the elasticity and stiffness of the resulting composites, Vistamaxx™ propylene-based elastomer has been added to the mixture blends in a relative high weight percentatge which appears to deliver good impact properties (Kumar et al. 2017), but still moderate flexibility.

3.2 Thermal properties

The impact of the type of fibre additivation on the thermal characteristics of rPP compounds can be assessed from the results obtained from DSC thermographs that are graphically presented in Figure 2. The crystalization (X_c) and melting (T_m) behaviour was evaluated from the 2nd heating scan, while the crystallization temperature (CT) of the neat recycled polymer and composites was studied from the cooling scan. The results are shown in Table 3.

The thermal stability of the composites with recycled PP and recovered cellulose/newsprint fillers were similar to those of neat rPP. However, the enthalpy of fusion for the composites progressively decreased with the addition of cellulose and newsprint fibres, which can be attributed to the lower content of the polymer in final material composition. In fact, cellulose-based fibres does not essentially contribute to the melting endotherm, since this type of fillers does not present any transitions within the temperature range of DSC scan. Furthermore, if the obtained values of the melting enthalpies are normalized on the basis of pure polymer content of each sample, still a modest decrease enthalpy with the fibre content can be observed for most cases. This effect suggests that some interactions between cellulose/newsprint fibres and polyolefin matrix take place. The degree of crystallinity, calculated using the Eq. 1, is higher for the composite than for the neat rPP (Table 3). This behaviour indicates that newsprint or cellulose fibres can induce crystal nucleation of the recycled polymer matrix, which implies that both of the utilized fillers can probably be used as a nucleating agent for rPP. Similar observations were made by other authors (Lopez-Machado et al. 2000). By comparsion between the two types of composites, a slightly higher crystallinity yield is observed for the rPP/CF composites as compared to the rPP/NP. The stronger adhesion between the rPP matrix and the NP fibres, as imposed by the surface morphology features of the composites, could hinder the motion of the polymer chains which are close to the NPs. This decrease in mobility could be an explanation of the lower crystalline ratio.

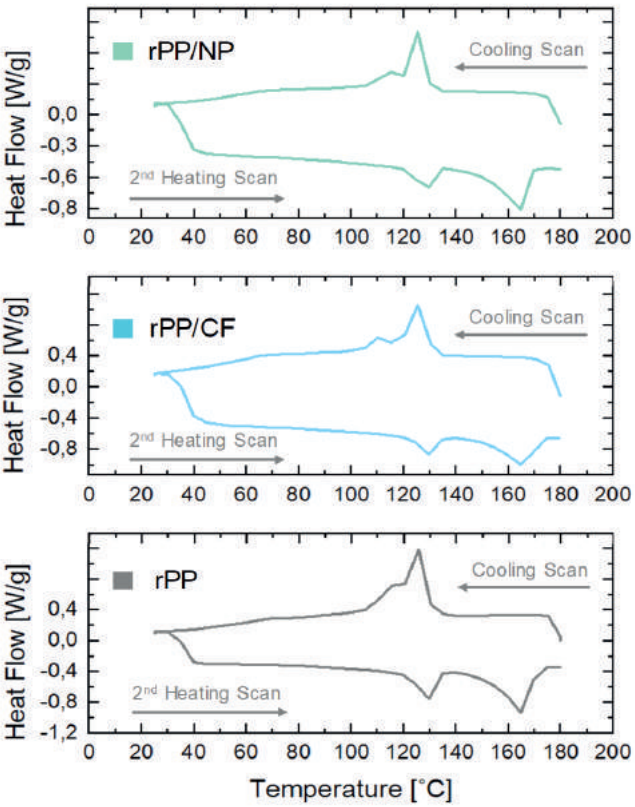

FIGURE 2: DSC thermograms of rPP and composites with reclaimed CF and NP fibres during the cooling and the second heating scan.

What was more interesting is that the DSC results revealed the occurrence of the two distinct melting transitions, implicating that the examined materials are not based on pure PP, but are rather blends of HDPE (peak melting temperature at around 130°C) and PP (melting of about 165°C) (Camacho and Karlsson, 2001). Pure or homogeneous PP resin should yield a single melting event and the presence of the smaller endothermic transition, evolved at lower melting temperatures (130°C), indicates

TABLE 3: DSC data of neat rPP and composites with respect to different fillers during the first and second heating scan.

	1st heating scan		2nd heating scan							Contamination	
Sample	Melt. temp.		Melt. temp.		CT	Cristallinity [%]		Enthalpy [J/g]		HDPE	PP
	Tm^1 [°C]	Tm^2 [°C]	Tm^1[°C]	Tm^2[°C]	T_c [°C]	$X_{c\ HDPE}$	$X_{c\ PP}$	$\Delta H_{m\ (HDPE)}$	$\Delta H_{m\ (PP)}$	[%]	[%]
rPP	129	166	129	165	124.3	5.51	20.44	16.15	42.31	28	72
rPP/CF	129	166	130	166	124.9	6.33	24.29	9.65	26.15		
rPP/NP	128	165	128	164	124.8	6.24	21.82	9.52	23.49		

the presence of HDPE, which could be accidentally mixed with the PP recycled containers or resins. A substantial part of public solid waste (MSW) streams is composed of mixed polymers, like polyethylene (PE), polypropylene (PP), polyvinyl chloride (PVC) and polyethylene terephthalate (PET), which are among the most common plastics waste, since they are the most frequently used commercial plastics in our daily lives as well as in industries. PP and HDPE have similar densities and by using the conventional physical separation technique (i.e. floating drop process) is almost impossible to separate them. The misclassification of these two types of plastic waste is highly probable in the daily waste sorting routine and explains the reason for the presence of HDPE in the PP matrix.

According to the application guide of the original equipment manufacturer of DSC measuring devices, the DSC heats of melting do not only detect the contaminant, but can also determine its percent level in the final resin (Sichina, 2000). To make a rapid qualitative assessment of the polyolefin blend composition we need to divide the measured melting enthalpy of the "contaminant" ($\Delta H_{m\ HDPE}$) with the total ΔHm of the rPP recyclate. The estimated percent level of the HDPE in the final material composition was, according to this calculation, equal to 30%.

3.3 Chemical Composition

The ATR-FTIR spectroscopy analysis was elaborated as a qualitative (aiding polymers identification based on their specific absorption bands) method for assessing the chemical composition of the recyclate PP. The representative FTIR spectra of virgin PP and HDPE, and the spectra of recycled PP are presented in Figure 3. In order to differentiate between the HDPE and PP the 3000-2750 cm^{-1} spectral region has been firstly taken into consideration. This frequency range is related to different vibration types of methyl groups, wherein the absorption bands between 2950 and 2850 cm^{-1} represents the -CH2- asymmetric and symmetric stretching vibration that typically belongs to HDPE,

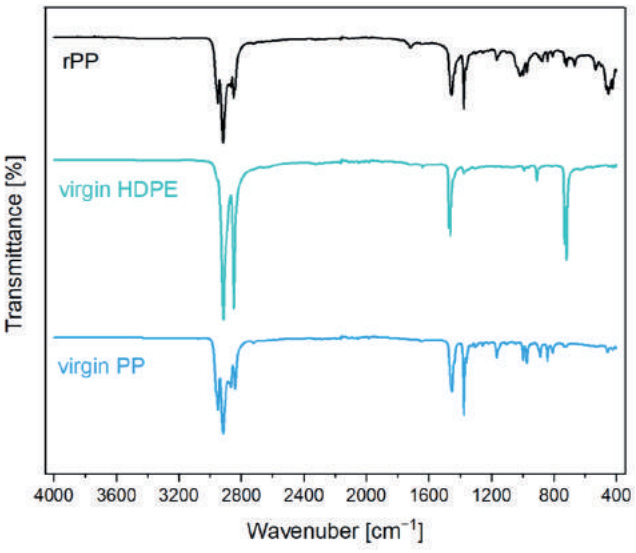

FIGURE 3: FTIR spectral comparison of rPP, virgin high-density polyethylene and virgin polypropylene.

while four superimposed absorption bands in between 2985 cm^{-1} and 2810 cm^{-1} correspond to the asymmetric and symmetric stretching vibration of methylene and methyl groups, and are subscribed to PP (Lin et al. 2015). Variations between the spectra were also observed in the 1475-1350 cm^{-1} domain, where absorption bands correspond to scissoring vibration of the methylene group (1470-1460 in HDPE, and 1475-1440 cm^{-1} in PP spectrum) and to symmetric deformation of the methyl group (1380-1370 cm^{-1} only in PP spectrum). Supplementary, a doublet with the maxima at 730 and 720 cm^{-1}, corresponds to bending and rocking vibrations of crystalline and amorphous methylene group, is characteristically assigned to HDPE. The frequency ranges of different functional groups of PP and HDPE polymers, with assigned vibration type are summarized in Table 4.

By comparing the rPP spectrum to the reference spectra of virgin PP and HDPE it can be argued that the main chemical structure of the recyclate belongs to PP and, in lower amount to high density polyethylene (HDPE). On the other hand, all the characteristics peaks of PP and HDPE can be found also in rPP spectrum, confirming the co-existence of both polymer types as formerly speculated by the results of DSC analysis.

3.4 Morphology Analysis

The interface in any fibre-matrix composite system is responsible for transmitting the load stresses from the polymer to the fibres. This stress transfer efficiency largely depends on the fibre-matrix interface and fibres quality, i.e. morphology and mechanical characteristics (Kalia et al. 2011).

SEM images of recovered bleached cellulose fibres and recycled newsprint fibres were taken to investigate their surface structure and are shown in Figure 4a and 4b, respectively. The results illustrated smooth and clean surface of bleached cellulose fibres, while the mechanically reclaimed newsprint fibres indicated rougher surface texture, signifying the presence of impurities such as hemicellulose, lignin, pectin and waxy substances. Furthermore, the average diameters of the measurable newsprint fibres (36 ± 10 μm) were higher than those of chemically bleached cellulose fibres (30 ± 12 μm). This can be explained by the fact that bundles of individual newsprint fibres are linked together with lignin, which acts like a cementing material around the fibre strands.

The original pulping process for newsprint fibres is high yield mechanical pulping, consequently, the external

TABLE 4: FTIR spectra analysis of PP and HDPE polymers.

Wave number (cm^{-1})	Functional group	Vibration type	Assigned to
2985 - 2810	-C-H	Streching	PP
2950 - 2850	$-CH_2$	Streching	HDPE
1475 - 1440	$-CH_2$	Bending	PP
1470 - 1460	$-CH_2$	Bending	HDPE
1380 - 1370	$-CH_3$	Bending	PP
730 - 700	$-CH_2$	Rocking	HDPE

surface of fibres tends to be rich in lignin, hence to some extent hydrophobic (Gregersen et al. 1995; Backström et al. 1999), and with lower strength properties (Kibblewhite, 1983). By contrast, the removal of lignin and extractives during the chemical bleaching will result in a hydrophilic fibre surface due to carbohydrates (cellulose, hemicelluloses) and better strength compared to newsprint fibre. The aim of the present study was, inter alia, to compare the effect of mechanically recycled newsprint fibres and bleached cellulose fibres on the ultimate mechanical properties of the resulting composites. The quality of the fibres for their reinforcement potential, including the developed surface characteristics (Figure 4), is therefore closely related to the fibre pre-treating process.

Figure 5 shows a comparison of the effect of filling the recycled polypropylene matrix with 40% of reclaimed cellulose and newsprint fibres. We can observe the difference between the morphology of the composites, depending of the chosen natural fibres — longer cellulose fibres seem to be more coherent and break perpendicularly to the polymer matrix (Figure 5a, b), while newsprint fibres are firmly embedded within the polymer matrix (Figure 5c, d) suggesting a strong interfacial adhesive bond. On the fractured surfaces of the composites, we can observe that some fibres are pulled out from the matrix, but most of them are still tightly linked to the matrix. This last statement is factual for both types of composites and can be attributed to the compatibilizing agent effect. The results of thermal and mechanical analysis indicated higher cristallinity and improved tensile strength for cellulose-reinforced composites as opposed to recycled newsprint fibre composites, therefore, the assumption that chemically bleached fibres express a higher reinforcing potential can be clearly confirmed.

4. CONCLUSIONS

The present study has shown that composites based on recycled polypropylene filled with natural reclaimed fibres obtained from post-consumer waste, can be an interesting alternative to virgin polymer materials modified by artificial fibres like glass or aramid. This leap to natural fibre reinforcements reduces the mechanical properties of the composites, when compared to glass or aramid fibres. Nevertheless, the resulting materials show good specific properties due to the lower density of the natural cellulose-based fibres. Moreover, these fibres are more flexible and less abrasive than glass fibres, protecting the machinery and allowing higher recyclability rates. In the case of adding the recovered newsprint fibres (without special aperture and expensive chemical pre-treatment), we can observe higher improvement of tensile modulus compared to cellulose fibre filled rPP, which has a special bleaching pre-treatment and a higher price. In that perspective the selection of the newsprint fibre reinforcement provides a better economic decision. Moreover, the increase of the tensile strength and morphological characteristics of the composites confirmed good adhesion between the natural fibres and rPP. The addition of fillers significantly limited the chain movements in the polymer system and resulted in higher stiffness and lowered the elongation at break values. It seems that these composites can be processed with classical plastic transformation technologies, like injection moulding or conventional extrusion compounding. The addition of recovered natural fibres to waste plastic matrices thus renders the resulting composites to be viable from both the mechanical properties and the environmental points of view. Besides, these types of materials may be reclaimed and recycled for the production of second-generation composites, when mechanical recycling is applied. Through the mentioned recycling method, the materials can be efficiently re-processed excluding the energy recovery or disposal practices, without changing their chemical structure.

AKNOWLEDGEMENTS

The research leading to these results has received funding from the European LIFE Programme under the sub-program for environment and resource efficiency with the grant agreement n° LIFE17 ENV/SI/000119. Special acknowledgement goes also to all project partners: AITIIP, ITB, ECOPULP, ADRIA Mobil and OMAPLAST, and to the Department of Wood Science and Technology (Chair of Wood Pests, Modification and Protection of Wood) from Biotechnical Faculty of University of Ljubljana for their technical assistance in FT-IR measurements.

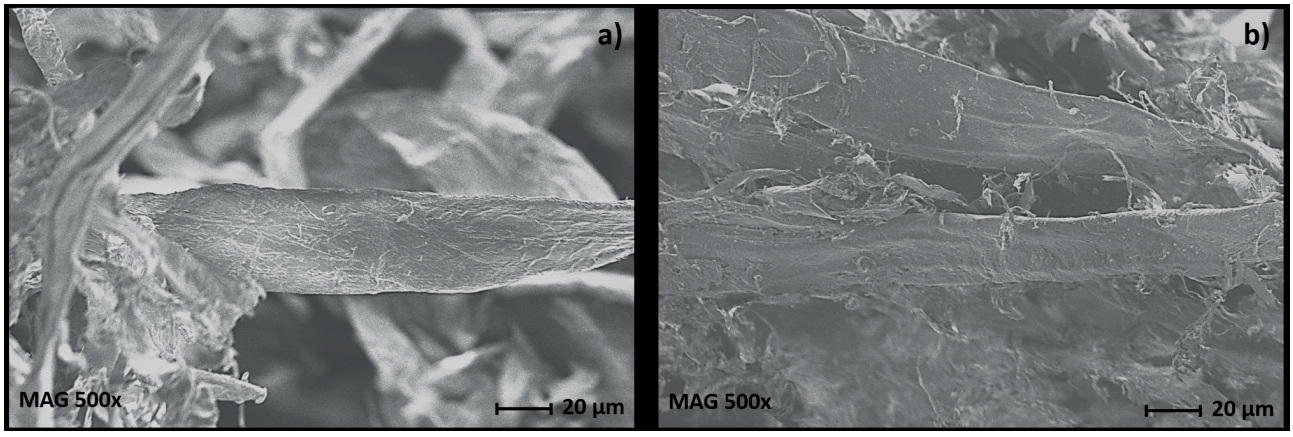

FIGURE 4: SEM micrographs of a) chemically pulped and bleached cellulose fibers, and b) mechanically recycled newsprint fibers.

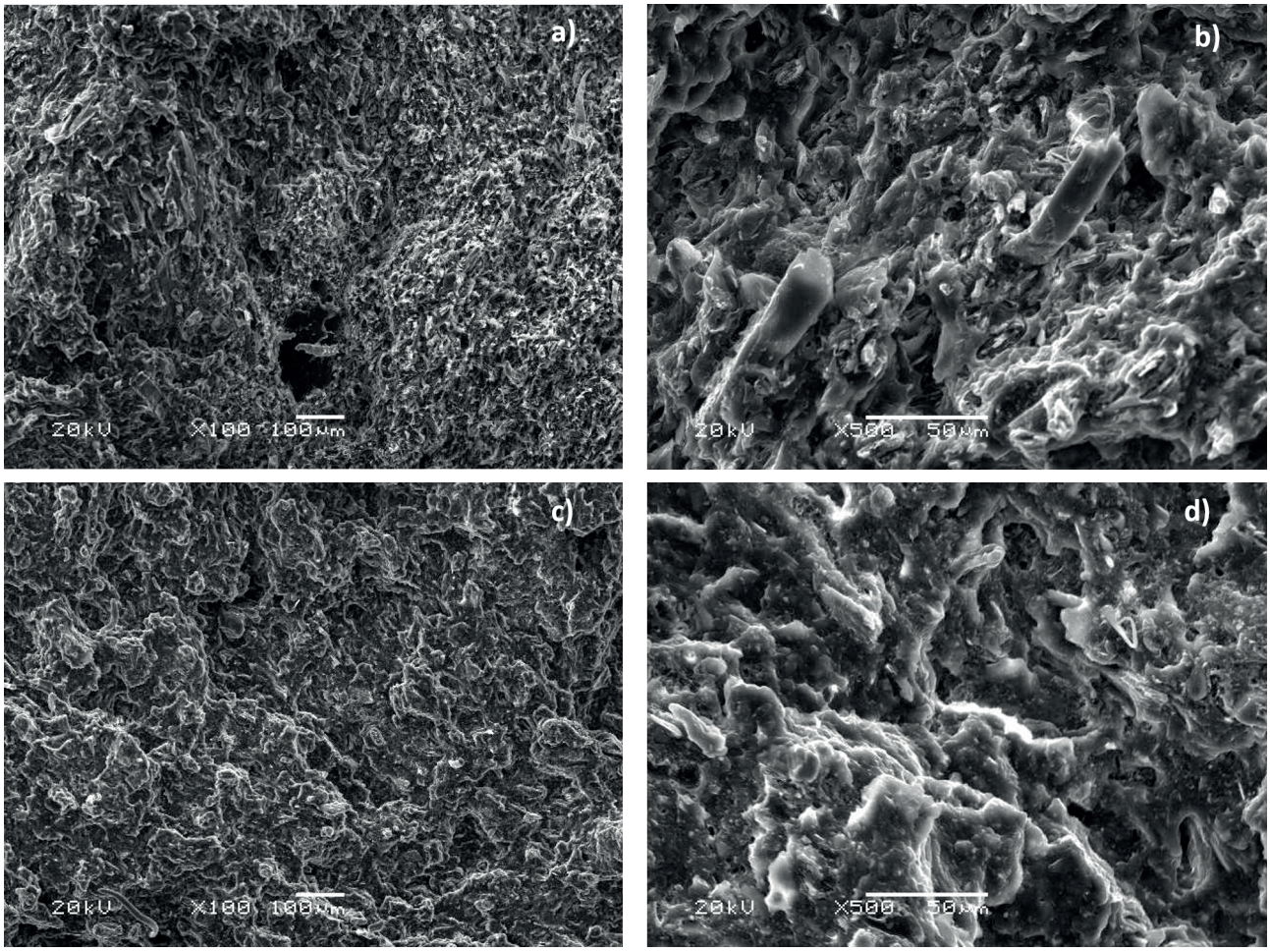

FIGURE 5: Tensile fractured surfaces of a) rPP filled with 40 wt.% of CF, b) higher magnification of Figure 5a, c) rPP filled with 40 wt.% of NP, and d) higher magnification of Figure 5c.

REFERENCES

Ashori, A., Nourbakhsh, A. 2008. A comparative study on mechanical properties and water absorption behavior of fiber-reinforced polypropylene composites prepared by OCC fiber and aspen fiber. Polym. Compos., 29:574–78.

Backström, M., Fellers, C., and Htun, M. 1999. The influence of kappa number and surface energy on paper-to-paper friction. Nord. Pulp Pap. Res. J., 14(3): 204-208.

Camacho, W., Karlsson, S. 2001. NIR, DSC, and FTIR as quantitative methods for compositional analysis of blends of polymers obtained from recycled mixed plastic waste. Polym Eng Sci, 41: 1626-1635.

EC (2015). Communication from the Commission to the European Parliament, the Council, the European Economic and Social Committee and the Committee of the Regions, Closing the loop – An EU action plan for the Circular Economy, COM. 2015, 614 final, Brussels/BE, 2 December 2015.

EMF and McKinsey. 2015. Growth within: a circular economy vision for a competitive Europe, Ellen MacArthur Foundation and McKinsey Center for Business and Environment: 126

European Paper Recycling Council (EPRC) monitoring report. 2017. European Declaration on Paper Recycling 2016-2020. Available at http://www.paperforrecycling.eu/publications/

Gregersen, Ø.W., Skinnarland, I., Johnsen, P.O., et al. 1995. Qualitative Methods for the Study of Lignin Distribution in Wood and Surface layers of unbleached Pulp fibers and Paper. J. Pulp Pap. Sci., 21(8): 285-287.

Holbery, J., Houston, D. 2006. Natural-fiber-reinforced polymer composites inautomotive applications. JOM, 58(11):80.

Jariwala, H., Jain, P. 2019. A review on mechanical behavior of natural fiber reinforced polymer composites and its applications. Journal of Reinforced Plastics and Composites, 38 (10): 441-453.

Kalia, S., Kaith, B.S., Kaur, I. 2011. Cellulose Fibers: Bio- and Nano-Polymer Composites, Green Chemistry and Technology. Springer, Heidelberg/Dordrecht/London/New York, 2011.

Kibblewhite R.P. 1983. The fibers of radiata pine mechanical pulps. Appita J., 36(4): 272.

Kowaluk G. 2017. Lignocellulosic Fibers Composites: An Overview, Handbook of Composites from Renewable Materials, 293-308

Kumar, A., Choudhary, V., Khanna, R., Cayumil, R., Ikram-ul-Haq, M., Sahajwalla, V., Kumar, I. Angadi, S., E. Paruthy, G., S. Mukherjee, P., Park, M. 2017. Recycling polymeric waste from electronic and automotive sectors into value added products. Frontiers of Environmental Science & Engineering, 11(5):4

LIFE17 ENV/SI/000119. Implementation of a new Circular Economy through the valorisation of postconsumer PLAstic waste and reclaimed pulp FIBer. https://ceplafib.eu/

Lin, J.H., Pan, Y.J., Liu, C.F., Huang, C.L., Hsieh, C.T., Chen, C.K., Lin, Z.Y. and Lou, C.W. (2015) Preparation and Compatibility Evaluation of Polypropylene/High Density Polyethylene Poly-blends. Materials, 8, 8850-8859.

Lopez-Manchado, M., Biagiotti, J., Torre, L., Kenny, J. 2000. Effects of reinforcing fibers on the crystallization of polypropylene. Polymer Engineering and Science, 40:2194-2204.

Mochane, M.J., Mokhena, T.C., Mokhothu, T.H., et.al. 2019. Recent progress on natural fiber hybrid composites for advanced applications: A review. eXPRESS Polymer Letters, 13 (2), 159–198.

PlasticsEurope. 2018. Plastics – the Facts 2018. PlasticsEurope-Association of Plastic Makers. Available at http://www.plasticsrecyclers.eu/plastic-recycling

Shen, Li., and Ernst Worrell. 2014. Plastic Recycling. In Handbook of recycling: State-of-the-art for practitioners, analysts, and scientists. Edited by Ernst Worrell and Markus A. Reuter, 179–90. Amsterdam [etc.]: Elsevier.
Sichina, W.J. 2000. Characterization of the quality of recycled polymers using DSC. Perkin Elmer Instruments.
Sydow, Z., Bieńczak, K. 2018. The overview on the use of natural fibers reinforced composites for food packaging. Journal of Natural Fibers, 00(00), 1–12.
TN 48 Polymer Heats of Fusion. TA Instruments, 23.
Wunderlich, B. 1990. Thermal Analysis, 417–431, Academic Press, USA, 1990.
Yang, H.-S., Kim, H.-J., Park, H.-J., Lee, B.-J., and Hwang, T.-S. 2007. Effect of compatibilizing agents on rice-husk flour reinforced polypropylene composites. Composite Structures, 77(1): 45–55.
Žepič, V., Poljanšek, I., Oven, P., Čop, M. 2016. COST-FP1105: Properties of PLA films reinforced with unmodified and acetylated freeze dried nanofibrillated cellulose. Holzforschung, 70:1125–1134

detritus | Multidisciplinary Journal for Waste Resources & Residues

CISA

DEVELOPMENT OF A MSW GASIFICATION MODEL FOR FLEXIBLE INTEGRATION INTO A MFA-LCA FRAMEWORK

Geneviève Groleau [1], Fabrice Tanguay-Rioux [1], Laurent Spreutels [1], Martin Héroux [2] and Robert Legros [2,*]

[1] *Chaire de Recherche sur la Valorisation des Matières Résiduelles (CRVMR), Chemical Engineering Department, Polytechnique Montreal, Montreal, Canada*
[2] *Department of Environment, City of Montreal, Montreal, Canada*

Article Info:
Received:
19 November 2018
Revised:
15 August 2019
Accepted:
27 August 2019
Available online:
26 September 2019

Keywords:
MSW
MFA-LCA
Kinetic models
Gasification
Downdraft moving bed
Fluidized bed

ABSTRACT
This paper presents the development of a comprehensive gasification module designed to be integrated in a MFA-LCA framework. From existing gasification models present in the literature, the most appropriate modelling strategy is selected and implemented into the module. This module needs to be able to capture the influence of input parameters, such as gasification reactor type, oxidizing agent, feedstock composition and operating conditions on the process outputs, including syngas yield, its composition and LHV, as well as tar and char contents. A typical gasification process is usually modelled in four steps: drying, pyrolysis, oxidation and reduction. Models representing each of these steps are presented in this paper. Since the type of gasification reactor is taken into account in the module, models for downdraft moving bed and bubbling fluidized bed reactor are also reviewed. The gasification module will be integrated into a MFA framework (VMR-Sys), which enables calculation of relevant gasifier feedstock parameters, such as moisture content, composition, properties and particle size distribution. Outputs from the module will also include elemental compositions obtained from VMR-Sys calculations. Finally, all outputs from the module will be used to build LCA-inventory data.

1. INTRODUCTION

In most developed countries, recyclables have been collected separately for several decades. More recently, source-sorted collections of organics are being implemented, with the aim of recycling this fraction of Municipal Solid Waste (MSW) through anaerobic digestion and composting. Once recyclables and organics are diverted and reintroduced into the circular economy, other recovery loops need to be implemented to deal with the remaining waste stream, often referred to as refuse. At the moment, this stream is mostly disposed of in landfills, but still contains valuable resources (e.g. recyclables and organic wastes) and a potential for energy recovery. Thermochemical treatments, which are characterized by an important waste reduction in mass (70-80%) and in volume (80-90%), appear to be interesting options to recover either resources or energy from the refuse stream (Arena, 2012). More precisely, gasification appears to be particularly well suited to convert a great variety of waste components present in the refuse stream into a quality syngas, appropriate for multiple applications: combined heat and power (CHP), production of valuable chemicals and fuels (Arena, 2012).

Several tools are used in waste management planning to guide decisions. In the past few years, Material Flow Analysis (MFA) gained in popularity as a decision-making tool. MFA models are able to predict output stream characteristics of a given waste treatment process and may be combined with a Life Cycle Assessment (LCA) in order to estimate environmental impacts of a given waste management system. However, since transfer coefficients from empirical data are often used in LCA inventory databases to model material conversions in treatment plants, effects of input stream characteristics and operating conditions are not taken into accounts. In order to capture these effects, a gasification model based on constitutive equations (mass and energy balances, reaction kinetics, transport phenomena) need to be developed. Therefore, the aim of this work is to select the most appropriate modelling strategy in order to develop a comprehensive gasification module designed to be integrated in a MFA-LCA framework.

1.1 Abbreviations and symbols

ABM	Agent-Based Model
CHP	Combined heat and power

* Corresponding author:
Robert Legros
email: robert.legros@polymtl.ca

https://doi.org/10.31025/2611-4135/2019.13850
© 2018 Cisa Publisher. Open access article under CC BY-NC-ND license

CRVMR	Chaire de Recherche sur la Valorisation des Matières Résiduelles
CSTR	Continuous stirred tank reactor
DST	Decision Making Tool
MSW	Municipal solid waste
LCA	Life cycle assessment
LHV	Lower heating value
PFR	Plug flow reactor
WMS	Waste Management Systems

List of symbols

A_j	Pre-exponential factor of reaction j (1/s)
A_c	Reactor cross sectional area (m^2)
a_c	Particle volumetric surface area (1/m)
C_i	Concentration of component i ($kmol/m^3$)
Cp_i	Specific heat constant of component i (J/kmol.K)
D_i	Diffusivity of component i (m^2/s)
d_p	Particle diameter (m)
E_j	Activation energy of reaction j (J/kmol)
F_i	Molar flow of component i (kmol/s)
f_P	Pyrolysis fraction
k_j	Kinetic rate constant of reaction j (m/s)
k_{m_i}	Mass transfer coefficient of component i (m/s)
L	Reactor length (m)
ΔH_{Rxj}	Heat of reaction of reaction j (J/kmol)
M	Molecular weight (kg/kmol)
m_0	Initial fuel mass (kg)
m_∞	Final fuel mass at t=∞ (kg)
n_i	Number of moles of component i (kmol)
r_j	Reaction rate of reaction j ($kmol/m^3s$)
R	Universal gas constant (J/kmol.K)
Sh_i	Sherwood number of component i (-)
U_0	Superficial gas velocity (m/s)
U_{mf}	Minimum fluidization velocity (m/s)
U_t	Terminal velocity (m/s)
V	Volume of the reactor (m^3)
X	Extent of conversion (-)
Y_i	Mass fraction of component i (-)

Greek letters

ε	Void fraction (-)
ρ_g	Gas density (kg/m^3)
ρ_s	Solid density (kg/m^3)
τ	Residence time (s)
v_{ij}	Stoichiometric coefficient of component i in reactions j
v	Volumetric flow rate (m^3/s)
v_0	Initial volumetric flow rate (m^3/s)
μ_g	Gas viscosity (kg/m.s)
ω	Order of reaction

Subscripts

0	Initial
b	Bed
D	Drying step
g	Gas phase
i	Species
j	Reactions
O	Oxidation step
P	Pyrolysis step
R	Reduction step
s	Solid
T	Total

1.2 Gasification process

During the gasification process, the combustible fraction of MSW is mostly converted into carbon monoxide (CO), hydrogen (H_2) and methane (CH_4) (Arena, 2012). These three gases are the main constituents of syngas. The syngas may also contain vapor, carbon dioxide (CO_2), large amounts of nitrogen (N_2) in the case of air-blown gasifier, and a wide variety of non-desirable components (e.g. H_2S) (Sikarwar et al., 2016). In addition to these gases, solid residues such as char and ash are also formed during gasification, which are both composed of elemental carbon, minerals and metals (Klinghoffer et al., 2011). While char contains mainly elemental carbon, ash is primarily composed of minerals and metals, with minimal elemental carbon (Klinghoffer et al., 2011). Depending on the MSW feedstock, the quality of the syngas may greatly vary (Sikarwar et al., 2017). The effects of MSW moisture content, chemical composition and particle size on the gasifier outlet streams are discussed in the following sections.

1.3 MSW moisture and ash content

MSW components are separated into wet and dry materials, based on their water contents. Dry combustible materials such as plastics, textiles, rubber, leather and wood are characterized by a water content of 0-30%. Wet combustible materials, such as green residues, food and other organic wastes usually contain 40-90% of water. Dry non-combustible materials such as metals, glasses and other inorganic compounds do not contain water and are considered inert (Themelis et al., 2002). The allowable feedstock moisture content depends on the type of reactor. In this study, only downdraft moving bed and bubbling fluidized bed reactors are considered. Downdraft reactor can handle feedstock characterized by less than 20% moisture content, while bubbling fluidized bed reactor feedstock must not exceed 55% moisture content (Arena, 2012). Therefore, in order to meet reactors criteria in terms of moisture content, wet combustible materials should be removed or partially dried before entering the gasification. Finally, the fraction of dry non-combustibles in the feedstock should also be removed prior to the process to reduce its fraction below 20% (Bailie et al., 1997; Themelis et al., 2002; US department of Energy, 2008).

1.4 MSW chemical composition

Since MSW may contain element traces such as sulfur (S) chlorine (Cl) and nitrogen (N), the produced syngas may contain contaminants such as hydrogen sulfide (H_2S), carbonyl sulfide (COS), hydrochloric acid (HCl), ammonia (NH_3) and hydrogen cyanide (HCN) (Sikarwar et al., 2016; US department of Energy, 2008). Furthermore, due to traces of alkali metals in MSW, syngas may also contain traces of sodium (Na) and potassium (K) (Sikarwar et al., 2016). H_2S causes equipment corrosion, while NH_3, HCl and trace

metals contribute to deactivation of catalysts used in the syngas downstream conversion (Sikarwar et al., 2016). MSW feedstock may also contain fluorine (F), arsenic (As) and phosphorus (P), known as catalyst poisons for liquid fuels synthesis processes, as well as volatile metals such as cadmium (Cd) and mercury (Hg, known as potential catalyst poisons and are particularly difficult to remove (US department of Energy, 2008). Finally, the produced syngas from MSW gasification may also contain particulates and tars (Sikarwar et al., 2016). Presence of tars can lead to equipment blockages (Sikarwar et al., 2016). The two types of reactors reviewed in this work, fluidized bed and downdraft moving bed reactors, are selected because of their performance in reducing the amount of tar emitted. In fact, fluidized bed produces tar concentration in syngas of the order of 10 g/m^3, while downdraft moving bed reactor produces tar concentration around 1 g/m^3 of syngas (Milne et al., 1998; Basu, 2013).

1.5 MSW particle size

Feedstock particle size distribution has direct impacts on the syngas yield (Sikarwar et al., 2016). In fact, with smaller particles, fluid-particle heat transfer is improved and gasification rate is enhanced exponentially (Sikarwar et al., 2016). Higher heat transfer resistance caused by larger particles results in higher residual char yield, due to incomplete pyrolysis (Lv et al., 2004). Finer particles may be elutriated from fluidized beds before complete conversion, thus reducing gasification efficiency and increasing fly ash. In addition a reduction in particle size also increases H_2 yield and decreases tar production (Hernándezet al., 2010; Luo et al., 2009; Sikarwar et al., 2016). Therefore, in order to improve the syngas quality, pretreatment including removing or shredding/compacting of large waste articles should be considered before the gasification process (US department of Energy, 2008). Downdraft moving bed reactors can treat particles as large as 50 mm, while fluidized bed reactors usually accept smaller particles of the order of 6 mm (Basu, 2013), although some bubbling fluidized bed reactors have overbed feeding of very large particles.

1.6 Context

The present work aims at developing a comprehensive gasification process module, to be integrated in a Mass Flow Analysis and Life Cycle Assessment (MFA-LCA) framework. The Chaire de Recherche sur la Valorisation des Matières Résiduelles (CRVMR, Research Chair on Advanced Waste Recovery) at Polytechnique Montreal, is currently developing a methodology to assess the sustainability of Waste Management Systems (WMS), based on the integration of three distinct tools:

- VMR-Gen: Agent-Based Model (ABM) to predict the behaviour of the waste generator, providing the MSW flows and compositions of the source-sorted waste streams;
- VMR-Sys: MFA based framework to calculate waste and products flows and stocks throughout the WMS. Comprehensive process modules, one for each waste treatment technology, are developed and integrated into this framework;
- VMR-Imp: Waste LCA modelling to evaluate the WMS impacts.

The VMR-Sys tool is composed of different process modules (e.g. composting, anaerobic digestion, etc.) all tied together by a MFA calculation framework. Detailed results from VMR-Sys are then used to build the LCA-inventory in VMR-Imp tool. Imbedded in the MFA framework VMR-Sys, the gasification process module will receive detailed information on the feedstock, such as its moisture content, composition and particle size distribution and will capture the influence of a variation of waste flows or compositions for different types of gasification reactors (downdraft moving bed or bubbling fluidized bed). Based on the type of reactor selected, the module will identify the required sets of feedstock properties and thus provide targets for the pretreatment sequence of operations, as shown in Figure 1. The gasification module will then predict the output results in terms of syngas yield, composition and lower heating value (LHV) as well as the composition of tar and char. These outputs will be used in VMR-Imp to build the LCA-inventory data. In order to build a gasification process module, models for each step of the process (drying, pyrolysis, reduction and oxidation) and for the reactor hydrodynamics must be selected. A survey of available modelling strategies is presented in section 2.

2. LITERATURE REVIEW

Typically, gasification processes are separated into four steps: drying, pyrolysis, oxidation and reduction. Figure 2 presents the simplified input and output streams for each step, with their respective chemical compositions. Descriptions of the different modelling approaches for each gasification step and each reactor type are presented in the next sub-sections.

2.1 Gasification process

2.1.1 Drying step

The first step of the gasification process consists of drying. Since the drying characteristic time is considerably shorter than other reaction times in the overall gasification process, this step is often assumed to be instantaneous (Di Blasi, 2000). Stoichiometric relations are the simplest ways to represent the phenomena. In this approach, it is assumed that a fixed fraction of water initially contained in the feedstock is evaporated. The produced vapor is directly added to the other gas components, without the use of kinetic models (Gupta & Bhaskaran, 2018). For example, in the study of Gerber et al. (2010) it is assumed that 10% of the water contained in the feedstock is evaporated.

In order to consider the effects of temperature on the drying yield, kinetically controlled models are used. A typical drying kinetic model is presented in Eq. 1, where r_D, A_D, E_D, T_D and $C_{H_2O(l)}$ represent the evaporation rate (kmol/m^3.s), the pre-exponential drying factor (1/s), the activation energy of water evaporation (J/kmol), the drying temperature

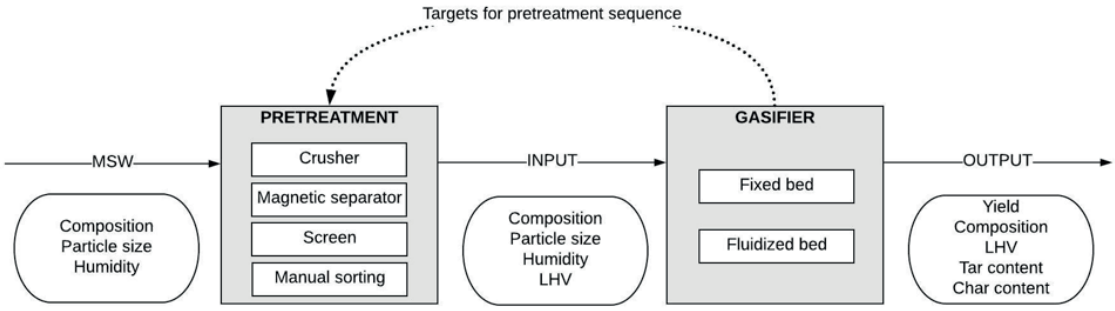

FIGURE 1: Gasification module structure.

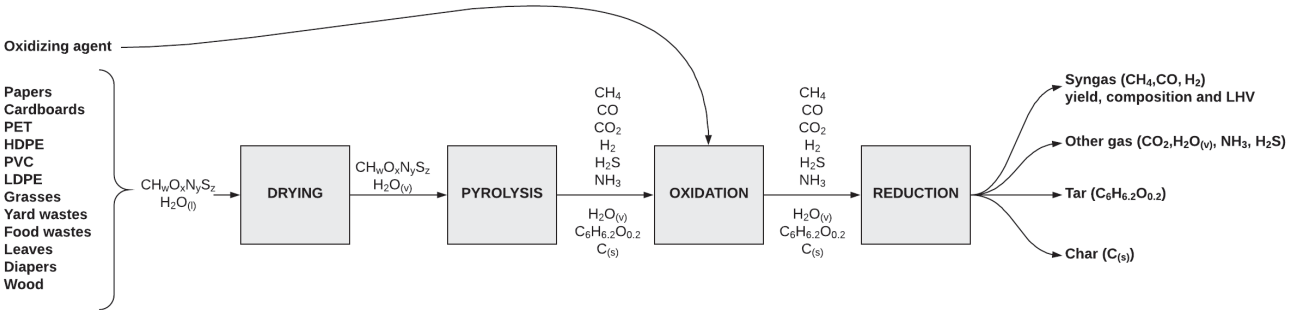

FIGURE 2: Chemical inputs and outputs of the four steps of the gasification process: drying, pyrolysis, oxidation and reduction.

(K) and the water concentration (kmol/m^3), respectively (Salem & Paul, 2018). Constant temperature or a certain temperature profile may be used to describe the drying step. For example, a temperature of 400K is used in the study of Salem & Paul (2018) while a temperature profile ranging from 368K to 473K is used by Dejtrakulwong & Patumsawad (2014).

$$r_D = A_D exp\left(-\frac{E_D}{RT_D}\right) C_{H_2O_{(l)}} \quad (1)$$

Other drying models exist in the literature. For example, in studies by Di Blasi & Branca (2013) and Sharma (2011), a diffusion controlled process is used to describe the drying step. In such models, evaporation rate is limited by vapor diffusion throughout the particle pores (Shokri & Or, 2011). Finally, an isothermal evaporation process is used in a study by Gerber & Oevermann (2014). In this model, the evaporation process is described by a lumped method at a constant evaporation temperature (373K), where a certain amount of water is evaporated over a short time period (Gerber & Oevermann, 2014; Gupta & Bhaskaran, 2018). Since this process is usually very rapid, its kinetic is often neglected.

2.1.2 Pyrolysis step

Once water is partially evaporated, the feedstock is devolatilized into volatiles, tar and char (Sharma, 2011). In the literature, pyrolysis fraction (f_P) and kinetic models are used to describe the mass loss. In the most simplified models, pyrolysis is assumed to occur instantaneously at the feeding location, along with the drying step (Gupta & Bhaskaran, 2018). In a study by Giltrap et al. (2003), the pyrolysis fraction f_P is introduced in order to represent the degree of devolatilization of an instantaneous pyrolysis process. A f_P of zero indicates no pyrolysis while a f_P of one indicates that feedstock is completely devolatilized into volatiles, tar and char (Giltrap et al., 2003). A f_P of 0.5 is assumed in a study by Giltrap et al. (2003).

Devolatilization process described by a kinetic model is shown in Eq. 2, where m_0, m_∞, X and ω represent the feedstock mass at t=0 (kg), the feedstock mass at t=∞ (kg), the extent of conversion and the order of reaction, respectively (Grammelis et al., 2009; Gupta & Bhaskaran, 2018). The reaction rate constant is expressed by the Arrhenius reaction rate.

$$-\frac{dm}{dt} = (m_0 - m_\infty) \cdot A_P exp\left(\frac{-E_P}{RT}\right)(1-X)^\omega \quad (2)$$

Several pyrolysis kinetic models exist, such as the one-step global model, the one-stage multi-reaction model and the two-stage semi-global model (Gupta & Bhaskaran, 2018; Sheth & Babu, 2006). These pyrolysis models are presented in Table 1, where n represents the number of moles and K_p represents the kinetic rate constant (Di Blasi, 2000; Gupta & Bhaskaran, 2018; Sheth & Babu, 2006). In the one-step global model, pyrolysis is considered as a single-step reaction, where volatiles, tar and char are produced simultaneously (Gupta & Bhaskaran, 2018). On the other hand, in the one-stage multi-reaction model, pyrolysis is represented with several simultaneous competing reactions. Finally, in the two-stage semi-global model, pyrolysis is considered as a two-stage reaction, where the final product (primary tar) of the first reaction produces a secondary tar (Sheth & Babu, 2006).

While pyrolysis fraction f_P and kinetic models predict the mass loss of the solids, other models are used to estimate the volatiles composition (Sharma et al., 2006). In the literature, volatiles usually comprise CO, CO_2, H_2, H_2O, CH_4,

TABLE 1: Pyrolysis kinetics models used in the gasification process modelling (Babu & Sheth, 2006; Di Blasi, 2000; Gupta & Bhaskaran, 2018).

Models	Equations
One-step global model	$n_{Fuel} \xrightarrow{k_{P1}} n_{volatiles} + n_{Tar} + n_{Char}$
One-stage multi-reactions model	$n_{Fuel} \xrightarrow{k_{P2,1}} n_{volatiles}$
	$n_{Fuel} \xrightarrow{k_{P2,2}} n_{Tar}$
	$n_{Fuel} \xrightarrow{k_{P2,3}} n_{Char}$
Two stage semi-global model	$n_{Fuel} \xrightarrow{k_{P3,1}} n_{volatiles,1} + n_{Tar,1} + n_{Char}$
	$n_{Tar,1} \xrightarrow{k_{P3,2}} n_{volatiles,2} + n_{Tar,2}$

as shown in Eq. 3 (Sharma et al., 2006).

$$n_{Fuel} \xrightarrow{pyrolysis} n_{H_2} + n_{H_2O} + n_{CO} + n_{CO_2} + n_{CH_4} + n_{Tar} + n_{Char} \quad (3)$$

In order to predict pyrolysis product compositions, different methods are used. For example, in a study by Giltrap et al. (2003), an equivalent amount of CO, H_2O and CH_4 was assumed. Other studies use experimental data to estimate the composition. For example, in the work of Di Blasi (2000), experimental data on gasification of wood chips and rice husks are used to estimate the volatiles distribution in terms of CO, CO_2, H_2, H_2O and CH_4.

Other studies such as that by Tinaut et al. (2008) use the method suggested in the work of Thunman et al. (2001), where a set of equations composed of elementary balances and enthalpy balances is solved for the mass fractions of volatile species. Experimental data for ratios of CO/CO_2 and C_xH_y/CO_2 are used to solve the system (Sharma et al., 2006; Thunman et al., 2001).

Finally, in the work of Sharma et al. (2006), a model describing the biomass devolatilization in terms of cellulose, hemicellulose and lignin is used. In order to solve the system of equations composed of elementary balances, experimental ratios of CO/CO_2, H_2O/CO_2 and CH_4/CO_2 are used (Sharma et al., 2006). These ratios are presented in Eq. 4, Eq. 5 and Eq. 6, where represents the mass fraction (Sharma et al., 2006). To close the system of equations, mass fractions of cellulose, hemicellulose and lignin are used as input information to solve for n_{Char}. In the model, it is considered that each of these constituents of dry and ash-free biomass decomposed into a fixed fraction of char and volatiles (Sharma, 2011). Transformation of sulfur (S) and Nitrogen (N) atoms initially contained in the solid are not taken into account in these studies.

$$Y_{CO}/Y_{CO_2} = exp\left(-1.845 + \frac{7730.3}{T_P} - \frac{5019898}{T_P^2}\right) \quad (4)$$

$$Y_{H_2O}/Y_{CO_2} = 1 \quad (5)$$

$$Y_{CH_4}/Y_{CO_2} = 5.10^{-16} \cdot T_P^{5.06} \quad (6)$$

2.1.3 Oxidation step

After the pyrolysis step, volatiles, tar and char are oxidized by reacting with an oxidizing agent (either pure oxygen or air in this work) or with each other (e.g. water-gas shift reaction) (Gupta & Bhaskaran, 2018). The reaction rates of homogeneous reactions and heterogeneous reactions involving char, are presented in Table 2.

In the literature, different approaches are used to predict the oxidation yield. Since all oxidation reaction rates are faster by a few orders of magnitude than those of char reduction reactions, the oxidation step is often assumed to be instantaneous (Babu & Sheth, 2006; Giltrap et al., 2003; Sharma, 2011). For example, in the studies by Giltrap et al.(2003) and Babu & Sheth (2006) an instantaneous and complete oxidation process was assumed at the feeding location.

Other studies, such as the one by Sharma (2011) and Salem & Paul (2018), use a heuristic approach to predict the oxidation yield. In this approach, the oxidation and pyrolysis products are allowed to react with the oxidizing agent available, in a sequence of descending order of reaction rates (Sharma, 2011). Reaction rates listed in Table 2 are only used as a guide to establish the sequence of oxidation reactions described below:

1. Oxidation of hydrogen (reaction O-4)
2. Oxidation of carbon monoxide (reaction O-2)
3. If oxygen remains, the oxidation of methane takes place (reaction O-3)
4. If oxygen still remains, char and tar are oxidized simultaneously according to their reaction rates (reactions O-1 and O-5)

Finally, in studies by Di Blasi & Branca (2013) and Tinaut et al. (2008), kinetic models are used to predict the quantity of gases produced during the oxidation step. Reaction rates presented in Table 2 are used to represent the kinetics of homogeneous reactions (O-2, O-3, O-4, O-5 and WG).

2.1.4 Reduction step

After the oxidation step, the products go through the reduction step in an oxidant-free environment. This step is primarily dominated by heterogeneous reactions, where the char is converted into gaseous products (Gupta & Bhaskaran, 2018). Reactions occurring during the reduction step are presented in Table 3.

These heterogeneous reduction reactions involve the diffusion of a variety of gases (O_2, CO_2, H_2O, H_2) from the bulk gas phase to the outer surface and then into the pores of the char particles (Gupta & Bhaskaran, 2018). As the char reacts, its particle size decreases while its porosity increases, leading to more active sites available for the gas to react and, as a result, to an increase of the extent of reaction (Sharma, 2011). In order to capture these effects, the unreacted shrinking core model, as well as the char reactivity factor model, are used in the literature. The unreacted shrinking core model is described by Eq. 7, where k_j, C_i, a_c and k_{mi} represent the kinetic constant (m/s) of the heterogeneous reactions presented in Table 3, the concentrations (kmol/m^3) of the species i (O_2, CO_2, H_2O, H_2), the particle volumetric surface area (1/m) and the mass transfer coefficient (m/s) for the species i, respectively (Di Blasi, 2000).

$$r_j = a_c \frac{C_i}{\left(\frac{1}{k_{mi}}\right) + \left(\frac{1}{k_j}\right)} \quad (7)$$

Equation of the particle volumetric surface area (a_c) is presented in Eq. 8, where ε and d_p represent the bed void-

TABLE 2: Chemical reaction rates in oxidation zone (Sharma, 2011; Tinaut et al., 2008).

	Reactions	Reaction rates (mol/m³s)
O-1	$C + 0.5O_2 \xrightarrow{k_{O1}} CO$	$r_{O1} = 0.554exp\left(-\frac{89\,990}{RT}\right)[C_{O_2}]$
O-2	$CO + 0.5O_2 \xrightarrow{k_{O2}} CO_2$	$r_{O2} = 1.3x10^8 exp\left(-\frac{166\,280}{RT}\right)[C_{CO}][C_{O_2}]^{0.25}[C_{H_2O,v}]^{0.5}$
O-3	$CH_4 + 1.5O_2 \xrightarrow{k_{O3}} CO + 2H_2O$	$r_{O3} = 9.2x10^6 exp\left(-\frac{80\,230}{RT}\right)T[C_{O_2}][C_{CH_4}]^{0.5}$
O-4	$H_2 + 0.5O_2 \xrightarrow{k_{O4}} H_2O$	$r_{O4} = 1x10^{11} exp\left(-\frac{42\,000}{RT}\right)[C_{O_2}][C_{H_2}]$
O-5	$C_6H_{6.2}O_{0.2} + 2.9O_2 \xrightarrow{k_{O5}} 6CO + 3.1H_2$	$r_{O5} = 59.8exp\left(-\frac{101\,430}{RT}\right)TP^{0.3}[C_{O_2}][C_{Tar}]^{0.5}$
WG	$CO + H_2O \xrightarrow{k_{WG}} CO_2 + H_2$	$r_{WG} = 2.78exp\left(-\frac{12\,600}{RT}\right)\left[C_{co}C_{H_2O,v} - \frac{C_{CO_2}C_{H_2}}{k_{eq}}\right]$ $k_{eq} = 0.0265exp\left(-\frac{32\,900}{RT}\right)$

TABLE 3: Chemical reaction rates in reduction zone (Tinaut et al., 2008).

	Reactions	Reaction rates (mol/m³s) & Reaction rate constants (m/s)	
R-1	$C + CO_2 \xrightarrow{k_{R1}} 2CO$	$r_{R1} = a_c\left(\frac{k_{R1}k_{m,CO_2}}{k_{R1} + k_{m,CO_2}}\right)[C_{CO_2}]$	$k_{R1} = (3.42 \cdot T)exp\left(-\frac{129\,700}{RT}\right)$
R-2	$C + H_2O \xrightarrow{k_{R2}} CO + H_2$	$r_{R2} = a_c\left(\frac{k_{R2}k_{m,H_2O}}{k_{R2} + k_{m,H_2O}}\right)[C_{H_2O}]$	$k_{R2} = 1.67k_{R1}$
R-3	$C + 2H_2 \xrightarrow{k_{R3}} CH_4$	$r_{R3} = a_c\left(\frac{k_{R3}k_{m,H_2}}{k_{R3} + k_{m,H_2}}\right)[C_{H_2}]$	$k_{R3} = 0.001 \cdot k_{R1}$
R-4	$CH_4 + H_2O \xrightarrow{k_{R4}} CO + 3H_2$	$r_{R4} = 3015exp\left(-\frac{125\,520}{RT}\right)[C_{CH_4}][C_{H_2O,v}]$	

age and the particle diameter (m) (Di Blasi, 2000).

$$a_c = \frac{6(1-\varepsilon)}{d_p} \quad (8)$$

The mass transfer coefficient k_{m_i} is defined by Eq. 9, where D_i and Sh_i represent the diffusivity coefficient of species i in the gaseous boundary layer (m^2/s) and the Sherwood number obtained from correlation involving Reynold and Schmidt numbers for species i (Fogler, 2016).

$$k_{m_i} = \frac{D_i}{d_p}\mathrm{Sh}_i \quad (9)$$

In the literature, a second approach to model heterogeneous reactions consists of the use of a char reactivity factor (CRF). This approach is specifically used in the case of downdraft moving bed gasifier as it directly represents the reactivity of the char along the moving bed (Babu & Sheth, 2006). CRF is used as a multiplier of the pre-exponential factor present in the reaction rates presented in Table 4. In the work of Giltrap et al. (2003), a constant CRF value of 1000 is proposed. In the study by Babu & Sheth (2006), an exponential increment of CRF along the length of the reactor is suggested in order to avoid rapid reaction completion at the beginning of the reduction zone.

2.2 Reactor hydrodynamics

Depending on the number of dimensions being considered, hydrodynamics models can be classified into zero-dimensional, one-dimensional, two-dimensional or three-dimensional models (Basu, 2010). Characteristics of these models are shown in Table 5. In the following sections, selected models are presented for the downdraft moving bed reactor and for the fluidized bed reactor.

2.2.1 Downdraft moving bed reactors

Pressure and temperature profiles exist along the length of downdraft moving bed reactors. In this type of reactors, the bed pressure drop is proportional to the gas velocity (Levenspiel & Kunii, 2012). Assuming that the reactor operates under steady state conditions and that there is no radial gradients in concentrations, temperature and reaction rates, the downdraft moving bed may be approximated as a plug flow reactor (PFR) (Fogler, 2016). This assumption is mostly valid for large reactors and caution should be applied in the case of small downdraft gasifiers. A few studies, such as those by Di Blasi (2000), Giltrap et al. (2003) and Tinaut et al. (2008), use this type of approximation for downdraft reactors.

2.2.2 Fluidized bed reactors

Fluidized bed reactors are widely used in the industry due to excellent heat and mass transfers, followed by uniform temperature distribution and concentrations throughout the reactor volume (Bandara et al., 2017). It is often considered that the temperature remains constant within the fluidized bed, and that the gas pressure drop across the bed of particles remains constant (Rhodes, 2008).

Since fluidized bed reactors are well mixed, they are often assumed to be analogous to continuous stirred tank reactors (CSTR), resulting in no spatial variation of concentra-

TABLE 4: Reduction reactions used with char reactivity factor (Babu & Sheth, 2006).

	Overall reaction rates (mol/m³s)
R-1	$r_{R1} = CRF \cdot 3.616x10^4 exp\left(-\frac{77\,390}{RT}\right)\left[P_{CO_2} - \frac{P_{CO}^2}{k_{eq,1}}\right]$
R-2	$r_{R2} = CRF \cdot 1.517x10^7 exp\left(-\frac{121\,620}{RT}\right)\left[P_{H_2O} - \frac{P_{CO}P_{H_2}}{k_{eq,2}}\right]$
R-3	$r_{R3} = CRF \cdot 4.189exp\left(-\frac{19\,210}{RT}\right)\left[P_{H_2}^2 - \frac{P_{CH_4}}{k_{eq,3}}\right]$
R-4	$r_{R2} = CRF \cdot 73.01exp\left(-\frac{36\,150}{RT}\right)\left[P_{CH_4}P_{H_2O} - \frac{P_{CO}P_{H_2}^3}{k_{eq,4}}\right]$

TABLE 5: Hydrodynamic models present in literature (Bandara et al., 2017; Fogler, 2016; Liu et al., 2013).

Models	Characteristics
Zero-dimensional (stirred tank reactor)	Algebraic equations
One-dimensional (plug flow)	Differential equations with respect to volume or catalyst mass
Two-dimensional Three-dimensional	Conservation of mass, momentum and energy: • Euler-Euler approach: - Solid and gas: continuous, Navier-Stokes equation - Transport properties of solids: kinetic theory of granular flow • Eulerian-Lagrange approach: - Gas phase: continuous, Navier-Stokes equation - Solid phase: Newtonian equation of motion for each individual particle

tions, temperature and reaction rates (Fogler, 2016). It must be noted that modelling fluidized bed reactors as CSTR may give relatively accurate results, higher precision results usually require complex models that capture more closely the hydrodynamics of such reactors (Fogler, 2016). These effects may be roughly captured by a single-phase PFR model, which considers the gas flowing through the bed in manner similar to a PFR, assuming an average bed voidage, an uniform solid distribution and that high particle mixing and high superficial gas velocities are reached (Mostoufi et al., 2001). Two-phase models are used for higher precision, where the bubbles and the emulsion phases are either represented with CSTR in series, PFR, or with a combination of CSTR and PFR (Jafari et al., 2004). The latter are the most common type of two-phase models used, where the bubble phase is modelled as a PFR and the emulsion phase as a CSTR (Jafari et al., 2004). Other more complex models also exist in the literature, such as three-phase models, capturing the interactions of the bubbles, emulsion and cloud phases (Levenspiel & Kunii, 2012).

3. GASIFICATION MODULE DEVELOPMENT

Keeping with the aim of developing a flexible, yet accurate gasification module capable of capturing the effect of reactor types, simplified models for the drying, pyrolysis, oxidation and reduction steps are selected. Since characteristic times for moisture evaporation, devolatilization and oxidation are considerably shorter than those for char reduction, these processes are often considered to be instantaneous (Di Blasi, 2000). Therefore, stoichiometric relations are used to represent these steps.

3.1 Drying model

An evaporation of 10% of the water initially contained in the MSW is assumed during the drying step. Water content of MSW is provided by VMR-Sys.

3.2 Pyrolysis model

Since the reaction is assumed to be instantaneous and complete, a pyrolysis fraction of 1 is assumed in order to predict the solids mass loss during the pyrolysis step. Therefore, all of the carbon (C), oxygen (O) and hydrogen (H) atoms initially contained in the MSW are transformed into CO, CO_2, CH_4, $H_2O_{(v)}$, H_2 and char during this step. Itis also assumed that the nitrogen (N) and sulfur S) atoms contained initially in the MSW are transformed into NH_3 and H_2S during this step (Sikarwar et al., 2016).

To take into account the effects of MSW composition, the devolatilization of MSW is described by the breakdown of cellulose, hemicellulose and lignin (Sharma, 2011). The contents of cellulose, hemicellulose and lignin of different MSW components are presented in Table 6. To consider the plastics fraction of the MSW, the feedstock is also separated into HDPE, LDPE, PP, PS, PVC and PET.

Having the MSW composition of plastics, cellulose, hemicellulose and lignin provided by VMR-Sys, the distribution of CO, CO_2, H_2, H_2O, CH_4 is predicted for a certain char yield. In order to predict the amount of char produced, pyrolysis char yields of different plastics and organic fractions of the MSW are used. These fractions are presented in Table 7.

3.3 Oxidation model

Since it is assumed to be instantaneous, a heuristic approach is chosen to describe the reaction sequence during the oxidation step. In this step, the effects of the oxidizing agent type and quantity are taken into account.

3.4 Reduction model

In order to capture the effects of the MSW particle size for both the downdraft reactor and the bubbling fluidized bed reactor in the reduction step, the unreacted shrinking core model is chosen. Particle size distribution is provided by VMR-Sys in order to calculate the overall reaction rate.

3.5 Hydrodynamics models

Keeping with the aim of developing a flexible, yet accurate gasification module capable of capturing the effect of

TABLE 6: Cellulose, hemicellulose and lignin contents (wt.% dry) of organic fraction of MSW (Agarwal et al., 2014; Couhert et al., 2009; Komilis & Ham, 2003; Wang et al., 2015).

	Cellulose	Hemicellulose	Lignin
Papers	64.7	13.0	0.9
Cardboards	59.7	13.8	14.2
Grasses	59.0	38.0	3
Yard wastes	26.82	10.23	24.54
Food wastes	46.09	0.0	12.03
Leaves	9.48	3.24	33.88
Diapers	33.7	4.6	-
Wood	49.8	20.8	26.7

TABLE 7: Pyrolysis char yield (wt%) of different plastics (HDPE, LDPE, PP, PS, PVC, PET) and organic constituents (cellulose, hemicellulose, lignin) (Sharma, 2011; Williams & Williams, 1999).

	HDPE	LDPE	PP	PS	PVC	PET	Cellulose	Hemicellulose	Lignin
Char yield	0	0	0.2	3.5	13.8	15.6	5	10	55

reactor types, simplified reactor models are selected. The downdraft moving bed reactor is modelled as a PFR, while the fluidized bed reactor is approximated as a single-phase model using a CSTR.

3.5.1 Plug flow reactor model

Since the drying, pyrolysis and oxidation steps are assumed to be instantaneous at the feeding location, oxidation products represent the initial molar flows F_{i0} of the reactor (kmol/s). In a PFR, concentrations, temperature, pressure and velocity vary along the reactor length. In order to capture the variation of molar flows along the length, the design equation of the PFR is used. This equation is shown in Eq. 10, where v_{ij} represents the stoichiometric coefficient of species i in reactions j and A_c represents the cross-sectional area of the reactor (m^2) (Fogler, 2016).

$$\frac{dF_i}{dz} = A_c \sum \nu_{ij} r_{ij} \tag{10}$$

Since gas-phase reactions are present in the reduction zone, concentrations are expressed in terms of temperature and pressure, as shown in Eq. 11 (Fogler, 2016). Having the inlet molar flows (F_{i0}), the entrance volumetric flow rate v_0 (m^3/s) can be obtained.

$$C_i = \frac{F_{T0}}{v_0}\frac{F_i}{F_T}\frac{P}{P_0}\frac{T_0}{T} \tag{11}$$

The initial temperature (T_0) and pressure (P_0) for the model are those of the gas coming out of the oxidation zone. Assuming no work and an adiabatic reactor, the temperature profile along the length is described by Eq. 12, where Cp_i and ΔH_{Rxj} represent the mean heat capacity of species i (J/kmol.K) and the heat of reaction of reactions j (J/kmol) (Fogler, 2016).

$$\frac{dT}{dz} = \frac{A_c \sum r_j \Delta H_{Rxj}}{\sum F_i Cp_i} \tag{12}$$

The pressure drop across the reduction zone can be evaluated by the Ergun equation, presented in Eq. 13, where μ_g, ρ_g and U_0 represent the gas viscosity (kg/m.s), the gas density (kg/m^3) and the superficial gas velocity (m/s) (Fogler, 2016).

$$\frac{dP}{dz} = 150\frac{(1-\varepsilon)^2 \mu_g U_0}{\varepsilon^3 d_p^2} + 1.75\frac{(1-\varepsilon)\rho_g U_0^2}{\varepsilon^3 d_p} \tag{13}$$

The interstitial gas velocity profile (U_g) is expressed in Eq. 14 and the superficial gas velocity profile is shown in Eq. 15 (Di Blasi & Branca, 2013; Rhodes, 2008).

$$\frac{dU_g}{dz} = \frac{1}{\rho_g}\sum_i \sum_j \nu_{ij} M_i r_j \tag{14}$$

$$\frac{dU_0}{dz} = \varepsilon \frac{dU_g}{dz} \tag{15}$$

Since the char particles shrink during the reduction step, the particle diameter d_p decreases with respect to the char mass loss, as shown in Eq. 16, which assumes spherical particles (Sharma, 2011). Assuming a constant bed voidage and particle density, a decrease in the particle diameter causes a decrease in the solid velocity (Di Blasi & Branca, 2013). The void fraction is expressed in Eq. 17, where ρ_b and ρ_s represent the bed density (kg/m^3) and the particle density (kg/m^3) (Rhodes, 2008). Finally, the solid velocity profile is presented in Eq. 18, where r_j only takes into account the heterogeneous reactions (Di Blasi & Branca, 2013).

$$d_p = \sqrt[3]{d_{p0}^3 \frac{F_{char}}{F_{char_0}}} \tag{16}$$

$$\varepsilon = 1 - \frac{\rho_b}{\rho_s} \tag{17}$$

$$\frac{dU_s}{dz} = -\frac{M_{Char}}{\rho}\sum_j r_{j_{Char}} \tag{18}$$

3.5.2 Continuous stirred tank reactor model

The design equation of a CSTR is shown in Eq. 19 (Fogler, 2016). Gas-phase concentrations used in reaction rates are expressed in Eq. 11. The entrance volumetric flow rate υ_0 (m^3/s) is assumed to be the volumetric flow rate of the gas produced during the oxidation step, since drying, pyrolysis and oxidation steps are assumed to be instantaneous.

$$V = \frac{F_{i0} - F_i}{-r_i} \tag{19}$$

The initial temperature (T_0) and pressure (P_0) for the model are those of the MSW entering the CSTR. The uniform temperature of the fluidized bed (T) is calculated with Eq. 20, assuming no work and an adiabatic reactor (Fogler, 2016). Since the pressure drop can be approximated as the apparent bed weight, Eq. 21 is used, where L represent the bed height (m) (Rhodes, 2008).

$$T = T_0 + \frac{V \sum r_{ij} \Delta H_{Rxij}}{\sum F_i Cp_i} \tag{20}$$

$$\Delta P = L(1-\varepsilon)(\rho_s - \rho_g)g \tag{21}$$

Assuming a constant bed voidage and particle density, particle shrinkage causes a decrease in the solid velocity (Di Blasi & Branca, 2013). In order to calculate the particle diameter and the bed voidage, Eq. 16 and Eq. 17 are used (Rhodes, 2008; Sharma, 2011). In order to predict the residence time of the MSW in both gasifiers, Eq. 22 is used, where τ represents the residence time (s) (Fogler, 2016).

$$\tau = \frac{V}{v_0} \tag{22}$$

3.6 Elements partitioning

In order to complete the mass balance for the gasification process, all non-reactive elements must be partitioned between the outlet gas and solids streams. This is achieved by partitioning the non-reactive elements that are tracked by the VMR-Sys using coefficients obtained from different studies. A compilation of these partitioning hypotheses is presented in Table 8.

TABLE 8: Partitioning of non-reactive elements (Arena & Di Gregorio, 2013; Clarke & Sloss, 1992; Gupta & Bhaskaran, 2018; Jung et al., 2005; Kamińska-Pietrzak & Smoliński, 2013; Tanigaki & Ishida, 2014; Vejahati, et al., 2010; Wilk et al., 2011).

	Group 1	Group 1-2	Group 2	Group 2-3	Group 3
Elements	Fe, K, Mn, Al	Ba, Be, Co, Cr, Cu, Mo, Ni,	As, Ca, Na, P, Pb, S, Si, Sn, Tl, Zn	B, Se	Br,Hg, I, F, Cl, N
Hypothesis	0.25: Fly Ash 0.75: Bottom Ash	0.5: Fly Ash 0.5: Bottom Ash	0.75: Fly Ash 0.25: Bottom Ash	0.5: Fly Ash 0.5: Gas	1: Gas

4. VALIDATION OF THE GASIFICATION MODULE PREDICTIONS

The predictions obtained with the gasification module are validated with the syngas compositions of CO, N_2, H_2, CH_4 and CO_2 presented in two experimental studies: 1. Jayah et al. (2003), with wood as feedstock; 2. Garcia-Bacaicoa et al. (2008), with a mixture of wood and HDPE as feedstock. Both studies were carried out in pilot scale fixed beds operating under a co-current mode. Characteristics of these flows and the operating conditions are presented in Table 9.

Predicted syngas composition from the module are presented in Figure 3 for the two experimental sets of conditions. It can be seen that the predictions agree generally well with results obtained in the two experimental studies. For the comparison with the experimental results from by Jayah et al., (2003), the elementary compositions in terms of C, H, O, N, S and volatile materials, fixed carbon, ash and wood moisture content presented in their work were used. It is possible to observe good agreement between the module predictions and the experimental results for CO_2, CH_4 and CO, while larger amounts of H_2 are predicted.

With regard to comparison between the module predictions and the experimental results presented in the work of Garcia-Bacaicoa et al., (2008), where the feedstock was composed of wood mixed with HDPE, the elementary compositions were determined using data provided by VMR-Sys since they were not provided by the authors. This enabled a first validation of the integration between the gasification module and the MFA-LCA framework. The results are very encouraging as seen in Figure 3. However, looking at the data presented in Figure 3, it is possible to see that the module predicts larger amounts of H_2 and CO_2 and lower amounts of CO. This could be attributed to the fact that the elementary compositions describing wood and HDPE provided by VMR-Sys might be slightly different from the actual elementary compositions of the feedstocks used in this study.

TABLE 9: Composition of feedstocks and gasifier operating conditions for two experimental studies.

	1 (Jayah et al., 2003)	2 (Garcia-Bacaicoa et al., 2008)
Feedstock	**Wood**	**17.4% HDPE 82.6% Wood**
Flowrate dry basis (kg/h)	18.6	30.9
Moisture content (%)	14.7	25.0
Solids density (kg/m3)	330	450
Mean particle size (m)	0.055	0.02
Gasifier diameter (m)	0.9	0.44
Gasifier height (m)	0.3	2.0
Air flowrate (kg/h)	34.6	62.1
Drying zone temperature (K)	373	395
Pyrolysis zone temperature (K)	873	634
Oxydation zone temperature (K)	1273	1365
Reductio zone temperature (K)	1173	1084
Oxydant	Air	Air

In regard to the larger quantities of H_2 predicted by the module compared with the experimental results, this may be explained by the limitations associated with the Water-Gas Shift (WGS) reaction in the reduction zone to adequately predicts the balance of CO, CO_2, H_2O and H_2. Since the WGS reaction is characterized by slow reaction kinetics, very little H_2 and CO_2 are converted into CO and H_2O. These effects therefore slightly increase the H_2/CO ratio and reduce the H_2/CO/CO_2 ratio of the syngas produced. However, given the general consistency of the module predictions with the two experimental studies used for data validation, it is reasonable to conclude that the developed gasification module offers a very useful tool to be integrated in a MFA-LCA framework since it is able to capture the influence of feedstock composition and properties, together with the operating conditions of the gasifier.

5. CONCLUSIONS

In order to develop a comprehensive gasification process module to be integrated in a MFA-LCA framework, a review of available models was presented. The gasification process was divided into four steps: drying, pyrolysis, oxidation and reduction. Drying, pyrolysis and oxidation are assumed to be instantaneous. Four models representing the drying step were presented: stoichiometric relations, kinetic models, diffusion-controlled models and isothermal evaporation processes. Instantaneous evaporation of 10% of the initial water contained in the MSW was assumed during the drying step. For the pyrolysis step, two approaches to model the mass loss were presented, that is kinetics models and pyrolysis fraction (f_p). The latter was chosen. To predict the distribution of CO, CO_2, H_2, H_2O, CH_4, tar and char, a few methods were presented. To take into account the effects of MSW composition, the devolatilization of MSW described by the breakdown of cellulose, hemicellulose and lignin was chosen. All of the nitrogen (N) and sulfur (S) initially contained in the MSW are assumed to be completely transformed into NH_3 and H_2S during the pyrolysis step. Three approaches were presented to model the oxidation step: stoichiometric conversion, heuristic and kinetic models. The heuristic approach that takes into account a sequence of reactions,

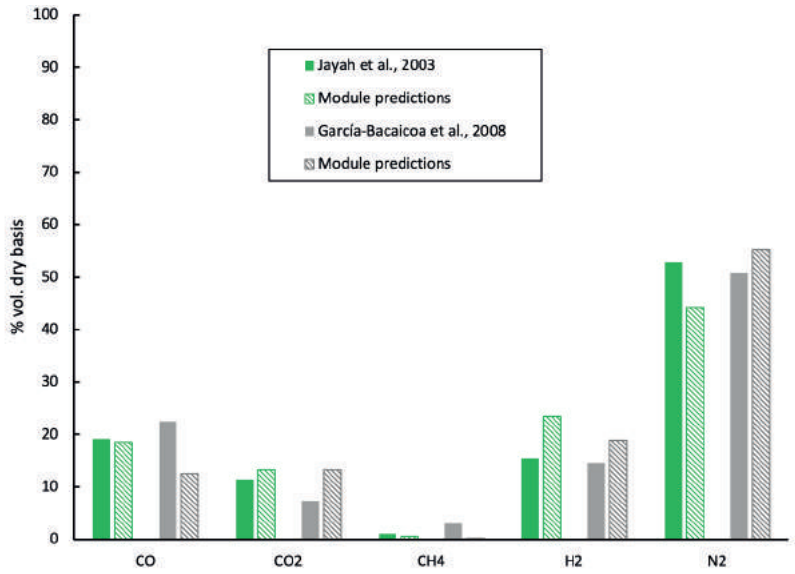

FIGURE 3: Comparisons between the gasification module predictions and experimental results from Jayah et al. (2003) and Garcia-Bacaicoa et al. (2008).

was chosen for this step. Two approaches were presented for the reduction step: the unreacted shrinking core model and the char reactivity factor model. The former model was selected since this model may be applied for both PFR and CSTR reactors, while the latter is specific to PFR only. Finally, the downdraft moving bed reactor was approximated as a PFR, while the fluidized bed reactor was approximated as a CSTR. Water content, MSW composition and average particle size are provided by VMR-Sys as inputs to the gasification module. The module predicts syngas yield, composition and LHV as well as the tar and char contents as functions of the oxidizing agent, operating conditions, reactor types and feedstock composition. The next step will be to integrate this gasification module into VMR-Sys, hence providing a more robust mean of building LCA-inventory data for VMR-Imp.

REFERENCES

Agarwal, G., Liu, G., & Lattimer, B. (2014). Pyrolysis and Oxidation of Cardboard. Fire Safety Science, 11, 124–137. https://doi.org/10.3801/IAFSS.FSS.11-124

Arena, U. (2012). Process and technological aspects of municipal solid waste gasification. A review. Waste Management, 32(4), 625–639. https://doi.org/10.1016/j.wasman.2011.09.025

Arena, U., & Di Gregorio, F. (2013). Element partitioning in combustion- and gasification-based waste-to-energy units. Waste Management, 33(5), 1142–1150. https://doi.org/10.1016/j.wasman.2013.01.035

Babu, B. V., & Sheth, P. N. (2006). Modeling and simulation of reduction zone of downdraft biomass gasifier: Effect of char reactivity factor. Energy Conversion and Management, 47(15), 2602–2611. https://doi.org/10.1016/j.enconman.2005.10.032

Bailie, R. C., Everett, J. W., Liptak, B. G., Liu, D. H. F., Rugg, F. M., & Switzenbaum, M. S. (1997). Solid waste. In Environmental Engineers' Handbook (Second Edition). Boca Raton: CRC Press. Retrieved from https://www.taylorfrancis.com/books/9781584888598

Bandara, J., Eikeland, M., & Moldestad, B. M. E. (2017). Analyzing the effects of particle density, size, size distribution and shape for minimum fluidization velocity with Eulerian-Lagrangian CFD simulation (pp. 60–65). Presented at the Proceedings of the 58th Conference on Simulation and Modelling (SIMS 58) Reykjavik, Iceland, September 25th – 27th, 2017. https://doi.org/10.3384/ecp1713860

Basu, P. (2010). Gasification Theory and Modeling of Gasifiers. In Biomass Gasification Design Handbook (pp. 117–165). Elsevier. https://doi.org/10.1016/B978-0-12-374988-8.00005-2

Basu, P. (2013). Biomass Gasification, Pyrolysis and Torrefaction: Practical Design and Theory. San Diego, UNITED STATES: Elsevier Science & Technology. Retrieved from http://ebookcentral.proquest.com/lib/polymtl-ebooks/detail.action?docID=1319046

Clarke, L. B., & Sloss, L. L. (1992). Trace elements - emissions from coal combustion and gasification. London: IEA Coal Research.

Couhert, C., Commandre, J.-M., & Salvador, S. (2009). Is it possible to predict gas yields of any biomass after rapid pyrolysis at high temperature from its composition in cellulose, hemicellulose and lignin? Fuel, 88(3), 408–417. https://doi.org/10.1016/j.fuel.2008.09.019

Dejtrakulwong, C., & Patumsawad, S. (2014). Four Zones Modeling of the Downdraft Biomass Gasification Process: Effects of Moisture Content and Air to Fuel Ratio. Energy Procedia, 52, 142–149. https://doi.org/10.1016/j.egypro.2014.07.064

Di Blasi, C. & Branca, C. (2013). Modeling a stratified downdraft wood gasifier with primary and secondary air entry. Fuel, 104, 847–860. https://doi.org/10.1016/j.fuel.2012.10.014

Di Blasi, C. (2000). Dynamic behaviour of stratified downdraft gasifiers. Chemical Engineering Science, 55(15), 2931–2944. https://doi.org/10.1016/S0009-2509(99)00562-X

Fogler, H. S. (2016). Elements of chemical reaction engineering: H. Scott Fogler (Fifth edition). Prentice Hall.

Garcia-Barcaicao, P., Mastral, J.F., Ceamanos, J., Berrueco, C., and Serrano, S. (2008). Gasification of biomass/high density polyethylene mixtures in a downdraft gasifier. Bioresource Technology, 99(13), 5485-91. https://doi.org./10.1016/j.biortech.2007.11.003

Gerber, S., Behrendt, F., & Oevermann, M. (2010). An Eulerian modeling approach of wood gasification in a bubbling fluidized bed reactor using char as bed material. Fuel, 89(10), 2903–2917. https://doi.org/10.1016/j.fuel.2010.03.034

Gerber, S., & Oevermann, M. (2014). A two dimensional Euler–Lagrangian model of wood gasification in a charcoal bed – Part I: model description and base scenario. Fuel, 115, 385–400. https://doi.org/10.1016/j.fuel.2013.06.049

Giltrap, D. L., McKibbin, R., & Barnes, G. R. G. (2003). A steady state model of gas-char reactions in a downdraft biomass gasifier. Solar Energy, 74(1), 785–791. https://doi.org/10.1016/S0038-092X(03)00091-4

Grammelis, P., Basinas, P., Malliopoulou, A., & Sakellaropoulos, G. (2009). Pyrolysis kinetics and combustion characteristics of waste recovered fuels. Fuel, 88(1), 195–205. https://doi.org/10.1016/j.fuel.2008.02.002

Gupta, S., & Bhaskaran, S. (2018). Numerical Modelling of Fluidized Bed Gasification: An Overview. In S. De, A. K. Agarwal, V. S. Moholkar, & B. Thallada (Eds.), Coal and Biomass Gasification (pp. 243–280). Singapore: Springer Singapore. https://doi.org/10.1007/978-981-10-7335-9_10

Hernández, J. J., Aranda-Almansa, G., & Bula, A. (2010). Gasification of biomass wastes in an entrained flow gasifier: Effect of the particle size and the residence time. Fuel Processing Technology, 91(6), 681–692. https://doi.org/10.1016/j.fuproc.2010.01.018

Jafari, R., Sotudeh-Gharebagh, R., & Mostoufi, N. (2004). Modular Simulation of Fluidized Bed Reactors. Chemical Engineering & Technology, 27(2), 123–129. https://doi.org/10.1002/ceat.200401908

Jaya, T.H., Aye, L., Fuller, R.J., and Stewart, D.F. (2003). Computer simulation of a downdraft wood gasifier for tea drying. Biomass and Bioenergy, 25(4), 459-469. https://doi.org/10.1016/S0961-9534(03)0037-0

Jung, C.H., Matsuto, T., & Tanaka, N. (2005). Behavior of metals in ash melting and gasification-melting of municipal solid waste (MSW). Waste Management, 25(3), 301–310. https://doi.org/10.1016/j.wasman.2004.08.012

Kamińska-Pietrzak, N., & Smoliński, A. (2013). Selected Environmental Aspects of Gasification and Co-Gasification of Various Types of Waste. Journal of Sustainable Mining, 12(4), 6–13. https://doi.org/10.7424/jsm130402

Klinghoffer, N., Castaldi, M. J., & Nzihou, A. (2011). Beneficial use of ash and char from biomass gasification. In Proceedings of the 19th Annual North American Waste-to-Energy Conference NAWTEC19. Lancaster, Pennsylvania, USA. Retrieved from http://citeseerx.ist.psu.edu/viewdoc/download?doi=10.1.1.471.6269&rep=rep1&type=pdf

Komilis, D. P., & Ham, R. K. (2003). The effect of lignin and sugars to the aerobic decomposition of solid wastes. Waste Management, 23(5), 419–423. https://doi.org/10.1016/S0956-053X(03)00062-X

Levenspiel, O., & Kunii, D. (2012). Fluidization Engineering (2nd ed.). Elsevier.

Liu, H., Elkamel, A., Lohi, A., & Biglari, M. (2013). Computational Fluid Dynamics Modeling of Biomass Gasification in Circulating Fluidized-Bed Reactor Using the Eulerian–Eulerian Approach. Industrial & Engineering Chemistry Research, 52(51), 18162–18174. https://doi.org/10.1021/ie4024148

Luo, S., Xiao, B., Guo, X., Hu, Z., Liu, S., & He, M. (2009). Hydrogen-rich gas from catalytic steam gasification of biomass in a fixed bed reactor: Influence of particle size on gasification performance. International Journal of Hydrogen Energy, 34(3), 1260–1264. https://doi.org/10.1016/j.ijhydene.2008.10.088

Lv, P. M., Xiong, Z. H., Chang, J., Wu, C. Z., Chen, Y., & Zhu, J. X. (2004). An experimental study on biomass air-steam gasification in a fluidized bed. Bioresource Technology, 95(1), 95–101. https://doi.org/10.1016/j.biortech.2004.02.003

Milne T.A., Evans R.J., Abatzoglou N. (1998). Biomass gasifier "tars": their nature, formation and conversion. National Renewable Energy Laboratory, Golden, CO, report no: NREL/TP-570-25357

Mostoufi, N., Cui, H., & Chaouki, J. (2001). A Comparison of Two- and Single-Phase Models for Fluidized-Bed Reactors. Industrial & Engineering Chemistry Research, 40(23), 5526–5532. https://doi.org/10.1021/ie010121n

Rhodes, M. J. (2008). Introduction to Particle Technology. Wiley. Retrieved from https://ebookcentral.proquest.com/lib/polymtl-ebooks/detail.action?docID=351230

Salem, A. M., & Paul, M. C. (2018). An integrated kinetic model for downdraft gasifier based on a novel approach that optimises the reduction zone of gasifier. Biomass and Bioenergy, 109, 172–181. https://doi.org/10.1016/j.biombioe.2017.12.030

Sharma, A.K. (2011). Modeling and simulation of a downdraft biomass gasifier 1. Model development and validation. Energy Conversion and Management, 52(2), 1386–1396. https://doi.org/10.1016/j.enconman.2010.10.001

Sharma, A.K., Ravi, M. R., & Kohli, S. (2006). Modelling product composition in slow pyrolysis of wood, 13.

Sheth, P. N., & Babu, B. V. (2006). Kinetic Modeling of the Pyrolysis of Biomass. In National Conference on Environmental Conservation (NCEC-2006) (pp. 453–458). Pilani, India.

Shokri, N., & Or, D. (2011). What determines drying rates at the onset of diffusion controlled stage-2 evaporation from porous media? Water Resources Research, 47(9). https://doi.org/10.1029/2010WR010284

Sikarwar, V. S., Zhao, M., Clough, P., Yao, J., Zhong, X., Memon, M. Z. & Fennell, P. S. (2016). An overview of advances in biomass gasification. Energy & Environmental Science, 9(10), 2939–2977. https://doi.org/10.1039/C6EE00935B

Sikarwar, V. S., Zhao, M., Fennell, P. S., Shah, N., & Anthony, E. J. (2017). Progress in biofuel production from gasification. Progress in Energy and Combustion Science, 61, 189–248. https://doi.org/10.1016/j.pecs.2017.04.001

Tanigaki, N., & Ishida, Y. (2014). Waste Gasification Technology with Direct Melting for Energy and Material Recovery, 14. Retrieved from http://www.vivis.de/phocadownload/Download/2014_wm/2014_wm_365_378_tanigaki.pdf

Themelis, N. J., Kim, Y. H., & Brady, M. H. (2002). Energy recovery from New York City solid wastes. Waste Management and Research, 20(3), 223–233. Retrieved from https://doi.org/10.1177/0734242X0202000303

Thunman, H., Niklasson, F., Johnsson, F., & Leckner, B. (2001). Composition of Volatile Gases and Thermochemical Properties of Wood for Modeling of Fixed or Fluidized Beds. Energy & Fuels, 15(6), 1488–1497. https://doi.org/10.1021/ef010097q

Tinaut, F. V., Melgar, A., Pérez, J. F., & Horrillo, A. (2008). Effect of biomass particle size and air superficial velocity on the gasification process in a downdraft fixed bed gasifier. An experimental and modelling study. Fuel Processing Technology, 89(11), 1076–1089. https://doi.org/10.1016/j.fuproc.2008.04.010

US department of Energy. (2008). Municipal Solid Waste (MSW) to Liquid Fuels Synthesis, Volume 1: Availability of Feedstock and Technology.

Vejahati, F., Xu, Z., & Gupta, R. (2010). Trace elements in coal: Associations with coal and minerals and their behavior during coal utilization – A review. Fuel, 89(4), 904–911. https://doi.org/10.1016/j.fuel.2009.06.013

Wang, X., De la Cruz, F. B., Ximenes, F., & Barlaz, M. A. (2015). Decomposition and carbon storage of selected paper products in laboratory-scale landfills. Science of The Total Environment, 532, 70–79. https://doi.org/10.1016/j.scitotenv.2015.05.132

Wilk, V., Aichernig, C., & Hofbauer, H. (2011). Waste Wood Gasification: Distribution of Nitrogen, Sulphur and Chlorine in a Dual Fluidised Bed Steam Gasifier, 9.

Williams, P. T., & Williams, E. A. (1999). Interaction of Plastics in Mixed-Plastics Pyrolysis. Energy & Fuels, 13(1), 188–196. https://doi.org/10.1021/ef980163x

detritus | Multidisciplinary Journal for Waste Resources & Residues

CISA

GRAIN SIZE-RELATED CHARACTERIZATION OF VARIOUS NON-HAZARDOUS MUNICIPAL AND COMMERCIAL WASTE FOR SOLID RECOVERED FUEL (SRF) PRODUCTION

Alexander Curtis *, Josef Adam, Roland Pomberger and Renato Sarc

Montanuniversitat Leoben Department fur Umwelt- und Energieverfahrentechnik Ringgold standard institution - Chair of Waste Processing Technology and Waste Management Franz-Josef-Strasse 18, Leoben 8700 Austria

Article Info:
Received:
21 June 2019
Revised:
18 July 2019
Accepted:
24 July 2019
Available online:
26 September 2019

Keywords:
Solid Recovered Fuel
Grain size-related characterization
Screening
Commercial waste
Municipal waste

ABSTRACT
This article deals with studies on the grain size-related characterization of various types of waste for the production of Solid Recovered Fuel (SRF) for the cement industry. By implementing a suitable combination of the mechanical processes and adjusting the proportions of the waste types used, different properties of SRF in certain parameters can be set. In addition to the process technology, the treated solid waste types themselves have the greatest impact on the final quality of SRF. Here, the practical investigation for the characterization of various grain size classes generated of different solid waste types (packaging waste and commercial waste) used for the production of SRF is described. These investigations have been divided into a series of tests (12) with an industrial waste screen and in further tests with a laboratory screen and chemical analyses of all of the produced grain size classes. The mass distribution of the investigated grain size classes for each type of waste show significant differences. As assumed, the parameters calorific value and dry mass content of all types of waste increase with growing grain size. For most heavy metals and chlorine, no clear trend can be shown. For example, nickel accumulates in the commercial waste types in the grain size class 0-20 mm, in the packaging waste in class > 65 mm. The data on waste input material and generation of proper input waste mix is required for production of quality assured and homogeneous SRF for energy recovery in cement industry.

1. INTRODUCTION

The introductory chapter describes in more detail the quality criteria for waste for the production of substitute fuels for use in the cement industry in Austria.

The cement production process is quite energy-intensive with 3,839 GJ per tonne of clinker (Mauschitz, 2018), which is why the search for alternatives for the standard fossil fuels such as coal has been going on for quite some time now. The thermal substitution rate, that is to say the share of energy from solid recovered fuels (SRF) that are burned instead of primary standard fuels (e.g. coal) in relation to the demand for energy in a cement production facility, was at 80.6% (Mauschitz, 2018) in the year 2017. In order to attain this high substitution rate, the input of energy in the cement production process must occur in several stages (primary firing, calciner firing, rotary kiln inlet) with various substitute fuels (Sarc et al., 2015). The SRF being used at the input positions must be adjusted with regard to its chemical (heavy metals, chlorine) and physical parameters (calorific value, grain size distribution).

On the one hand, the SRF used must meet the facility's own quality criteria as well as the criteria for the heavy metals (Sb, As, Pb, Cd, Cr, Co, Ni, and Hg) for the threshold values as per the Austrian Incineration Ordinance (AVV) (Bundeskanzleramt, 2010). The facility's own quality requirements for SRF are to ensure that even with a high degree of substitution both process stability and product quality are to be guaranteed. The demands on the SRF for use in the primary firing are particularly high. The input of SRF into the rotary kiln via the primary firing, is carried out pneumatically via a channel on the burner gun and this must incinerate completely within a quite brief retention time, during the trajectory. With an optimal burn-out, only incombustible fuel components (i.e. ashes) get into the clinker and are then utilized materially (from a technical point of view). Any changes in the fuel properties have an impact on the conveying characteristics, the dosing, the burn-out behaviour, the flame form, the flame temperature, the clinker quality, etc., and are thus able to be determined by means of si-

* Corresponding author:
Alexander Curtis
email: alexander.curtis@unileoben.ac.at

Detritus / Volume 07 - 2019 / pages 55-67
https://doi.org/10.31025/2611-4135/2019.13847
© 2019 Cisa Publisher. Open access article under CC BY-NC-ND license

mulations and practical tests and to be carefully coordinated with the operator of the cement facility. The demands on a calciner fuel are not as high, however, this SRF also has to fulfil many criteria (e.g. calorific value, chlorine content). For the production of SRF for the cement industry, the most various combustible materials are put to use. A large part of these are commercial waste of the most various pre-treatment intensity or residual fractions from sorting packaging waste. Further fundamental and subject-specific statements on the topic of the production of SRF for energy-oriented exhaustion in the cement industry as well as on the topic of quality assurance and the normal market qualities have been described and discussed by Lorber et al. (2012), Sarc et al. (2013), Sarc et al. (2014) and Aldrian et al. (2016). The aim of the present work was to determine the combustion properties as well as the concentration of heavy metals in different grain size classes in comparison to the legal limits for waste types suitable for SRF production.

2. MATERIALS AND METHODS

The extensive tests with an industrial screen were conducted between March and May 2018 on the premises of a waste treatment plant in Austria. The subsequent screening trials and chemical analyses of each of the individual screen fractions were conducted during the same time period in the laboratory of the Chair of Waste Processing Technology and Waste Management of the Montanuniversitaet Leoben.

2.1 Test Material

Four input materials important for SRF production were tested, whereby one of these was from packaging waste (PW): F1 (PW) and the other three materials were from mixed commercial waste (MCW): F2 (MCW 1), F3 (MCW 2), F4 (MCW 3) (note: F = fraction).

Quality assured, high-calorific and medium-calorific SRF ready for incineration for the use in the cement facilities are able to be produced from these input materials by means of suitable mechanical treatment steps.

2.1.1 F1 (Packaging Waste PW)

The fraction F1 is the sorting residue from the processing of plastic packaging waste. Due to the standardized collection and processing (defined requirements such as quotas) the material is rather homogeneous. The test material comes from several sorting facilities in Austria and neighbouring countries. Large plastic films, hollow items, metals and in part the fine contents (approx. 40 mm) are separated from the entire mixed packaging waste in the sorting process. The remaining sorting residue consists of smaller, partly more highly soiled sheets of plastic, paper, cardboard, small hollow plastic items which, due to the high plastic content, exhibits a high calorific value (> 20 MJ/kgOS).Performed Tests: T1, T2, T3.

2.1.2 F2 (Mixed Commercial Waste 1)

The fraction F2 consists of mixed commercial waste, household trash and bulky materials and comes from Austria. The material was subject to ground sorting, whereby approx. 10-15% recyclable material (wood, metals, rigid plastics (buckets used in the construction industry, etc.), plastic films and impurities (inert)) were separated and came from commercial enterprises in Graz and its surroundings. It contained high amounts of plastic films and fine contents. The material was quite inhomogeneous, which is something that was reflected in the results of the tests. Performed Tests: T5, T7, T8, T13.

2.1.3 F3 (Mixed Commercial Waste 2)

The fraction F3 consists of mixed processed commercial waste (Mixed Commercial Waste) and came from various processing facilities in neighbouring country 1. Most of the recyclable materials and impurities were already separated in the processing facilities. Performed Tests: T4, T6, T9.

2.1.4 F4 (Mixed Commercial Waste 3)

The fraction F4 consists of mixed commercial waste (Mixed Commercial Waste) and came from various processing facilities in neighbouring country 2. Most of the recyclable materials and impurities were already separated in the processing facilities. Performed Tests: T12, T14.

The individual tests conducted and the abbreviations used

Three to five screening trials each were conducted with each of the four input materials (F1 to F4, with two tonnes of test material for each test) with an industrial waste screen (IFE circular vibratory screen) with a screen deck with 65 mm screen cut and a screen deck with 10 mm mesh size. As has already been mentioned, additional screen categories were produced in the laboratory.

Each individual test was abbreviated with the letter T and in addition to that with a serial number (in chronological order) e.g.T12 (test number). A 2 tonne sample of the various types of waste (i.e. F1, F2, F3, and F4) was examined for each test. Since several individual tests were conducted for each type of waste, the name of the respective test materials is comprised of the name of the type of waste and the test number, e.g. F4 T12.

Examples (compare Figure 2):

F4 T12 is thus the test material of the total of the twelfth test and the first 2 tonne sample of the type of waste F4.

F4 T14 is thus the test material of the total of the fourteenth test and the second 2 tonne sample of the type of waste F4.

2.2 Methods

The following chapters describe the trial scheme, the test materials and the procedure for the implementation of the examinations on site and in the laboratory.

2.2.1 Test scheme

To obtain a better overview the following Figure 1 illustrates the process of the entire tests conducted.

2.2.2 Test Material

Initially sample material was collected from each type of waste (F1, F2, F3, F4) observed and placed in interme-

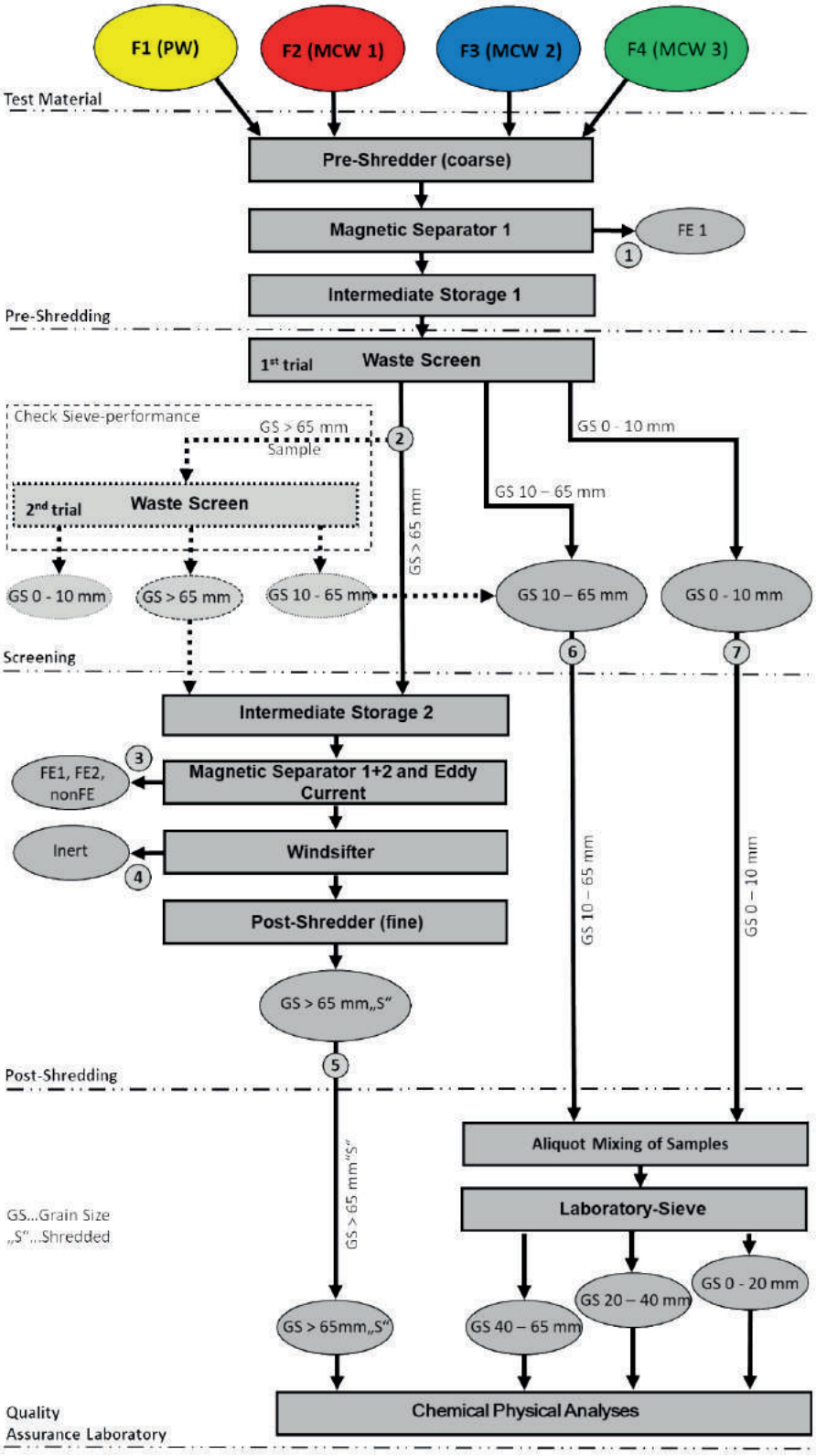

FIGURE 1: Trial scheme with locations of samples taken.

diate storage. Approx. two tonnes of test material was made available for each of the 12 observed tests.

2.2.3 Pre-Shredding

The previously described test materials were stored separately and pre-shredded coarsely using a pre-shredder (grain size (GS) ~ 350 mm), at the same time iron being separated using the magnetic separator 1 FE 1 (iron) and samples were taken at sampling location 1. The pre-shredded test material was weighed and placed in intermediate

storage 1.

The pre-shredder was a low speed device manufactured by the Lindner Recyclingtech Company.
Name: Meteor 2500
Screening basket: screening brace with 110 mm gap
Revolutions per minute: 50 rpm
Blade: Trapezoid blades in good condition

2.2.4 Screening

The test materials coarsely pre-shredded were taken from the intermediate storage bunker 1 and, using a wheel loader and with manual support (dosage) were transported on a conveyor belt to the waste screen. A mechanical dosage device, which guarantees even a dosage of the test materials used, will not be available on the market anytime in the near future (Feil et al., 2018). The quality of the manual dosage is not optimal, it is however, for lack of alternatives, the only possibility to place the material onto the circular vibratory screen fairly evenly. A direct interconnection of the pre-shredders with the circular vibratory screen was not possible for technical reasons. The possibility of using one of the additional shredders as a dosage device was discussed, however this idea was dismissed since the already pre-shredded material would have had to undergo an additional shredding step.

Waste screen used

The waste screen from the IFE Aufbereitungstechnik GmbH Company used is a double deck circular vibratory screen machine with waste screens (eight individual screen segments arranged in four stages) on the upper deck and the resonance system VARIOMAT with polymer screening mats on the lower deck.

Data and Name of the waste screen:
Name/Type: Waste Screen SMV 1200x4000 F-UW24
Unbalance shaft drive: P = 18.5 kW; n = 740 rpm
Frequency: f = 9 – 14 Hz
Total weight: mges = 6,300 kg
Vibrating mass: mvib = 4,170 kg

The width of the screening holes was 83 mm. Tilting the waste screen segments caused smaller effective screening holes (projected surface) which in this case corresponds to a 65 mm screen cut. Tests with the grain size GS 10-65 mm using these waste screening segments revealed that 95% of the particles were smaller than 65 mm. Thus, in the remaining part of the article the screen cut of 65 mm will be specified for these screening stages. The laboratory screening machine is specified with the actual screening hole diameter (20 mm and 40 mm).

The upper deck of the waste screen is equipped with eight screening segments and the total surface was 5 m². Six of the screening segments with a 65 mm screen cut had a screening surface area of 3.75 m², and two screening segments with 45 mm wide screening holes situated on the screening inlet, had a surface of 1.25 m².

On the lower deck there were polymer screening mats with squared screening holes of 10 mm built in (Resonance system VARIOMAT) (IFE Aufbereitungstechnik GmbH, 2019). The grain size GS 0 - 10 mm separated with the lower deck was caught by means of 600 Liter plastic boxes, taken into consideration in the weight assessment, mixed aliquot with the grain size GS 10-65 mm in the laboratory to create the grain size GS 0-65 mm for further lab screening.

Tests

The test duration was approx. 1 hour for the each of the two tonnes test materials, which corresponds to a screening throughput of 0.4 t/(m²*h). The throughput of the screening for these materials is approx. 0.8 t/(m²*h) according to the manufacturer.

The grain size GS 10 - 65 mm was transported via a conveyor belt and samples were able to be taken from the entire dropping area along the entire width with a 60 L box (sampling location 6 in Figure 1).

The entire oversize fraction GS > 65 mm (screen overflow) from each test and each trial (1st trial and 2nd trial) was caught directly at the screening outlet with the wheel loader scoop and weighed (sampling location 2 in Figure 1) and was placed in intermediate storage 2 for the subsequent post-shredding.

Check Sieve Performance

In order to determine, how much of the grain size GS 10 – 65 mm still remained in the grain size GS > 65 mm, a partial sample was taken (1 to 2 wheel loader scoops) of the grain size GS > 65 mm at the sampling location 2 (GS > 65 mm sample). This material was sieved a second time (2nd trial) at 65 mm (Figure 1). The remaining amount of material in the grain size GS > 65 mm, the grain size GS 10 - 65 mm, after the first screening throughput was determined with approx. 20 M-% for most of the tests. The fraction GS > 65 mm from this check was also collected in the intermediate storage bunker 2.

The impact of the second screening of a partial flow of the grain size GS > 65 mm (screen overflow) was insignificant.

A third screening cycle only exhibits quite a minor impact. Samples of the grain size GS 10-65 mm were taken from both screening cycles (1st trial and 2nd trial) and the rest were discarded. Since the circular vibratory screen used was equipped with an additional lower deck with 10 mm mesh size, separate samples of the partial flow of the grain size GS 0-10 mm (from the 1st trial and the 2nd trial) were taken in addition to that (sampling location 7 in Figure 1) and taken into consideration in the assessment (for more details see chapter 2.2.6 Quality Assurance Laboratory).

2.2.5 Post-Shredding

The post-shredding process step was carried out in order to be able to better sample the coarse fraction GS > 65 mm for later laboratory tests. A particle size analysis was not provided.

Process: The entire amount (1st trial and 2nd trial) of the grain size GS > 65 mm was taken from the intermediate storage bunker 2 for each individual trial, and fed via several separators (magnetic separator 1+2, Eddy current, wind sifter) to the (fine) post-shredder and shredded to a grain

size of < 10 mm (GS 0 - 10 mm). The fractions FE1, FE2, non-ferrous and inert were removed from the separators, weighed, samples were taken and the rest was discarded. The shredded material is labelled as GS > 65 mm„S“ („S“... shredded).

The shredded material GS > 65 mm“S“ from the post-shredder was discharged by means of a trough chain conveyor. The sample collection was carried out via a sampling flap (sampling location 5 in Figure 1). The rest was discarded.

Sampling locations and samples obtained from the waste screen and the post-shredder

The following samples were obtained during each trial: The sampling locations are shown in Figure 1.

- **Sampling location 1:** samples Fe-metals taken for the sorting analyses in the laboratory.
- **Sampling location 2:** a partial sample of one to two wheel loader scoops taken and sieved once again to determine the screening quality (check sieve performance) in a second cycle (2nd trial). The entire amount of the grain size GS > 65 mm from cycle one (1st trial) and cycle two (2nd trial) is collected in the intermediate storage bunker 2 and is subsequently shredded with a post-shredder to < 10 mm.
- **Sampling locations 3, 4:** weighing the material flows Fe, NonFE and inert and representative samples taken for the determining the metal content and the inert content in the laboratory.
- **Sampling location 5:** representative samples taken from the shredded grain size GS > 65 mm“S“ (S=shredded) for determining the chemical and physical fuel parameters in the laboratory.
- **Sampling location 6:** representative samples taken from the grain size GS 10-65 mm for screening analyses and determining the chemical and physical parameters of the individual screen categories in the laboratory.
- **Sampling location 7:** weighing the fine particles of the grain size GS 0-10 mm and representative samples taken. Aliquot dosage of the grain size GS 0-10 mm to the samples of the grain size GS 10-65 mm, subsequently screening analysis and after that chemical, physical analysis in the laboratory of the grain sizes obtained from the screening analysis.

2.2.6 Quality Assurance Laboratory

The samples of the grain sizes GS 10-65 mm and GS 0 - 10 mm were aliquotly mixed in the laboratory (aliquot mixing of samples) in a mass ratio, such as was obtained during the screening with the waste screen, causing the grain size GS 0-65 mm. The grain size GS 0-65 mm was subsequently sieved with a lab screen in the grain sizes GS 0-20 mm, GS 20-40 mm and GS 40-65 mm.

These grain sizes and the samples taken of the post-shredded material (post-shredder (fine)) GS > 65 mm“S“ were subject to chemical and physical analyses.

The chemical and physical analyses were conducted in the laboratory of the Chair of Waste Processing Technology and Waste Management at the Montanuniversitaet Leoben.

Determining the grain size distribution in the grain size GS 0 - 65 mm

The grain size GS 0 - 65 mm was sieved with a lab screening machine with the screening holes of 20 mm and 40 mm.

Resulting from the screening tests on site and the screening analyses in the laboratory are the following grain sizes: GS 0-20 mm, GS 20-40 mm, GS 40-65 mm, GS > 65 mm and GS > 65 mm”S” after shredding with the post-shredder.

Selecting the screening cuts/screening hole sizes was primarily based on the Austrian Standard ÖNORM EN 15415-1 (Austrian Standards Institute, 2011a). The standard fundamentally recommends a gradual doubling of the hole sizes or mesh size.

Technical data for the laboratory screening machine used

- Manufacturer: Fritsch, type AS 400 control;
- Dimensions: 400 x 530 x 650 mm (width x depth x height);
- Mass: approx. 11 kg (max), approx. 5 kg (empty);
- Sieve movement: uniform and circular (radius 15mm);
- Speed: 170-180min-1;
- Duration: 7-10min;
- Diameter test sieves: 400 mm.

Determining the metal and inert material contents in all material flows

In order to be able to determine the metal content (FE, nonFE) and inert portion, samples of the individual grain sizes were manually sorted.

Analyses

The individual grain sizes of each of the trial materials were subject to an in-depth chemical and physical analysis.

The calorific value was determined according to the standard DIN 51900-1 (Austrian Standards Institute, 2000). The inferior calorific value (Hi, TS) is determined at constant volume, the superior calorific value (Hs, TS) at constant pressure. The analyzes were carried out using a device from IKA (type C 7000). The superior calorific value is calculated from the experimentally determined inferior calorific value at constant volume. The calculation is carried out with a given correction factor of f = 0.92 according to the German RAL Quality Label Directive (May 2001). The conversion takes place according to Hs, TS = Hi, TS * 0.92.

The dry mass was determined according to the standard ÖNORM EN 14343 (Austria Standards Institute, 2007).

The heavy metals content (parameters AVV) was determined according to the standard ÖNORM EN 15411 (ICP-MS). (Austrian Standards Institute, 2011b).

AVV: Austrian Incineration Ordinance

3. RESULTS

The results of the screening trials on site and the lab tests are shown in detail in the following chapters.

3.1 Mass distribution of the individual grain sizes (grain size classes)

The mass distribution of the investigated grain size classes is shown as bars in Figure 2 for each type of waste and each test. After the individual tests the corresponding average values (arithmetic mean values) are shown for the respective type of waste (FiØ) as outlined bar determined in the tests.

The average distribution of the mass to the individual grain sizes for the individual types of waste is as follows:

F1Ø: 50% of the mass is in the grain size GS > 65 mm, 13 % in the grain size GS 40-65 mm, 19% in the grain size GS 20-40 mm and 17% in the grain size GS 0-20 mm. In contrast to the types of commercial waste F2-F4 the amount of the grain size GS < 65 mm of waste type F1 is higher. With tests on the pre-shredded type of waste F1 (Test T1, T2, T3) it can be seen that no noteworthy fluctuation in the mass distribution of the individual grain sizes appears between the individual tests. These types of waste are much more homogeneous than the types of commercial waste F2 and F3 due to the standardized collection defined and treatment given (sorting).

When treating these types of waste extensive sheets and hollow items are specifically separated, leaving only small-scale packaging film, screw tops and small hollow items.

F2Ø: 66% of the mass is in the grain size GS > 65 mm, 12 % in the grain size GS 40-65 mm, 10% in the grain size GS 20-40 mm and 13% in the grain size GS 0-20 mm. Great fluctuation appears in the mass distribution of the individual grain sizes between the individual tests.

F3Ø: 63% of the mass is in the grain size GS > 65 mm, 10 % in the grain size GS 40-65 mm, 12% in the grain size GS 20-40 mm and 15% in the grain size GS 0-20 mm. Similar to F2, great fluctuation appears in the mass distribution of the individual grain sizes between the individual tests.

F4Ø: 63% of the mass is in the grain size GS > 65 mm, 14 % in the grain size GS 40-65 mm, 9% in the grain size GS 20-40 mm and 14% in the grain size GS 0-20 mm. A greater fluctuation appears between the grain sizes 0-20 mm and 20-40 mm.

In contrast to type of waste F1 (Packaging Waste), there were many large plastic films in the Mixed Commercial Waste types F2, F3 and F4. When using a coarse pre-shredding the plastic films are often only pulled through the cut gap and the tooth gap of the shredders and thus are hardly shredded (selective crushing). This leads to a greater mass portion of the grain size GS > 65 mm in the types of waste F2, F3 and F4.

3.2 Calorific value and dry mass

In the following Figure 3 a) and b) the calorific values and the dry mass for each grain size and each test material are shown as a bar and the arithmetic mean value for the respective grain sizes are shown as framed bars. In addition, the weighted arithmetic mean values of the calorific values are marked with a dotted line for each type of waste (F1 to F4). It is calculated from the arithmetic mean value of the calorific values of the individual grain classes, taking into account the mass distribution on the individual grain classes.

The calorific value was calculated from the energy value taking the dry mass into consideration.

As is to be expected, the calorific value (arithmetic mean value) rises in most of the cases with the grain size.

- F1: the calorific value of 25.2 MJ/kg in the grain size GS 0-20 mm is the lowest. Contrary to expectations, the grain size 40-65 mm exhibits the highest value at 30.1 MJ/kg. The reason for this deviation was not able to be determined. Relatively large amounts of hollow items (beverage bottles) containing liquids can be found in the grain size GS > 65 mm and they might have a negative impact on the calorific value. In this case, the high dry substance content of 89% is an argument against that impact. As is to be expected, the type of waste F1 (packaging waste) exhibits the highest averages (weighted mean value) of calorific values in contrast to types of commercial waste in all grain sizes. The weighted arithmetic mean value of the calorific values is 28.2 MJ/kg;
- F2: the average calorific value at 11.4 MJ/kg in the grain size GS 0-20 mm is the lowest. The grain size GS > 65 mm exhibits the greatest calorific value at 22.5 MJ/kg. In trial T13 (F2 T13) with less than 6 MJ/kg, the type of waste F2 exhibits in the grain size 0-20 mm a quite low

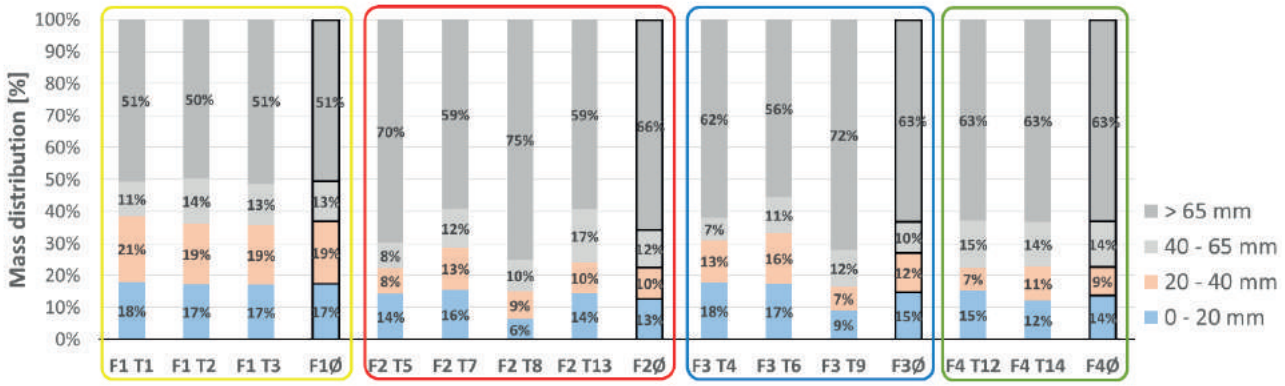

FIGURE 2: Results of the mass distribution of grain size (related to the original substance (OS)) for each waste type and test.

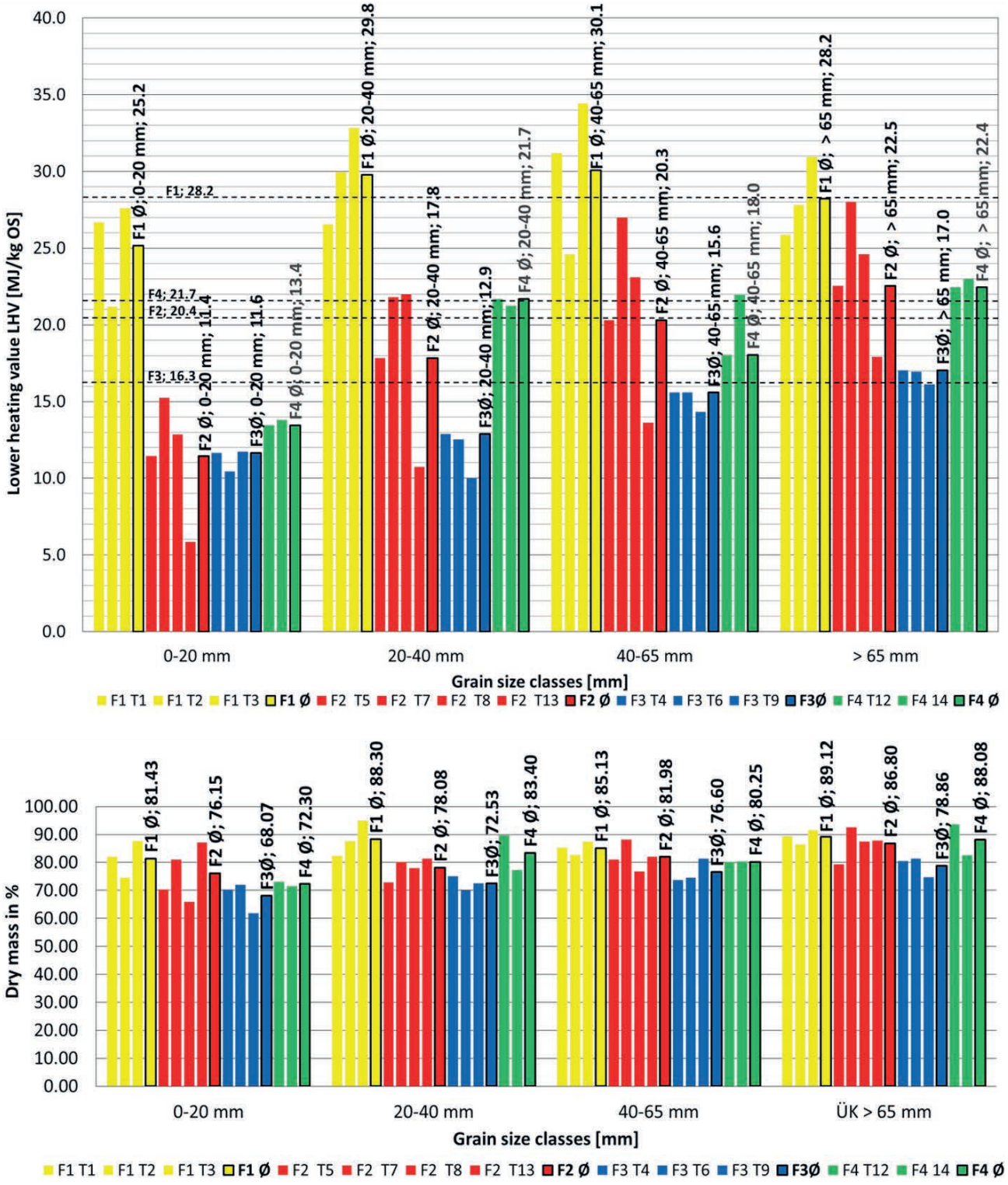

FIGURE 3: a) Results of the calorific values, and b) dry mass for each test material and grain size.

calorific value. The weighted arithmetic mean value of the calorific values is 20.2 MJ/kg;

- F3: the average calorific value at 11.6 MJ/kg is the lowest in the grain size GS 0-20 mm. The grain size GS > 65 mm exhibits the greatest calorific value at 17.0 MJ/kg. The fluctuation of the calorific values between the individual tests in the respective grain sizes are relatively low. The weighted arithmetic mean value of the calorific values is 16.3 MJ/kg;
- F4: the average calorific value at 13.4 MJ/kg in the grain size GS 0-20 mm is the lowest. The grain size GS > 65 mm exhibits the greatest calorific value at 22.4 MJ/kg. The fluctuation of the calorific values between the individual tests are quite low. The weighted arith-

metic mean value of the calorific values is 21.7 MJ/kg.

The dry substance (arithmetic mean value) rises in all types of waste with the grain size, as is to be expected. The fluctuation for the individual tests are low.

- F1: The dry substance is between 81.43% in the grain size GS 0-20 mm and 89.12% in the grain size GS > 65 mm. F1 has in all grain size classes the highest dry substance (arithmetic mean value) of all fractions;
- F2: The dry substance is between 76.15% in the grain size GS 0-20 mm and 86.80% in the grain size GS > 65 mm;
- F3: The dry substance is between 68.07% in the grain size GS 0-20 mm and 78.86% in the grain size GS > 65 mm;
- F4: The dry substance is between 72.3% in the grain size GS 0-20 mm and 88.08% in the grain size GS > 65 mm.

3.3 Chlorine

In Figure 4, the chlorine content for each grain size and each test material is shown as a bar and the arithmetic mean values of the chlorine are shown as framed bars.

In the grain size GS 20-40 mm the type of waste F4 exhibits the highest average concentration of chlorine at 4.4%. The type of waste F3 exhibits the lowest concentration in all grain size classes except GS > 65 mm. The types of waste F1 and F2 are in the range of 1%. Part of the chlorine content of the type of waste F1 comes from table salt that has remained in the sorting residue of the sorted packaging by clinging onto food packaging or food waste.

3.4 Metals

Table 1 summarizes the measured values for the heavy metals according AVV for each test material and grain size class. The values are given as % of the limit values.

3.4.1 Antimony

In the grain size GS 40-65 mm, the type of waste F4 exhibits the highest average values of antimony. The value rises with the grain size in the type of waste F1, and displays an erratic rise which is to be traced back to an accumulation of PET beverage bottles in this grain size. In the types of waste F2 and F3 the highest values are in the grain size GS > 65 mm as well. All of the values are below the threshold values of the AVV.

3.4.2 Arsenic

The type of waste F4 exhibits highest average values of arsenic at 14.2% for the threshold value in the grain size GS > 65 mm. All of the values are markedly less than the threshold values of the AVV.

3.4.3 Lead

The fraction F3 has the highest lead content across all grain size classes. At 216.4% the type of waste F3 exhibits the highest values of lead in the threshold value for the grain size GS 20-40 mm. The values of the other types of waste are less than the threshold value.

3.4.4 Cadmium

All of the values are markedly below the threshold values of the AVV. No clear trend is discernible.

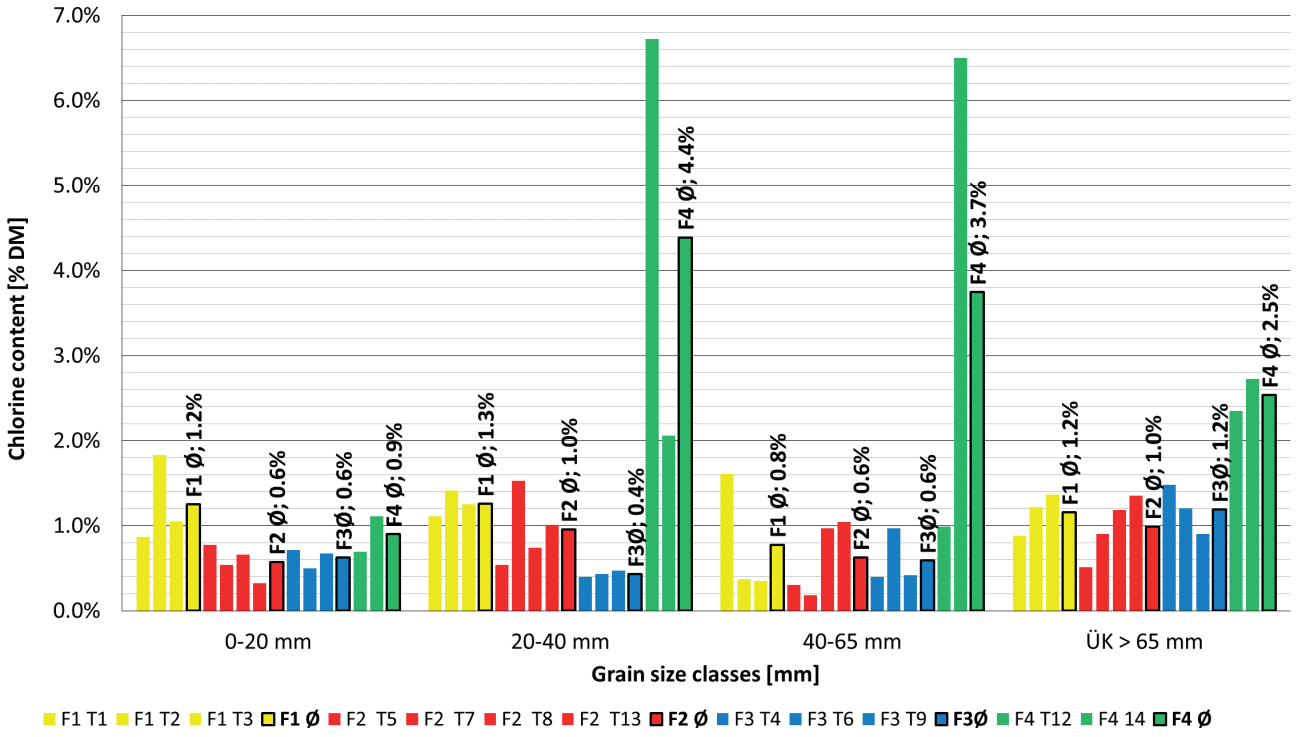

FIGURE 4: Results of the chlorine content [% DM] in each test material and particle grain size class.

TABLE 1: Results of the heavy metal content.

	% of limit value	F1 T1	F1 T2	F1 T3	F1Ø	F2 T5	F2 T7	F2 T8	F2 T13	F2 Ø	F3 T4	F3 T6	F3 T9	F3 Ø	F4 T12	F4 T14	F4 Ø
		%	%	%	%	%	%	%	%	%	%	%	%	%	%	%	%
Sb median: 7 [mg/MJ], 80th perzentile: 10 [mg/MJ]	0 - 20 mm	2,0	7,0	4,8	4,6	13,1	21,3	5,0	10,6	12,5	19,3	13,8	21,6	18,2	8,9	4,8	6,9
	20 - 40 mm	7,1	3,5	2,9	4,5	13,9	14,7	2,2	5,9	9,2	6,5	25,7	79,7	37,3	6,5	8,4	7,4
	40 - 65 mm	0,9	14,8	0,7	5,5	18,5	4,9	1,3	7,2	8,0	1,3	5,3	7,4	4,7	35,8	4,0	19,9
	> 65 mm	11,0	8,4	32,5	17,3	18,1	19,1	18,4	5,8	15,4	43,9	67,0	50,8	53,9	12,8	15,3	14,1
As median: 2 [mg/MJ], 80th perzentile: 3 [mg/MJ]	0 - 20 mm	2,6	2,9	2,6	2,7	9,5	5,0	4,3	30,8	12,4	4,6	5,7	4,4	4,9	14,7	4,5	9,6
	20 - 40 mm	2,6	2,4	2,4	2,5	3,6	3,1	3,0	37,9	11,9	3,9	4,7	12,8	7,1	3,4	6,3	4,8
	40 - 65 mm	2,3	2,8	2,1	2,4	3,9	2,7	2,8	14,9	6,1	3,7	4,0	4,7	4,1	4,7	3,1	3,9
	> 65 mm	2,9	2,6	2,5	2,6	3,4	2,8	3,0	4,4	3,4	3,7	4,0	3,9	3,9	25,4	3,0	14,2
Pb median: 20 [mg/MJ], 80th perzentile: 36 [mg/MJ]	0 - 20 mm	1,2	2,1	5,8	3,0	18,2	6,5	10,5	39,4	18,7	4,8	7,3	89,2	33,7	15,5	8,9	12,2
	20 - 40 mm	0,6	1,6	8,8	3,7	1,3	3,9	3,4	15,2	6,0	1,7	7,3	640,1	216,4	7,5	1,5	4,5
	40 - 65 mm	0,3	2,1	0,6	1,0	1,0	3,1	1,4	16,7	5,6	1,5	2,9	102,6	35,7	56,8	1,1	29,0
	> 65 mm	3,9	2,4	13,1	6,5	3,9	8,3	16,7	7,5	9,1	10,5	6,0	48,6	21,7	10,9	4,9	7,9
Cd median: 0.45 [mg/MJ], 80th perzentile: 0.7 [mg/MJ]	0 - 20 mm	2,9	1,3	3,6	2,6	2,6	8,4	1,8	12,2	6,2	6,6	2,5	4,4	4,5	3,6	1,9	2,7
	20 - 40 mm	1,1	1,0	1,0	1,1	1,6	1,3	1,3	32,5	9,1	1,7	2,0	3,3	2,3	1,4	1,3	1,4
	40 - 65 mm	1,0	11,1	0,9	4,3	1,7	13,5	1,2	18,9	8,8	1,6	1,7	2,0	1,8	4,0	1,3	2,6
	> 65 mm	6,9	11,5	1,2	6,5	2,1	1,2	1,3	4,4	2,3	35,4	4,0	7,3	15,6	1,5	25,1	13,3
Cr median: 25 [mg/MJ], 80th perzentile: 37 [mg/MJ]	0 - 20 mm	4,3	2,6	3,8	3,6	20,9	18,7	6,9	108,9	38,9	29,9	102,5	6,8	46,4	21,1	12,5	16,8
	20 - 40 mm	0,9	0,9	0,8	0,9	2,2	6,5	3,4	47,1	14,8	10,2	36,2	13,3	19,9	1,5	1,8	1,7
	40 - 65 mm	0,6	0,7	0,6	0,6	1,4	8,0	1,3	42,3	13,3	6,0	64,7	8,4	26,4	3,5	1,4	2,5
	> 65 mm	14,9	3,7	3,0	7,2	5,1	5,7	2,3	24,1	9,3	27,6	55,8	11,6	31,7	26,4	3,5	14,9
Co median: 1.5 [mg/MJ], 80th perzentile: 2.7 [mg/MJ]	0 - 20 mm	2,2	6,1	3,6	4,0	28,7	23,6	10,6	939,7	250,7	9,8	33,2	19,5	20,8	24,8	21,1	23,0
	20 - 40 mm	1,2	1,2	0,9	1,1	8,4	5,2	2,9	218,9	58,8	7,2	11,0	34,9	17,7	3,1	5,0	4,1
	40 - 65 mm	1,3	1,9	1,0	1,4	9,8	6,7	2,0	200,8	54,8	3,6	12,2	10,9	8,9	10,1	3,8	6,9
	> 65 mm	17,9	7,2	3,3	9,5	8,3	6,1	2,5	67,7	21,2	7,1	14,9	9,5	10,5	40,8	3,9	22,4
Ni median: 1.5 [mg/MJ], 80th perzentile 2.7 [mg/MJ]	0 - 20 mm	30,8	28,7	20,0	26,5	70,5	124,1	76,0	829,2	275,0	77,8	536,4	33,1	215,8	126,2	76,8	101,5
	20 - 40 mm	4,1	10,5	5,0	6,6	13,8	44,9	26,3	392,8	119,5	43,1	206,9	93,9	114,6	22,5	11,7	17,1
	40 - 65 mm	4,0	3,2	10,3	5,9	9,6	41,2	6,8	379,3	109,2	22,7	389,9	46,3	153,0	25,3	9,2	17,2
	> 65 mm	35,7	13,8	59,1	36,2	18,0	40,5	17,2	84,0	39,9	42,9	302,2	37,8	127,7	188,5	18,9	103,7
Hg median: 0.075 [mg/MJ], 80th perzentile: 0.15 [mg/MJ]	0 - 20 mm	5,1	5,9	5,3	5,4	71,4	8,9	8,5	885,6	243,6	9,2	11,5	18,2	13,0	30,5	24,2	27,4
	20 - 40 mm	5,2	4,9	4,8	5,0	21,2	6,1	5,9	222,2	63,9	7,8	9,3	27,5	14,9	7,0	6,1	6,5
	40 - 65 mm	4,6	5,6	4,2	4,8	11,7	5,4	5,5	176,7	49,9	7,3	8,0	15,9	10,4	9,5	6,1	7,8
	> 65 mm	5,8	5,2	4,9	5,3	20,8	5,5	5,9	69,1	25,3	7,4	8,0	64,6	26,7	53,7	6,1	29,9

3.4.5 Chromium

All of the average values of the individual types of waste are less than the threshold value. In the grain size GS 0-20 mm the fraction F2 T13 at 108.9% exceeds the threshold value and the fraction F3 T6 at 102.5% slightly exceeds the threshold value of the AVV. All of the other values are markedly lower than the threshold values of the AVV. No clear trend is discernible.

3.4.6 Cobalt

The type of waste F2 exhibits the highest average values for Cobalt for the threshold value in the grain size GS 0-20 mm at 250.7%.

Individual test materials of the type of waste F2 exceed the threshold value in the grain sizes GS 0-20 mm at 939.7%, GS 20-40 mm at 218.9% and GS 40-65 mm at 200.8%. The reason for these high values was not able to be determined. All of the other values are markedly below the threshold values of the AVV. The values are higher in the smaller grain sizes.

3.4.7 Nickel

In all types of waste with the exception of the type of waste F1 there is in part a high level of threshold value exceedance. The type of waste F2 in the grain size GS 0-20 mm at 829.2% has the highest exceedance and an average value of 275.0%, the values drop with increasing grain size, and falls well below the threshold value in the grain size

GS > 65 mm. The average values of the type of waste F3 exceed the threshold value in all grain sizes, whereby the highest values are in the grain sizes GS 0-20 mm and GS 40-65 mm. The average values of the type of waste F4 exceed the threshold value in the grain sizes GS > 65 mm and GS 0-20 mm. The reason for these high values was not able to be determined. It is discernible that the highest values are found in the small grain sizes.

3.4.8 Mercury

The type of waste F2 in the grain size GS 0-20 mm has the highest values at a threshold value exceedance of 885.6% in the test material F2 T13. The values drop with increasing grain size and in the grain size GS > 65 mm are markedly less than the threshold value. The values of all of the other types of waste are markedly less than the threshold value of the AVV.

4. DISCUSSION

In the following chapters, the results or values from the individual chemical investigations are summarized and discussed. The arithmetic mean values are the mean values of the individual grain classes from several experiments with the same type of waste. The weighted arithmetic mean values across all grain sizes correspond to the value of each type of waste prior to screening.

4.1 Calorific values

In Figure 5 the arithmetic mean values of the calorific values of the individual grain sizes are shown as bars and the weighted arithmetic mean (weighted average) values for each type of waste are shown as framed bars.

As is to be expected the calorific value (arithmetic mean value) rises in most of the cases with the grain size.

The weighted average of the arithmetic mean values of the respective grain classes is for:

- F1: 28.2 MJ/kg. The type of waste F1 (packaging waste) is relatively homogeneous since the processing and collection are precisely defined process stages. This fact is also reflected in the results of the chemical and physical analyses. The material is quite dry and thus also has a quite high calorific value in the small grain size ranges;
- F2: 20.4 MJ/kg;
- F3: 15.59 MJ/kg;
- F4: 20.50 MJ/kg.

4.2 Chlorine

Figure 6 shows the arithmetic mean values of the chlorine levels of the individual grain sizes shown as bars and the weighted arithmetic mean values for each type of waste shown as framed bars.

The weighted arithmetic mean chlorine values of the respective grain sizes (classes) is for:

- F1: 1.14%. The differences between the individual grain sizes are slight.
- F2: 0.890%.
- F3: 0.959%. The small grain sizes contain less chlorine than the grain size > 65 mm and show with values between 0.4 and 0.6% the lowest Cl values.
- F4: 2.65%. Rather great differences appear between the individual grain sizes. The maximum value of all of the test materials of 4.4% was measured in the grain size GS 20-40 mm. Thus this material can only be pro-

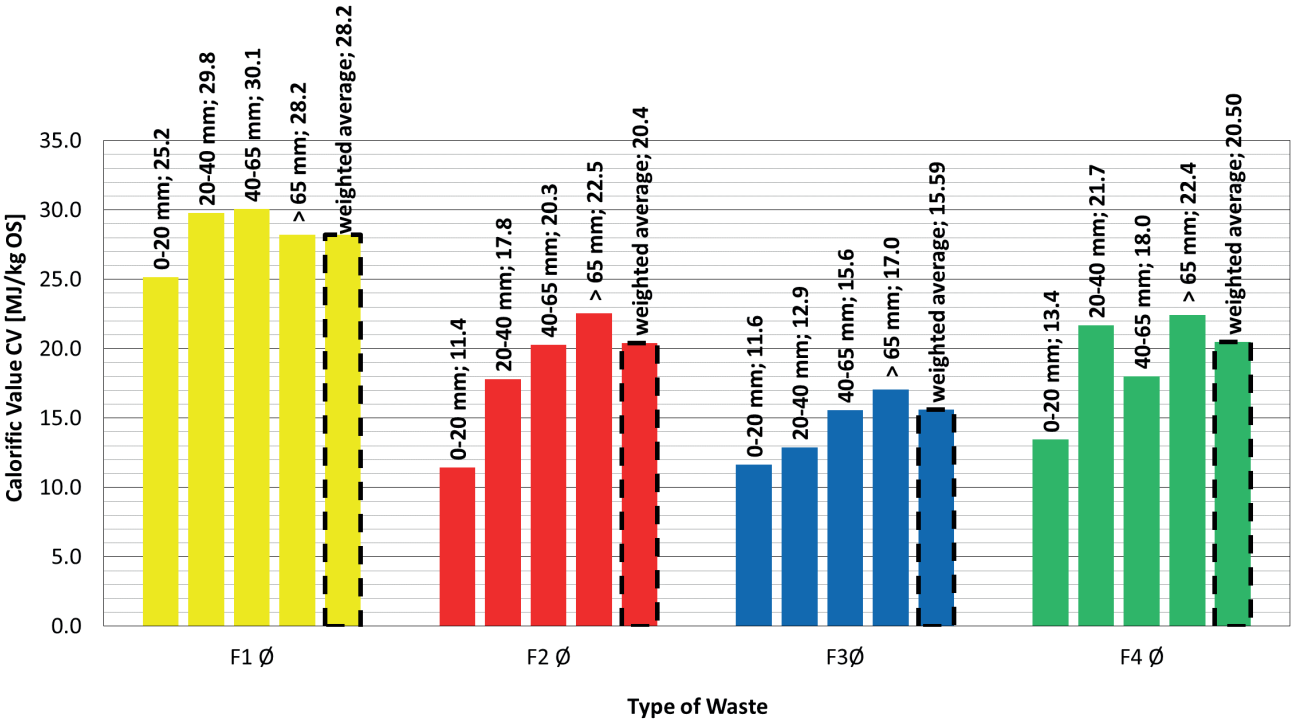

FIGURE 5: Calorific values of the types of waste examined.

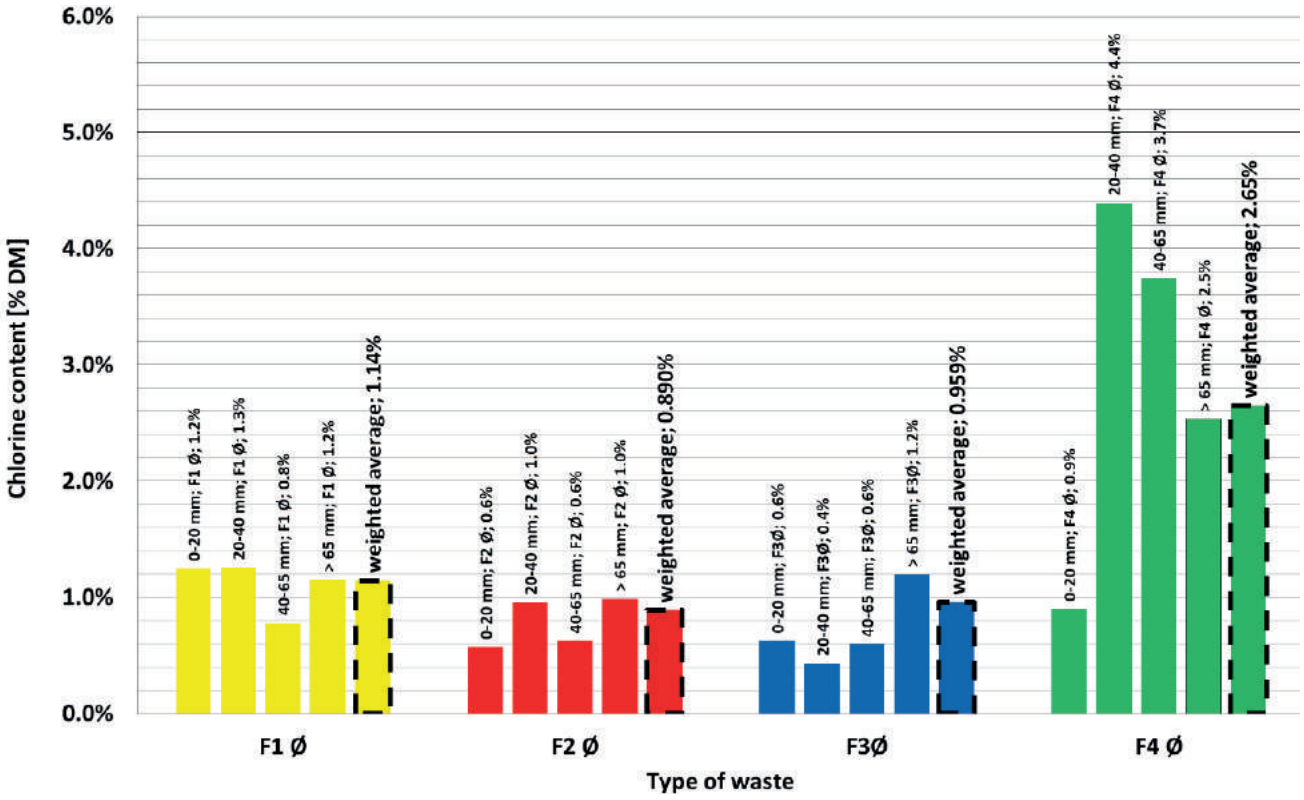

FIGURE 6: Chlorine levels of the types of waste examined.

cessed into substitute fuel as a mixture with other low chlorine waste.

4.3 Heavy metals

In Figure 7 the threshold value exhaustion for heavy metals is shown as a percentage of the threshold values for each type of waste and grain size. In addition, the weighted mean values (weighted average w.a. = average value) for the respective heavy metal for each type of waste are also shown as black bars. The weighted mean value is the value of the entire respective type of waste prior to the screening.

Most of the mean values (weighted arithmetic mean values) of the individual types of waste are lower than the threshold values of the AVV. The reasons for individual threshold value exceedance were not able to be determined.

- F1: The values for all parameters in all grain sizes are markedly lower than the threshold values of the AVV.
- F2: Most of the values are markedly lower than the threshold values of the AVV. Individual threshold value exceedance can be found in the grain size GS 0-20 mm for Co, Ni and Hg as well in grain sizes GS 20-40 mm and GS 40-65 mm for Ni. The weighted arithmetic mean is below the threshold values.
- F3: Most of the values are markedly less than the threshold values of the AVV. The weighted arithmetic mean value for Ni exceeds the threshold value with 138.5% markedly. Individual threshold value exceedance can be found in all grain sizes for Ni and in grain size GS 20-40 mm for lead.
- F4: Most of the values are markedly lower than the threshold values of the AVV. Individual slight threshold value exceedance can be found in the grain sizes GS 0-20 mm and GS > 65 mm for Ni. The weighted arithmetic mean values for all parameters are lower than the threshold values of the AVV.

5. CONCLUSIONS

The quality in the various grain sizes of the types of waste examined fluctuated quite heavily. The calorific values are higher such as is to be expected in the larger grain sizes. The highest calorific value is to be found in the type of waste F1. The chlorine levels are with the exception of F4 (2.65%) lower and can be found in the range of 1%. The mean values (weighted arithmetic mean values) of the heavy metal contents are markedly less than the threshold values of the AVV.

But the type of waste F2 exceeds the threshold value in some grain sizes for Ni, Hg and Co. In the type of waste F3 the weighted mean value exceeds the Ni-threshold value markedly with 138.5%. The cause for the exceedance was not able to be determined.

Basically all types of waste are suitable for the production of SRF:

- F1: The high-calorific type of waste F1 (Packaging Waste) is ideally suitable for the production of SRF. The type of waste F1 can compensate for lower calorific value types of waste, such as e.g.F3, however it exhibits higher chlorine levels which in turn are evened out by the low chlorine types of waste;

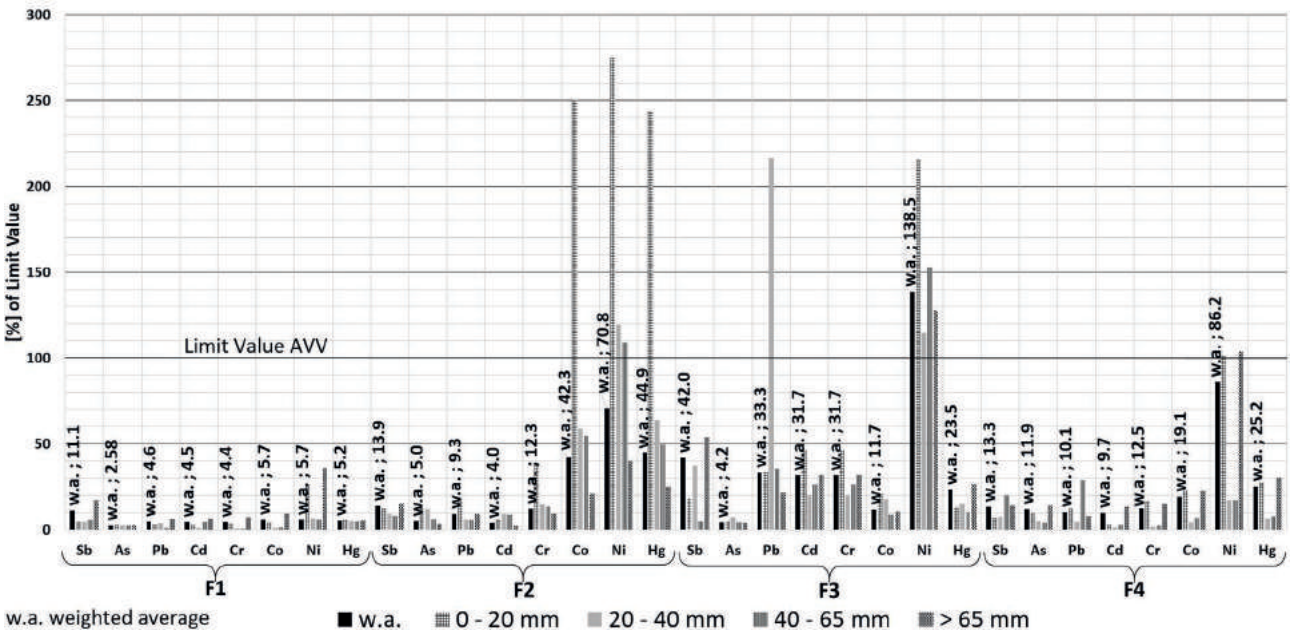

FIGURE 7: AVV parameters (heavy metals) of the types of waste F1, F2, F3 and F4 examined.

- F2: The type of waste F2 (Mixed Commercial Waste 1) is suitable in the mixture with other high-calorific waste for the production of SRF;
- F3: The type of waste F3 (Mixed Commercial Waste 2) can be used in the mixture with other types of waste with higher calorific values as an input material for the production of SRF particularly as they display relatively low chlorine values;
- F4: The type of waste F4 (Mixed Commercial Waste 3) is suitable due to the high chlorine values only in the mixture with low chlorine waste for the SRF production.

None of the types of waste are suitable as a monofraction for the production of substitute fuels or for the direct use in the cement facilities' processes (e.g. to low heating value, to high water content, to high chlorine content etc.). It is the right mixture that produces the flexibility important to be able to produce high quality assured substitute fuels. Disadvantageous properties, such as higher chlorine values or lower calorific values of individual types of waste or individual batches, can thus be compensated, thereby allowing to ensure constant and stable quality properties and high substitution rates.

CONFLICT OF INTEREST

The authors declare no conflict of interest.

ACKNOWLEDGEMENTS

The Center of Competence for Recycling and Recovery of Waste 4.0 (acronym ReWaste4.0) (contract number 860 884) under the scope of the COMET – Competence Centers for Excellent Technologies – financially supported by BMVIT, BMWFW and the federal state of Styria, managed by the FFG.

REFERENCES

Aldrian, A., Sarc, R., Pomberger, R., Lorber, K.E., Sipple, E.-M., 2016. Solid recovered fuels in the cement industry-semi-automated sample preparation unit as a means for facilitated practical application. Waste management & research: the journal of the International Solid Wastes and Public Cleansing Association, ISWA 34 (3), 254–264. 10.1177/0734242X15622816.

Austrian Standards Institute, 2000. DIN 51900-1 Prüfung fester und flüssiger Brennstoffe - Bestimmung des Brennwertes mit dem Bomben-Kalorimeter und Berechnung des Heizwertes - Teil 1: Allgemeine Angaben, Grundgeräte, Grundverfahren (Testing of solid and liquid fuels - Determination of the calorific value with the bomb calorimeter and calculation of the calorific value - Part 1: General information, basic equipment, basic method).

Austrian Standards Institute, 2007. ÖNORM EN 14343 Charakterisierung von Abfällen — Berechnung der Trockenmasse durch Bestimmung des Trockenrückstandes oder des Wassergehaltes (Characterization of waste - Calculation of waste Dry matter by determination of the Dry residue or water content).

Austrian Standards Institute, 2011a. ÖNORM EN 15415-1 Feste Sekundärbrennstoffe - Bestimmung der Partikelgrößenverteilung Teil 1: Siebverfahren für kleine Partikel (EN 15415-1 Solid recovered fuels - Determination of particle size distribution Part 1: Screening method for small particles). Österreichisches Normungsinstitut (ON), Wien. (Last access: 6 February 2019).

Austrian Standards Institute, 2011b. ÖNORM EN 15411 (ICP-MS Feste Sekundärbrennstoffe - Verfahren zur Bestimmung des Gehaltes an Spurelementen (As, Ba, Be, Cd, Co, Cr, Cu, Hg, Mo, Mn, Ni, Pb, Sb, Se, Tl, V und Zn) (Solid secondary fuels - Method for determining the content of trace elements (As, Ba, Be, Cd, Co, Cr, Cu, Hg, Mo, Mn, Ni, Pb, Sb, Se, Tl, V and Zn).

Bundeskanzleramt, 2010. Austrian Incineration Ordinance https://www.ris.bka.gv.at/GeltendeFassung.wxe?Abfrage=Bundesnormen&Gesetzesnummer=20002239 (Last access: 27. march 2019).

Feil, A., Pretz, T., 2018. Unused potential in waste processing. Recy & DepoTech 2018_ conference book presentations.pdf, in: Recy & DepoTech 2018_ conference book presentations , Vol. 1, 153-160.

IFE Aufbereitungstechnik GmbH, 2019. Waste screens: Brochure Waste screens. Last access: 31 January 2019.

Lorber, K.E., Sarc, R., Aldrian, A., 2012. Design and quality assurance for solid recovered fuel. Waste management & research : the journal of the International Solid Wastes and Public Cleansing Association, ISWA 30 (4), 370–380. 10.1177/0734242X12440484.

Mauschitz, G., 2018. Emissionen aus Anlagen der Österreichischen Zementindustrie Berichtsjahr 2017 (Emissions from Austrian cement industry reporting year 2017). Available online at: https://www.zement.at/beton-2/nachhaltigkeit-und-umwelt/emissionen. (Last access: 01 march 2019).

Sarc, R., Lorber, K.E., 2013. Production, quality and quality assurance of Refuse Derived Fuels (RDFs). Waste management (New York, N.Y.) 33 (9), 1825–1834. 10.1016/j.wasman.2013.05.004.

Sarc, R., Lorber, K.E., Pomberger, R., Rogetzer, M., Sipple, E.M., 2014. Design, quality, and quality assurance of solid recovered fuels for the substitution of fossil feedstock in the cement industry. Waste management & research : the journal of the International Solid Wastes and Public Cleansing Association, ISWA 32 (7), 565–585. 10.1177/0734242X14536462.

Sarc, R, Pomberger, R, Eferdinger, S., 2015. „REUQ-Ausweis" für EBS Entwicklung eines Ressourcen-, Energie-, Umwelt-, Qualitätsausweises (REUQ) für Ersatzbrennstoffe (EBS) ("REUQ certificate" for SRF Development of a resource-, energy-, environmental-, quality certificate (REUQ) for solid recovered fuels (SRF), Association of Austrian Waste Management Companies (VÖEB)), Verband Österreichischer Entsorgungsbetriebe (VÖEB), Wien, Austria.

detritus | Multidisciplinary Journal for Waste Resources & Residues

CISA

A TECHNO-ECONOMIC FEASIBILITY ANALYSIS FOR THE GASIFICATION OF SCRAP TIRES FOR ENERGY GENERATION IN TURKEY

Iskender Gökalp [1,*], Oguz Kaya [2], Serden Keçecioglu [3] and Deger Boden [4]

[1] *Centre National de la Recherche Scientifique - ICARE, 1C Avenue de la Recherche Scientifique 45071 Cedex 2, Orléans, France*
[2] *PRO-SIS Mühendislik, Pro-Sis Enerji Teknolojileri Mühendislik ve Üretim Ltd. Mustafa Kemal Mahallesi, 2146 Sok. No: 7/8, 06520 Çankaya, Ankara, Turkey*
[3] *Kristal Partners, Istiklal Caddesi Tünel Meydanı, Geçit Han C Blok, No.130, 34430 Beyoğlu, Istanbul, Turkey*
[4] *Boden-Law, Maslak Mahallesi, İz Plaza Giz No:9, 34398 Sarıyer, Istanbul, Turkey*

Article Info:
Received:
19 February 2019
Revised:
25 June 2019
Accepted:
02 July 2019
Available online:
22 August 2019

Keywords:
End-of-life tire
Gasification
Electricity generation
Techno-economic feasibility

ABSTRACT

A techno-economic feasibility analysis for a 5 MWe scrap tire granulés gasification facility is presented. Electricity generation is based on gas engines with the option of waste heat recovery. Based on our previous work, it is demonstrated that the best thermochemical option for waste tire disposal and energetic valorization is gasification using a mixture of preheated air and steam as the gasification agent. Also based on our previous work, the best gasification technology is shown to be the circulating fluidized bed technology. The study shows that under the regulatory and financial conditions prevalent in Turkey, the project is both technically and economically feasible.

1. INTRODUCTION

End-of-life tires ("ELT") constitute a global and growing environmental issue. We must deal with their recycling and/or disposal in an environment-friendly manner. According to reports from the largest associations of tire and rubber manufacturers, about 1 billion new units of end-of-life tires are turning into waste annually and must be properly managed. In some parts of the World, hundreds of millions of tires are stockpiled and are posing severe health problems:

> *"They are breeding grounds and havens for mosquitoes and other vectors, resulting in the spread of dengue fever, yellow fever, encephalitis, West Nile virus, and malaria. Once ignited, tire fires are difficult to extinguish. When water is applied to fight the fire, serious air, ground water, and surface water contamination may result. Toxic emissions from tire fires, such as sulfuric acid and gaseous nitric acid, can irritate the skin, eyes, and mucus membranes, and can affect the central nervous system, cause depression, have negative respiratory effects and, in extreme cases, cause mutations and cancer" (EPA, 2010).*

In better regulated geographies, ELTs are used either in recycling (granulation) or in energy generation. However, recycling is just a palliative care which does not address the absolute removal of the waste. On the other hand, the demand for scrap tires from the recycling industry is not sustainable and reliable. As for the energy recovery, the main user of scrap tires is cement kilns. The problem with this type of use is pollutant emissions from scrap tire combustion.

As detailed in the later sections, gasification of scrap tires is a clean technology that only generates a synthetic gas with a high calorific value. When granulated scrap tires are gasified with the appropriate technology, about 95% in mass are transformed into synthetic gas and the remaining is just inert ash (inorganics). Therefore, gasification of ELT offers the solution for an absolute disposal of scrap tires while proposing an economically beneficial and sustainable energy production route. This work is a techno-economical study of ELT gasification for energy generation based on our previous studies on solid fuel gasification and on a thorough analysis of regulatory and financial conditions prevalent in Turkey.

2. REGULATORY ASPECTS OF THE ELT SECTOR IN TURKEY

Waste-to-Energy programs are among the most impor-

* Corresponding author:
Iskender Gökalp
email: iskender.gokalp@cnrs-orleans.fr

https://doi.org/10.31025/2611-4135/2019.13843
© 2019 Cisa Publisher. Open access article under CC BY-NC-ND license

tant priorities of International Financial and Developmental Institutions (IFDIs), such as World Bank, IFC and EBRD. According to "IFC Climate Implementation Plan, April 2016", sustainable waste management projects are estimated to triple in the fastest growing low to middle income countries driven by a growing waste problem, enhanced regulatory environment, increased public pressure, urbanization and land scarcity. IFC's waste management strategy has four pillars: Focus on waste-to-energy, refuse-derived fuel, e-waste recycling and integrated waste management (IFC, 2016).

In addition to the IFDIs, local banks, green bond issuers and green funds are seeking investment opportunities that have solid financials and addressing global environmental issues. Consequently, it is very likely to easily have access to local and international long term project financing with competitive pricing for ELT gasification projects.

In Turkey, over the last decade, policymakers have taken important measures to diversify the energy supply mix of the country and to reduce reliance on imported natural gas for power generation. To this aim, the Government has been supporting the use of non-fossil energy sources (hydro-electricity, wind, solar, geothermal, biomass, etc.) throughout long term governmental offtake agreements.

"The Law on the Utilisation of Renewable Energy Resources for the Purpose of Generating Electrical Energy", published in May 2005, initiated attractive feed-in tariff mechanisms to encourage renewable energy investors. In June 2016, an amendment to the above-mentioned law enlarged the definition of "biomass" and included "by-products formed after the processing of scrap tires" into its definition. As a consequence, generating electricity using the synthetic gas produced by scrap tire gasification has become eligible to benefit from 13.3$ Cent/kWh feed-in tariffs for the first 10 years of operations. It is also possible to receive additional incentives for the first 5 years of operations if locally manufactured equipment is used. Under such conditions, the 10-year Government offtake supported by the feed-in tariffs makes the ELT Gasification not only an environmental sustainability project but also a highly profitable investment decision.

2.1 Supply of scrap tires

Scrap tires constitute a global environmental issue but also they are a valuable resource. To address the environmental issue and to benefit from its economic value, developed economies, mainly EU, US and Japan, have adopted local regulatory measures over the past decades.

> *"The cornerstone of an effective scrap tire management program is developing diverse applications, or purposes for which to apply this resource, preferably ones that (i) can be developed reasonably quickly; (ii) use large quantities; iii) are technically and environmentally sound; and (iv) are economically feasible and sustainable. The largest application in the United States, Europe, and Japan, among others, is using scrap tires as a supplemental energy resource" (EPA, 2010).*

EU appears to have the best practice in the World, given the success of its ELT recovery program. Turkey has also chosen to deploy European Union's environmental practices and has adopted "Extended Producer Responsibility (EPR)" approach in 2006, to implement an effective scrap tire management program. Extended producer responsibility means that the original manufacturer has a duty of care to ensure that the waste from the products it has created is disposed of responsibly, in an environmentally sound manner. This makes the producer responsible for the waste that the consumer generates.

This Extended Producer Responsibility may be implemented in various ways: (i) by a single ELT management company dealing with ELT collection and treatment in the country, such as in Portugal, the Netherlands or Sweden; (ii) by multiple ELT management companies, such as in Italy, France or Spain; or (iii) by individual producers' responsibility such as in Hungary. EPR is today the most widespread system in Europe with 21 countries (most of EU28 countries + Norway and Turkey) having adopted a legal framework assigning the responsibility to the producers (tire manufacturers and importers) to organise the management chain of ELTs (ETRMA, 2015).

In Turkey, a Communiqué regarding end-of-life tires has been drafted by the Ministry of Environment and Urbanisation and published in the Official Journal on 25th of November 2006. The Communiqué identifies the roles and responsibilities of all relevant parties to create an effective ELT management program. According to the article 17 of the Communiqué, all manufacturers (including the authorised importers) are obliged to collect end-of-life tires from the local market and they should submit proving documents regarding the disposal and/or recycling of collected tonnage to the Ministry. The required amount of collection is equal to 80% of the previous year's domestic sales to the replacement market by the relevant vendor. Given the loss of the caoutchouc during the life of the tire, 80% collection rate is assumed to correspond to the full recovery of the tires sold in the domestic market.

In April 2007, major tire manufacturers and importers in Turkey, namely BRİSA, CONTINENTAL, GOODYEAR, MICHELIN and PIRELLI came together to establish LASDER, the Association of Tyire Manufacturers. With the subsequent participation of BAYTUR, İNCİTAŞ and ANLAŞ, the Association is now serving as the only organisation to implement the Extended Producer Responsibility Program on behalf of 8 the member firms.

2.2 Volume of the End-of-Life Tires in Turkey and its present use

World tire market has grown 12% since 2011 to reach 1.77 Billion units of sale in 2016. The same year, In Turkey, 22.6 Million units have been sold to domestic market. 16 million tires (70%) were sold to the "replacement" market and the remaining 6.6 million were sold to car manufacturers. According to ELT management approach, the total amount of tires sold on a specific market is equal to an equal amount of used tires dismounted from vehicles (1:1 correlation). This is generally the case, except for winter tires. Therefore, in Turkey, tire manufacturers and importers

are obliged to collect 80% of the tonnage equivalent of 16 million tires sold to the domestic replacement market. This amount roughly corresponds to 80% of 300,000 tons per year, which is 240,000 tons per year. As a comparison, one can estimate that the World tire market has to deal with ~19 million tons of scrap tires annually. EU used tire stock is estimated to ~4 million tons per year.

LASDER member companies are controlling about 70% of the replacement market in Turkey. Therefore, LASDER's mission is to coordinate and control the collection and disposal/recovery of ~168,000 tons of scrap tires annually, through a tender process. Apart from LASDER, management of remaining ELTs are under the responsibility of other producers and importers which control 30% market share in the replacement market. However, according to 2015 results shared by the Ministry of Environment, 137,000 tons of ELTs have been effectively managed, which corresponds to a ~57% success rate (137K/240K). LASDER has successfully managed 110,000 tons of ELT and other players have managed to dispose/recycle only 27,000 tons of scrap tires.

The potential of the ELT market in Turkey is summarised in Table 1. This table also contains information on the amount of granulated tires, given a widely accepted yield rate of 65%, after removing all the metallic and textile parts and also taking into account lost caoutchouc during the granulations processes.

2.2.1 Recycling (Granulation) - (Tire-Derived Materials TDM)

In Europe, the ELT sector is evenly divided between recycling and energy recovery. However, in Turkey, material recycling has a larger portion, given the unstable demand of cement kilns (depending on the price of alternative fuels). Tires are made from a range of constituent components such as rubbers, steel, and textiles. The types of rubbers vary with the type of tire and the compounds used. The ratio of steel may vary from one tire type to another, and textiles are generally only used in passenger car and light truck tires today. In the case of granulation, when non-rubber parts are separated from the rubber, there remains about 65% of the scrap tire.

The rubber in recycled tires is often treated as a complex resource and recycled in its entirety as shred, crumb, granulate or powder. Each of these stages of size reduction has its own characteristics and properties and a given size reduction is used for a specific end-product (ETRMA, 2015). Granulated rubber is used in "rubberised asphalt", "athletic tracks", "stadium surfaces" and in "rail transportation" for noise mitigation and anti-vibration solutions. In Turkey, there is a much more limited use and mainly in "child parks", "synthetic football pitches", and "animal beds". In many cities, small to medium scale firms have invested into scrap tire granulation technology. It should however be noted here that the use of used tire granules for synthetic sport lawns is a controversial issue for its potential health hazards (Environmet & Human Health Inc., 2017).

TABLE 1: The present potential of the ELT market in Turkey.

Total sales to replacement market (tons)	300,000
Legal obligation of ELT management	80%
Annual tonnage of ELT to be managed (tons)	240,000
Percentage of granulated tyre out of ELT	~65%
Maximum possible amount of granulated ELT (tons)	156,000
Market share of LASDER member firms	~70%
LASDER's maximum possible granule output (tons)	109,200

2.2.2 Energy Recovery - (Tire-Derived Fuel TDF)

The single highest volume and quickest route to the valorisation of scrap tires is to use them for their heat energy content and cement kilns are the main users for tire derived fuel (TDF). In the EU, ~49% of ETLs go to the energy recovery market and 91% of them are used in cement kilns (ERTMA, 2015). In Turkey, each year 3 to 6 cement producers join the LASDER tender for their upcoming fuel needs. Out of 300,000 tons of total inquiries, a maximum of 60-70,000 tons are received from cement factories. Capacity utilisation of cement plants, on the one hand, alternative fuel (natural gas, sewage sludge) costs, on the other hand, determine the effective demand of cement producers in the ELT market. However, there are environmental concerns regarding scrap tire combustion even under controlled conditions such as in cement kilns. Under such conditions combustion emissions are much lower compared to uncontrolled combustion (such as stockpiled tire fires). But serious concerns still exist on the full controllability of tire combustion in cement kilns (EPA, 1997; Richards and Agranovski, 2017).

Pyrolysis is another TDF use technology. Pyrolysis is the thermal decomposition under oxidant free environment where the decomposition products are combustible gases, liquid components (pyrolytic oil) and carbon black. This technology has also been tried in Turkey but it is now clear that this process is not sustainable both economically and environmentally. The liquid components are mostly heavy hydrocarbons that need refining to be used as fuel to be converted into energy in a clean way and the market for carbon black is mostly missing.

3. THE PROPOSED TECHNOLOGY: GASIFICATION OF ELT GRANULES

Carbon containing materials are used for energy production since ages: wood, coal, oil and natural gas are the main such materials transformed into heat and power by combustion. This thermochemical process converts the organic source into CO_2 and H_2O but also to other emissions such as nitric and sulphur oxides and particulates matter (soot), and of course ash in the case of coal or biomass.

Carbon containing energetic materials can be classified in two types: Fossils (such as coal, oil and natural gas, mainly) on the one hand, and biomass and other organic materials such as various waste streams both municipal and industrial, on the other hand. This last category is named "renewable" as biomass can be grown in short and continuous periods and waste streams are also generated on a continuous basis by human activity.

The fuels under the fossils category have been accu-

mulated in the Earth underground during a process of several hundred million years (due to the decomposition and compression of various biomass resources). Therefore, they are of a given (finite) amount by definition and subject to depletion. Coal and natural gas power plants emit huge amounts of CO_2 hence contribute to the global warming issue. Combustion of "new" biomass (not fossilized) can be considered as CO_2 free because of the reuse of the emitted CO_2 for plant growth through photosynthesis.

3.1 General considerations on solid fuel gasification

Gasification of scrap tires is a clean technology that only generates synthetic gas (essentially CO, H_2, CH_4 and CO_2) with a high calorific value. De-metallized and granulated (with dimensions of few millimetres) scrap tires can be efficiently gasified in well-designed fluidized bed gasifiers. As a result about 95% in mass of the granulés are transformed into synthetic gas and the remaining is just inert ash (inorganics). After some cleaning, the energetic gas can be converted into electricity in gas engines (with an efficiency of about 40%). The available engine waste heat can also be recovered and used as process heat or steam or for heating purposes and even to generate additional electricity using a Rankine cycle turbine.

Gasification studies of carbon containing materials have a long history. The first large scale application goes back to coal gasification in Germany to produce synthetic gas from which synthetic liquid fuels were generated during the Second World War. This process was further developed during the post-war period in South Africa by the company Sasol.

Gasification can be best explained as incomplete combustion. By reducing the amount of the air (and thus of the oxygen) supplied to oxidize, for example, coal, the oxidation process is limited and instead of CO_2 + H_2O as end-products in complete combustion, one obtains a gaseous mixture composed essentially of H_2 + CO, called synthetic gas or syngas. This produced gas is obviously reactive and can be burned in a gas turbine, a gas engine or in a burner similar to natural gas. Compared to the direct combustion of coal (or biomass etc.) the gasification temperatures in the gasification reactor are lower; this reduces the production of pollutant emissions such as nitric and sulphur oxides. Furthermore, without going into details, we can also mention that gasification permits more easily the capture CO_2 (pre-combustion capture) compared to direct combustion (post-combustion capture).

The produced gas (syngas) can be combusted to generate heat and power but can also be further processed essentially by catalytic processes (as in the German example we mentioned above). In addition, gasification is also a hydrogen production process. Gasification systems can handle several feedstocks and also co-gasification approaches are possible such as co-gasification of coal and biomass blends. Gasification is therefore a multi fuel and multi product technology.

The quality of the syngas (its calorific value, the H_2/CO ratio etc.) depends on many parameters such as the gasification temperature, the oxygen/fuel ratio, the residence time of the fuel within the gasifier, but also on the gasification reactor design. To optimize the gasification process for a given feedstock, several studies should be conducted, starting with laboratory type studies to determine the gasification kinetics (essentially the carbon conversion rate meaning that in the ideal case there should be no carbon atom in the ashes) using sophisticated laboratory equipment and several thermochemical computation techniques. Once this gasification thermochemistry is established, pilot and demonstration facilities can be designed, built and operated. All these studies contribute to give confidence to move to commercial level designs at various capacity levels, to build up the learning by doing process and initiate a virtuous cycle for unit cost reduction. There are several reviews in the literature which justify the advantages of scrap tire gasification (Molina et al., 2013; Oboiriena and Northa, 2017; Machin et al., 2017; Rowhani and Rainey, 2017). The present work is based on our previous studies concerning solid fuel gasification research and fluidized bed gasification demonstration facilities.

3.2 Previous studies on which this project is based

Several previous studies conducted by our team paved the way for the proposed technology. First, the gasification kinetics has been established in laboratory type studies for various scrap tire samples (both for cars and trucks). These studies used thermogravimetric analyzers coupled with mass spectrometry and gas chromatography to characterize used tire gasification kinetics (for various heating rates up to 1000 K/min, gasification temperatures between 800 and 900°C and for different gasification agents such as air, steam and CO_2 and their various mixtures (Kandasamy and Gökalp, 2015).

The pilot and demonstration phases have also been accomplished for the gasification of lignite in the framework of a large-scale European Union FP7 project (the OPTIMASH project, 2011-2016, supported by the EU for about 5.5 million Euros). Within the OPTIMASH project a 1 MWth high pressure circulating fluidized bed gasifier was designed, built, commissioned and successfully tested. This facility is now in operation at the company THERMAX in Pune, India (Figure 1). The Turkish Coal Enterprise TKI was also a partner of this project, together with the French CNRS, IIT Madras, India and ECN, Netherlands (Kandasamy and Gökalp, 2018). The present project is therefore capitalizing on this accumulated knowledge and expertise.

3.3 Technical and financial characteristics of the project

We designed a scrap tire gasification facility of 5 MWe capacity using gas engines, shown schematically in Figure 2. The gasification reactor design is adapted to the thermo-physical characteristics of various scrap tire samples especially the gasification kinetics, obtained during laboratory studies. Based on the expertise gained during the OPTIMASH project, a circulating fluidized bed gasifier for various thermal capacities has been designed. The synthetic gas obtained from the gasification island is cleaned

FIGURE 1: 1 MWth circulating fluidized bed solid fuel gasification facility developed during the FP7 OPTIMASH project (2011-2016).

and converted to heat and power in gas engines. The most critical and innovative part of this system is obviously the gasification reactor. Its design criteria are based on our knowledge, experience and expertise in the gasification area. The circulating fluidized bed gasifier uses a mixture of preheated air and steam as the gasification agent. A global layout of the gasification facility is presented on Figure 2.

The power plant consists basically of the following elements:

- the scrap tire granules storage area and feeding system, together with the limestone and silica sand storage and feeding areas;
- the gasification reactor composed mainly of the circulating Fluidized Bed Reactor with its support structure, cyclone separator, loop-seal system, start-up burner, primary & secondary air fans, ash take-off system with ash cooler screw, cooling water system with circulating water cooling radiators, air preheater, primary & secondary air pipes, instruments, valves and dampers, MCC & control panel;
- the reactor steam supply system mainly composed of the superheated steam boiler where the required heat shall be provided by the hot syngas through a heat recovery system, feed water pumps, deaerator and storage tank with instruments, valves, water treatment unit with storage tank, MCC & control panel;
- the syngas system with the syngas piping ensemble including the by-pass system, the syngas heat recovery system and/or syngas cooler with air, instruments and control dampers;
- the syngas cleaning system with spray scrubber 1 and 2, condenser with gas/water separator, bag filter protected with nitrogen, circulating water system with waste water treatment, circulating pumps;
- the flare system with the knock-out drum, the water seal tank, flare LPG pilot flame, control panel;
- the gas engine generator sets including lube oil system, intake air filters, generator control panel, fuel control skid, start air system, acoustic enclosure, exhaust gas system and stack, air ducts and radiators also including the gas engines heat recovery system with the engines' jacket water heat exchangers, exhaust gas boiler with valves & pumps.

The flare system will insure the safe disposal of syngas during start-up or short term upsets. The flare includes a LPG fired pilot flame to ensure that the flare is continually operating. Water for gas cleaning and cooling will be used in a circulating way without any environmental pollution after it is treated through water treatment facilities. A small amount of make-up water will be however required. The main water loss is through the steam to be fed to the gasification reactor to increase the gasification efficiency.

We expect to reach 8,000 hours of net operations annually. This will allow a net electricity generation of about 40,000,000 kWh. The yearly needed scrap tire granules amounts to about 14,000 tons. The technical and financial details of the facility are given in the sections below.

3.3.1 Gasification mass and energy balance details

The gasification reactor is based on the circulating fluidized bed concept that we optimized in the OPTIMASH project (Kandasamy and Gökalp, 2018). The main advantages of this technology are its high conversion efficiency, its fuel flexibility, high turn-down ratio and low emissions. The heat and mass balances of the gasification reactor are based on the determination of the scrap tire samples gasification kinetics in detailed laboratory studies (Kandasamy and Gökalp, 2015). The average scrap tire characteristics that we used for the heat and mass balances are presented in Table 2.

The gasification reactor mass balance only for electricity is given in Table 3 for a reactor bed temperature of 850°C and for a cold gas efficiency of 70%.

To generate electricity from syngas, we use 3 GE Jenbacher J620 GS-F63 gas engines with 40% efficiency. Under such conditions the net electricity efficiency of the system is 26.3%. Using the data given by GE, we estimated the waste heat recovery potential from the engine cooling water and the hot exhaust gases. From the 3 engines, the recoverable cooling water heat (as hot water)

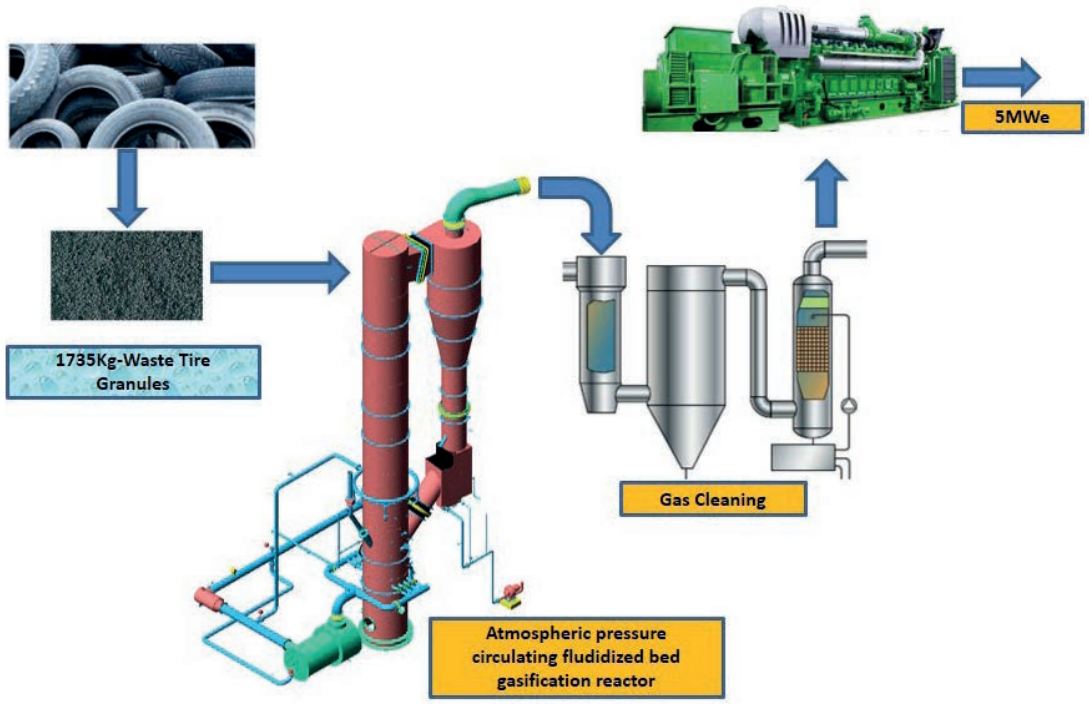

FIGURE 2: Schematic presentation of the 5 MWe scrap tire gasification and electricity generation facility designed based on the technology developed during the OPTIMASH project.

is 2607 kWth and the recoverable heat (as steam) from the exhaust gases is 3465 kWth, giving a total recoverable heat of 6072 kWth. For the exhaust gases case, the hot gas temperature is given as 465°C by GE. We cooled down the gases to 155°C to be ejected from the chimney and we accepted a heat loss coefficient of 2%. Under those conditions, the total energy efficiency of the system becomes 61.7%. To estimate the natural gas equivalent of the recovered heat, we used a natural gas with a calorific value of 8250 kcal/Nm^3 and a boiler efficiency of 94%. Under such conditions the natural gas equivalent of the total recoverable heat is 673 Nm^3/h. These figures will be used below for the financial analysis of the project.

TABLE 2: Averaged characteristics of scrap tire samples used for the energy and mass balances of the gasification reactor.

Total humidity %	1.09
Ash %	4.95
Volatile matter %	73.74
Fixed carbon %	20.22
C %	81.46
H %	6.84
N %	2.27
S %	1.38
O	2.01
LHV / HHV, kcal/kg	8478 / 8853

TABLE 3: Mass balance for 5000 kWe generation.

Scrap tire granules flow rate	1735 kg/h
Air flow rate	6250 kg/h
Steam flow rate	780 kg/h
Ash flow rate	86 kg/h
Syngas flow rate	8529 Nm^3/h
Syngas LHV	5276 kJ/Nm^3
Syngas HHV	5713 kJ/Nm^3
Electric generation / Net	5 000 kWe / 4 500 kWe

3.3.2 Financial details of the project

A full economic feasibility analysis has been performed using various sensitivity parameters and options, for a 30 years operation period of the facility. One important parameter is the cost of waste tire granulés. A detailed sensitivity analysis has been performed for this parameter, including the options of either buying the granulés from the market (with long term purchase agreements) or investing in a waste tire granulés production facility. Initial investment costs (capex + opex during the facility installation and commissioning phases) and the opex for the facility running phase have been estimated. Different loan strategies have been also investigated (including a preferential loan possibility through the EBRD). The operating phase opex also considers the maintenance of the whole system including the gas engines. Finally the generated cash flow, the NPV and the IRR have been calculated for two scenarios. One scenario considers only the electricity generation sold using the power purchase agreement mentioned above. The second scenario also includes the valorization of the waste heat from the engines and valued at the market price of natural gas to generate the same heat output. In both cases the IRR is much higher than other renewable energy investments. The details of

the cost-income analysis are given in Table 4 where more conservative efficiency figures than above are used. The cost for a ton of scrap tire granules is taken here as 80 USD / ton. To estimate the yearly income figures, the government feed in tariff of 0.15 USD/kWe and the substituted natural gas price of 222 USD/Nm^3 are used.

4. CONCLUSIONS

A techno-economic feasibility analysis for a 5 MWe scrap tire granulés gasification facility is presented. Electricity generation is based on gas engines with the option of waste heat recovery. Based on our previous work, it is demonstrated that the best thermochemical option for waste tire disposal and energetic valorization is gasification using a mixture of preheated air and steam as the gasification agent. Also based on our previous work, the best gasification technology is shown to be the circulating fluidized bed technology. The study shows that under the regulatory and financial conditions prevalent in Turkey, the project is both technically and economically feasible.

The existing and upcoming ELT volumes in Turkey tells us that an installation of 10 MWe capacity power plant, fed by about 30,000 tons of granulated scrap tire per year, has no supply risk. The installed capacity shall be gradually increased to 30 MWe, provided that tire manufacturers and their related body, LASDER, support the use of scrap tire in energy recovery. In order to achieve 30 MWe installed capacity, about 60% of the annual scrap tire tonnage (90,000 tons in granulé form) have to be allocated to ELT gasification.

Given the fact that 20 million tons of ELTs should be managed worldwide each year, power generation capacities of hundreds MW can be installed all around the World based on the Turkish examples The eagerness of IFDIs, private lenders and regulators creates a favourable investment climate to boost this development. Such an expansion requires obviously due diligence to understand the supply side and sell side risks of the relevant country jurisdictions.

ACKNOWLEDGMENTS

This work has benefited from the support of the Conseil Regional Centre, France through the project VALESTO to establish the chemical kinetics of the scrap tire gasification. It has also benefited from the support of the European Commission to Project OPTIMASH, FP7-ENERGY, 2011-2016, Project No 283050 for the optimization of the circulating fluidized bed gasification system.

REFERENCES

Air Emissions from Scrap Tire Combustion, 1997. U.S. Environmental Protection Agency

Environment & Human Health, Inc., 2017. Synthetic turf. Industry claims versus the Science, 112 p.

EPA, 2010. Scrap Tires: Handbook on Recycling Applications and Management for the U.S. and Mexico. U.S. Environmental Protection Agency

ETRMA, 2015. End-of-life Tyre Report 2015. European Tyre & Rubber Manufacturers' Association

TABLE 4: A financial feasibility analysis for 5MW electricity generation from scrap tire gasification under Turkish economic conditions.

AIMED POWER OF THE PLANT: 5 Mwe (5000 kWe)
NECESSARY SCRAP TIRE FLOW RATE : 1735 kg/h
AUTO CONSUMPTION OF THE PLANT : 500 kWe
NET ELECTRICTY GENERATION POWER : 4500 kWe
GLOBAL PLANT EFFICIENCY FOR ELECTRIC GENERATION ONLY : %25
GLOBAL PLANT EFFIICIENCY FOR ELECTRIC GENERATION + WASTE HEAT USE : %59

INVESTMENT COST OF THE PLANT	**USD**
BUILDINGS CONSTRUCTION	320,000
GRANULATED TIRE FEEDING SYSTEM	190,000
GASIFICATION ISLAND	1,750,000
GAS CLEANING ISLAND	850,000
3 GAS ENGINES	2,625,000
FLARE AND OTHER TUBING	190,000
ELECTRIC SYSTEM	280,000
CONTROL AND AUTOMATION SCADA	350,000
ENGINEERING	150,000
TOTAL	**6,705,000**

YEARLY OPERATING COST	
COST OF TIRES PREPARED FOR GASIFICATION	2,435,000
OPERATIONAL COST OF THE PLANT	580,000
MAINTENANCE	250,000
INSURANCE	25,000
TOTAL	**3,290,000**

YEARLY INCOME (0.15 USD/kWe and 8000 hour/year)	**5,400,000**
NET YEARLY INCOME	**2,110,000**
RETURN ON INVESTMENT (electricty generation only)	**3,2 YEAR**
WHEN THE WASTE HEAT IS USED	
TOTAL AVAILABLE HEAT	6,018 kWth
NATURAL GAS EQUIVALENT	696 Nm^3/h
ADDITIONAL INCOME (222 USD /Nm^3/h) FOR 8000 HOURS	1,776,000

TOTAL INCOME	**7,176,000**
TOTAL NET INCOME	**3,886,000**
ADDITIONAL INVESTEMENT TO USE THE WASTE HEAT	**600,000**
TOTAL INVESTMENT COST	**7,305,000**
RETURN ON INVESTMENT (electricity + waste heat)	**1,9 YEAR**

IFC, 2016. Climate Implementation Plan
Kandasamy Jayarama and Gökalp Iskender, 2015. Pyrolysis, Combustion, and Steam Gasification of Various Types of Scrap Tires for Energy Recovery. Energy & Fuels 29, 346-359
Kandasamy Jayaraman and Gökalp Iskender, 2018. Pyrolysis and Gasification Characteristics of High Ash Indian and Turkish Coals in http://dx.doi.org/10.5772/intechopen.73536 Chapter 11, pp. 209-235
Machin Einara Blanco, Travieso Pedroso Daniel, de Carvalho Júnior João Andrade, 2017. Technical assessment of discarded tires gasification as alternative technology for electricity generation. Waste Management 68, 412–420
Molino Antonio, Alessandro Erto, Francesco Di Natale, Antonio Donatelli, Pierpaolo Iovane and Dino Musmarra, 2013. Gasification of Granulated Scrap Tires for the Production of Syngas
and a Low-Cost Adsorbent for Cd(II) Removal from Wastewaters. Ind. Eng. Chem. Res. 52, 12154–12160
Oboiriena, B.O and Northa, B.C., 2017. A review of waste tyre gasification. Journal of Environmental Chemical Engineering 5, 5169–5178
Richards Glen and Agranovski Igor E., 2017. Dioxin-like pcb emissions from cement kilns during the use of alternative fuels. Journal of Hazardous Materials 323, 698–709
Rowhani Amir and Thomas J. Rainey, 2016. Scrap Tyre Management Pathways and Their Use as a Fuel-A Review. Energies 9, 888

detritus | Multidisciplinary Journal for Waste Resources & Residues

CISA

DEVELOPMENT OF A METHOD FOR DESIGNING LEACHATE DESALINATION PROCESS USING LANDFILL CELL MODEL

Kazuo Tameda *, Tong Li, Jiaxing Liu and Sotaro Higuchi

Research Institute for Resource Recycling and Environmental Pollution Control, Fukuoka University, 10, Koyo-cho, Wakamatsu-ku, Kitakyushu, Fukuoka 808-0002, Japan

Article Info:
Received:
21 February 2019
Revised:
18 July 2019
Accepted:
29 July 2019
Available online:
26 September 2019

Keywords:
Landfill cell model
Leachate treatment plant
Cl^-
Open type
Closed type

ABSTRACT

During the design of leachate treatment plants at Japanese landfill sites, the main examined design parameters have been leachate treatment plant capacity and raw leachate quality. However, the scientific basis for characterizing raw leachate quality has been less robust, especially for the Cl^- concentration. This characterization is usually based on the precedent of other operating leachate treatment plants. However, regarding the quantity and quality of leachate at landfill sites, there is a close relationship between these parameters and Cl content in waste cells or the waste cell placement method, and these parameters depend on the landfilling method, dilution zone (no dumping area) and the quantity of leachate. Based on the landfill shape, dilution zone (no dumping area), waste cell placement method, and property of the waste cell, the Landfill Cell Model can predict leachate concentration. In this research, we used a process of leachate treatment plant capacity and the Landfill Cell Model together to investigate an early method for stabilizing landfill and dilution zones. The results revealed the possibility of characterizing the optimal leachate treatment plant capacity by balancing leachate reservoir capacity and the predicted Cl^- concentration of raw leachate in landfill.

1. INTRODUCTION

When designing leachate treatment plants in Japanese landfill sites, the capacity of such plants and the quality characteristics of raw leachate are the main examined parameters. There are two types of landfill in Japan: 1) conventional open landfill sites without a roof and 2) closed landfill sites with a roof. In the case of open type landfill sites (hereinafter referred to as "open type"), the capacity of leachate treatment plants has been researched during the last decade and a half based only on calculations using meteorological data. In the case of closed system landfill sites (hereinafter referred to as "closed type"), the same as for the open type, methods for capacity calculation during the past 15 years have used meteorological data or alternatively liquid:solid ratio in the range of 1–3 (liquid: solid ratio>3 in the case of desalination treatment) (Japan Waste Management Association, 2010). The characterization of raw leachate quality has had less of a robust scientific basis, especially the characterization of Cl^-concentration. Instead, this has generally been based on existing practices at other operating leachate treatment plants (Japan Waste Management Association, 2010). However, regarding the amount of leachate and the raw leachate quality in actual landfill sites, a close relationship of these variables with Cl content and waste cell placement method can be found; furthermore, this relationship changes depending on the landfill method and dilution zone (no dumping area) or the amount of water.

In the conventional method of calculating the capacity of leachate treatment plants, the planned raw water quality can be characterized according to the landfill shape (the height of one landfill layer), dilution zone (no dumping area), waste cell placement method and leachate landfill property. By combining this with the Landfill Cell Model (Kazuo et al., 2016, 2017a, 2017b), it is possible to characterize the optimal leachate treatment plant capacity, balancing reservoir capacity and the expected concentration of Cl^- in raw leachate for both open and closed types. Besides, the volume of water for sprinkling in the closed type can also be established, as described here.

2. MATERIALS AND METHODS

2.1 Calculation methods

2.1.1 Methods of calculating the peak concentration of Cl^- in leachate (Kazuo et al., 2016, 2017a, 2017b)

The peak concentration of Cl^- can be predicted according to the following parameters: "Cl content in incin-

* Corresponding author:
Kazuo Tameda
email: tameo@j-hac.com

Detritus / Volume 07 - 2019 / pages 76-82
https://doi.org/10.31025/2611-4135/2019.13845
© 2019 Cisa Publisher. Open access article under CC BY-NC-ND license

eration residues," "peak concentration of Cl^- in the height of one landfill layer," "dilution zone in landfill sites," and "landfill by stacking up." The predicted flow is shown in Figure 1. In this research, to estimate the peak concentration of Cl^-, the Landfill Cell Model is used. As shown in Figure 2, Hi~Hn was integrated in the x-direction. Vi~Vn was integrated in the y-direction. Di~Dn was integrated in the z-direction. The assumed calculation steps are explained as below.

Step ① The daily landfill capacity of the target landfill site is calculated and the capacity and size (length × width × height) of the Landfill Cell Model are set (capacity per cell is about 10–30 days).

Step ② The numbers of cells in the x-direction (Hi~Hn), y-direction (Vi~Vn), and z-direction (Di~Dn) of the Landfill Cell Model are set to ensure the correct shape of landfill sites.

Step ③ The volume of water for sprinkling is set according to the daily precipitation of the Landfill Cell Model in the case of the open type or through the liquid: solid ratio in the case of the closed type.

Step ④ The peak concentration of Cl^- is set by the Cl content in incineration residues from the landfilling target.

Step ⑤ A formula for predicting landfill cell peak concentration is produced from the Cl content in Step ④ and using the results of temporal changes in the leachate quality in the experiment on a simulated landfill layer, which is filled with incineration residues. At the branching point of the rate of reduction of Cl^- concentration, it is divided into the initial stage, the intermediate stage, the end stage, and the stable stage of the landfill. The predictive formula is presented in Figure 3. Depending on the parameters, the

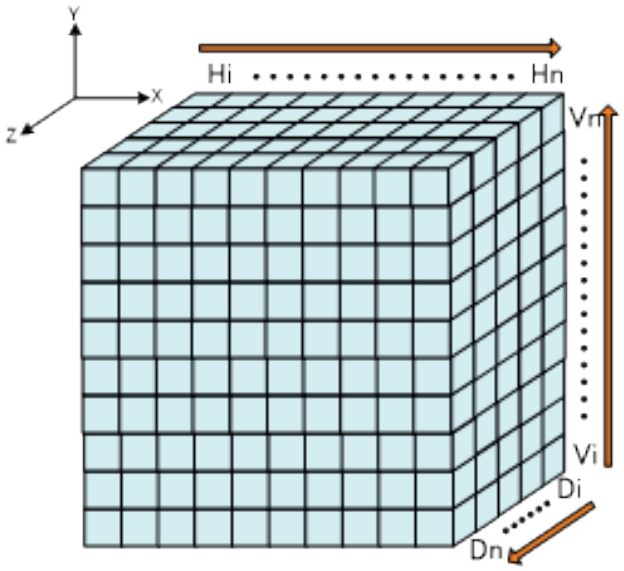

FIGURE 2: Landfill Cell Model.

predictive formula sometimes stays the same from the initial stage to the stable stage. In this study, we used the daily variation of Cl^- in the leachate from the simulated landfill site filled with incineration residue (mixing ratio=main ash: fly ash=7:3) with a Cl content of 67 g/kg. The results show that the predictive formulas are Y=−3.31X + 114,971 in the early period, Y=−0.52X + 31,553 in the middle period, Y=−0.041X + 7,003 in the late period, and Y=495 in the stable period of landfill.

Step ⑥ The leaching properties upon increasing the landfill cell are characterized. Details of the leaching prop-

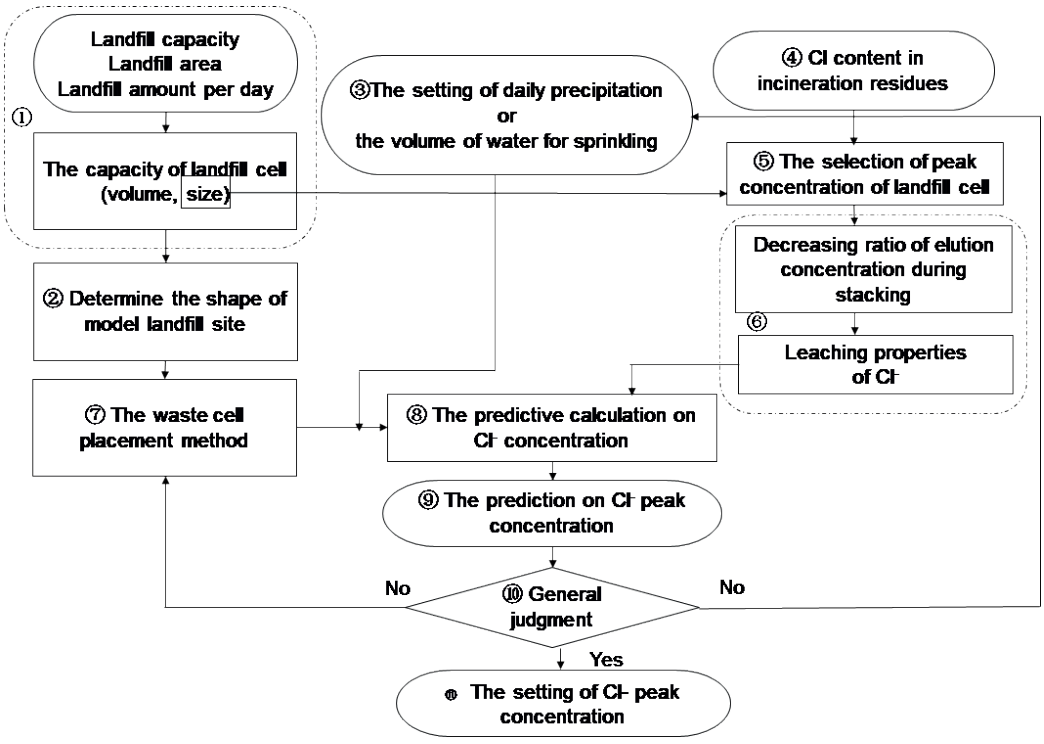

FIGURE 1: The setting flow of peak concentration of Cl^-.

erties of a cell stacked up on others are described later in "Leaching properties of one cell."

Step ⑦ The waste cell placement method is characterized by considering the timing of addition. (The x-direction indicates the landfill process and the y-direction expresses the timing of addition.)

Step ⑧ A calculation for predicting the Cl^- concentration is performed according to the waste cell placement method in Step ⑦.

Step ⑨ The peak concentration of Cl^- during the duration of existence of the landfill is estimated.

Step ⑩ A general judgment on the peak concentration of Cl^- is made; then, one proceeds to Step ⑪ or back to Step ③ and Step ⑦ to perform the examination again.

Step ⑪ The peak concentration of Cl^- is characterized.

Reduction ratio of Cl^- concentration in leachate penetration (Kazuo et al., 2017a)

1) Leachate concentration α_i (mg/L) on the number of days after landfill n_i (Day n_i) is obtained from Figure 4 using the daily precipitation (the volume of water for sprinkling) on Day n_i (i=1, 2, 3, 4...). Migration properties of leachate concentration α_i (mg/L) of Day n_i cell is calculated by multiplying migration rates and α_i (mg/L). When a migration rate for the case (V_m) in which Day n_i cell is landfilled at the m-th cell from the basement is defined as M_m%, the rate of migration (M_m) from Day n_i cell to the cell immediately below it is 100%, and those to the second and subsequent cells below it are preset as M_{m-1}%,...M_3%, M_2%, M_1%. (The migration rate is the ratio to the initial leachate quality relative to the initial leachate quality with α_i mg/L that migrates to the cell below and is expressed as a percentage.) The migration rate M_m% is set based on the rate of decrease of the peak concentration about landfill by stacking up.
2) Leachate concentration at the m-th cell from the basement on Day n_i is determined according to the location (V_m) of Day n_i cell in the y-direction.
   The location (V_m) of Day n_i cell in the y-direction gives the following calculations:
   Leachate concentration of all Day n_i cells at the basement of the landfill site, V_1, is expressed by the following equation: α_i (mg/L)×100%,
   where Day n_1 is the number of days required to landfill one cell, which was set at Step ①.
   Migration of Day n_i cell at V_m starts {m×n_1} days after Day n_i, that is, at Day $N_i = n_i + \{m \times n_1\}$, and it ends at Day $N_i + n_1 \times j$ (j = 1, 2, 3, 4...),
   where M_1%, the rate of migration to outside of the landfill site, of the Day n_i cell is calculated until the initial leachate quality M_m = 100% completely migrates outside of the landfill site. In other words, calculation is performed until an equation 100% − $\Sigma M_{1,k} < M_1$ holds, where the sum of the migration rates outside of the landfill site is $\Sigma M_{1,k} = (M_{1,1} + M_{1,2} + ... + M_{1,k})$ (k = 1, 2, 3, 4...).
   Therefore, the leachate concentration of Day n_i cell on Day N_i is expressed by the following equation: α_i (mg/L) × $M_{1,k}$%.
   Next, the leachate concentration of Day n_i cell on Day $N_i + n_1 \times j$ when the migration of the leachate concentration α_i (mg/L) ends is expressed as follows: α_i (mg/L) × (100 − $\Sigma M_{1,k}$)%.
3) The calculation described above in 2) is performed for all cells in the landfill area in this Landfill Cell Model and the volume of water for sprinkling in the dilution zone is added to it at the end to obtain the total leachate concentration.
4) The following is an example of the calculation described above of the case where four cell layers are stacked up (Figures 5, 6).
   Assume that:

   - landfill is advanced from V_1 to V_4,
   - only the migration property from V_4 is considered,
   - the leachate concentration from V_4 is α_i mg/L (i re-

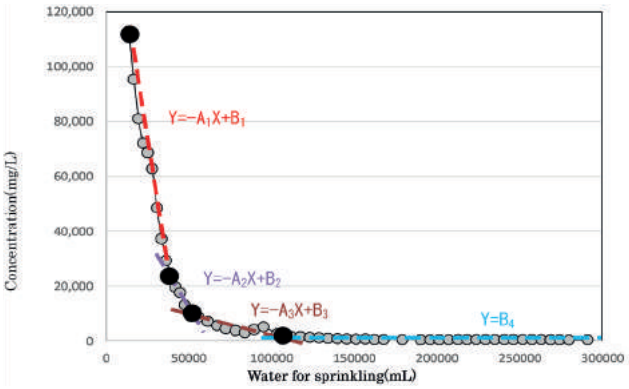

FIGURE 3: Conceptual diagram of formula for predicting landfill cell peak concentration.

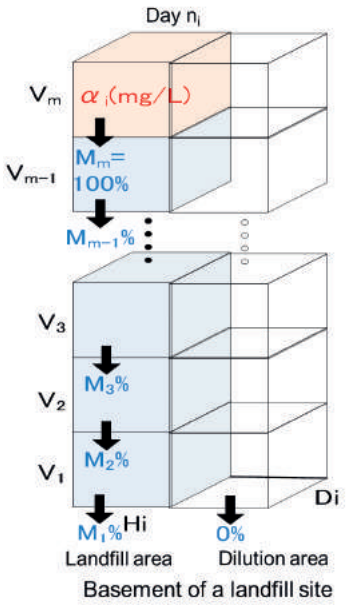

FIGURE 4: Conceptual diagram of the reduction ratio of Cl- during the landfill by stacking up.

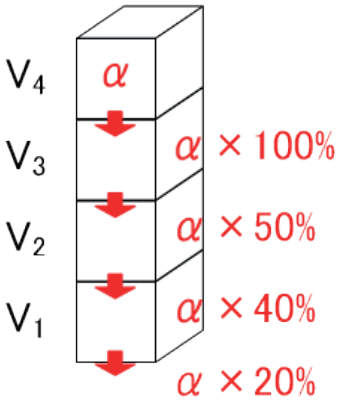

FIGURE 5: The reduction ratio of Cl^- in the case where four cell layers are stacked up.

presents the number of days; i = 10, 20, 30,...), and

- the migration rates from V_4 in the y-direction: first layer, 100%; second layer, 50%; third layer, 40%; and fourth layer, 20%.
- 10 days after the landfill: The leachate quality α_{10} × 100 migrates from V_4 to V_3.
- 20 days after the landfill: The leachate quality α_{20} × 100% migrates from V_4 to V_3 and the leachate quality α_{10} × 50% migrates from V_3 to V_2.
- 30 days after the landfill: The leachate quality α_{30} × 100% migrates from V_4 to V_3, the leachate quality α_{10} × 60% migrates from V_3 to V_2, the leachate quality α_{20} × 50% migrates, the leachate quality α_{10} × 40% migrates from V_2 to V_1.
- 40 days after the landfill: The leachate quality α_{40} × 100% migrates from V_4 to V_3, the leachate quality α_{20} × 50% migrates from V_3 to V_2, the leachate quality α_{30} × 50% migrates, the leachate quality α_{10} × 40% migrates from V_2 to V_1, the leachate quality α_{20}×40% migrates, and the leachate quality α_{10} × 20% migrates from V_1 to outside of the landfill site.

Conduct the subsequent calculations in the same way.

2.1.2 The calculation method for characterizing the planned raw water quality in open type (Kazuo et al., 2017b)

Figure 7 shows the flow for designing a leachate treatment plant (the capacity of the leachate treatment plant, the capacity of the adjustment dam, and the quality of planned raw water).

① The maximum and minimum capacities of both the leachate treatment plant and the adjustment dam are calculated from the average daily precipitation and monthly maximum precipitation in the last 15 years. (The possible amount of evaporation can be calculated by using the Blaney-Criddle method and the seepage coefficient C can be characterized)

② The same as in the conventional method, the capacity of both the leachate treatment plant and the adjustment dam are calculated within the capacity range in Step ① from water balance analysis using the daily precipitation series in the last 15 years.

③ The Landfill Cell Model is used to calculate the predicted peak concentration and load amount.

④ The possible daily precipitation through the seepage coefficient is calculated from the capacity of the leachate treatment plant, which was calculated in Step ②. Then, the quantity of supplied water is calculated by subtracting the daily precipitation that was set in the landfill model for this amount.

⑤ The range of the predicted peak concentration is calculated, which was considered to represent the quantity of supplied water.

⑥ The optimum capacity of the leachate treatment plant, that of the adjustment dam, and the quality of planned raw water are calculated through Step ② and Step ⑤.

2.1.3 The calculation method for characterizing the planned raw water quality in closed type (Kazuo et al., 2018)

Figure 8 shows the flow for designing a leachate treatment plant (the capacity of the leachate treatment plant, the capacity of the adjustment dam, and the quality of planned raw water).

① The Landfill Cell Model was used to calculate the predicted peak concentration and load amount.

② The capacity range of the leachate treatment plant was set using the same method as in [2.1.2 ①].

③ The daily leachate amount was calculated from the volume of water for sprinkling according to the liquid: solid ratio.

④ According to the concentration of Cl^- predicted in Step ①, the target Cl^- concentration can be set and the dilution amount can be calculated.

⑤ The daily amount of leachate can be calculated by the sum of the amounts in Step ③ and Step ④, and the total level should be less than or equal to the amount in Step ②.

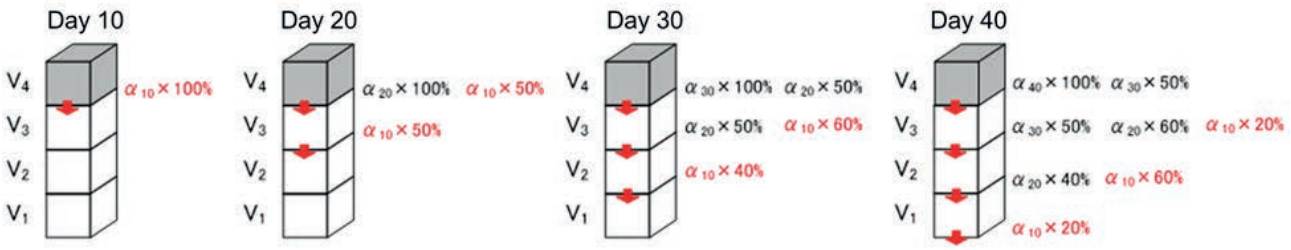

FIGURE 6: The migration concept of Cl^- in leachate of Landfill Cell Model.

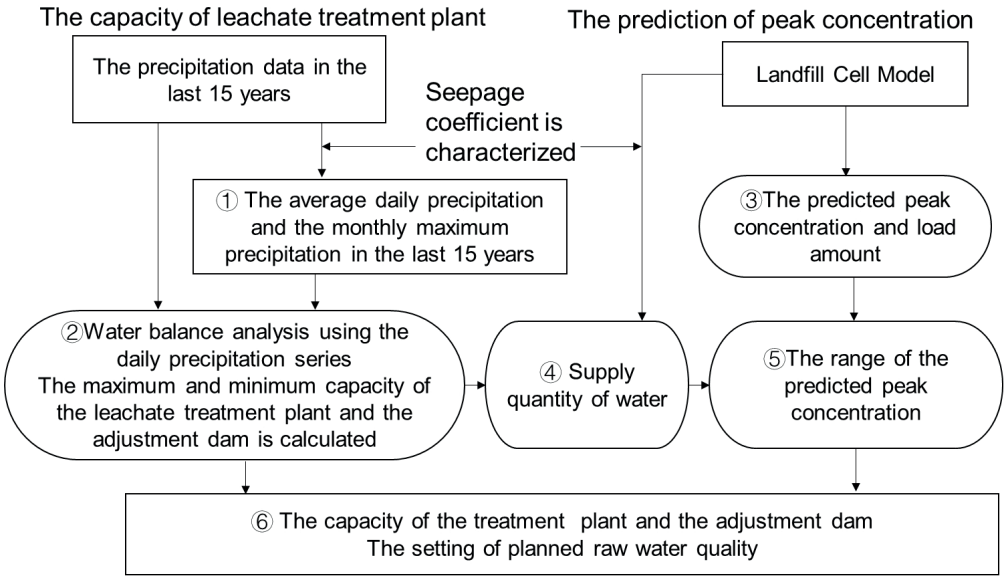

FIGURE 7: The flow for designing a leachate treatment plant.

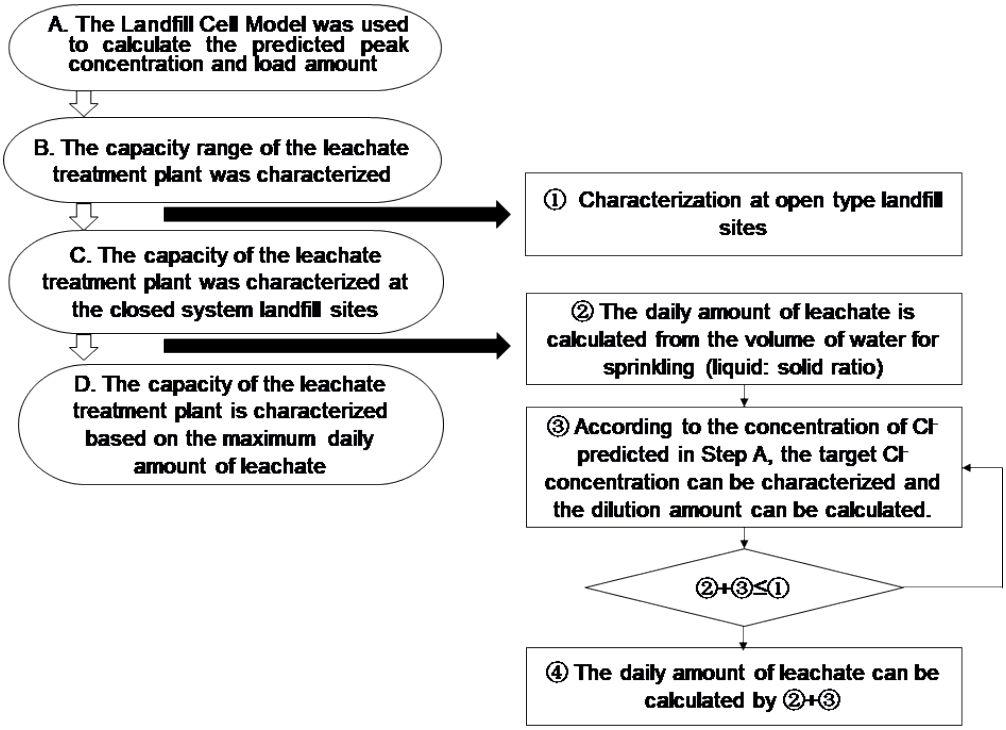

FIGURE 8: The flow for designing a leachate treatment plant.

2.2 Case study

2.2.1 The conditions in the case study

The case study in this research focused on a treatment plant for a population of 100,000 people, with a capacity of municipal solid waste (MSW) landfill sites of nearly 90,000 m^3, a landfill area of about 9,000 m^2, a landfill height of 10 m, a landfill duration of 15 years, and incineration residues with Cl content of 67 g/kg (bottom ash: flying ash ratio of 7:3). The one-cell landfill duration of the Landfill Cell Model was set to 10 days (landfill capacity ~160 m^3).

The capacity of the leachate treatment plant was examined using the past meteorological data of F city. In the last 15 years (2002–2016), the mean annual precipitation was 1,702 mm (4.7 mm/day), the maximum monthly precipitation was 620 mm (20 mm/day) in July 2009, the landfill area was A1=4,500 m^2 in the process of the landfilling and A2= 4,500m^2 in the case of the completed landfill, the seepage coefficient is 0.63 during the duration of landfilling, and will be 0.38 when the landfill is completed. The minimum capacity of the leachate treatment plant is 20 m^3/day and

its maximum capacity is 90 m^3/day (Sotaro, 2017). This investigation was carried out within this capacity range. The formula for calculating Q is as follows: Q= (1/1000) × I × (C1 × A1 + C2 × A2).

2.2.2 Open type (Kazuo et al., 2016 and 2017b)

The peak concentration of Cl^- in leachate and the load amount of Cl were set by using the method in [2.1.1]. The results as shown in Figure 9 indicate that the concentration fluctuates drastically at the initial stage of the landfill, the peak concentration of Cl^- is about 24,863 mg/L, and the load amount of Cl increases to about 7,640 kg/10 days when the volume of water for sprinkling is 107,520 m^3.

Then, the capacity of the leachate treatment plant is set. As mentioned in [2.2.1], the minimum capacity of the leachate treatment plant (Qop) is 20 m^3/day and its maximum capacity is 90 m^3/day. As a result, the target peak concentration of Cl^- is below 10,000 mg/L; dilution water was added to the leachate treatment plant, and the peak concentration of Cl^- was adjusted. When the daily precipitation is 38 m^3, the amount of dilution water is 40 m^3 and the capacity of the leachate treatment plant is 65 m^3/day (Table 1).

The desalination treatment installation determines the capacity of the membrane surface area based on the load amount obtained from the product of the water quantity and the water quality. Therefore, finding the peak load amount and using the maximum load amount to determine the equipment capacity makes it economical. In other words, even if the peak value of water quality is high, if the amount of load at this time is smaller than the maximum value, stable processing can be performed.

For this reason, the quality of Cl^- planned raw water is set from the maximum load amount. However, under these conditions, as the landfill method affects a lot, it is necessary to connect the maximum load amount with the landfill method. Besides, since unpredictable situations often occur in actual operations, it is important to have a margin that allows a response to such situations by changing the landfill method used.

2.2.3 Closed type (Kazuo et al., 2018)

Based on the method in [2.1.1], the peak concentration of Cl^- and the load amount of Cl in leachate were set. In this case, the liquid: solid ratio used for setting the volume of water for sprinkling is 3:1 (advanced treatment).

As shown in Figure 10, the predicted concentration of Cl^- peaks at the initial stage of the landfill, reaching about 101,200 mg/L. The load amount of Cl becomes the maximum at the end of the landfill, at 2,260 kg/day. At that time, the volume of water for sprinkling is about 137,670 m^3 and the total liquid: solid ratio is 1.5:1. Besides, 11,540 days (about 31.6 years) after the end of the landfill, the predicted concentration of Cl^- is below 1,000 mg/L, the volume of water for sprinkling is about 424,090 m^3, and the total liquid: solid ratio is 4.8:1. Then, the setting of the volume of water for sprinkling and the quality of Cl^- planned raw water is made.

Regarding the volume of water for sprinkling, the liquid: solid ratio is increased to 3:1 (desalination treatment); in this setting, the liquid: solid ratio is 1.5:1 at the end of the landfill. In this study, the quality of Cl^- planned raw water and the capacity of the leachate treatment plant in closed-system landfill sites are set, and we estimate the capacity of leachate treatment plant at first. We used the result of setting the capacity of the leachate treatment plant in the case of the open type in [2.2.1]. The minimum capacity of leachate treatment plant is 20 m^3/day, while the maximum value is 90 m^3/day. Our study was conducted within this range. Besides, in the case of setting the volume of water for sprinkling, when the liquid: solid ratio was increased to 3:1 (desalination treatment), the predicted peak concentration of Cl^- is 101,200 mg/L at the initial stage of the landfill. To reduce the burden on the leachate treatment plant, dilution water was added to reduce the concentration of Cl^-. Regarding the amount of dilution water to be added, we should make sure that the capacity of the leachate treatment plant is within the range of 20-90 m^3/day. Considering the volume of dilution water under the above conditions, the upper limit for the reduction of Cl^- concentration is 26,000 mg/L. However, when the value is above 26,000 mg/L, the volume of dilution water to be added is set to below 49 m^3/day in the leachate treatment plant. The result is shown in Figure 11. In the case of the volume of dilution water, the maximum value is 49 m^3/day. At the same time, the volume of water for sprinkling is 137,665 m^3. Then, when the volume of water for sprinkling is 325,720 m^3, the volume of dilution water gradually decreases to 0 m^3/day. Therefore, when the capacity of a leachate treatment plant, which is the sum of the amount of leachate and dilution

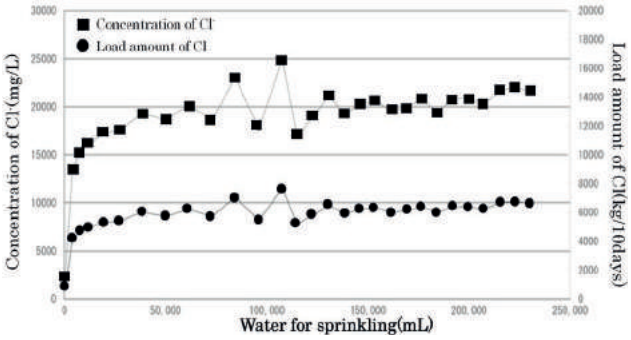

FIGURE 9: The daily changes of the peak concentration of Cl^- and load amount of Cl.

TABLE 1: The capacity of the leachate treatment plant.

Items	UM	Values
The predicted peak concentration of Cl^-	mg/L	24,863
The predicted load ammount	Kg	7,638
Daily precipitation of Landfill Cell Model	m^3	38
The target peak concentration of Cl^-	mg/L	10,000
The supply quantity of water	m^3	40
The peak concentration of Cl^- after diluition	mg/L	9,742
Possible ammount of precipitation	m^3	78,40
Seepage coefficient	C	0.8
The capacity of leachate treatment	m^3/day	63

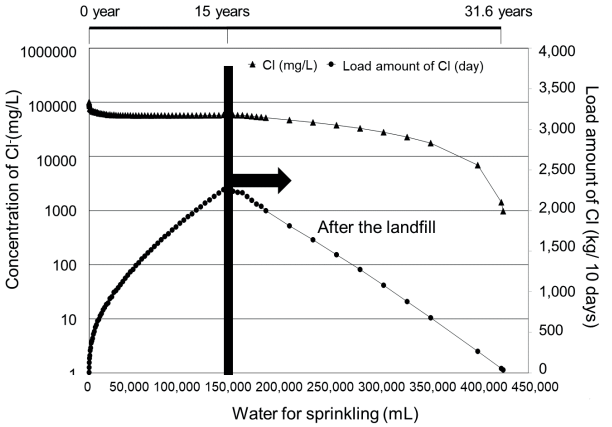

Items		UM	Values
The maximum predicted value of Cl^- concentration		mg/L	~101,200
The maximum load amount of Cl	After the landfill	Kg/day	~2,260
	The volume of water for sprinkling	m^3	~137,670
	The liquid: solid ratio		1.5:1
The predicted concentration of Cl^- below 1,000 mg/L	After the landfill	Kg/day	11,540 (~31.6)
	The volume of water for sprinkling	m^3	~424,090
	The liquid: solid ratio		4.8:1

FIGURE 10: The predicted peak concentration of Cl^- and the load amount of Cl (liquid:solid ratio: 3:1).

water, reaches 90 m^3/day, the quality of Cl^- planned raw water is 26,000 mg/L.

3. CONCLUSIONS

The results of this study can be summarized as follows:

(1) When designing MSW landfill sites, it is possible to estimate the peak concentration of Cl^- and make a prediction of the quality of raw water regarding its Cl^- concentration through the Cl content in landfill incineration residues and landfill methods.

(2) When the predicted peak concentration of Cl^- is generated, it is possible to reduce the peak concentration by adjusting the volume of dilution water at the dilution zone and leachate treatment plant in the case of open type or adjusting the volume of water for sprinkling and dilution in the case of closed type.

(3) In the design of closed-type leachate treatment plants, referring to the peak concentration of Cl^- and the load amount of Cl that is predicted by the Landfill Cell Model and the capacity of open-type leachate treatment plants, it is possible to calculate the volume of dilution water to reduce the concentration of Cl^-. As a result, the optimal quality of Cl^- planned raw water and the optimal capacity of the leachate treatment plant can be set.

(4) By using the Landfill Cell Model in the open type, it is possible to identify an appropriate landfill method that can achieve stabilization at an early stage.

(5) By using the Landfill Cell Model in the closed type, it is possible to identify an appropriate landfill method, adjust the volume of water for sprinkling, and reduce the Cl^- concentration to achieve early stabilization.

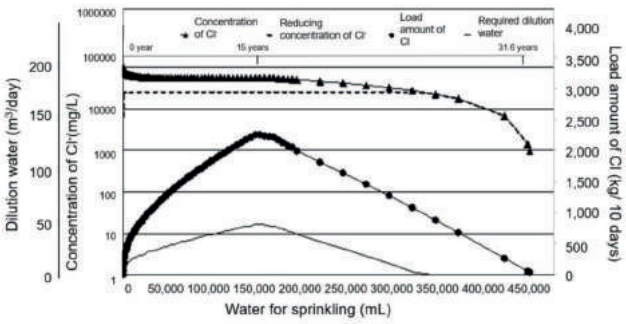

Items	UM	Values
Peak concentration (at the initial stage of the landfill)	mg/L	101,200
The maximun load ammount	Kg/day	2260
The reduction of peak concentration	mg/L	set below 26,000
The maximun volume of dilution water	m^3 / day	49
The capacity of leachate treatment plant	m^3 / day	90

FIGURE 11: The amount of dilution water and the reduction of predicted peak concentration of Cl^-.

REFERENCES

Japan Waste Management Association (2010). Plan, design and management guidelines for the improvement of MSW landfill sites (2010 revised edition), p.364, pp.417-438.

Kazuo, T et al. (2016). A study on the development of the predictive method of Cl^- concentration in leachate. Research presentation in the 27th Material Cycles and Waste Management Conference, pp.431-432.

Kazuo, T et al. (2017a). A study on the development of a predictive method of Cl^- concentration in leachate. Japan Waste Management Association and Research, 70(399). pp.101-107.

Kazuo, T et al. (2017b). The development of leachate desalination design method using Landfill Cell Model. Research presentation in the 28th Material Cycles and Waste Management Conference, pp.371-372.

Kazuo, T et al. (2018). The development of leachate desalination process design method of closed system landfill sites using Landfill Cell Model. Proceedings of 39th Japan Waste Management Association and Research, pp.124-126.

Sotaro, H. (2017). Technology for final disposal-waste management and technology for final disposal (No. 21). The City and the Waste, 47(10), pp.45-51.

detritus | Multidisciplinary Journal for Waste Resources & Residues

CISA

AEROBIC BIOLOGICAL TREATABILITY STUDIES ON LANDFILL LEACHATE WITH NITRIFICATION AND DENITRIFICATION

Tim Robinson *

Phoenix Engineering, Phoenix House, Scarne Mill Industrial Estate, Launceston, Cornwall, PL15 9GL, United Kingdom

Article Info:
Received:
01 March 2019
Revised:
07 June 2019
Accepted:
02 July 2019
Available online:
01 August 2019

Keywords:
Ammoniacal-N removal
Biological treatment
Denitrification
Landfill leachate
Leachate treatment
Nitrification
Treatability trials

ABSTRACT

Large pilot-scale treatment trials have examined the treatment of a leachate typical of those found at many closed landfill sites, containing approximately 200mg/l of ammoniacal-N. At such sites, treatment of these leachates with nitrification of ammoniacal-N alone, will not allow discharges of treated leachate to be made into sensitive surface watercourses, because of concerns about nitrate-N. The trials therefore included denitrification processes, by modification of an SBR process configuration, using the waste product glycerol, widely available as a by-product from the production of biodiesel, as the carbon source for denitrification. Initially a nitrification-only Stage 1 treatment trial treated strong, methanogenic leachate containing 2000mg/l of ammoniacal-N and 4000mg/l COD, completely nitrifying all ammoniacal-N to nitrate-N. Following the successful treatment of strong leachate through nitrification, the innovative combined nitrification and denitrification treatment system was constructed. Stage 2 of the treatability trial used this newly designed system to incorporate both aeration and anoxic phases within a single reactor; enabling full nitrification and denitrification of weaker leachate from a closed landfill, containing 150mg/l ammoniacal-N and 200mg/l COD. In particular, the development of an innovative, stable, robust and relatively simple combined nitrification and denitrification process will have wide application at many closed landfill sites, where a reliable and robust treatment process is required, whilst full denitrification of nitrate-N is essential if treated leachate is to be discharged locally into small watercourses. The relative simplicity of the new process, in a single tank, with readily-automated operation and few chemical additions, means that it can be used at remote closed landfills, to produce high quality effluents suitable for discharge into many surface watercourses.

1. INTRODUCTION

The reliable and consistent on-site treatment of leachate is now a common requirement at modern landfill sites. That treatment must achieve complete removal of all degradable organic compounds in the leachate, as well as nitrification, and increasingly denitrification, of very high concentrations of ammoniacal nitrogen and nitrate nitrogen.

Aerobic biological processes have widely been shown to be capable of achieving these treatment objectives, and the Sequencing Batch Reactor (SBR) process configuration has been used successfully in many countries, and regularly shown to provide the robustness of treatment required (Environment Agency, 2007). However, an effective method of treating medium strength leachates from closed landfills, whilst incurring low running, operational and maintenance costs has yet to be adopted; whereby both nitrification and denitrification are successfully achieved within a single reactor, prior to appropriate discharges to sensitive watercourses.

The study reported in this paper first involved proving the success of large pilot scale treatment studies at treating strong methanogenic leachate through nitrification, which is very typical of leachates from large landfill sites in many countries of the world (Christensen, 2011).

At many closed landfill sites however, treatment of weaker leachates (containing approximately 200mg/l of ammoniacal-N) with nitrification only will not allow discharges of treated leachate into highly sensitive surface watercourses (Wilson, et al., 2015), because of concerns about nitrate-N and possible eutrophication problems. Therefore, the Stage 2 treatability trial incorporated the denitrification process, by modification of the process configuration, to provide complete nitrification and denitrification within a single treatment reactor.

Full scale leachate treatment plants which not only achieve nitrification of high concentrations of ammonia-

* Corresponding author:
Tim Robinson
email: tim.robinson@phoenix-engineers.co.uk

Detritus / Volume 07 - 2019 / pages 83-95
https://doi.org/10.31025/2611-4135/2019.13840
© 2019 Cisa Publisher. Open access article under CC BY-NC-ND license

cal-N, but also full denitrification of the nitrite-N produced, have been designed and commissioned in recent years (Robinson, 2007). The Vissershok plant at the main landfill serving the city of Cape Town is one such plant, designed to treat more than 400m³/d of leachate containing more than 2000mg/l of ammoniacal-N (Plate 1). The full-scale Vissershok plant has two aeration tanks, overflowing into an anoxic tank, before being transferred into a post anoxic tank and an ultra-filtration unit.

Such large plants, although demonstrated to be capable of reliable and robust operation, are relatively complex, and generally require daily attendance by a plant operator. In particular, the process of nitrification, denitrification and post anoxic aeration take place in separate reactors, as follows, so that acidity produced during nitrification, and alkalinity generated during denitrification, can balance each other to minimize addition of pH chemicals, as mixed liquor circulates around the various reactors (Robinson, et al., 2017).

It would not be possible to operate such a plant in a single reactor, because alternating nitrification during Aerobic phases, denitrification during Anoxic phases, and aeration during Post-Anoxic Aeration phases, would cause wide swings in pH value, which would be damaging to both nitrifying and denitrifying bacteria. The Stage 2 trials would therefore investigate whether treatment of weaker leachates, found at many hundreds of older closed landfills in the UK, could achieve complete nitrification and denitrification of ammoniacal-N in a simpler, single reactor system.

The paper describes the design and operation of both Stage 1 and Stage 2 of the trials, presenting detailed analytical and operational results, and discusses the implications of these.

2. MATERIALS AND METHODS

The same 240-litre capacity pilot-scale treatment unit was used for Stage 1 nitrification trials on strong leachates and Stage 2 combined nitrification and denitrification trials on weaker leachate from a closed landfill. The unit was constructed as shown in Plate 2 and was modified to allow anoxic mixing and carbon dosing during the denitrification phase of the Stage 2 Trials.

2.1 Stage 1 Experimental Design

The strong methanogenic leachate treated during Stage 1 contained COD values of about 4000mg/l, and concentrations of ammoniacal-N of just below 2000mg/l. This trial achieved the degree of nitrification treatment required, demonstrating that no leachate contaminants were causing inhibition to complete ammoniacal-N removal.

Figure 1 displays the design of the treatment unit used during Stage 1, to allow operation in a fully-automated way, as a Sequencing Batch Reactor (SBR). The aerated reactor had a minimum operating volume of 160 litres, and could be aerated and mixed by means of a fine air diffuser pipe in the base, which received air from a small electric compressor, controlled by a simple timer. Dosing of leachate for treatment was provided by a small dosing pump, mounted on a 100-litre capacity feed tank.

Pre-set volumes of leachate were dosed into the reactor every 15 minutes during aeration periods. Following a daily period of quiescent settlement, clarified effluent was decanted over a small bellmouth weir, when a small solenoid valve was energized by a timer, and opened.

A 20mm pipe was inserted to act as the bellmouth overflow weir, to allow effluent discharge down to a bottom water level of 160 litres capacity. The discharge

PLATE 1: Vissershok Landfill Leachate Treatment Plant, Cape Town, South Africa.

PLATE 2: View of the experimental units, showing feed tank and dosing pump, the 240 litre SBR reactor, electrical control panel, and treated leachate tank.

end of this pipe was fitted with a solenoid valve (CEME 9914 ½"series), which, when energized, opened to allow discharge of treated leachate into an effluent collection container.

To allow nitrification to take place during an aerobic phase, a small 0.25kW Compton air compressor (model AMDE 90L/A4) supplied aeration via a 25mm diameter fine pore diffuser pipe in the base of the unit. This also provided vigorous mixing. Air flow rates from 10 to 35 l/min through the diffuser could be achieved accurately.

A diaphragm chemical dosing pump (Siemens AA1409 Premia75 Mono Pump) was programmed to dose leachate slowly at precise low rates into the aeration unit every 15 minutes from the 100-litre feed tank. This feed tank was calibrated to allow volumes dosed each day to be measured accurately to the nearest 0.1 litre.

Automated operation of the treatability unit was controlled from an electrical panel, where timers for each device were located in a series of sockets. A 200W tank heater/thermostat maintained treatment temperatures in the range 23-25°C, which would be typical of a large scale biological treatment plant (Robinson, 2015).

The treatment process was operated on a 24-hour cycle as shown below:

(1) 20 hours: Aeration and leachate addition every 15 minutes.
(2) 2 hours: Quiescent settlement and clarification.
(3) 2 hours: Effluent decant and idle.

pH values were controlled within an optimum range of 7.2 to 7.8 by manual daily addition of measured amounts of sodium bicarbonate into the reactor. Samples of effluent discharged were tested each day for concentrations of ammoniacal-N, nitrate-N and nitrite-N, using test strips, and samples of leachate feed, mixed liquor, and treated leachate were submitted to a laboratory once or twice each week, for more detailed analysis.

Leachate to be treated in the initial nitrification only trials was selected to be typical of strong, stable methanogenic leachates that are found at large landfill sites in many countries of the world (Robinson, 2007). 1000 litres of the leachate was obtained from a large landfill site in East Anglia, UK, to be transported in an airtight IBC container to the laboratory, for storage and use in the trials. Regular testing of the leachate feed demonstrated that no significant changes in leachate composition took place during the period of the trials (Table 2).

Leachate feeding began on Day 0, and gradually increased until by Day 10, about 10 litres were being treated each day, at a mean Hydraulic Retention Time (HRT) of about 16 days. Feed rates continued to be increased, and between Days 29 and 45 leachate was being treated at rates of 16 or 17 litres per day with full nitrification. For the last week of the trials, up to Day 54, dosing rates of 21 or 22 litres per day were consistently treated successfully, however when increased further, to above 25 litres daily, breakthrough of ammoniacal-N took place.

Figure 2 shows the mean HRT (in days) that was maintained during the Stage 1 trials, and Table 2 presents detailed results for the quality of the raw leachate feed, and of treated leachate once stable conditions of operation had been established.

2.2 Stage 2 Experimental Design

The initial Stage 1 series of trials had demonstrated that the pilot-scale treatment units which had been designed and constructed, were capable of operating reliably and efficiently to provide stable treatment of a relatively strong methanogenic landfill leachate.

Leachates from closed landfill sites are weaker than those from large operational sites (Kjeldsen et al., 2002), but typically still contain 100 to 200mg/l of ammoniacal-N. Furthermore, discharge of treated leachates containing equivalent concentrations of nitrate-N to watercourse or sewer remains problematic (Robinson, 2017).

The second stage of the trials would therefore examine the practicality of using a single vessel modified SBR process to treat such leachates, using an innovative process design shown below in Figure 3. The overall treatment process was simplified, to enable it to be carried out within a single treatment tank; very important for operation of leachate treatment facilities at unmanned closed landfill sites, where availability of space may also be an issue. Glycerol was used as the carbon source for denitrification, since it

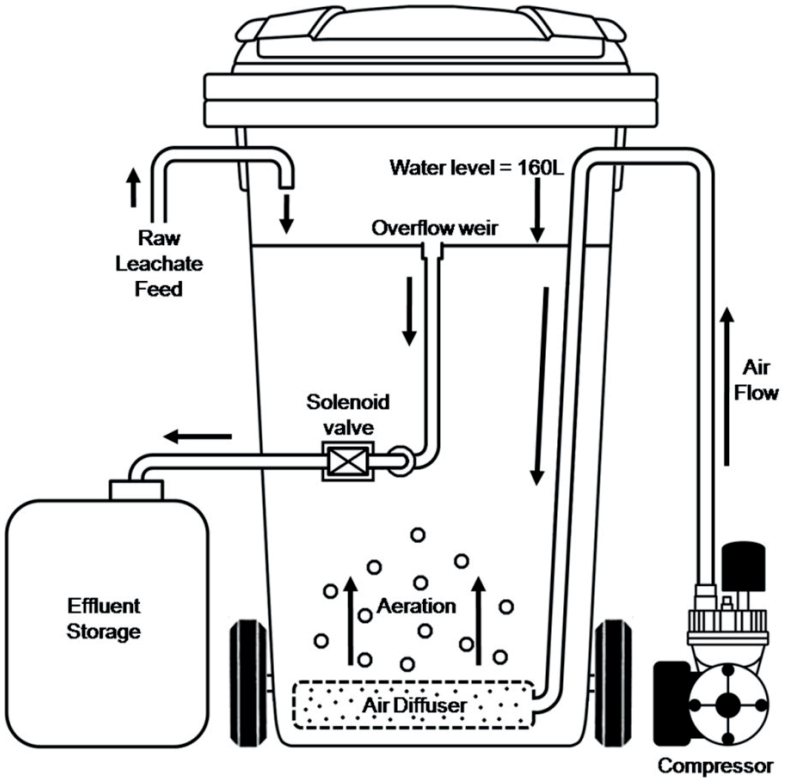

FIGURE 1: Layout of the pilot-scale SBR treatment system.

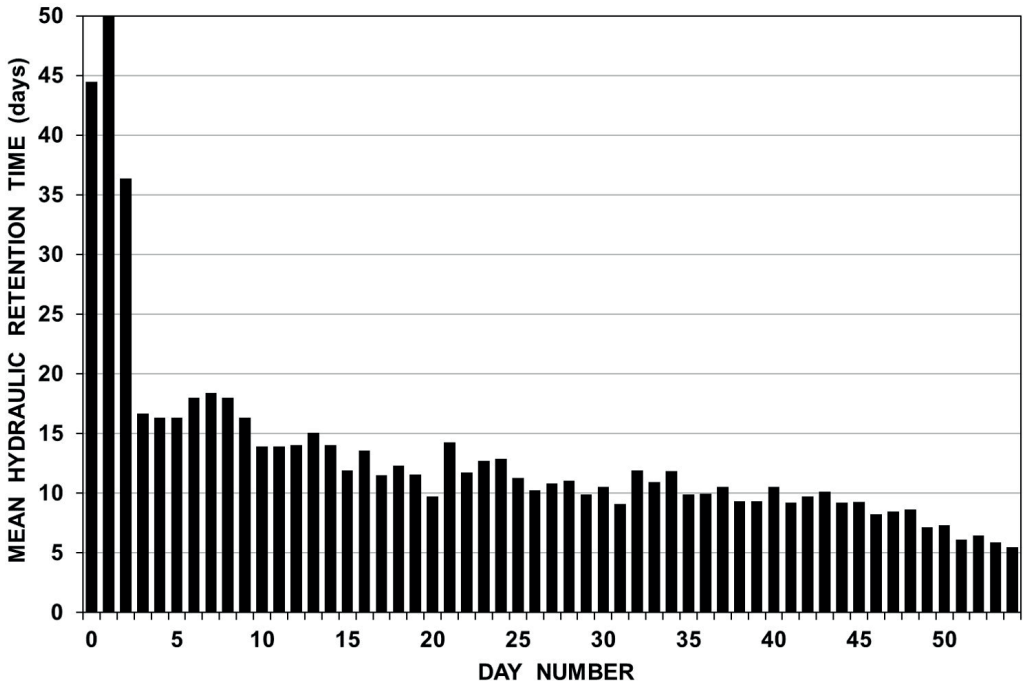

FIGURE 2: Mean hydraulic retention time (HRT, in days) during the Stage 1 trials.

is widely available as a by-product from the production of biodiesel.

Biological nitrogen removal using denitrification is common in wastewater treatment, where nitrate in effluent discharges causes concerns about eutrophication. The presence of any dissolved oxygen seriously inhibits the denitrification process, even at concentrations as low as 0.2mg/l. Denitrification operates well between 5°C to 40°C, and the process is typically three times as fast as nitrification (e.g. see USEPA, 1993, and Hartley, 2013, page 42). pH-values outside a narrow optimum range of 6.0 to 8.0 rapidly reduce rates of denitrification (Environment Agency,

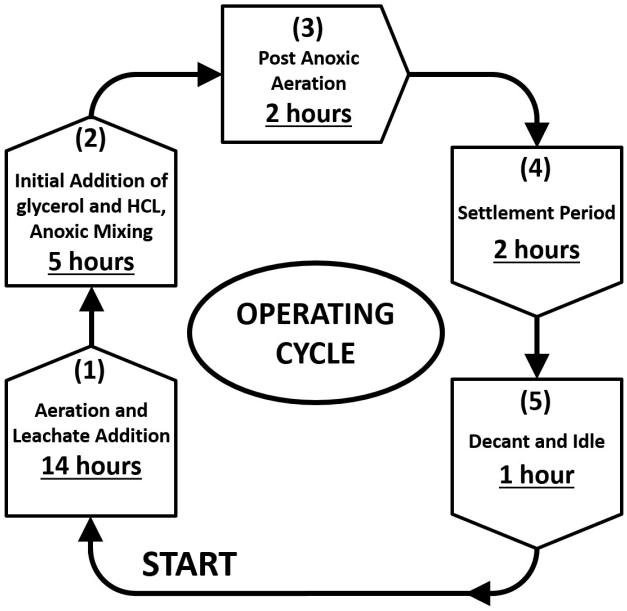

FIGURE 3: Process design for Stage 2 of the trials.

2007), and because the denitrification process releases alkalinity (3.57 grams of alkalinity as $CaCO_3$ for every gram of nitrate-N reduced; see Metcalf and Eddy, 2004, page 619), it is sometimes necessary to add acid to prevent inhibition.

To incorporate an anoxic phase for denitrification, the 240-litre wheeled bin reactor was equipped with a stirrer motor (Prominent model 791503), attached to the lid. The 0.18kW motor turned a small propeller at 1400rpm, which completely mixed the contents of the reactor without aeration; allowing anoxic phases of treatment to be carried out successfully.

To allow controlled dosing of the glycerol carbon source and acid for pH control, a combined solution was made up which initially contained 12% glycerol waste, 4% HCl and 84% water (which was later adjusted as required). To dose this solution at the start of every anoxic phase, an accurate peristaltic pump was used (Watson Marlow, model 323), via a timer. The peristaltic pump and solution container are on the desk displayed in Plate 2.

The Stage 2 treatment process again operated as a 24-hour cycle with phases as follows:

(1) 14 hours: Aerobic treatment with gradual addition of leachate.
(2) 5 hours: Initial addition of glycerol (containing some acid or alkali for pH control as determined), and stirred Anoxic treatment to achieve denitrification.
(3) 2 hours: Post-anoxic aeration, to strip off bubbles of nitrogen generated in Phase (2), and degrade any residual glycerol.
(4) 2 hours: Quiescent sludge settlement and clarification of effluent.
(5) 1 hour: Effluent decant, then idle, before returning to Phase (1).

In order to carry out the Stage 2 trials, the trials units used for the initial treatment studies were modified as follows, to allow the process design shown in Figure 3 above to be carried out in a fully automated manner. First, a stirrer motor and propeller were attached to the lid of the treatment reactor (see the motor in Figure 4 and Plate 2 earlier), to enable the contents of the reactor to be completely mixed without any oxygen inputs, during Anoxic phases of treatment. Second, a feed bottle providing a carbon source for denitrification, in the form of diluted waste glycerol (Grabinska-Loniewska et al., 1985) was supplied. A small peristaltic pump could dose this solution into the treatment reactor in a very precise manner, under timer control at the start of each Anoxic period. Low concentrations of acid or alkali could then be added into this glycerol feed bottle, in amounts calculated to provide an accurate control of overall pH values in a simple manner. Figure 4 displays these additions to the modified SBR treatment reactor design.

A suitable leachate was selected from a closed landfill site in the South of England (Environment Agency, 1996), which is presently being tankered a significant distance for disposal to sewer. The leachate contained 150-160mg/l of ammoniacal-N, and is typical of leachates at many similar landfills in the UK (Robinson, et al., 2009; 2011).

1000 litres of leachate was collected on two separate occasions, for use in the trials, and was stored in a sealed IBC container, to be pumped into the trials feed tank as required.

The biological sludge from the Stage 1 trials was used as the seed sludge for the Stage 2 work, and during initial operation of the second trials these were operated in a nitrification-only manner, to acclimatize the bacteria to the new leachate, and also to flush through the treatment system with several bed volumes of the weaker leachate. During both sets of trials, suspended solids concentrations within the reactor were maintained well, without either significant loss or accumulation of excess biological sludge mass.

During the nitrification/denitrification phase of the combined Stage 2 treatability trials, ORP and pH results were used to optimize conditions for the nitrifying and denitrifying bacteria. While operating these trials, pH and ORP were recorded extensively during the 24-hour treatment cycle, enabling observations to be made of the effects that both nitrification and denitrification processes had on the conditions within the combined treatment reactor (Robinson, T., 2014). Outside a narrow optimum range of 6.0 to 8.0 pH-values can rapidly reduce rates of denitrification (Environment Agency, 2007).

Because in theory, during denitrification, 3.57 grams of alkalinity is produced as $CaCO_3$ for every gram of nitrate-N reduced (Metcalf and Eddy, 2004; WPCF, 1983), small volumes of hydrochloric acid (0.5 l/m^3 treated) were required. Additionally, the overall process could be managed using pH and ORP as control parameters.

Figure 5 presents results for the overall mean Hydraulic Retention Time (HRT) achieved during the entire Stage 2 trial, which from Day 0 to Day 39 was operated on a nitrification-only basis.

A feed pump failure between Days 28 and 30 meant that no leachate was dosed into the reactor during this period, but the process very rapidly achieved previous feed rates when the pump was repaired. Between Day 40 and

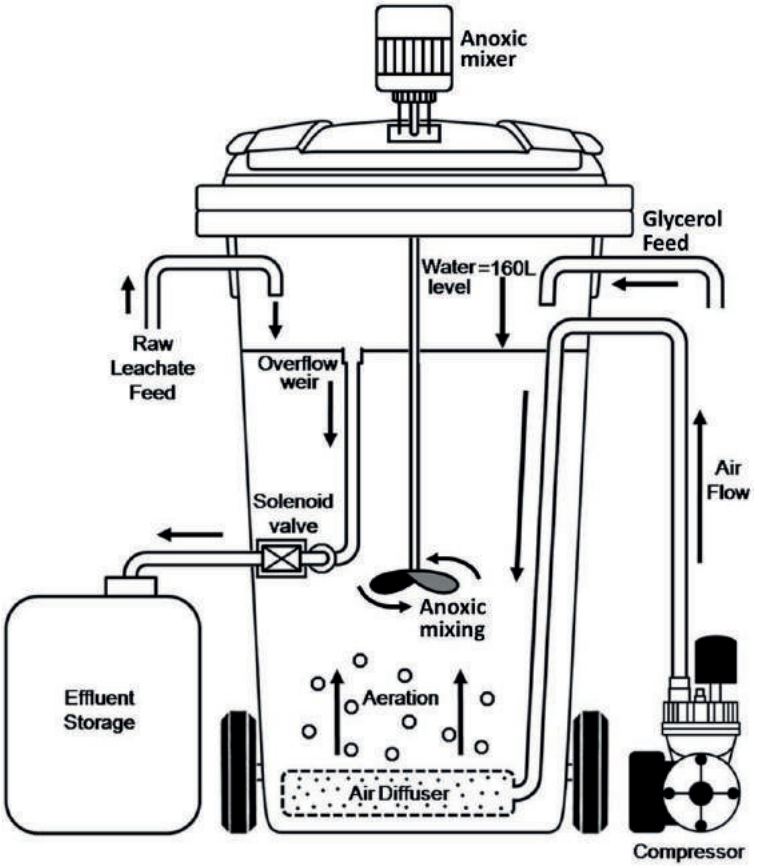

FIGURE 4: Layout of the modified SBR treatment system for Stage 2, incorporating both aeration and anoxic phases.

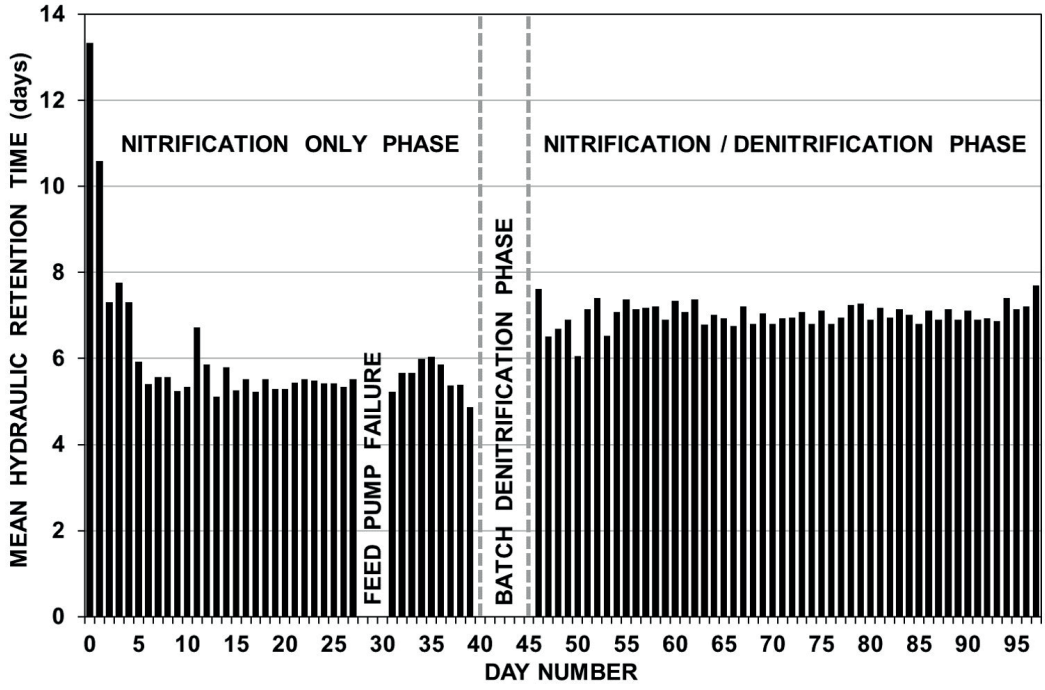

FIGURE 5: Mean Hydraulic Retention Time (HRT) during the Stage 2 trial on weaker leachate from a closed landfill site.

Day 45, at the end of the nitrification-only phase of treatment, no leachate addition took place, as a "batch denitrification" period of treatment was carried out, following addition of a small quantity (2-litres) of additional seed bacteria via thickened sludge from a full-scale leachate treatment plant in Buckinghamshire, UK, where a combined nitrifica-

tion/denitrification process was being operated. Suitable batch doses of the glycerol were added into the reactor, sufficient to allow concentrations of nitrate-N and nitrite-N to be reduced to below detection limits, before the automated nitrification/denitrification process, and further leachate additions began on Day 46; continuing to the end of the trial on Day 97.

2.3 pH control

The pH was controlled within an optimum range of 7.2 to 7.8 by manual daily addition of measured amounts of either sodium bicarbonate (Stage 1) or hydrochloric acid (Stage 2) into the reactor. pH-values were obtained using a handheld Palintest Micro 500 meter, which could measure to the nearest 0.01 pH, and was routinely calibrated against buffer solutions.

During the aeration period of Stage 1, the mass of sodium bicarbonate added to the reactor each day to buffer acidity was determined by weighing out an appropriate amount (using scales accurate to 0.01 gram), after observing pH-value within the reactor.

No additions of sodium bicarbonate were required during the nitrification-only treatment of the weaker leachate in Stage 2, as the leachate itself contained sufficient alkalinity to buffer the acidity generated during nitrification of the lower concentrations of ammoniacal-N. It was only when the denitrification phase of the trials was introduced that small additions of hydrochloric acid were dosed with the daily glycerol feed solution, to effectively control pH-values, at rates of 0.51 litres per m^3 of leachate treated. This was due to the slight alkalinity produced following the denitrification phase of treatment.

2.4 Carbon source for denitrification

In sewage treatment, readily-degradable organic compounds in the wastewater are usually used as a carbon source for denitrification (e.g. Ludzack and Ettinger, 1962), but for leachates from landfills in methanogenic stages of decomposition containing much higher concentrations of ammoniacal-N and low levels of readily-degradable BOD_5, external carbon sources must be used.

Several soluble organic compounds can be used, such as acetate, ethanol or glucose, but methanol (CH_3OH) is absorbed rapidly and degraded easily, so is most commonly used in sewage treatment (Gerardi, 2006; Water Environment Federation, 1998; USEPA, 1993).

For leachate treatment with far higher concentrations of nitrate-N to denitrify, methanol is relatively expensive, and also has explosive/flammability issues, representing a hazard on remote and unmanned closed landfills.

For these studies, a decision was made to investigate glycerol ($C_3H_8O_3$) as a carbon source for denitrification. Glycerol is readily-degradable, available as a waste product from biodiesel production (1 litre is produced for every 10 litres of biodiesel), and has far lower levels of risk associated with storage and use. Although glycerol has previously been used occasionally for denitrification (e.g. see Akunna et al., 1993; Bodik et al., 2009; Grabinska-Loniewska et al., 1985), its use has increased in very recent years (including for leachate treatment – see below), and it would be a safe carbon source for use at closed landfill sites, if demonstrated to be suitable.

2.5 ORP

Oxidation-Reduction Potential (ORP, also known as Redox and measured in millivolts, mV) is a measure of the net charge of oxidised and reduced compounds in solution, and their tendency to acquire electrons and be reduced. Nitrate and sulphate ions are examples of oxidised compounds, and ammonium ions of reduced compounds. ORP is readily measured, and managed to encourage required processes, see Table 1.

In practice, results from individual ORP instruments may be consistent, but difficult to calibrate precisely against standards, although most authors agree that results in the range -100mV to -200mV are ideal to achieve efficient denitrification, avoiding reduction of sulphate to release sulphide (e.g. Gerardi, 2002; Schuyler, 2013; Elefsiniotis et al., 1989).

During the Stage 2 trials, two separate devices were used, to obtain consistent and accurate ORP results. First a Palintest Micro 500 ORP monitor was used on three different days to measure ORP manually. Results were taken every minute, especially during the anoxic phase. Additionally, an automated recording device (YSI Professional Plus, ProCommII multiparameter recorder) was used on four different dates during the trial. This device had both an ORP and pH probe, and automatically recorded variables every fifteen minutes (Figure 6 and Figure 7 respectively).

2.6 Lab analysis of routine samples

Although regular daily testing was carried out manually with a pH-meter and test strips for Ammoniacal-N, Nitrate-N and Nitrite-N, giving a good indication of whether treatment was successful and stable, for more detailed analysis to be achieved samples were submitted to ALcontrol; a specialist laboratory in Chester, UK. After initial samples of leachate were sent off following on-site collection, leachate was sampled weekly from the beginning of both trials, in order to prove no changes in composition took place during storage. Sampling of treated effluent was carried out frequently throughout both the Stage 1 and Stage 2 trials, with samples being taken following settlement and clarification within the reactor. During the Stage 1 trials, settled effluent samples were taken weekly, for an overview of key determinands; ammoniacal-N, COD, BOD_5, TOC, nitrate-N, nitrite-N, alkalinity, pH-value, sodium, and chloride. During Stage 2, when thorough observation of effluent quality was required, both settled and filtered samples (through 45µm GF/D papers) were submitted to the laboratory twice each week for the same analytical suite. The benefit of filter-

TABLE 1: Nitrification, denitrification and ORP (mV) (After Gerardi, 2002).

ORP	Bacterial Process
>150 mV	Degradation of BOD and nitrification of NH_4^+ and NO_2^-
+150 to -150 mV	Degradation of BOD with NO_2^- and NO_3^-
< -150 mV	Degradation of BOD with NH_4^+ and SO_4^{2-}

ing samples through 45µm GF/D filter paper is that only results for dissolved determinands would be reported in those samples; however, there was very little difference between concentrations in filtered and unfiltered samples. Occasional, more comprehensive analysis (including the nine heavy metals) was required for leachate and effluent quality. Therefore, further samples were taken at the start, midpoint and end of both trials, to prove the consistent removal that both pilot-scale treatment systems provided (see Tables 2 and 4).

All samples were submitted to arrive at the ALcontrol Laboratory within 24 hours of sampling, for analysis. Routine laboratory protocol for analysis of such samples involved separate filtration through a 0.45µm filter upon receipt at the lab.

To determine the COD in water samples, ALcontrol Laboratories use sulphuric acid and potassium dichromate in the presence of a silver sulphate catalyst to oxidize well shaken samples. 2ml of sample is then added to the reagent tube and mixed. The tube is put into a heating block at 148°C for 2 hours. After allowing cooling, the result is read using a photometer, to a detection limit of 7mg/l.

To test for Total Organic Carbon (TOC) the samples are well shaken before being taken for analysis. The analysis is carried out by automated wet oxidation, where the CO_2 produced is purged from the acidified sample and detected by a non-dispersive infrared (NDIR) detector. Following removal of the inorganic carbon, CO_2 produced by persulphate oxidation is purged from the sample and detected by NDIR. The mass of CO_2 produced from this reaction is proportional to the mass of TOC present in the sample. The detection limit for this analysis is 3mg/l, whilst the range is 3-125mg/l.

Analysis for dissolved metals incorporates operation of the Thermo Scientific X Series Inductively Coupled Plasma Mass Spectrometer (ICP-MS) for multi-element determination. All samples are essentially run neat, thus low levels of detection can be achieved. Following acidification, the samples in solution pass into the plasma source in a flow of argon where atomisation and ionisation occur. The quadrupole MS separates out ions by their mass to charge ratio, which is element specific. The intensity of the signal at each mass is directly proportional to the concentration of the element in question in the solution.

3. RESULTS

3.1 Results from Stage 1 nitrification trials

The pilot-scale SBR unit was seeded with bacterial sludge from a full-scale treatment plant in Southern England, which was treating a similar strength leachate.

During the period from Day 29 to Day 45, when leachate feed rate was maintained at very stable levels of 16 to 17 litres per day, a total of 271.8 litres of leachate was treated, at a mean HRT of very close to 10 days (10.01 days). By Day 43, for which detailed analysis of the effluent are provided in Table 2, a total of 561.4 litres of leachate had been treated, representing more than 3.5 bed volumes of the treatment reactor.

Table 3 presents mean concentrations for key determinands within the raw leachate feed and the final effluent during Stage 1. The percentage removal of these determinands highlights how successful the treatability trial was at nitrifying all ammoniacal-N to produce nitrate-N.

During the period of stable operation from Day 29 to 45, it was necessary to add a total of 1620.5 grams of sodium bicarbonate, equivalent to 5.96 grams of $NaHCO_3$ to every litre of leachate treated. This rate of addition can be confirmed to within 6 percent by the observed increase in concentrations of sodium from leachate to effluent (85 percent increase).

The Stage 1 trials performed very well indeed, achieving and maintaining complete nitrification of over 1,800 mg/l ammoniacal-N, and substantial reduction in BOD_{20} and BOD_5 at all times, and allowing leachate dosing rates to be increased steadily with no breakthrough of either ammoniacal-N or nitrite-N.

In practice, for a full-scale leachate treatment plant, alkalinity would not be added as sodium bicarbonate, but instead a solution of sodium hydroxide (NaOH) would be used. A 32 per cent solution (w/w) would be most likely to be used in a temperate climate, as stronger solutions can freeze at temperatures above 5°C. In this case, an equivalent alkalinity dosing rate would be 7.45 litres of 32% NaOH solution to be dosed into every cubic meter of leachate treated. This is a typical dosing rate for similar full-scale treatment plants, and data obtained from these trials would allow the volume of a suitable NaOH storage tank to be optimized.

3.2 Results from the Stage 2 trials

Treatment within the combined nitrification and denitrification phase of treatment, between Days 46 and 97, was extremely stable, with very consistent full nitrification and denitrification of 150 mg/l of ammoniacal-N during the entire 52-day period. A total of 1186.1 litres of leachate was treated, at an average rate of 22.8 litres per day.

Acidity produced during a nitrification phase, and alkalinity produced during a subsequent denitrification phase, were balanced, without excessive cyclical swings in pH-value; this minimised any requirement for additions of pH control chemicals. Additions of glycerol amounted to rates much less than 1 litre of glycerol for every cubic metre of leachate treated, which would be relatively inexpensive to supply on a larger scale. pH-values were maintained automatically by additions of very low quantities of hydrochloric acid into the daily glycerol feed.

Table 4 presents a summary of the quality of raw leachate used and of treated leachate quality during both the initial nitrification only phase of treatment, and during the later stable nitrification and denitrification phase of the Stage 2 trials.

Table 5 highlights the removal of key determinands throughout the combined nitrification and denitrification phase of the Stage 2 trials. Importantly, this table demonstrates that both ammoniacal-N and nitrate-N concentrations within the final effluent remained low, following both the nitrification and denitrification processes. Daily test strip analysis of the effluent produced throughout the trials proved that all ammoniacal-N within the leachate was be-

TABLE 2: Results for quality of the raw and treated leachate during the Stage 1 trials.

	Leachate		Effluent		
Day	**0 (S)**	**43 (S)**	**40 (S)**	**43 (F)**	**43 (S)**
Determinand					
COD	3510	3530	1420	1440	1510
BOD_{20}	499	330	<300	<10	29.4
BOD_5	275	173	<10	<5	10.7
TOC	1140	1120	517	27.6	534
fatty acids (as C)	<10	<10	<10	<10	<10
Kjeldahl-N	1720	1980	76.9	177	172
ammoniacal-N	1850	1820	0.871	0.485	0.391
nitrate-N	<1.35	<1.35	1670	1700	1670
nitrite-N	<0.304	<0.304	<0.304	<0.304	<0.152
alkalinity (as $CaCO_3$)	9740	9420	236	140	150
pH-value	8.11	8.05	7.73	7.2	7.11
chloride	2390	2530	2440	2470	2470
sulphate (as SO_4)	513	517	564	603	598
phosphate (as P)	11.3	11.7	10.5	10.1	10.1
conductivity (µS/cm)	20,800	19,300	15,800	16,300	17,500
sodium	2000	2090	3890	3630	3820
magnesium	75.7	90.2	91.8	80.5	78.9
potassium	1280	1340	1390	1360	1310
calcium	73.1	<5.7	102	101	98.4
chromium	0.371	0.345	0.336	0.293	0.291
manganese	0.381	0.389	0.048	0.012	0.082
iron	0.709	<2.40	1.57	1.25	2.44
nickel	0.256	0.253	0.270	0.249	0.253
copper	<0.04	<0.04	<0.056	<0.04	<0.04
zinc	0.061	0.042	0.180	0.105	0.097
cadmium	<0.005	<0.005	0.014	<0.005	<0.005
lead	0.0174	0.0148	0.0118	<0.005	<0.005
arsenic	0.420	0.409	0.342	0.337	0.330
mercury	<0.00002	<0.00002	0.00005	0.00003	0.00004

Notes: All results in mg/l, except pH-value, and conductivity (µS/cm) / Alkalinity as $CaCO_3$ / (S) = Settled effluent sample. (F) = Filtered effluent sample through GF/D paper.

TABLE 3: Mean removal of key determinands during the Stage 1 trials.

Determinand	Mean leachate	Mean effluent	Mean removal (%)
COD	3520	1457	58.6
TOC	1130	360	68.2
ammoniacal-N	1835	0.6	99.9
nitrate-N	1.35	1680	-124,344
nitrite-N	<0.304	<0.304	0.0
alkalinity (as $CaCO_3$)	9580	175	98.2
chloride	2460	2460	0.0
sodium	2045	3780	-84.8

Notes: Increased concentrations of sodium, due to small additions of sodium bicarbonate when controlling changes in pH due to the acidity created through the nitrification process.

ing reduced to trace levels, whilst the denitrification phase was successfully removing nitrate-N.

The treatability trials demonstrated that a close balance could be achieved between consumption of alkalinity during nitrification of ammoniacal-N, and release of alkalinity during the denitrification stage in the Anoxic Reactor. In both the pilot-scale trials and at full-scale, controlled additions of small volumes of hydrochloric acid were required, into the Anoxic Tank, as denitrification of the high nitrate concentrations generated quantities of alkalinity with potential to inhibit the denitrification process (at pH values greater than about 8.0).

Figure 6 summarizes ORP data from several 24-hour treatment cycles during the Stage 2 trials. Vertical dotted lines mark the time of the start of each individual period during the cycle (as displayed in Figure 3), and labels

TABLE 4: Results for quality of raw and treated leachate during the Stage 2 trials.

Location	Raw leachate		Final effluent		
Treatment	**FEED**		**N**	**N plus DeN**	
Day	**37 (S)**	**60 (S)**	**37 (F)**	**67 (F)**	**67(S)**
Determinand					
COD	155	177	74	84	85
BOD_{20}	>16	30	<30	<1	3.23
BOD_5	8.4	12	<1	<1	<1
TOC	59	56	27	30	31
fatty acids (as C)	<10	<10	<10	<10	<10
Kjeldahl-N	141	146	23.7	2.5	3.1
ammoniacal-N	142	143	<0.2	<0.2	0.40
nitrate-N	0.223	0.591	151	0.52	<0.06
nitrite-N	0.222	1.40	<0.015	<0.015	<0.015
alkalinity (as $CaCO_3$)	1020	1030	75	325	325
pH-value	7.95	7.94	7.82	8.43	8.44
chloride	199	191	211	522	524
sulphate (as SO_4)	34	39	42	34	35
phosphate (as P)	<0.02	0.026	6.61	2.36	2.33
conductivity (µS/cm)	2370	2420	1930	1860	1840
sodium	179	198	208	287	293
magnesium	35	34	39	45	47
potassium	100	108	115	138	146
calcium	127	187	170	250	256
chromium	0.0065	0.0155	0.0073	0.0108	0.0112
manganese	0.0056	0.0137	0.0015	0.0490	0.0590
iron	4.93	22.6	0.060	0.027	0.134
nickel	0.0133	0.0169	0.0160	0.0168	0.0170
copper	<0.004	<0.004	0.015	0.0066	<0.004
zinc	0.0174	0.0771	0.0150	0.0093	0.0067
cadmium	<0.0005	<0.0005	<0.0005	<0.0005	<0.0005
lead	<0.0005	<0.0029	<0.0005	<0.0005	<0.0005
arsenic	0.0063	0.0215	0.0150	0.0010	0.0012
mercury	<0.00002	<0.00002	<0.00002	<0.00002	<0.00002

Notes: All results in mg/l, except pH-value, and conductivity (µS/cm) / Alkalinity as $CaCO_3$ / (S) = Settled effluent sample. (F) = Filtered effluent sample through GF/D paper / N = nitrification only phase of the trial / N plus DeN = nitrification and denitrification phase of the trial.

TABLE 5: Mean removal of key determinands during the nitrification and denitrification phase of the Stage 2 trials (days 46 to 97).

Determinand	Mean feed	Mean effluent	Mean removal (%)
COD	166	84.5	49.1
TOC	57.5	30.5	47.0
ammoniacal-N	142.5	0.25	99.8
nitrate-N	0.407	0.275	32.4
nitrite-N	0.811	<0.015	>98.2
alkalinity (as $CaCO_3$)	1025	325	68.3
chloride	195	523	-168.2
sodium	189	290	-53.8

Notes: Increased concentrations of chloride, due to small additions of hydrochloric acid when controlling changes in pH.

highlight each phase. Two different ORP instruments were used when recording ORP over 24-hour cycles, in order to increase the reliability of the readings obtained. Results from each instrument vary on specific days, but show a very clear pattern for ORP during each cycle.

During the 14-hour aeration and leachate dosing phase, ORP gradually rose, within an overall range from about +70mV to +140mV. Dosing of the glycerol/HCL solution, 30 minutes into the Anoxic Period, caused a very rapid fall in ORP, to between -80mV and -170mV for the YSI instrument, and -150mV to -180mV for the Palintest instrument. This allowed effective denitrification to take place, although there was variation in the response times of the two instruments, and between actual values being measured.

The Post Anoxic Aeration period began at 14:00 pm.

Sudden mixing and aeration caused a rapid increase in ORP, to +150mV on the Palintest instrument (equivalent to 100mV on the YSI recorder). After 2 hours (16:00 pm), aeration stopped and settlement began. During this quiescent period, ORP was stable or reduced slightly. At 19:00 pm, after effluent decant, the aeration period began again and the 24-hour cycle restarted.

Figure 7 shows equivalent pH data during the same 24-hour periods as Figure 6. These pH data reveal similar trends to the ORP graph:

- pH remained stable, between 7.8 and 7.9 during the aeration phase.
- After glycerol/acid addition at 09:00am a drop in pH is evident, to between 7.2 and 7.3; an ideal range for denitrification to occur.
- A sudden increase in pH to between 7.85 and 7.95 occurs during the 2 hours of the post anoxic aeration phase, possibly as carbon dioxide is stripped from solution.
- pH-values fall steadily from 7.95 to 7.6 during the settlement/decant phase, before gradually returning to between 7.8 and 7.9 at the start of the 14-hour aeration phase.

It is clear that pH and ORP can be used to optimize the operation of the treatment process, and detailed monitoring in a full-scale plant would enable additions of glycerol and acid to be optimized further, without reducing treatment efficiency.

All results from the Stage 2 trials have been extremely promising, in terms of the quality of effluent that was achieved and maintained consistently. Results for the combined treatment system, in which essentially complete removal of ammoniacal-N and nitrate-N were achieved using an innovative and relatively simple process design, demonstrated that the process has huge potential for application at relatively remote closed landfills. In instances such as these, leachates are presently being tankered long distances for disposal, at significant cost, and often with many tanker movements along small rural lanes, therefore an efficient and inexpensive on-site treatment solution would be very beneficial.

The discharge of treated leachates from such sites is coming under increased scrutiny in terms of nitrogen content, and this new combined treatment process can readily be implemented at relatively low additional cost, and can be operated with low personnel requirements for supervision on sites. One issue which may require further consideration in some locations is the increase in chloride concentrations which results from the use of low doses of hydrochloric acid for simple pH control. Where chloride in a discharge is an issue, then alternative acids may need to be considered.

4. CONCLUSIONS

The studies reported in this paper involved large pilot-scale treatment studies on leachates that are very typically produced at older, closed landfills. The leachate used contained about 160 mg/l of ammoniacal-N, and treatment sought to incorporate nitrification and denitrification processes within a single reactor, by design of an innovative process configuration, using the waste product glycerol as a carbon source, widely available as a by-product from the production of biodiesel (Bodik et al., 2009).

The paper describes the design and operation of the two stages of the trial, presents detailed analytical and operational results, and discusses the implications of these.

The first, nitrification-only stage of the trials generated very accurate process information, which is extremely valuable for the design of full-scale leachate treatment plants in many countries. Data demonstrated the value and operation of the pilot scale units, and showed that similar trials can be very valuable as a first stage in the design of full-scale treatment plants. In particular, they are able to demonstrate that specific leachates being tested do not contain any inhibitory substance, before large sums of money are spent developing a full-scale treatment plant.

The second stage of the trials was especially valuable, in which an innovative process design was developed and tested to provide a relatively simple, single-tank, treatment plant, which can provide full nitrification and denitrification of weaker leachates (ammoniacal-N from 150 to 200 mg/l) at closed landfill sites. The fact that the process can operate with only minimal supervision, is extremely important at all closed landfill sites, and will be tested at larger scale in the near future. The pilot-scale studies have provided sufficiently detailed data to allow a full-scale treatment plant to be designed.

In conclusion to the Stage 2 combined nitrification and denitrification trials, several important findings have been highlighted, which will be valuable in the consideration of managing those leachates produced at closed landfills in the future:

For relatively weak leachates from old landfill sites (ammoniacal-N of 100-200 mg/l), nitrification, denitrification, post-aeration and effluent clarification/decant can all be achieved simply and sequentially in a 24-hour cycle within a single reactor tank.

The acidity produced during a nitrification phase, and alkalinity produced during a subsequent denitrification phase, can be balanced, without excessive cyclical swings in pH-value which might inhibit the overall treatment process. This would minimise requirements for additions of pH control chemicals.

A biomass of denitrifying bacteria can be acclimatised successfully to use waste glycerol from biodiesel production, as a carbon source for denitrification, and that ORP can be used as a control parameter for the process.

The whole treatment process can be fully automated in a simple way, both in the laboratory studies, and for full-scale treatment systems on closed landfill sites.

Complete removal of ammoniacal-N and nitrate-N have been achieved using an innovative and relatively simple process design within a single reactor setup. This study demonstrated that the combined nitrification and denitrification process within a single reactor has huge potential for application at old, small and relatively remote closed landfills. This new process could readily be implemented at relatively low cost, and operated with low personnel re-

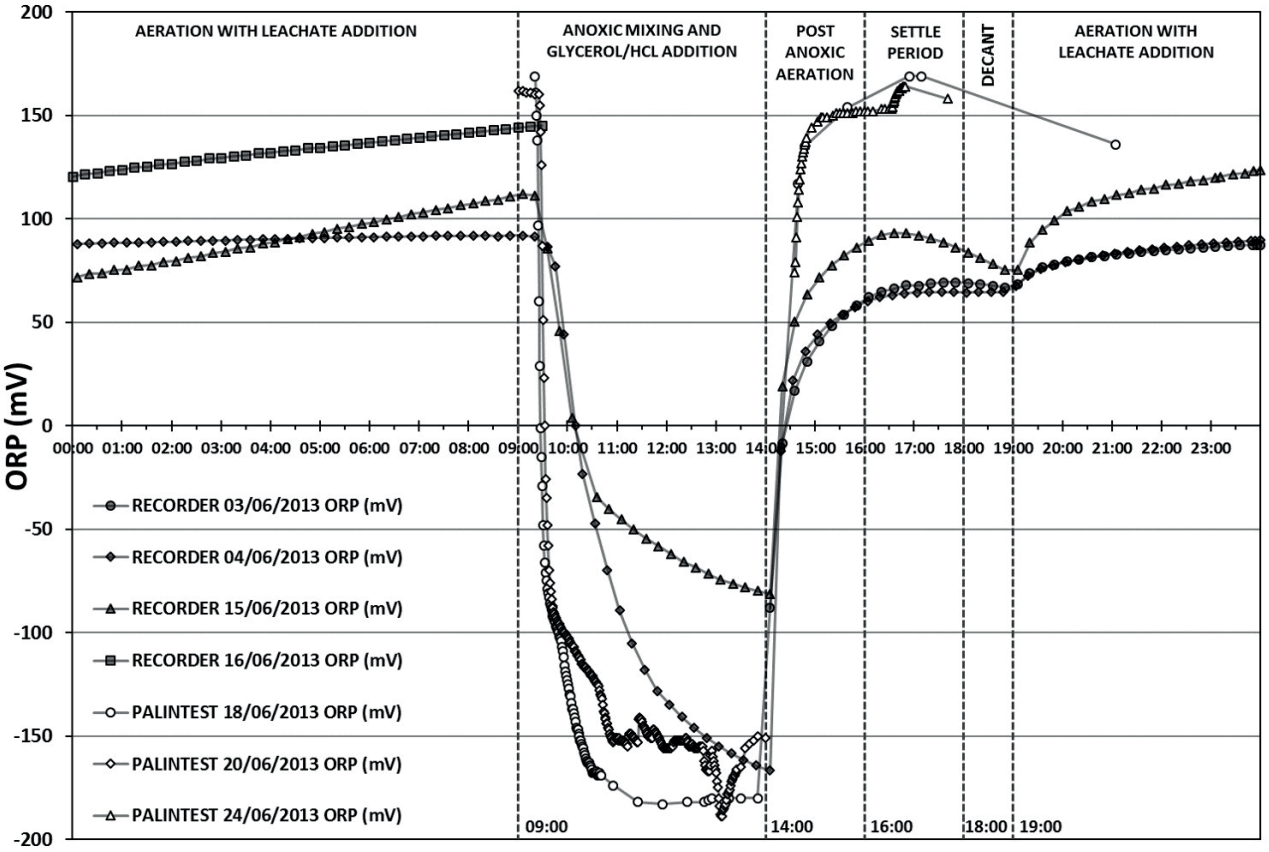

FIGURE 6: Changes in ORP during the 24-hour operating cycle of the Stage 2 trials, using data from two ORP devices on seven different days.

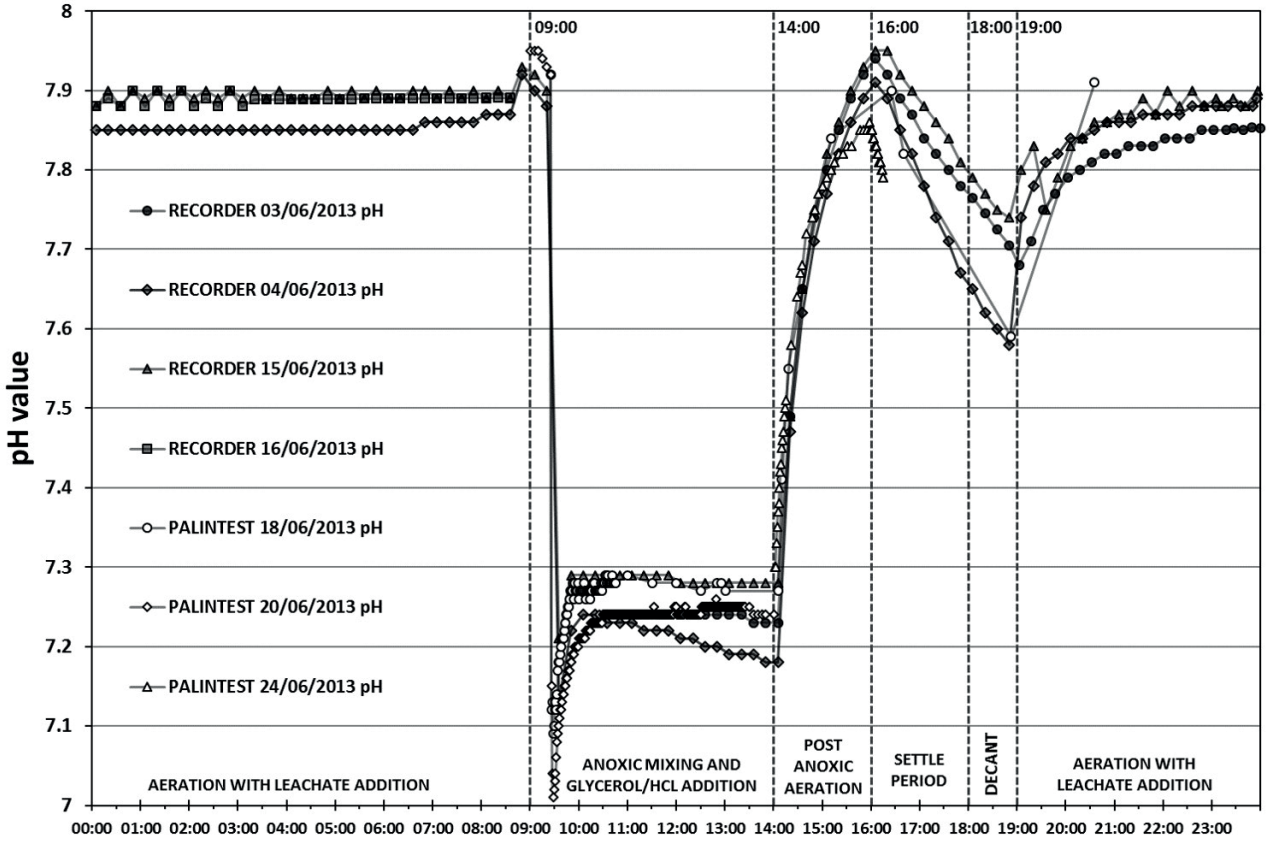

FIGURE 7: Changes in pH during the 24-hour operating cycle of the Stage 2 trials, using data from two pH devices on seven different days.

quirements for supervision. This is in contrast to an expensive treatment plant with separate reactors for aeration, anoxic treatment, post-aeration etc., where reactors must be sized and constructed before the plant is commissioned, and full-time supervision and monitoring is needed.

ACKNOWLEDGEMENTS

The author would like to acknowledge the help and assistance received from colleagues at SKM Enviros in undertaking this experimental study, which primarily represents a detailed research study undertaken as a final year thesis at the University of East Anglia (see Robinson, 2014). Many thanks to my supervisor, Professor Kevin Hiscock at the University of East Anglia, for his support and guidance.

Viridor Waste Management and East Sussex County Council were each extremely helpful in providing access to data and to landfill sites for collection of leachate samples.

REFERENCES

Akunna, J.C., C. Bizeau and R. Moletta, 1993, Nitrate and nitrite reductions with anaerobic sludge using various carbon sources: glucose, glycerol, acetic acid, lactic acid and methanol, Water Research, 27, 1303-1312.

Bodik, I., A. Blstakova, S. Sedlacek and M. Hutnan (2009). Biodiesel waste as source of organic carbon for municipal WWTP denitrification, Bioresource Technology, 100, 2452-2456.

Christensen, T.H., 2011, Landfilling: Leachate Treatment, Chapter 10.11 in: Christensen, T.H., Solid Waste Management and Technology, Blackwell Publishing Ltd, John Wiley & Sons, ISBN 9781405175173, 1026pp.

Elefsiniotis, P., R. Manohanaran and D.S. Mavinic, 1989, The effects of sludge recylce ratio on nitrification-denitrification performance in biological treatment of leachate. Environmental Technology Letters, 10, 1040-1050, p.1043.

Environment Agency (1996). A Review of the Composition of Leachates from Domestic Wastes in Landfill Sites. Report No. CWM 072/95, published by the Waste Technical Division of the Environment Agency, in the series "The Technical Aspects of Controlled Waste Management", 550pp, August 1996.

Environment Agency (2007). Guidance for the treatment of landfill leachate. Sector Guidance Note IPPC S5.03, February 2007. 182pp.

Gerardi, M.H. (2002), Settleability problems and loss of solids in the activated sludge process, John Wiley and Sons, USA and Canada, Wastewater Microbiology Series, ISBN 0-471-20694-6, 179pp.

Gerardi, M.H. (2006), Wastewater Bacteria, John Wiley and Sons, USA and Canada, Wastewater Microbiology Series, ISBN 0-471-20691-1, 255pp.

Grabinska-Loniewska, A., T. Slomczynski, and Z. Kanska (1985). Denitrification studies with glycerol as a carbon source, Water Research, 19, 1471-1477.

Hartley, K. (2013), Tuning Biological Nutrient Removal Plants, IWA Publishing, London, UK, 246pp.

Kjeldsen, P., M.A. Barlaz, A.P. Rooker, A. Baun, A. Ledin and T.H. Christensen (2002). Present and Long-Term Composition of MSW Landfill Leachate: A Review, Critical Reviews in Environmental Science and Technology, 32, 297-336.

Ludzack, F.J. and M.B. Ettinger, 1962. Controlling operation to minimize activated sludge effluent nitrogen. Journal of the Water Pollution Control Federation, 34, 920-931.

Metcalf & Eddy (2004), Updated by G. Tchobanoglous, F.L. Burton, and H.D. Stensel, Wastewater engineering, treatment and reuse, Mc Graw Hill, New York, 4.

Robinson, H., 2007, The composition of leachates from very large landfills: An international review, Communications in Waste and Resource Management, 8, 19-32.

Robinson, H. D., and Formby, R. W. (2009). The use of pilot-scale trials in the design of on-site leachate treatment plants. Proceedings of Sardinia 2009, The Twelfth International Waste Management and Landfill Symposium, Cagliari, Italy; 5-9 October 2009.

Robinson, H., Carville, M., Bailey, P., Farrow, S., Jones, D. and L.Gibbs (2011). Full-scale treatment of landfill leachates with full nitrification and denitrification. Proceedings of Sardinia 2011, Thirteenth International Waste Management and Landfill Symposium, S. Margherita di Pula, Cagliari, Italy; 3 - 7 October 2011.

Robinson, H., Wilson, K., Stokes, A., Olufsen, J., Robinson, T. (2017). Recent state-of-the-art leachate treatment plants in eastern England. Paper presented to Sardinia 2017, the Sixteenth International Waste Management and Landfill Symposium, S.Marguerita di Pula, Cagliari, Italy, 2 – 6 October 2017, in Proceedings.

Robinson, T. (2013). Aerobic Biological Treatability Studies on Landfill Leachate using Nitrification and Denitrification. Paper presented to Sardinia 2013, the Fourteenth International Waste Management and Landfill Symposium, S.Marguerita di Pula, Cagliari, Italy, 30 September – 4 October 2013, 9pp, in Proceedings.

Robinson, T. (2014). Aerobic Biological Treatability Studies on Landfill Leachate using Nitrification and Denitrification. Final Year Dissertation Project 2014, School of Environmental Sciences, University of East Anglia, Norwich, UK, 100 pages, Available from the UEA Library.

Robinson, T. (2015). Use of pilot-scale treatability trials in the design of full-scale leachate treatment plants. Paper presented to Sardinia 2015, the Fifteenth International Waste Management and Landfill Symposium, S.Marguerita di Pula, Cagliari, Italy, 5 – 9 October 2015, 128pp in Proceedings.

Robinson, T. (2017). Robust and reliable treatment of leachate at a closed landfill site in Sussex, UK. Paper presented to Sardinia 2017, the Sixteenth International Waste Management and Landfill Symposium, S.Marguerita di Pula, Cagliari, Italy, 2 – 6 October 2017, in Proceedings.

Shuyler, R.G., 2013, What every operator should know about ORP. Water Environment and Technology, January 2013, 25, 68-69.

United States Environmental Protection Agency (1993), Nitrogen Control Manual. Office of Research and Development, U.S. Environmental Protection Agency, Cincinnati, Ohio, USA, Report EPA/625/R-93/010, 311pp.

Water Environment Federation (1998), Biological and chemical systems for nutrient removal, Water Environment Federation, USA, ISBN 1-57278-123-8, 399pp.

Water Pollution Control Federation (1983), Nutrient Control: Manual of Practice FD-7, Facilities Design, WPCF, Alexandria, VA, USA, ISBN 0-943244-44-7, 205pp.

Wilson, K.S., Robinson, H., Robinson, T., Sibley, R., and Carville, M.S. (2015). Treatment of leachate from a closed landfill in West Sussex, UK. Paper presented to Sardinia 2015, the Fifteenth International Waste Management and Landfill Symposium, S.Marguerita di Pula, Cagliari, Italy, 5 – 9 October 2015, pp285 in Proceedings.

detritus | Multidisciplinary Journal for Waste Resources & Residues

CISA

EVALUATION OF BEHAVIOR OF WASTE DISPOSAL SITES IN KARACHI, PAKISTAN AND EFFECTS OF ENHANCED LEACHING ON THEIR EMISSION POTENTIAL

Ihsanullah Sohoo [1,2,*], Marco Ritzkowski [1] and Kerstin Kuchta [1]

[1] *Institute of Environmental Technology and Energy Economics, Hamburg University of Technology, Harburger Schlossstr. 36, 21079 Hamburg, Germany*

[2] *Department of Energy and Environment Engineering, Dawood University of Engineering and Technology, New M.A Jinnah Road, Karachi-74800, Pakistan*

Article Info:
Received:
28 March 2019
Revised:
13 June 2019
Accepted:
16 July 2019
Available online:
01 August 2019

Keywords:
Municipal solid waste
Waste disposal sites
Enhanced leaching
Landfill gas
Dry conditions
Leachate recirculation

ABSTRACT

This study aims to assess the efficiency of enhanced leaching on biodegradation of residual waste and gas emissions from waste disposal sites. The investigation simulated the waste disposal conditions in the landfill sites of Karachi, Pakistan in terms of waste composition, moisture content, and climatic conditions. For this purpose, a lysimetric analysis method was applied. Landfill sites in Karachi have typically no cover and the waste degrades in relatively dry conditions due to the lower moisture content of the waste as well as due to the low annual rainfall. Decomposition of organic waste with low moisture content and limited water introduction is causing prolonged emissions in the form of gas and leachate due to the slow biodegradation process. This paper focuses on the comparison of gaseous emissions from waste disposal sites in two different circumstances by applying two different experimental approaches. In the first approach, the actual dry conditions were simulated by means of limited water addition and without leachate recirculation.In the second approach, enhanced leaching conditions were provided with process water addition and leachate recirculation. The results from 100 days of experimental operation revealed that an enhanced leaching is able to increase gas formation in comparatively short periods and prolongs gaseous emissions from waste disposal sites can be controlled.This lab scale study can provide baseline data for further research and planning to transform waste dumpsites to sanitary landfills in the region.

1. INTRODUCTION

Open dumpsites of municipal solid waste (MSW) cause uncontrolled emissions for long duration. The physical, chemical and biological processes involved in the decomposition of landfilled waste cause emissions in both liquid (leachate) and gas (landfill gas) forms. Uncontrolled emissions from poorly managed landfills and open dumpsites are the major source of the greenhouse gases, contributing to the contemporary and perilous problem of climate change (Liu, Liu, Zhu, & Li, 2014). One of the major factors causing prolonged emissions from waste dumpsites is the slow biodegradation of waste due to unavailability of an environment that results favorable conditions for microorganisms to consume the organic content of the waste mass. The esnvironmental factors that cause significant effects on the anaerobic degradation of biogenic fraction in the waste include temperature, pH, moisture content, nutrients, non-existence of toxic materials, particle size and oxidation reduction potential (ORP) (D. R. and A. B. A.-Y. Reinhart, 1996). In order to curtail environmental and health problems associated with unmanaged waste practices, these raw dumping sites should be transformed into sanitary (bioreactor) landfills. Presently, Karachi does not have any properly engineered landfill facility for municipal solid waste disposal and all existing waste disposal sites are open dumps (Korai, M. S., et al 2015; Zuberi and Ali, 2015). Karachi is producing 12,000 tonnes of municipal waste on daily basis, of which about 60% is being collected and transported to dumpsites located outside of the city (Shahid, Muhammad et al, 2014; Korai MS et al. 2015). Municipal Solid Waste in Karachi contains 51% of biodegradable contents and 49% of non-biodegradable contents (Shahid, Muhammad et al. 2014). The waste disposal sites in Karachi receive moisture only in the form of rainwater. Consequently, due to low precipitation and deficiency of moisture content in the waste, decomposition processes develop in

* Corresponding author:
Ihsanullah Sohoo
email: sohoo.ihsanullah@tuhh.de

Detritus / Volume 07 - 2019 / pages 96-103
https://doi.org/10.31025/2611-4135/2019.13841
© 2019 Cisa Publisher. Open access article under CC BY-NC-ND license

relatively dry conditions and this has adverse environmental repercussions for a long duration. Due to insufficient moisture content, the optimum level of bio-decomposition in the overall disposed waste cannot be achieved in a limited timeframe. This situation leads to slow MSW degradation and biogas production from waste disposal facilities (Fei et al., 2016; Reinhart et al., 2002; Pohland, F. G., 2000). Previous experience and research show that controlling of the moisture content in waste is a very important aspect in enhancing waste degradation in landfills (Frank, R. R., et al. 2016; Pohland, 1975). For the moisture control, leachate recirculation was proven to be the most practical method (D. R. Reinhart et al., 2002). Moreover, several studies have elaborated the advantages of leachate recirculation in speeding-up the biodegradation processes of landfilled waste, which enhances the biogas production and improves the landfill space reduction. Furthermore, benefits like a renewable source of energy (landfill gas) can also be obtained (Liu et al., 2014; Rastogi et al., 2015; Nair et al., 2014; Reinhart et al., 2002; Clarke, 2000).

2. MATERIAL AND METHODS

2.1 Synthetic MSW Sample preparation

For this simulated landfill reactors (SLR) investigation, 30 kg of a fresh synthetic waste sample representing the average of MSW composition in Karachi, Pakistan was prepared in the laboratory at the Institute of Environmental Technology and Energy Economics, Hamburg University of Technology, Hamburg, Germany.The synthetic waste sample was prepared by acquiring different waste components and mixing them according to the average of MSW composition (% wet weight basis) inKarachi city (given in Table 1) reported by Shahid, Muhammad et al. 2014.

Where required, the size of waste material was reduced either manually or by means of a shredder (JBF Maschinen GmbH, Model: 28/35). Food and garden wastes were mixed and homogenized prior to the mixing with other components ofthe synthetic waste. All components of the waste were placed in a big steel tray and manually mixed for homogenization. Moreover, the synthetic waste mixture was further homogenized and its size was reduced by passing the waste mixture three times through a shredder, with a consequent particle size reduction to approximately 25 mm. The initial moisture content of the synthetic waste mixture after size reduction and homogenization was 45%. In order to increase the specific weight of the waste and to place more waste into the reactors, 10 liters of tap water were added to the waste mixture before filling in the reactors. This caused an increase in the moisture content of the waste mixture to 56%. The basic characteristics of the synthetic waste sample loaded in the landfill simulator reactor experiment are given in Table 2.

TABLE 2: Basic characteristics of the synthetic waste sample.

Parameter	Unit	Value
Initial Moisture content	[%]	45
Final Moisture content	[%]	56
Total solid (TS)	[%]	44
Total organic solids (oTS)	[%]	83

2.2 Reactors loading with the synthetic waste mixture

All reactors were weighed before and after loading the waste mixture. The synthetic waste mixture was filled in the reactors and slight compaction of waste was done by moderately pressing with a wooden stick. On average 3 kg of the synthetic waste were filled in each reactor for the landfill simulation experiment. After loading the reactors, the waste mixture was adjusted to field capacity by adding tap water. Afterwards, 250 ml leachate sample was taken from each reactor for initial examination.

2.3 Setup and operation of landfill simulation reactors

2.3.1 Landfill simulation Reactors setup

Four glass reactors used in the simulation experiment were installed in a climate controlled room and operated at a constant mesophilic temperature (36±1°C). Each reactor was sealed with a top cap having four ports; one used for aeration (which was closed after the pre-aeration); one for off-gas volume measurement and sampling; one for leachate recirculation and another one for water addition. Water addition and leachate recirculation were realized by means of a leachate distribution system provided at the top of the reactors. Leachate was collected in a storage cell provided below the perforated plate within the reactors. Leachate was recirculated by a port provided below the leachate storage cells of eachreactor and pumped to the leachate distributor at top of the reactors by means of pumps (Concept 9911/15TI, Artikel-Nr. 98157). Leachate sampling was realized from the sampling port provided at the connection between the pumps and the leachate distribution system. The volumes of off-gas during the per-aeration phase and anaerobic operation phase was measured by means of drum gas-meters and micro gas-meters, respectively. The pictorial view of the landfill simulation reactors (LSRs) experimental setup is illustrated in Figure 1.

Prior to the start of the landfill simulation experiment, a leakage test was conducted with all reactors by means of the eudiometric method. Nitrogen was introduced into sealed empty reactors connected with the eudiometric tube of a eudiometer from off-gas port individually and the change in the level of liquid inside the eudiometric tube was observed. At the same time, a liquid leak detector was also used to point out the position of leakage from joints, connections and ports of the reactors.

TABLE 1: MSW composition inKarachi, Pakistan (Shahid. M et al. 2014).

City	MSW composition	Food/ Kitchen waste	Green waste	Paper	Glass	Metal	Plastic	Dirt/ Fines	Nappies	Textile/ Clothing	Tetra Pack	Wood/ Cardboard
Karachi	% (w/w)	26.1	17	8	5.6	1.1	8	3.7	9.8	7.6	10	3.1

FIGURE 1: Setup of Landfill simulation reactor experiment.

2.3.2 Landfill Simulation Reactors operation

Two different conditions (dry and wet) were analyzed in this study to witness the behavior of waste under respective conditions in view of the situation in Karachi. For each case, two reactors were used for the experiment.In the first case, two rectors (R1-ACT and R2-ACT) were operated to observe the behavior of synthetic waste mixture through simulating dry (actual) conditions which are mainly perceived at waste disposal sites in Karachi. In the other case, two reactors (R3-MOD and R4-MOD) were operated under modified wet conditions (enhanced leaching) to compare the effect of supplementary water addition and leachate recirculation on the behavior of waste disposal sites in Karachi. Operational setup of landfill simulation reactor experiment is shown in Figure 2.

2.3.3 Pre-aeration Phase

Before starting the anaerobic experiment phase, a short pre-aeration phase was conducted. The aim of this aerobic pre-treatment was to reduce acid accumulationcaused by the high organic content in the waste mixture and to accelerate the initiation of methane formation phase. Excess liquid for leachate recirculation system was provided by adding 500 ml tap water in each reactor through the water distribution system. Air was supplied with a constant flow rate of 8 l/h adjusted by means of air flow meters (Tablar Masstechnik GmbH, Type DK 800 N).

For aeration, perforated pipes were installed in all the reactors and embedded in the waste mass along with the longitudinal position of the reactors. The aeration pipes were connected with the air supply system.

The pre-aeration phase was planned up to two weeks

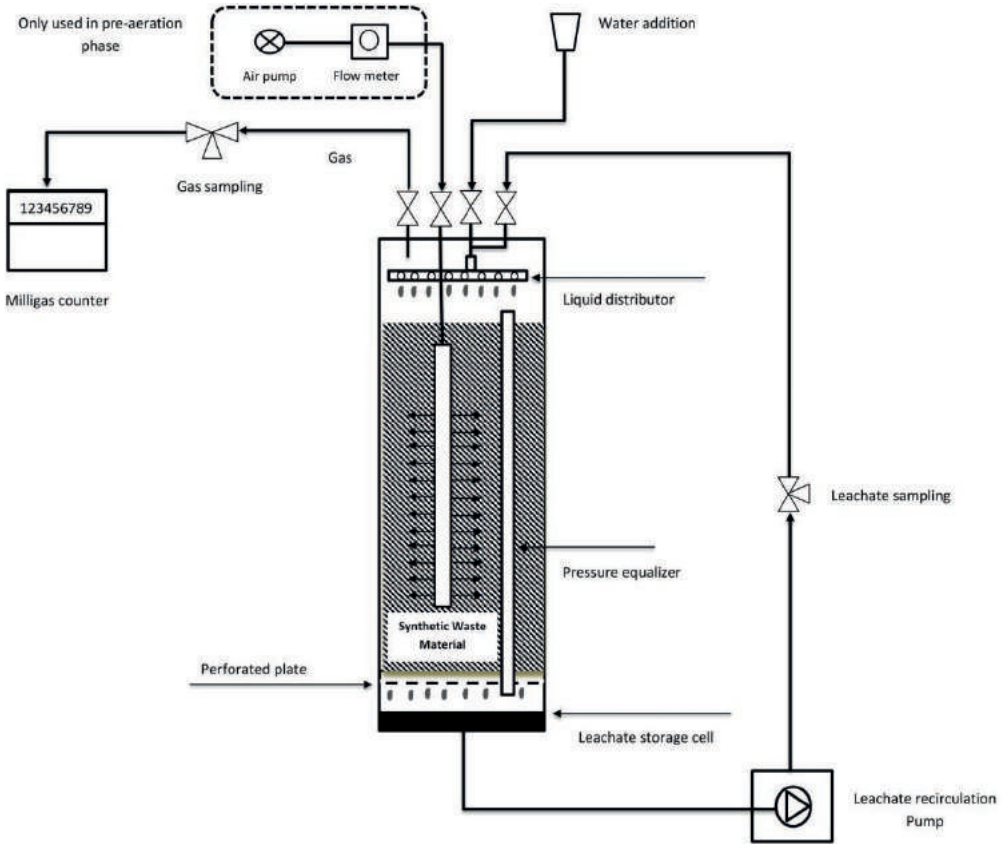

FIGURE 2: Schematic diagram of landfill simulation reactor experimental setup (amended from Ritzkowski et al., 2016).

initially. However, owing to feasibility reasons the aeration phase was enhanced to 16 days.

2.3.4 Anaerobic operation

After completion of the pre-aeration phase, aeration pipes were disconnected from the air supply system and removed from all reactors. Before starting the anaerobic operation mode, all the reactors were flushed with nitrogen gas for 15 minutes in order to purge the oxygen from the void spaces in the waste mass and to completely establish anaerobic conditions in the reactors. In the first two reactors (R1-ACT and R2-ACT) 56 ml tap water was added on a weekly basis in order to simulate 176 mm per year rainfall in Karachi (WMO, 2018). In the other two reactors (R3-MOD and R4-MOD) 250 ml tap water was added per week to provide process water for the recirculation system in order to realize an enhanced leaching effect. Operational details of anaerobic mode are explained in Table 3.

2.4 Analytical methods applied to LSRs

The gas composition (CO_2, N_2, O_2, CH_4) was analyzed by means of gas chromatography (HP 5890, Agilent).Total solids (TS) and volatile solids (VS) of the synthetic waste sample were determined according to DIN 38414 – S 2 and DIN 38409 – H 1-3, respectively.

3. RESULT AND DISCUSSION

3.1 Landfill gas (LFG) production and flow rate

All reactors observed one week of lag phase at the beginning of the anaerobic operation. From the second week of anaerobic phase, landfill gas production in the reactors R3-MOD and R4-MOD (equipped with enhanced leaching facility) was noticed more than in R1-ACT and R2-ACT (representing actual dry conditions). On the third week of anaerobic operation, landfill gas production from reactors operated on modified conditions was observed significantly more than reactors operated on actual conditions. During 105 days of the anaerobic operation time, the average gas production from R1-ACT and R2-ACT was 84.2 l/kg TS compared to a gas production of 156.4 l/kg TS from R3-MOD and R4-MOD. On average, 46% more landfill gas was produced form the reactors operated under the enhanced conditions than the reactors representing the actual circumstances of waste disposal sites. The cumulative landfill gas production from all reactors is shown in Figure 3.

The average landfill gasflow rate in all reactors was almost the same in the first week of anaerobic operation. In the second week, LFG flow rate from reactors R1-ACT and R2-ACT decreased from 81 ml/h and 54 ml/h to 21 ml/h to 17 ml/h, respectively. The higher flow rate noticed in the reactors R1-ACT and R2-ACT during the first week of operation was due to the available moisture content in the waste mass. In the second week, gas flow rate declined because of the slow biodegradation process due to leaching of the moisture containedin the waste. On the other hand, gas flowrate sharply increased from 69 ml/h to 133 ml/h in the second week in reactors R3-MOD and R4-MOD. This increase in the gas flow rate indicates the acceleration of biological processes in the enhanced leaching conditions. Figure 4 further depicts that, after one week of the lag phase gas flow rate from the reactors R3-MOD and R4-MOD, was exponentially increased and remained stable for two weeks and then deadly decreased and a long-term stationary phase was started. On the other hand,the gas flowrate from the reactors operated under the actual conditions remained almost stable until the 7th week of anaerobic operation but a moderate increase was observed in the flow rate afterwards. These results demonstrate that the enhanced leaching has stimulating effects on landfill gas production.

3.2 Methane concentration and flow rate

In the first week of the anaerobic operation mode, the landfill gas composition was analysed twice and the composition of gas from all reactors was relatively equal. After two weeks, the average methane (CH_4) and carbon dioxide (CO_2) concentration in the gas from reactors R3-MOD and R4-MOD reached 56% and 42%, respectively. In the same time, the average concentration of CH_4 and CO_2 in the off-gas from reactors R1-ACT and R2-ACT was 32% and 65%, respectively. An average concentration of methane above 50% (51.8%) in the reactors working on actual conditions was achieved after six weeks.In the stable methanogenic phase, landfill gas contains approximately 55-65% of methane and 35-45% of carbon dioxide (Farquhar, Grahame J., 1973;Christensen, T.H., Kjeldsen, P. and Lindhardt, 1996; Themelis and Ulloa, 2007). In this respect, the leaching effect helped to get the mature methanogenic phase in a shorter period of time (three-fold less) than the dry conditions. The methane flow rate is connected with the off-gas generation and concentration of methane in the off-gas. The off-gas production and methane concentration in the off-gas from reactors R1-ACT and R2-ACT was relatively

TABLE 3: Basic characteristics of the synthetic waste sample.

LSR#	Mode of operation	Leachate recirculation	Water addition	Leachate analysis	Landfill gas composition analysis	Landfill gas measurement
R1-ACT	AnA	-	56	once per month	once per week	Milligas counter
R2-ACT	AnA	-	56	once per month	once per week	Milligas counter
R3-MOD	AnA	Twice per day	250	bi-weekly	once per week	Milligas counter
R4-MOD	AnA	Twice per day	250	bi-weekly	once per week	Milligas counter

Rn-ACT: Reactors simulating actual conditions
Rn-MOD: Reactors simulating enhanced leaching conditions
AnA: Anaerobic

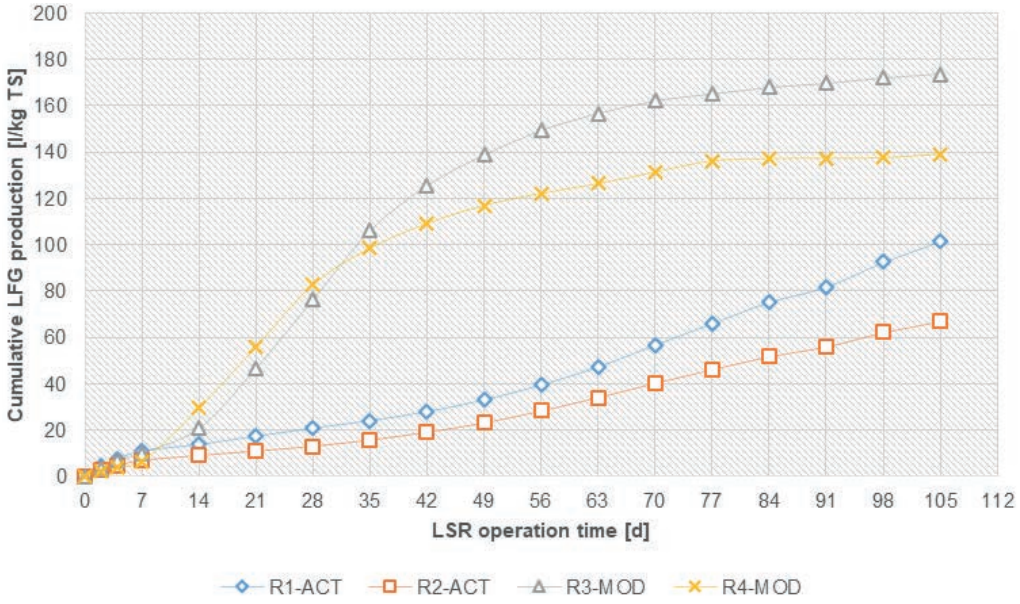

FIGURE 3: Cumulative landfill gas production from landfill simulation reactors.

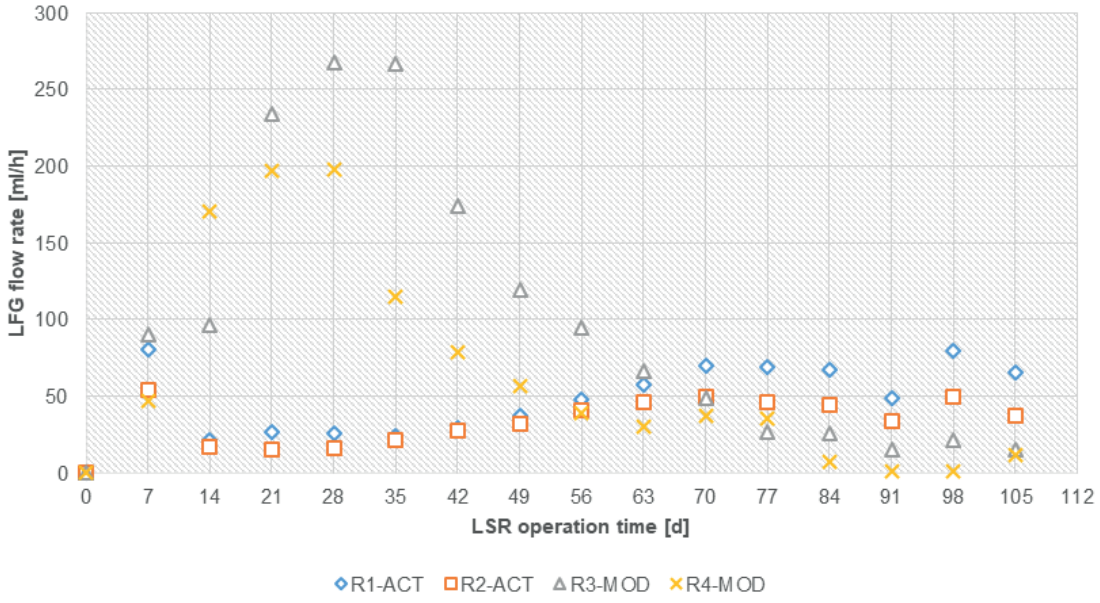

FIGURE 4: Landfill gas flow rate.

lower and increased slower than R3-MOD and R4-MOD in the starting of anaerobic operation. The average methane flow rate in all reactors was relatively equal (11.6 ml/h and 12 ml /h, representing actual and modified conditions, respectively) in the first four days of anaerobic operation. On the 7th day, the average methane flow rate of the reactors R3-MOD and R4-MOD increased to 81 ml CH_4 /h. Whereas, in the reactors R1-ACT and R2-MODflow rate was slightly increased to 18 ml CH_4 /h.

Cumulatively, a 38% increase in methane production rate was noticed in the reactors with leachate recirculation during the reported experimental period. Figure 5 shows the methane concentration and flow rate in both scenarios, revealing that the application of the enhanced leaching process increases the methane flow rate in the landfill operation.

3.3 Cumulative methane generation

It can be observed from graphs shown in Figure 6 that the methane generation in reactors R3-MOD and R4-MOD sharply increased and reached 11 lCH_4/kg TS and 9 lCH_4/kg TS within one week of anaerobic operation due to enhanced leaching, which ensures the availability of sufficient moisture to boost up the biological activity in the waste.In reactors R1-ACT and R2-ACT methane formation was observed very low in the first week, and noted as 3 lCH_4/kg TS and 2 lCH_4/kg TS, respectively. This very low methane formation was due to the limited biological activi-

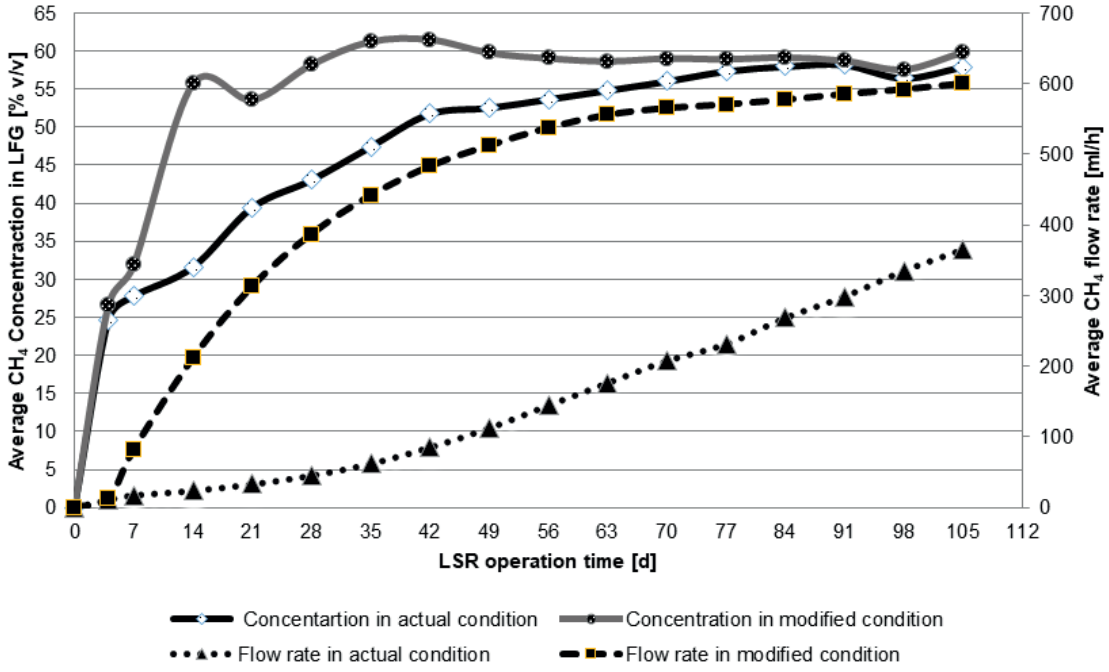

FIGURE 5: Average methane concentration and flow rate.

ty as a result of the low moisture content in the waste. The total quantity of methane formed from reactors R1-ACT, R2-KHI-ACT, R3-MOD and R4-MOD is noted as 60 lCH_4/kg TS, 36 lCH_4/kg TS, 87 lCH_4/kg TS and 57 lCH_4/kg TS, respectively. From the reactors R3-MOD and R4-MOD, the notable quantity of methane was produced in 70 days of anaerobic operational phase, in this time period the weekly methane production was reduced to 2% of total methane generated. Afterwards, the weekly methane productiondecreased to less than 0.7% of the total methane generated and remained at this level until the last reported day. On the contrary, the methane production from the reactors R1-ACT and R2-ACT increased gradually. During the 105 days of the anaerobic operation, the weekly methane production quantity reduecd to 8% of the total methane production during whole operation period. With leachate recirculation operation, the maximum methane production was achieved in 33% less time than the operation under dry conditions. The cumulative volumes of methane formed during investigation are illustrated in Figure 6.

3.4 Comparison of total volume of landfill gas and methane generated

In the 105 days of the anaerobic operation period, the average quantity of landfill gas and methane generated cumulatively from reactors R1-ACT and R2-ACT was 84 and 48 liters per kilogram of total solids, respectively. Whereas, from the reactors R3-MOD and R4-MOD, 156 l/kg TS landfill

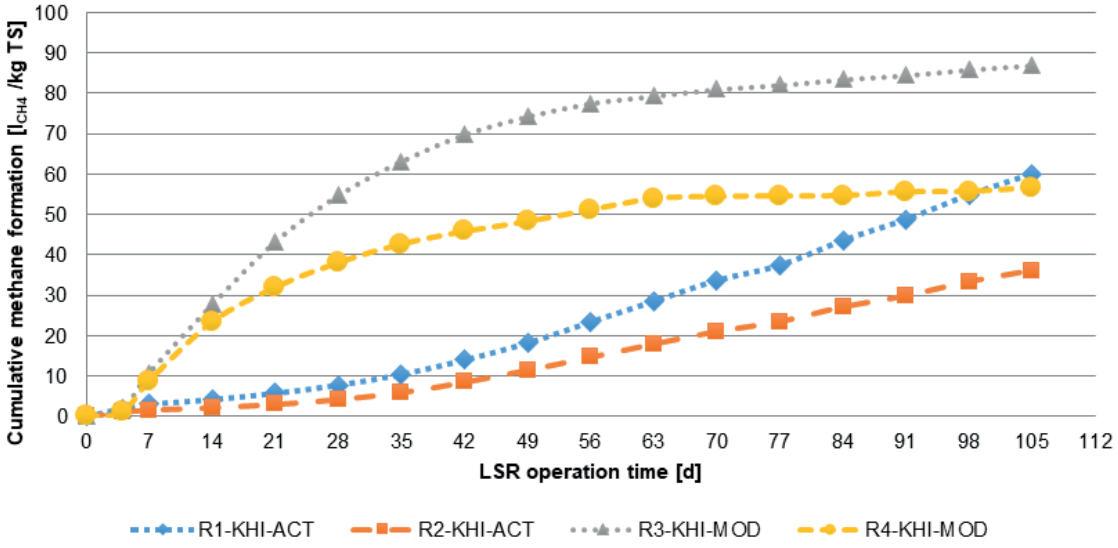

FIGURE 6: Cumulative methane generation.

gas and 72 l/kg TS of methane was recorded. The reactors in which operation was facilitated by water addition and leachate recirculation produced 54% more landfill gas and 66% more methane quantity than the reactors operated on actual dry conditions during the same period of operation. The results show that leaching effect have increased the landfill gas formation and methane generation potential of waste in a short time period. Considering the quantity and composition of the waste of generation in Karachi city and the results from this study, it is estimated that in current situation i.e., unmanaged waste dumping, the quantity of landfill gas going to the atmosphere is 4,264 m^3/day (with 2,436 m^3/day of methane). However, by using the landfills of the city as bioreactor (with enhanced moisture content and recirculation of leachate) and equipped with landfill capturing and processing technologies, 7,916 m^3/day of landfill gas (with 3,655 m^3/day of biomethane) can be produced. Figure 7 elaborates the average quantity of landfill gas and methane produced in the both circumstances (actual and enhanced leaching conditions) during 105 days of anaerobic operation.

4. CONCLUSION

In the existing uncontrolled waste dumping situation in Karachi, the waste disposal sites of the city are contributing to diverse environmental and health problems particularly at local and generally at a global level. This study provides a baseline for further research and planning for the rehabilitation of dumpsites in the region. Through this investigation, it is further affirmed that dry conditions at waste dumpsites are unfavorable for stabilization of the organic fraction of the waste in a limited time due to the absence of suitable conditions (moisture and nutrients) for microorganisms involved in waste stabilization. One of the major negative impact of dry conditions at waste dumpsites is low and prolonged gas emissions owing to the slow decomposition of the organic mass. Contrary to this, an enhanced leaching (water addition and leachate recirculation) has the highest effect on overall gas production and particularly on methane generation. During the study it was observed that enhanced leaching conditions in landfill simulation reactors developed methanogenesis phase faster than under dry conditions. Therefore, applying an enhanced leaching approach leads to environmental and energy gains, (in the form of renewable fuel production from waste) subject to the transformation of waste dumpsites to sanitary landfills with landfill gas capturing and power generation facilities in Karachi and other major cities of Pakistan.

ACKNOWLEDGMENT

Authors would like to thank the Institute of Environmental Technology and Energy Economics-IUE, Hamburg University of Technology-TUHH, Hamburg, Germany for facilitation and support in the conduction of this study. Special thanks to the laboratory and technical staff of Institute of Environmental Technology and Energy Economics-IUE for their guidance and support in establishment and analysis of the experimental work.

REFERENCE

Christensen, T.H., Kjeldsen, P. and Lindhardt, B. (1996). Landfilling of Waste: Biogas. In R. S. T. H. Christensen, R. Cossu (Ed.), Gasgenerating processes in landfills (pp. 27–50). London, GB: E & FN Spon.

Clarke, W. P. (2000). Cost-benefit analysis of introducing technology to rapidly degrade municipal solid waste. Waste Management and Research, 18(6), 510–524. https://doi.org/10.1034/j.1399-3070.2000.00157.x

Fei, X., Zekkos, D., & Raskin, L. (2016). Quantification of parameters influencing methane generation due to biodegradation of municipal solid waste in landfills and laboratory experiments. Waste Management, 55, 276–287. https://doi.org/10.1016/j.wasman.2015.10.015

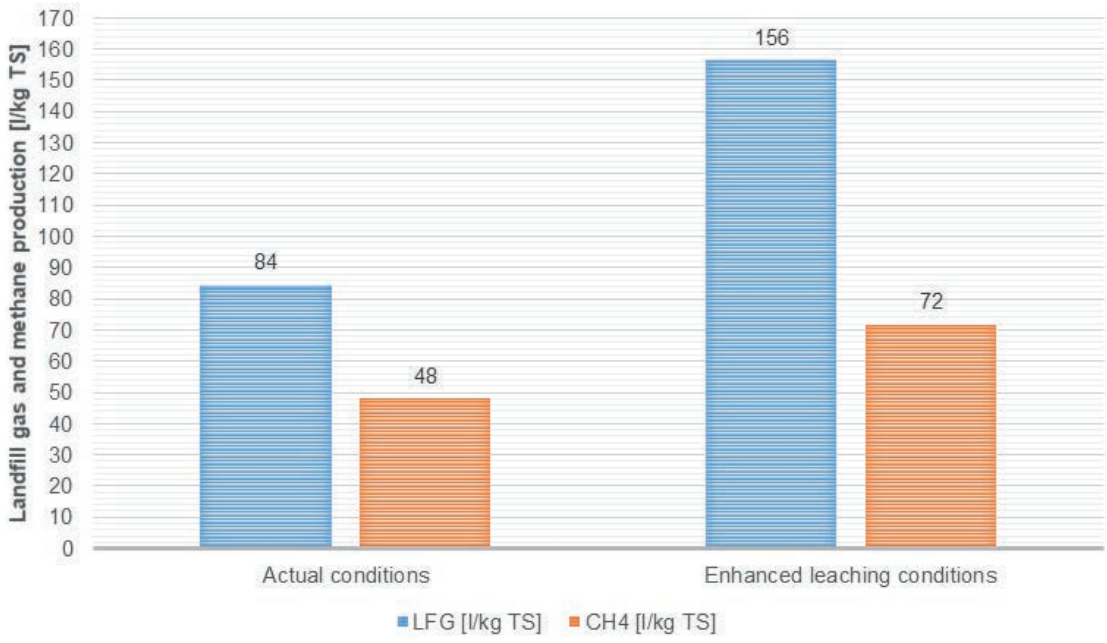

FIGURE 7: Average volume of landfill gas and methane produced.

Frank, R. R., Davies, S., Wagland, S. T., Villa, R., Trois, C., & Coulon, F. (2016). Evaluating leachate recirculation with cellulase addition to enhance waste biostabilisation and landfill gas production. Waste Management, 55, 61–70. https://doi.org/10.1016/j.wasman.2016.06.038

Korai MS, Mahar RB, Uqaili MA, B. K. (2015). Assessment of municipal solid waste management practices and Energy recovery potential in Pakistan. Proceedings of the 14th International Conference on Environmental Science and Technology Rhodes, Greece.

Liu, W., Liu, Y., Zhu, B., & Li, X. (2014). Enhanced biogas production from a stimulated landfill bioreactor for the co-disposal of municipal solid waste and coal wastes. Energy Sources, Part A: Recovery, Utilization and Environmental Effects, 36(11), 1186–1194. https://doi.org/10.1080/15567036.2010.540628

Nair, A., Sartaj, M., Kennedy, K., & Coelho, N. M. G. (2014). Enhancing biogas production from anaerobic biodegradation of the organic fraction of municipal solid waste through leachate blending and recirculation. Waste Management and Research, 32(10), 939–946. https://doi.org/10.1177/0734242X14546036

Pohland, F. G.,and J. C. K. (2000). Microbially mediated attenuation potential of landfill bioreactor systems. Water Science and Technology, 41(3), 247–254.

Pohland, F. (1975). Sanitary landfill stabilization with leachate recycle and residual treatment, 3(2), 100. Retrieved from https://smartech.gatech.edu/bitstream/handle/1853/34573/e-20-642_114709.pdf?sequence=1

Rastogi, M., Hooda, R., & Nandal, M. (2015). ChemInform Abstract: Review on Anaerobic Treatment of Municipal Solid Waste with Leachate Recirculation. ChemInform, 46(6), no-no. https://doi.org/10.1002/chin.201506317

Reinhart, D. R. and A. B. A.-Y. (1996). the Impact of Leachate Recirculation on. Waste Management & Reserach, 14(4), 337–346.

Reinhart, D. R., McCreanor, P. T., & Townsend, T. (2002). The Bioreactor Landfill: Its Status and Future. Waste Management & Research, 20(2), 172–186. https://doi.org/10.1002/chin.200318283

Ritzkowski, M., Walker, B., Kuchta, K., Raga, R., & Stegmann, R. (2016). Aeration of the teuftal landfill: Field scale concept and lab scale simulation. Waste Management, 55, 99–107. https://doi.org/10.1016/j.wasman.2016.06.004

Rovers, G. J. F. F. A. (1973). GAS PRODUCTION DURING REFUSE DECOMPOSITION. Water, Air, and Soil Pollution, 2(4), 483–495. https://doi.org/10.1007/BF00585092

Shahid, M., Nergis, Y., Siddiqui, S. A., & Farooq Choudhry, A. (2014). Environmental impact of municipal solid waste in Karachi city. World Applied Sciences Journal, 29(12), 1516–1526. https://doi.org/10.5829/idosi.wasj.2014.29.12.1908

Themelis, N. J., & Ulloa, P. A. (2007). Methane generation in landfills. Renewable Energy, 32(7), 1243–1257. https://doi.org/10.1016/j.renene.2006.04.020

Zuberi, M. J. S., & Ali, S. F. (2015). Greenhouse effect reduction by recovering energy from waste landfills in Pakistan. Renewable and Sustainable Energy Reviews, 44, 117–131. https://doi.org/10.1016/j.rser.2014.12.028

detritus | Multidisciplinary Journal for Waste Resources & Residues

CISA

GLOBAL DEVELOPMENT OF GREENHOUSE GAS EMISSIONS IN THE WASTE MANAGEMENT SECTOR

Christoph Wünsch * and Robin Kocina

Institute of Waste Management and Circular Economy, Department of Hydrosciences, Technische Universität Dresden - Pratzschwitzer Str. 15, 01796 Pirna, Germany

Article Info:
Received:
28 June 2019
Revised:
9 September 2019
Accepted:
19 September 2019
Available online:
26 September 2019

Keywords:
Greenhouse gas emissions
Global warming
National Inventory Reports

ABSTRACT

The Member States of the United Nations Framework Convention on Climate Change are required to periodically publish their national inventories of anthropogenic emissions in National Inventory Reports. The data used in this paper was extracted from these reports and applied to generate a study of the development of greenhouse gas emissions in the waste management sector. The results show a reduction of greenhouse gas emissions for developed contries/regions from 1990 to 2016 due to improved collection and treatment of landfill gas, a shift from landfilling to biological and thermal treatment, as well as a shift to separate waste collection and treatment. The developing countries and regions show another development of greenhouse gas emissions. On the one hand, their greenhouse gas emissions from the waste sector strongly increased due to higher generation of waste. And on the other hand, they increased due in most cases to unorganized and technically insufficent disposal of mixed waste on dumpsites along with better observation of disposal sites and therefore better registration of emissions. Nevertheless, the per capita emissions in developed countries/regions are with approx. 500 kg CO_2-eq./a much higher than for developing and emerging countries/regions, which just emit around 100 kg CO_2-eq./a.

1. INTRODUCTION

The First World Climate Conference took place in 1979 in Geneva. The conclusion of this conference was that if fossil fuels continued to be depleted as before, and deforestation rates persisted, there would be a further increase of the Carbon Dioxide (CO_2) concentration in the atmosphere; and thus a warning was given out. After the Toronto Conference in 1988, where targets were set for a 20% reduction of greenhouse gas (GHG) emissions by 2005 and a 50% reduction by 2050, the Second World Climate Conference in Geneva took place in 1990. At this conference the first progress report of the Intergovernmental Panel on Climate Change (IPCC) was reviewed, which led to the founding of the United Nations Framework Convention on Climate Change (UNFCCC). This treaty was adopted on the 9th of May 1992 in New York and signed by 154 countries (Parties) in June 1992 at the United Nations Conference on Environment and Development (UNCED) in Rio de Janeiro. The UNFCCC came into force on the 12th of August 1996.

Along with the ratification of this treaty "all Parties, ..., shall: develop, periodically update, publish and make available to the Conference of the Parties, ..., national inventories of anthropogenic emissions by sources and removals by sinks of all greenhouse gases not controlled by the Montreal Protocol, using comparable methodologies to be agreed upon by the conference of the Parties" (UN, 1992). These national inventories of anthropogenic emissions are published in National Inventory Reports (NIR). They include anthropogenic greenhouse gas emissions of different sectors, one of which being the waste sector. The NIR of the parties are available to the public and the data therein was used to make this overview of the global development of greenhouse gas emissions in the waste management sector.

2. METHODOLOGY

2.1 UNFCCC National Inventory submissions

The various parties which report their annual GHG-emissions to the UNFCCC can be devided into Annex I parties and non-Annex I parties. In general, Annex I parties include those countries that were members of the Organisation for Economic Co-operation and Development (OECD) in 1992 as well as countries (especially in Eastern Europe) with economies in transition (EIT Parties), whereas developing countries are considered non-Annex I parties (UNFCCC, 2006).

In accordance with the principle of "common but differentiated responsibilities and respective capabilities" the reporting requirements and timetabels are very different

* Corresponding author:
Christoph Wünsch
email: christoph.wuensch@tu-dresden.de

https://doi.org/10.31025/2611-4135/2019.13856
© 2019 Cisa Publisher. Open access article under CC BY-NC-ND license

for Annex I parties and non-Annex I parties. Therefore, the extent of data available depends on whether the country is an Annex I party (which provides information annually on the amount of GHG-emissions released) or a non-Annex I party (where significant data gaps are very common) (UNFCCC, 2006).

Within the submitted reports, GHG-emissions in the form of CH_4 and N_2O are usually stated on their own as well as in the form of CO_2-equivalents (CO_2-eq.) (IPCC, 2006). In order to enable a better comparison between the different kinds of GHG-emissions caused within the different kinds of waste streams, the following figures will show all GHG-emissions as CO_2-equivalents (CH_4 = 25 CO_2-eq. and N_2O = 298 CO_2-eq.) (UNFCCC, 2014). While all the data on released GHG-emissions is originally based on the reports submitted to the UNFCCC by the various parties, most of the data used in this study is taken directly from the website of the UNFCCC. Figure 1 outlines how GHG-emissions are generally segmented in the annual reports (IPCC, 2006).

Despite being part of the Waste sector in the Figure 1, GHG-emissions of "Wastewater Treatment and Discharge" were not included in any of the subsequent figures or calculations. Furthermore GHG-emissions declared as "Other" were also excluded. Lastly, in order to give a more complete picture of the waste management sector, GHG-emissions caused by waste incineration with energy recovery were transferred from the Energy sector (where they are usually reported) to the Waste sector. While they are mostly listed separately within the parties' reports, those GHG-emissions released through the incineration of waste with energy recovery and those without energy recovery will within this study be indicated combined.

2.2 System boundaries

In the country reports, only direct emissions produced in a sector are presented. Indirect up- and downstream emissions are assigned to the direct emissions of the corresponding sectors. For example, the indirect upstream emissions from the transportation of waste are assigned to the transportation sector and not included in the subsequent figures. The same applies for avoided GHG-emisions e.g. by energy and secondary raw material supply. These avoided indirect downstream emissions are also not included in the inventory of the waste sector and the subsequent figures.

Figure 2 shows the decided-upon system boundary around the waste sector and which direct emissions of this sector were considered exclusively.

2.3 Waste treatment options

2.3.1 Landfill and Dumpsite

In a global context, disposal of solid waste on landfills and dumpsites represents the most common kind of waste treatment. Especially in developed countries, landfills are frequently equipped with modern technologies; such as landfill gas collection systems, which – through the installation of vertically or horizontally positioned wells – allow the collection and utilization (e.g. for the production of electricity) of the emitted landfill gas. In contrast, most developing countries tend to deposit large amounts of their solid waste on mostly illegal and non-monitored dumpsites without modern technologies that prevent GHG-emissions from entering the atmosphere (IPCC, 2007).

GHG-emissions from landfilling occur under anaerobic circumstances, caused through the presence of moisture and the lack of oxygen. Aside from the release of

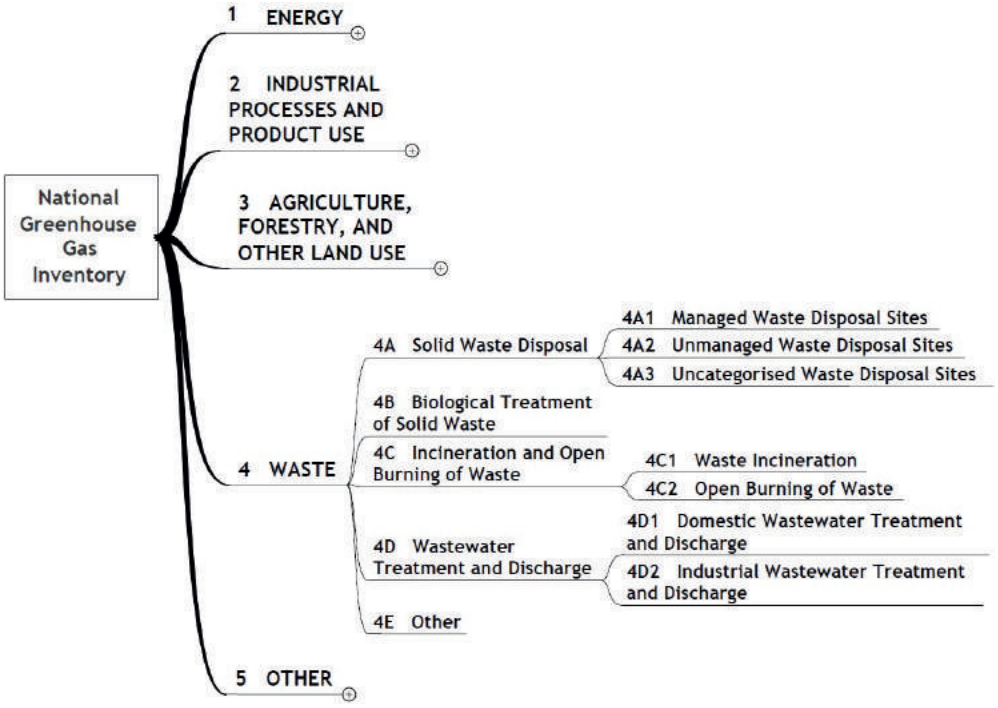

FIGURE 1: Structure of categories within the waste sector and coding of their IPCC categories (IPCC, 2006).

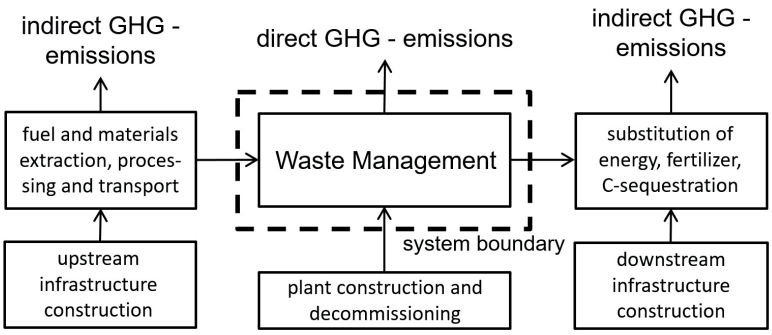

FIGURE 2: System boundary of the reported greenhouse gas emissions (own figure derived from Abu Qdais et al., 2019).

climate-damaging CH_4, waste disposal also leads to the release of carbon-neutral CO_2, N_2O, and small amounts of non-methane volatile organic compounds (IPCC, 2006). Apart from the presence of a modern landfill gas collection system, the amount of degradable organic matter (and therefore the amount of bioavailable carbon) in the form of organic waste within the landfill or dumpsite plays a key role in generating GHG-emissions (EUROSTAT, 2010).

2.3.2 Biological treatment

Biological treatment can take place in the form of composting (aerob) or digestion (anaerob). CO_2-emissions caused through biological treatment are of biogenic origin and can thus be considered carbon- and climate neutral. Climate-damaging GHG-emissions through the biological treatment of solid waste mainly occur as CH_4 and N_2O. Even though the amount of GHG-emissions generated through the biological treatment of waste compared to the amount of GHG-emissions caused by landfilling or waste incineration in general is significantly smaller, biological treatment of waste can still have a considerable influence on the amount of total GHG-emissions within the waste sector, since the amounts of separately collected organic waste treated biologically are not deposited in landfills (IPCC, 2006).

2.3.3 Waste incineration

Incineration of waste is another major source of GHG-emissions in the waste management sector. Whereas clinical waste is incinerated in many countries, the incineration of municipal waste is more common in developed countries. Waste incineration means the combustion of solid and liquid waste in controlled incineration facilities. GHG-emissions released through the incineration of waste consist mainly of CO_2, N_2O, and (as a result of incomplete combustion) CH_4. The CO_2-emissions are in most cases much higher than N_2O- and CH_4-emissions. While CO_2-emissions from the combustion of (partly) fossil originated waste should be included in national emissions by the parties, CO_2-emissions from the combustion of biomass should not be included (IPCC, 2006).

3. RESULTS - GREENHOUSE GAS INVENTORIES

To get an overview of the development of global GHG-emissions from 1990 to 2016, the emissions from the largest contributors were analysed. These are China with approx. 27.5%, the United States with approx. 14.8%, India with approx. 6.4%, Russia with approx. 4.9%, Japan with approx. 3%, Brazil with approx. 2.3%, Germany with approx. 2% and Canada with approx. 1.6%. These parties emit approx. 62.5% of the global emissions (based on the year 2014) (WRI, 2017).

Since the Annex I parties are required to report their emissions annually and a gapless data basis is available, these countries are analysed first. The selected non-Annex I parties are looked at separately since they do not report their GHG-inventories regulary and thus (particularly when comparing the selected larger regions) a few reasonable assumptions, oriented on the existing data, had to be made to fill in existing data gaps.

To get an even clearer picture of the development of global emissions, the larger regions of the European Union (EU28 + Iceland) with approx. 9.3%, North America (USA, Canada and Mexico) with approx. 18%, Russia and some of the New Independent States (Russian Federation, Kazakhstan, Uzbekistan and Ukraine) with approx. 6.9% and Asian states (China, India, Japan, South Korea, Turkey, Saudi Arabia, Malaysia, Thailand and Vietnam) with approx. 42.6% were analysed. These larger regions emitted 76.8% of the global GHG-emissions in 2014 (WRI, 2017). The selected states are the biggest polluters in their respective larger regions and provide the most sufficient data.

Figure 3 shows all countries and larger regions that were considered in this study on a global map.

3.1 Selected Annex I parties

3.1.1 United States of America

The United States of America is currently the second largest contributor with a relatively stable level of emissons between 6 and 7 billion Mg CO_2-eq. (6.356 Mg in 1990 and 6.511 Mg in 2016 with a peak of 7.351 Mg in 2006) generated over all sectors per year (UNFCCC, 2019).

Emissions of the waste sector decreased from approx. 188.2 million Mg CO_2-eq. in 1990 (2.96% of total emissions) to approx. 122.3 million (1.88% of total emissions) (UNFCCC, 2019). Figure 4 shows the development of GHG-emissions released by the waste sector of the United States of America between 1990 and 2016 by different disposal paths.

Since a lot of waste is still dumped and landfilled in the United States and older dumps and landfills are often not

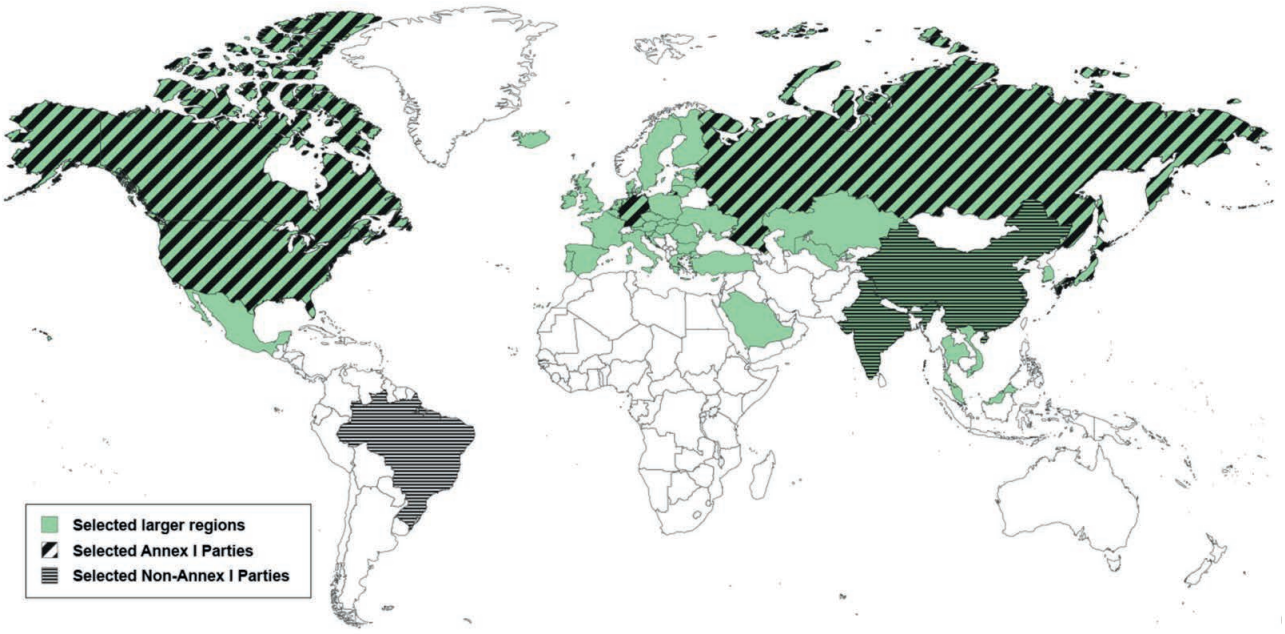

FIGURE 3: Map of the world with the considered parties/countries and larger regions (own figure).

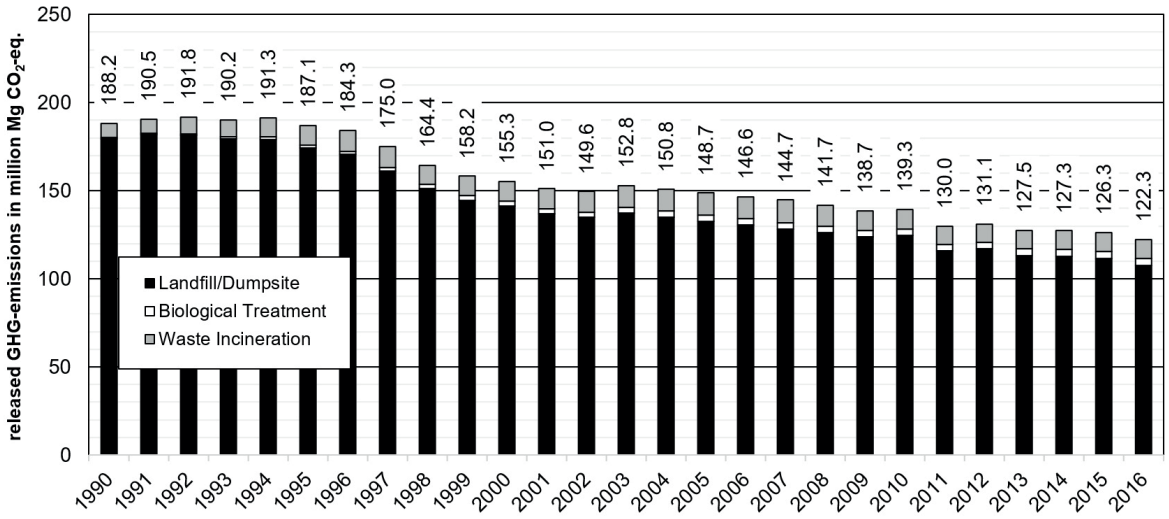

FIGURE 4: Greenhouse gas emissions released by the waste sector of the United States of America between 1990 and 2016 by disposal path (own figure derived from UNFCCC, 2019).

sufficiently equipped with landfill gas collection systems, a substantial amount of methane is produced and emitted into the atmosphere. Emissions from biological and thermal treatment of waste have increased from 1990 to 2016, however, compared to the greenhouse gases emitted from landfills and dumpsites, their contribution is far less significant (DOS, 2014).

The amount of GHG-emissions released in the US waste sector was reduced by approx. 65.9 million Mg CO_2-eq./a or approx. 35.00% from the base year 1990 until 2016.

3.1.2 Russian Federation

The Russian Federation is the fourth largest contributor worldwide with a decrease in GHG-emissions over all sectors from approx. 3.734 billion Mg CO_2-eq. (1990) to 2.644 billion Mg CO_2-eq. (2016) (UNFCCC, 2019). A decrease to a minimum of 2.217 billion Mg CO_2-eq. in 1998 was due to the decline of Russian industry in the early 90's. After 1998, GHG-emissions started to rise again.

Emissions of the waste sector increased from approx. 52.0 million Mg CO_2-eq. in 1990 (1.39 % of total emissions) to approx. 86.8 million (3.28% of total emissions). Figure 5 shows the development of GHG-emissions released in the waste sector of the Russian Federation between 1990 and 2016 by different disposal paths.

Almost all of the waste in the Russian Federation ends up on landfills or (in most cases) dumpsites. Some neglectable amounts of GHG-emissions (max. 70,000 Mg CO_2-eq. in 2012) were caused by biological waste treatment. Since a majority of waste is still dumped on

older dumpsites or landfills, which in most cases are not equipped with landfill gas collection systems, considerable amounts of methane are emitted into the atmosphere (IFC, 2012). Some waste incineration plants are being planned for the Moscow region and Kazan (Kanunnikova, 2016), but as of 2016 no emissions from waste incineration were reported by the Russian Federation.

The amount of GHG-emissions in the Russian waste sector increased by approx. 34.8 million Mg CO_2-eq./a, which is approx. 67.01% from the base year 1990 until 2016.

3.1.3 Japan

Japan is the fifth largest contributor in terms of overall amount of GHG-emissions. Japan's total released emissons over all sectors hovered within a relatively stable range between 1.267 billion Mg CO_2-eq. (1990) and 1.305 billion Mg CO_2-eq. (2016) (UNFCCC, 2019).

GHG-emissions in the Japanese waste sector remained fairly stable from approx. 35.0 million Mg CO_2-eq. in 1990 (2.76 % of total emissions) to approx. 34.6 million in 2016 (2.65% of total emissions) (UNFCCC, 2019). Between 1994 and 2008 GHG-emissions in Japan's waste sector increased slightly to around 40 million Mg CO_2-eq./a. Figure 6 shows the development of GHG-emissions released by the Japanese waste sector between 1990 and 2016 by different disposal paths.

Given its high population density and the lack of available area for landfill sites, incineration of waste is the most common disposal path in Japan (Vehlow et al., 2015). Therefore GHG-emissions caused by waste incineration (which also include the emissions from gasification melting furnace) are significantly higher than those caused from landfilling waste (Nojiri et al., 2018). The rise of GHG-emissions by waste incineration/thermal treatment in the middle of the 1990s was due to the increasing Japa-

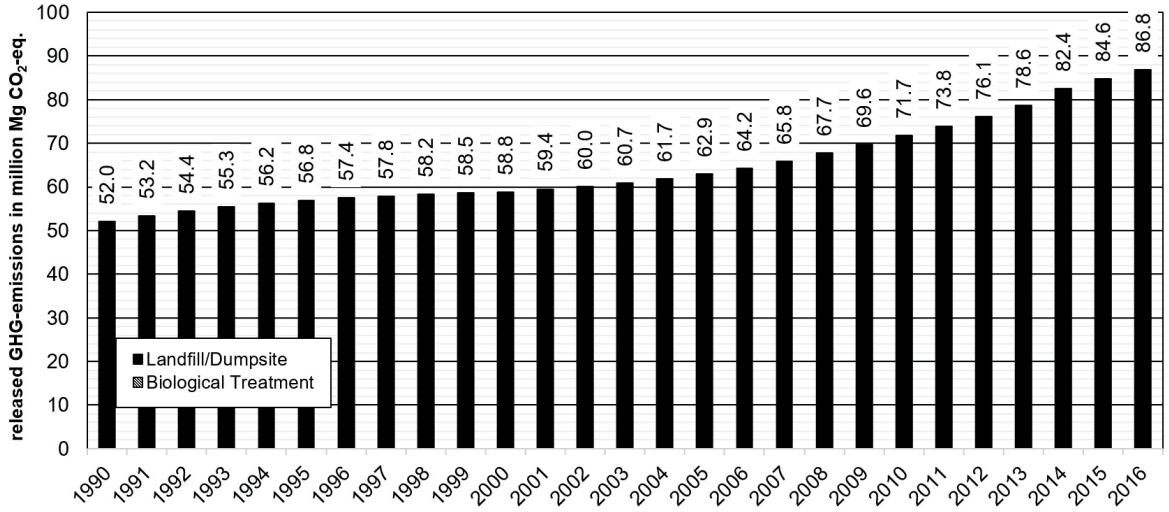

FIGURE 5: Greenhouse gas emissions released by the waste sector of the Russian Federation between 1990 and 2016 by disposal path (own figure derived from UNFCCC, 2019).

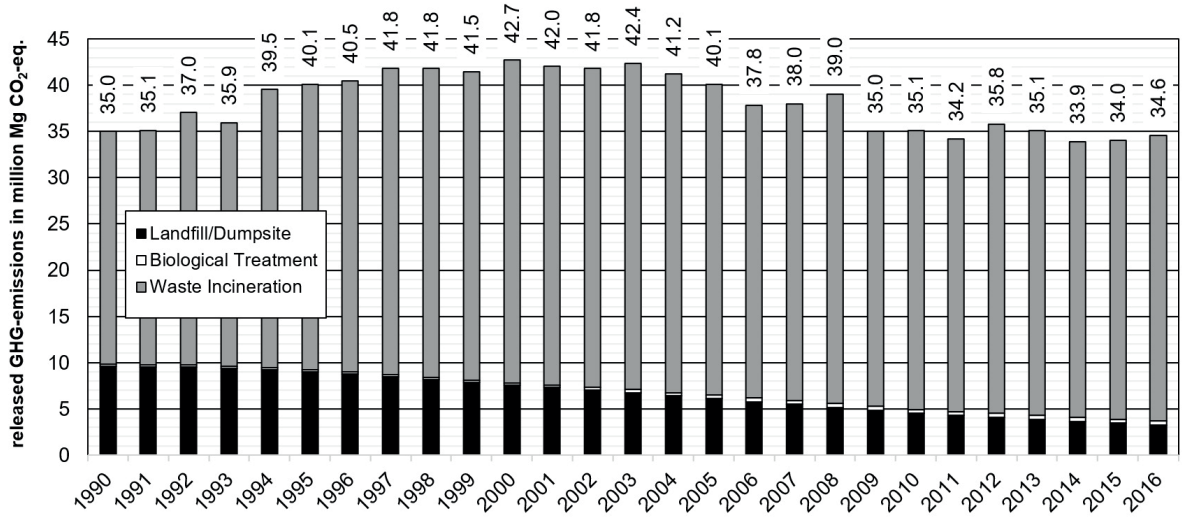

FIGURE 6: Greenhouse gas emissions released by the waste sector of Japan between 1990 and 2016 by disposal path (own figure derived from UNFCCC, 2019).

nese economy connected with growing waste generation (MOE, 2014) and the expansion of the capacity of pyrolysis and gasification plants. Due to a national regulation at this time that required incineration ashes to be melted down, the Japanese favored two-stage/combined processes (consisting of gasification/pyrolysis combined with slag smelting) rather than incineration with downstream slag smelting (Vaccani and Asato, 2014). The decrease from 2005 – 2009 was caused by changes in the Japanese industrial structure and economy with the effect that waste generation continued to decrease as a result of progress in sorted collection, recycling and in the development of a sound material-cycle society (MOE, 2014).

The levels of GHG-emissions released by Japan's waste sector decreased by approx. 0.4 million Mg CO_2-eq./a or approx. 1.15% from the base year 1990 until 2016.

3.1.4 Germany

As the seventh largest contributor, Germany decreased its total GHG-emissions from 1.252 billion Mg CO_2-eq. (1990) to 909 million Mg CO_2-eq. (2016) (UNFCCC, 2019).

Direct emissions in the waste sector decreased in the same range as the total emissions over all sectors, from 38.1 million CO_2-eq. in 1990 (3.04% of total emissions) to 28.7 million Mg CO_2-eq. in 2016 (3.16% of total emissions) (UNFCCC, 2019). Figure 7 shows the development of GHG-emissions released by the waste sector in Germany between 1990 and 2016 by different disposal paths.

Aside from a slight increase in GHG-emissions from biological waste treatment, a shift of GHG-emissions from landfill to waste incineration took place in the German waste sector. In 1990 more than 34 million Mg CO_2-eq. were released by landfills and dumpsites in the form of methane. This was reduced to approx. 8 million Mg CO_2-eq. by 2016. In contrast, the emissions from waste incineration increased from approx. 4 million Mg CO_2-eq. in 1990 to approx. 19 million Mg CO_2-eq. in 2016 (Gniffke and Strogies, 2018).

The extent of direct GHG-emissions released in the German waste sector was reduced by approx. 9.4 million Mg CO_2-eq./a or approx. 24.62% from the base year 1990 until 2016.

3.1.5 Canada

The eighth largest contributor of GHG-emissions is Canada with an increase of total emissions released over all sectors from 603 million Mg CO_2-eq. (1990) to 704 million Mg CO_2-eq. (2016) (UNFCCC, 2019).

Emissions of the waste sector increased between 1990 and 2006 from approx. 17.7 million Mg CO_2-eq. to approx. 20.8 million Mg CO_2-eq. and then decreased back to 17.8 million Mg CO_2-eq. in 2016 (UNFCCC, 2019). In 1990 the waste sector accounted for 2.93% of total emissions and in 2016 for approx. 2.53%. Figure 8 shows the development of GHG-emissions released in the waste sector of Canada between 1990 and 2016 by different disposal paths.

Most of Canada's waste is still dumped and landfilled, while older dumps or landfills are often not sufficiently updated with landfill gas collection systems. Therefore, large amounts of methane are still produced and emitted into the atmosphere. Emissions from the biological treatment of waste have increased between 1990 and 2016, but compared to the greenhouse gases emitted through disposing waste on landfills and dumpsites, their amounts are insignificant. (ECCC, 2017) GHG-emissions due to waste incineration remained relatively stable around 0.9 million Mg CO_2-eq./a.

The level of released GHG-emissions in the Canadian waste sector could not be reduced from the base year 1990 till 2016 and increased by less than 0.1 million Mg CO_2-eq./a or respectively approx. 0.19%.

3.2 Selected non-Annex I parties

3.2.1 China

China is currently the country with the largest amount of GHG-emissions released per year. As a non-Annex I party, the data about China's GHG-emissions submitted to the

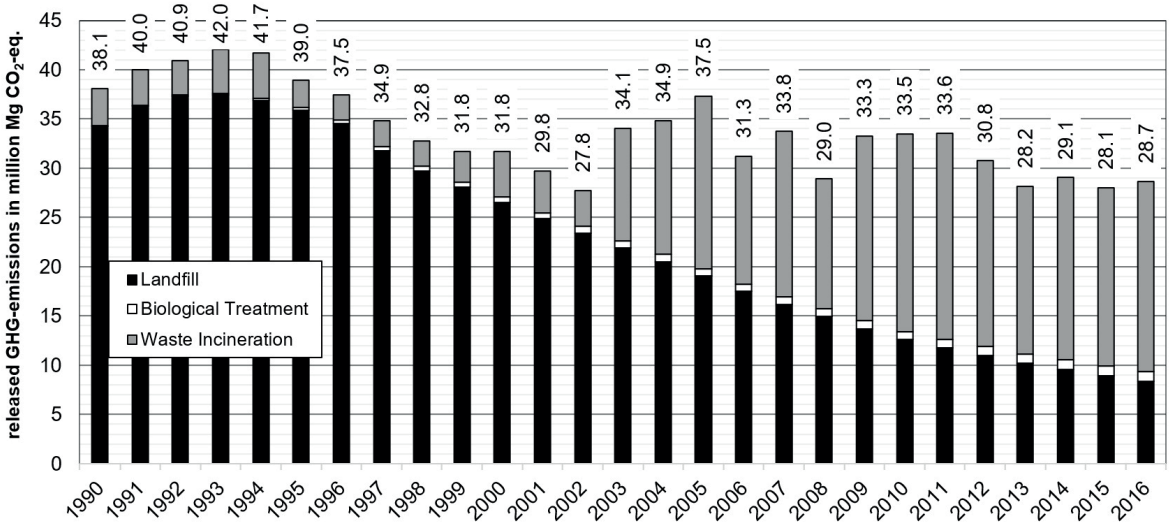

FIGURE 7: Greenhouse gas emissions released by the waste sector of Germany between 1990 and 2016 by disposal path (own figure derived from UNFCCC, 2019).

UNFCCC has many more gaps than that of Annex I parties, and only includes the three years of 1994, 2005 and 2012. Over this period, China's total GHG-emissions almost tripled, rising from 4.058 billion Mg CO_2-eq. (1994) to 11.896 billion Mg CO_2-eq. (2012) (UNFCCC, 2019).

Within the same period, GHG-emissions in China's waste sector also showed a significant rise, climbing from approx. 42.6 million Mg CO_2-eq. (1994) to 67.1 million Mg CO_2-eq. (2012) (UNFCCC, 2019). The waste sector accounted for 1.05% of China's total emissions in 1994. Even though the amount of GHG-emissions released in the waste sector increased, its share decreased to 0.56% in 2012 because of an even bigger emissions growth within the other sectors. Figure 9 shows the development of GHG-emissions released by the waste sector of China between 1994 and 2012 devided in the different disposal paths.

Despite an increase in the amount of waste incinerated over the last decades, discarding solid waste on landfills and dumpsites remains the preferred disposal path in China (Nelles et al., 2015). Since many of the landfills or dumpsites are not sufficiently equipped with landfill gas collection systems, a considerable amount of landfill gas is produced and emitted into the atmosphere, resulting in almost 80% of GHG-emissions within the waste sector being caused by the disposal of waste on landfills or dumpsites in 2012. In China, biological treatment of waste takes place to a certain extent in the form of composting. However, China's submitted GHG data does not include this kind of treatment and it can be assumed that the amount of GHG-emissions released through biological treatment compared to those released through landfilling and waste incinceration is negligible (Li et al., 2016).

The GHG-emissions in China's waste sector therefore showed an increase between 1994 and 2012 climbing from 42.6 million to 67.1 million Mg CO_2-eq./a, which is approx. 57.46%.

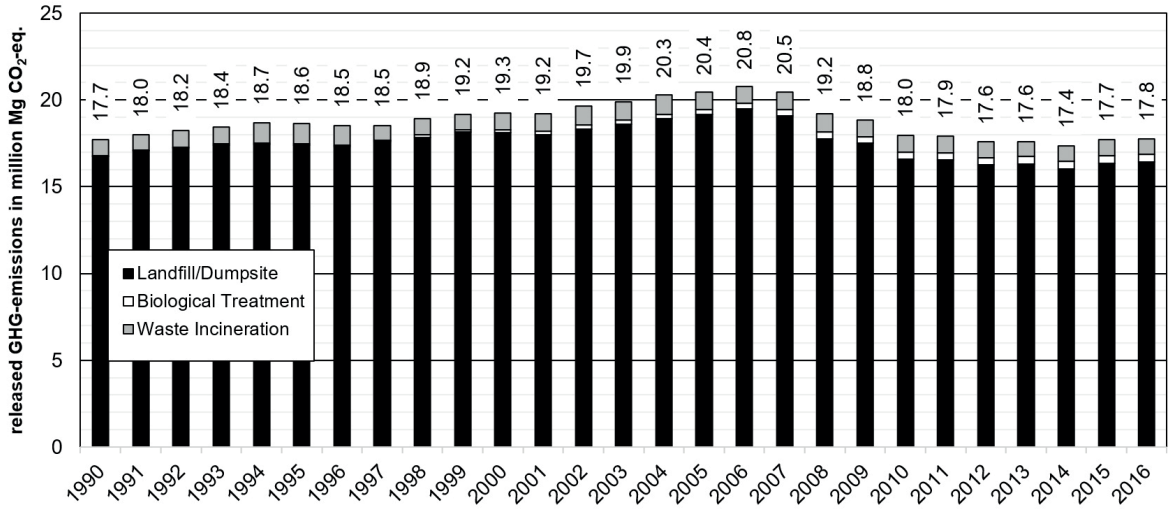

FIGURE 8: Greenhouse gas emissions released by the waste sector of Canada between 1990 and 2016 by disposal path (own figure derived from UNFCCC, 2019).

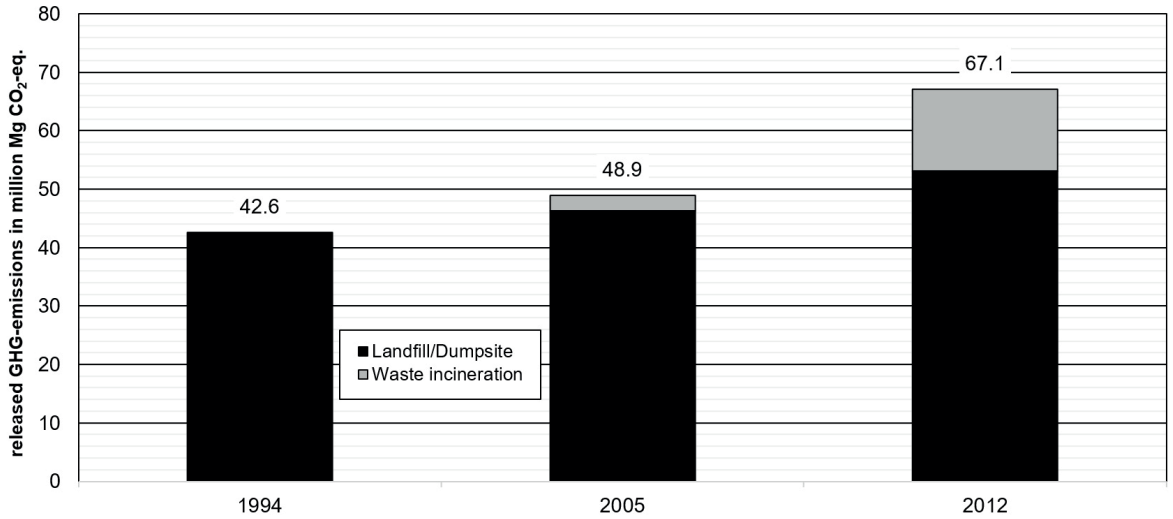

FIGURE 9: Greenhouse gas emissions released by the waste sector of China between 1994 and 2012 by disposal path (own figure derived from UNFCCC, 2019).

3.2.2 India

The third largest contributor of GHG-emissions is India. The data on released GHG-emissions submitted to the UNFCCC refers to the years 1994, 2000, 2010 and 2014. Within this period, India's total GHG-emissions rose consistently from 1.214 billion Mg CO_2-eq. (1994) to 2.607 billion Mg CO_2-eq. (2014) (UNFCCC, 2019).

While India's GHG-emissions within the waste sector decreased between 1994 and 2000 from 12.2 million Mg CO_2-eq. to 10.3 million Mg CO_2-eq., GHG-emissions subsequently increased again to a peak value of 15.1 million Mg CO_2-eq. in 2014 (UNFCCC, 2019). Though the total amount of released GHG-emissions in the Indian waste sector significantly rose, its share decreased over the years from 1.01% (1994) to 0.58% (2014), because similar to China there was an even stronger increase in the GHG-emissions released in the other sectors. Figure 10 shows the development of GHG-emissions released by the waste sector of India between 1994 and 2014.

Almost all the information on India's waste management refers to bigger cities, while the knowledge about rural areas of the country is very limited. Whereas an almost insignificant amount of waste seems to be composted or incinerated, a substantially larger amount is disposed of on dumpsites with no technologies installed to prevent occurring landfill gases from entering the atmosphere. Simultaneously India struggles with basic problems in their waste management, such as the lack of a nation-wide collection system for generated waste (Vogt et al., 2015).

The amount of released GHG-emissions in India's waste sector increased between 1994 and 2014 by 2.8 million Mg CO_2-eq./a, which is approx. 23.26%.

3.2.3 Brazil

Brazil is currently the sixth largest contributor in terms of total GHG-emissions released per year. Submitted data refers to all years from 1990 to 2010. Within this period, Brazil's GHG-emissions increased from 551 million Mg CO_2-eq. (1990) to 919 million Mg CO_2-eq. (2010) (UNFCCC, 2019).

In the waste sector, Brazil's GHG-emissions level steadily increased from 1990 to 2003 climbing steeply from 17.3 million Mg CO_2-eq. to 27.1 million Mg CO_2-eq., then it stabilized, reaching 27.9 million Mg CO_2-eq. in 2010 (UNFCCC, 2019). In 1990 the waste sector accounted for 3.14% of Brazil's total GHG-emissions. Despite a massive increase within the other sectors in 2010, the percentage of Brazil's total GHG-emissions still remained at 3.03% and hence did not show the same trend as China and India. Figure 11 shows the development of GHG-emissions released in the Brazilian waste sector between 1990 and 2010.

The reports Brazil submitted to the UNFCCC only contain information on GHG-emissions which were released through disposal of waste on landfills and dumpsites. Referring to the data of 2008, almost none (less than approx. 0.1%) of the municipal waste generated in Brazil is treated in waste incineration facilities and only approx. 2% is recycled or composted, while at the same time almost 60% is disposed of at organized landfills and almost 40% at unorganized dumpsites (without any technologies preventing landfill gases from entering the atmosphere). This results in significant amounts of methane emissions (Kling et al., 2018).

The extent of GHG-emissions released in the Brazilian waste sector increased between 1990 and 2010 by 10.6 million Mg CO_2-eq./a, which is approx. 60.97%.

3.3 Selected larger regions

3.3.1 European Union

The EU was able to reduce its total GHG-emissions from 5.646 billion in 1990 to 4.291 billion Mg CO_2-eq. in 2016 (UNFCCC, 2019). The GHG-emissions contribution of the waste sector increased from 207.4 million Mg CO_2-eq. in 1990 to 226.9 million Mg CO_2-eq. in 1995, before it began to decrease reaching 168.4 million Mg CO_2-eq. in 2016 (UNFCCC, 2019). The waste sector accounted for 3.67% of total emissions in 1990 and 3.92% in 2016. Figure 12 shows the GHG-emissions in the waste sector of the EU between 1990 and 2016, devided in the different disposal paths.

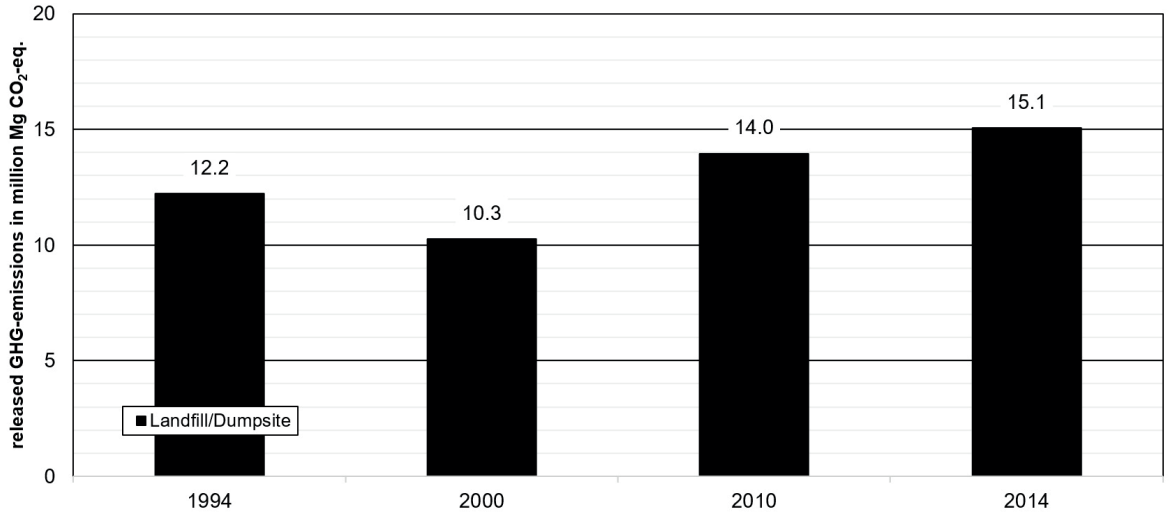

FIGURE 10: Greenhouse gas emissions released by the waste sector of India between 1994 and 2014 by disposal path (own figure derived from UNFCCC, 2019)

Over the last decades, incineration of waste became more and more popular in the EU Member States, but this went along with a simultaneous increase in GHG-emissions. However, even in 2016, landfilling still marks the disposal path with the largest amount of released GHG-emissions at 60%, while incineration covers approx. 36%. The GHG-emissions caused through biological treatment of waste also increased over the last decades, but they play a minor role compared to the GHG-emissions released through landfilling or waste incineration (UNFCCC, 2019).

The level of GHG-emissions released in the EU's waste sector decreased between 1990 and 2016 by 39.1 million Mg CO_2-eq./a, which is approx. 18.84%.

3.3.2 North America

The total GHG-emissions of North America (United States of America, Canada, and Mexico) increased from 7.363 billion Mg CO_2-eq. in 1990 to 8.707 billion Mg CO_2-eq. in 2007, before it began to fall again to 7.698 billion Mg CO_2-eq. in 2016 (UNFCCC, 2019). In the waste sector, GHG-emissions increased from 206.5 million Mg CO_2-eq. in 1990 to 212.0 million Mg CO_2-eq. in 1994, and then decreased again to 160.7 million Mg CO_2-eq. in 2016 (UNFCCC, 2019). While the waste sector accounted for 2.80% of total GHG-emissions in North America in 1990, in 2016 it only accounted for 2.09%. Figure 13 shows the GHG-emissions of the waste sector in North America between 1990 and 2016 by disposal path.

Disposal of waste on landfills and (especially in Mexico) dumpsites is the most common path for waste generated in the three observed countries in North America and therefore it accounts for the biggest portion of the GHG-emissions in the waste sector. While GHG-emissions released through the disposal of waste on landfills and dumpsites were able to be reduced over the last decades,

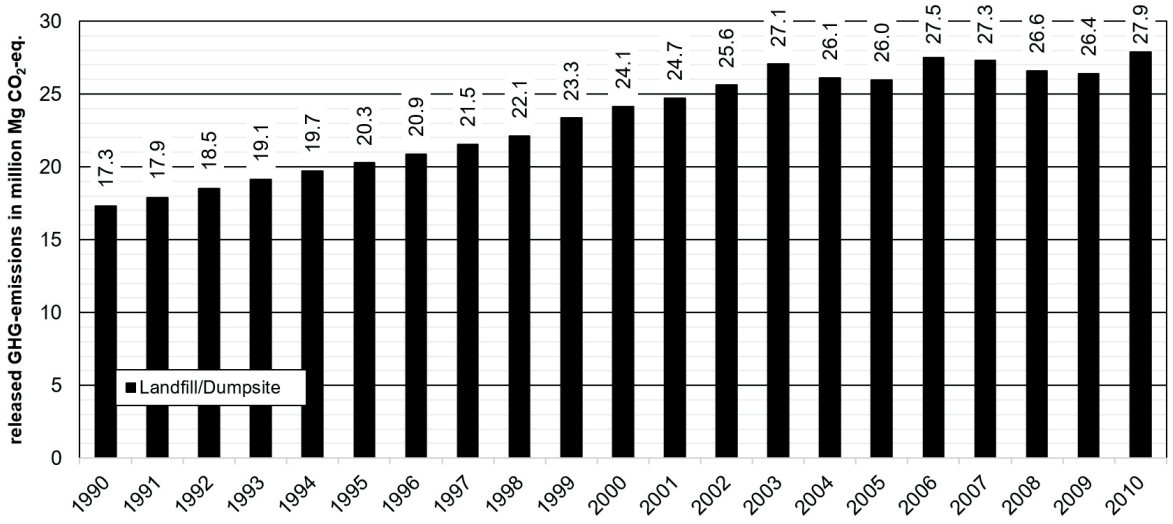

FIGURE 11: Greenhouse gas emissions released by the waste sector of Brazil between 1990 and 2010 by disposal path (own figure derived from UNFCCC, 2019).

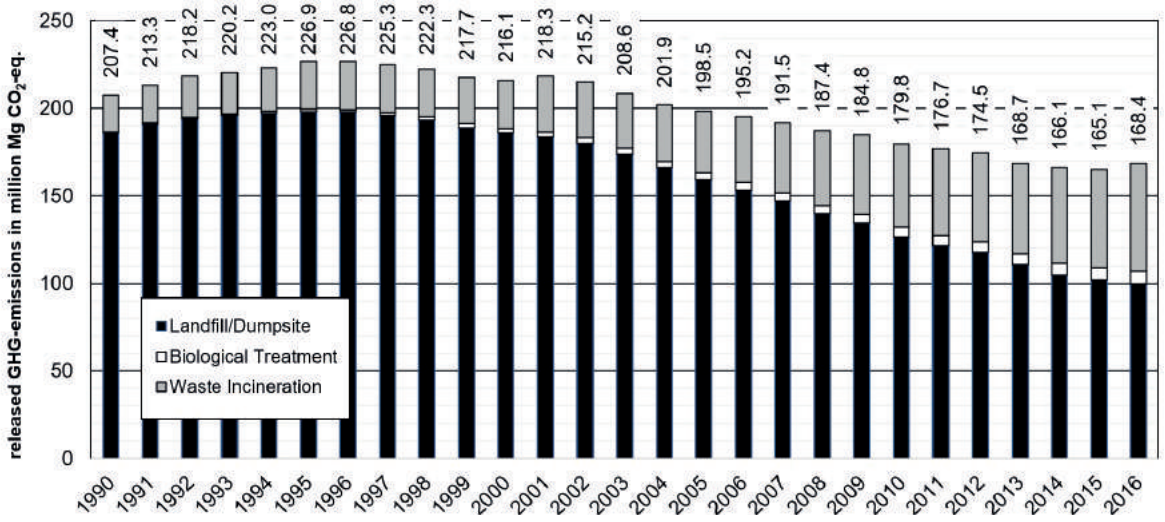

FIGURE 12: Greenhouse gas emissions released by the waste sector of the European Union between 1990 and 2016 by disposal path (own figure derived from UNFCCC, 2019)

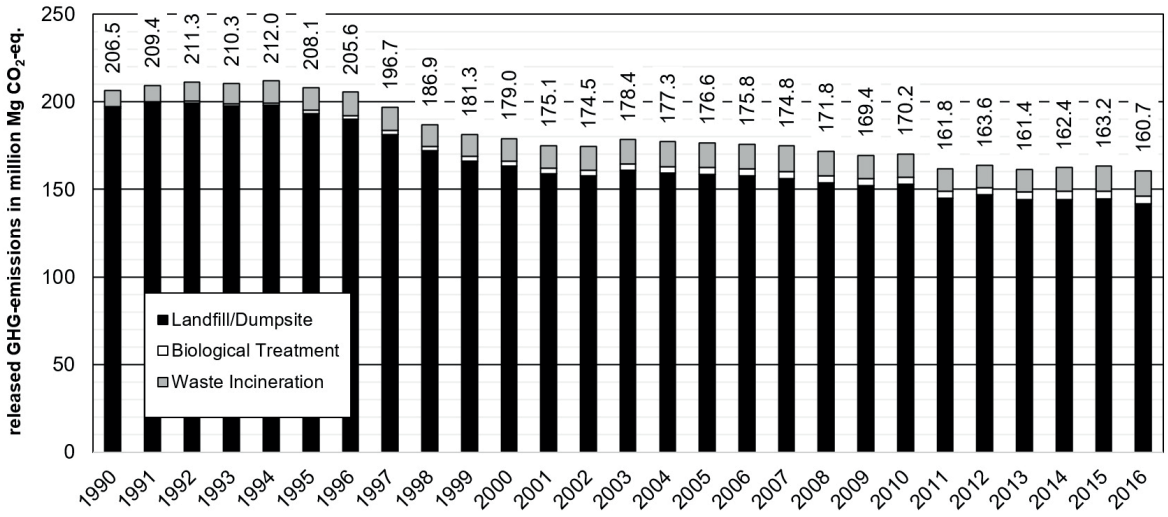

FIGURE 13: Greenhouse gas emissions released by the waste sector of North America between 1990 and 2016 by disposal path (own figure derived from UNFCCC, 2019).

those caused by waste incineration and biological treatment increased slightly (UNFCCC, 2019).

The USA accounted for the biggest part of released GHG-emissions in North America with 91.16% in 1990 and 76.04% in 2016. While the amount of Canada's waste related GHG-emissions did not change much, Mexico's share increased from 0.28% in 1990 to 12.98% in 2013 (UNFCCC, 2019).

The amount of released GHG-emissions in the North American waste sector decreased between 1990 and 2016 by 45.8 million Mg CO_2-eq., which is approx. 22.17%.

3.3.3 Russia, Kazakhstan, Ukraine and Uzbekistan

The total GHG-emissions of Russia and some of the Newly Independent States (NIS), Kazakhstan, Ukraine and Uzbekistan, decreased from 5.201 billion Mg CO_2-eq. in 1990 to 3.009 billion Mg CO_2-eq. in 1999. Then it increased again and stabilized at about 3.500 billion Mg CO_2-eq., later reaching 3.522 billion Mg CO_2-eq. in 2016 (UNFCCC, 2019).

In the waste sector of the observed states, GHG-emissions consistently increased from 64.0 million Mg CO_2-eq. in 1990 to 105.4 million Mg CO_2-eq. in 2016 (UNFCCC, 2019). While in 1990 GHG-emissions from the waste sector only accounted for 1.71% of the total emissions released in Russia and the observed NIS countries, they accounted for 3.99% in 2016. Figure 14 shows the increase of GHG-emissions in Russia and the observed NIS countries between 1990 and 2016 by disposal path.

Even though biological treatment and incineration of waste exist to a certain extent, those two disposal paths accounted for only 0.17% in 1990 and 0.08% in 2016 of all GHG-emissions in the waste sector, while the remaining GHG-emissions were caused by the disposal of waste on landfills and dumpsites. In most cases these landfills and dumpsites are not equipped with landfill gas collection systems, leading to substantial amounts of methane being emitted into the atmosphere (Skryhan et al., 2018). The Russian Federation accounts for 81.18% of the released GHG-emissions in the waste sector of the four observed countries in 1990, while in 2016 it accounted for 82.37%. The growth of released GHG-emissions within the waste sector not only took place in the Russian Federation, but also in the other three contries. None of the observed countries was able to reduce its waste-related GHG-emissions.

The amount of GHG-emissions released in the waste sector of Russia, Kazakhstan, Ukraine and Uzbekistan increased between 1990 and 2016 by 41.4 million Mg CO_2-eq./a or approx. 64.60%.

3.3.4 Selected Asian countries

The total GHG-emissions of selected Asian countries (including Turkey, Japan, China, India, South Korea, Saudi Arabia, Malaysia, Thailand, and Vietnam) consistently increased from 6.472 billion Mg CO_2-eq. in 1990 to 21.172 billion Mg CO_2-eq. in 2016 (UNFCCC, 2019). The GHG-emissions in the waste sector of these selected Asian countries also consistently increased from 124.4 million Mg CO_2-eq. in 1990 up to 219.6 million Mg CO_2-eq. in 2016 (UNFCCC, 2019). Even though they consistently increased, GHG-emissions of the waste sector accounted only for 1.04% of total emissions in 2016, while in 1990 they had accounted for 1.92%. This is mainly because of the even more rapid growth of GHG-emissions within other non-waste sectors. Figure 15 shows the GHG-emissions in the waste sector of the selected Asian countries between 1990 and 2016 by disposal path.

As can be seen in the Figure 15, GHG-emissions in the waste sector can largely be attributed to the disposal of waste on landfills and dumpsites, which accounted for 78.31% of released emissions in 1990 and 73.22% in 2016. Since in many of the observed countries landfills and dumpsites are not sufficiently equipped with landfill gas collection systems, serious amounts of methane are emitted into the atmosphere (Modak et al., 2017). Waste incineration in some of the observed countries is getting more and more popular as there was an increase to 26.57% of GHG-emissions in the waste sector in 2016, compared to 21.49% in 1990. Remaining GHG-emissions were released through biological treatment of waste and seem to be neg-

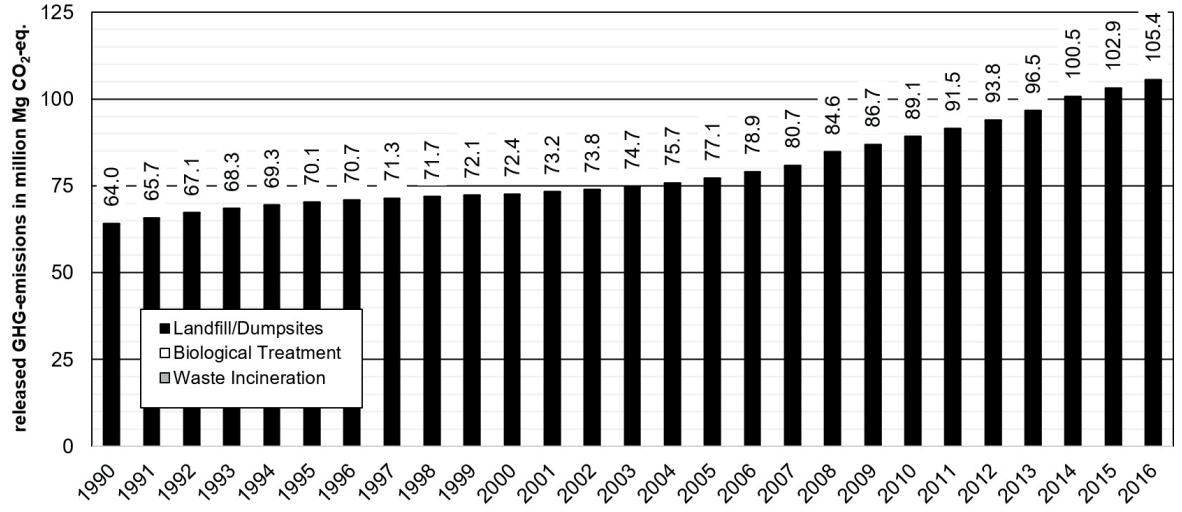

FIGURE 14: Greenhouse gas emissions released by the waste sectors of Russia, Kazakhstan, Ukraine and Uzbekistan between 1990 and 2016 by disposal path (own figure derived from UNFCCC, 2019).

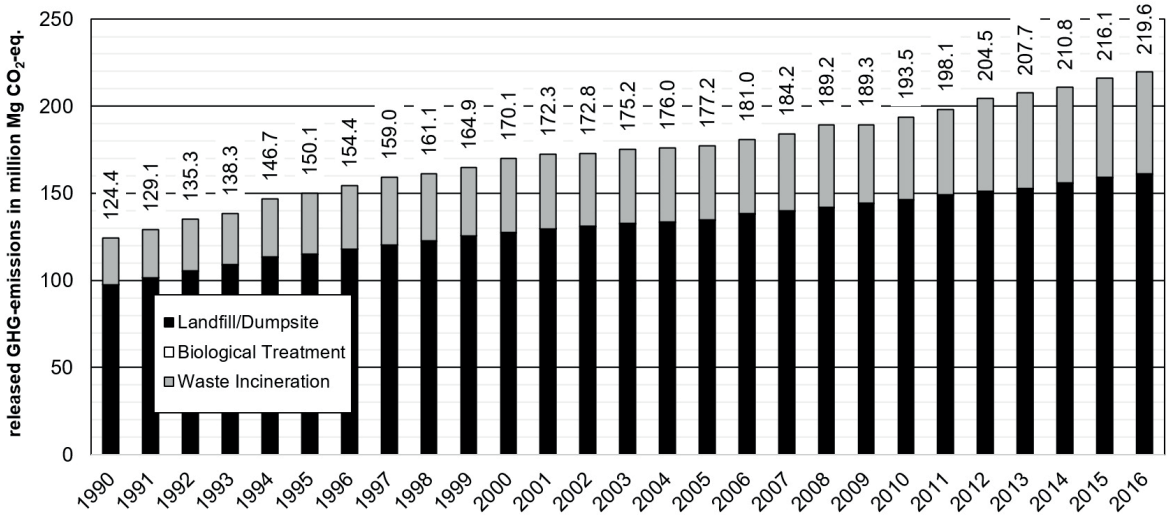

FIGURE 15: Greenhouse gas emissions released by the waste sector in selected Asian countries between 1990 and 2016 by disposal path (own figure derived from UNFCCC, 2019).

ligible in comparison with the other disposal paths.

China accounted for 31.05% of waste-related GHG-emissions in 1990, followed by Japan with 28.13%. When combined, South Korea, Saudi Arabia, Thailand, Vietnam and Malaysia accounted for 28.70% in 1990. In 2016, China was still accountable for 35.52% of the released GHG-emissions in the waste sector, while Japan only contributed 15.75% and the five smaller states 35.98%.

The GHG-emissions in the waste sector of the selected Asian countries increased between 1990 and 2016 by 95.2 million Mg CO_2-eq./a or approx. 76.53%.

3.4 Summary

3.4.1 Selected parties

The disposal path responsible for the largest amount of released GHG-emissions in the waste sector is for the majority of the observed countries disposal of waste on landfills or dumpsites. Germany and Japan are the exception by having the incineration of waste as the greatest source of released GHG-emissions. Even though Canada, the United States, and China are reporting about released GHG-emissions through waste incineration, those amounts are much smaller compared to emissions caused through the disposal of waste within each respective country. In Russia, India and Brazil, nearly all released GHG-emissions in the waste sector can be traced back to the disposal of waste on landfills and dumpsites. Figure 16 shows the GHG-emissions caused in the waste sectors of the observed countries in the base year (1990 for Annex I parties and Brazil, 1994 for China and India) and the year with the latest available data (2016 for Annex I parties, 2010 for Brazil, 2012 for China and 2014 for India). In addition to the total values, Figure 16 also shows the GHG-emissions converted to "per capita" values for each country in the respective year.

The United States is the leading contributor of GHG-emissions in the waste sector in the base year, as

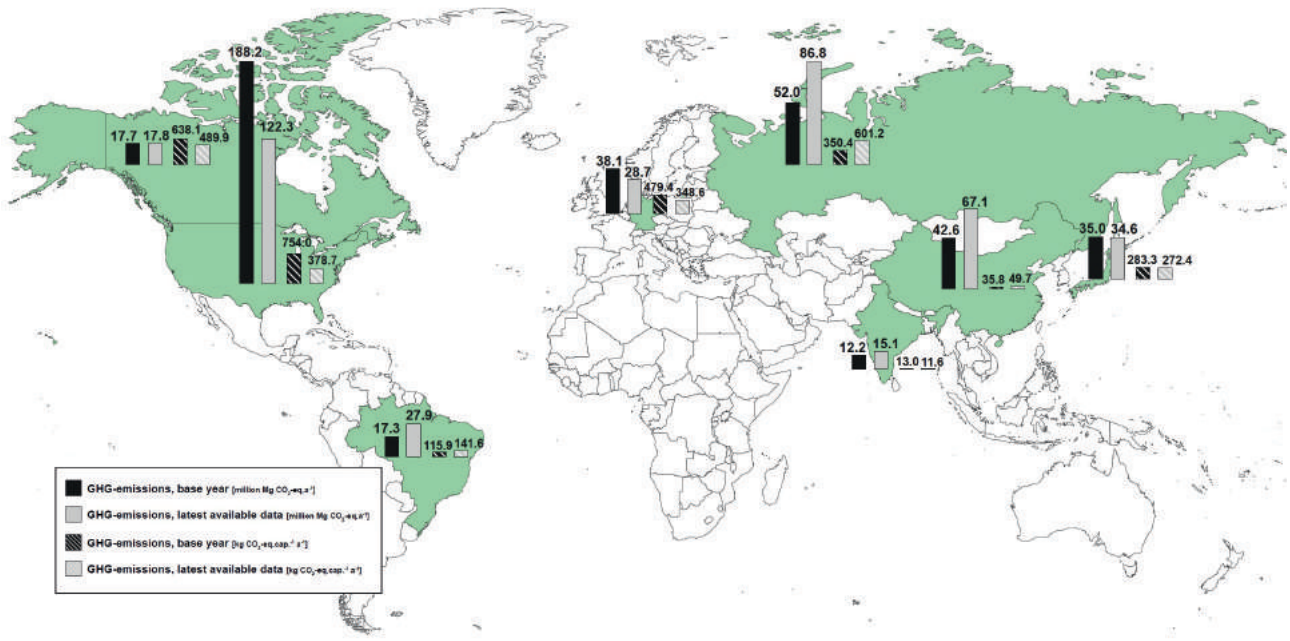

FIGURE 16: Greenhouse gas emissions released by the waste sector in the observed countries in the base year and the year with the latest available data (own figure derived from UNFCCC, 2019).

well as the year with the latest available data; followed by the Russian Federation and China. While only one of the five observed Annex I parties (the Russian Federation) showed a clear increase in waste-related GHG-emissions, two others (Canada and Japan) remained almost constant and another two (Germany and the United States) showed a clear decrease over the observed period. Meanwhile the GHG-emissions in the waste sectors of all three observed non-Annex I parties clearly changed for the worse.

Interestingly, the GHG-emissions per capita give another picture. With the very sizeable population of the observed non-Annex I parties, their GHG-emissions per capita are much smaller than those of the Annex I parties. In the year with the latest available data, Brazil accounted for approx. 142 kg CO_2-eq. per capita and year (kg CO_2-eq. cap.$^{-1}$ a^{-1}), China for 50 kg CO_2-eq. cap.$^{-1}$ a^{-1} and India for only 12 kg CO_2-eq. cap.$^{-1}$ a^{-1}. Russia, Canada and the United States released the biggest amounts of GHG-emissions per capita (with approx. 601, 490 and 379 kg CO_2-eq. cap.$^{-1}$ a^{-1} respectively), followed by Germany and Japan (with 349 and 272 kg CO_2-eq. cap.$^{-1}$ a^{-1}.

3.4.2 Selected larger regions

Within the larger regions, positive developments could be observed for the EU (168.4 million Mg CO_2-eq. in 2016) and North America (160.7 million Mg CO_2-eq. in 2016); with the EU's GHG-emissions level being slightly above that of North America in 1990 as well as in 2016. Meanwhile, Russia, Kazakhstan, Ukraine and Uzbekistan (105.4 million Mg CO_2-eq. in 2016) along with the selected Asian countries (219.6 million Mg CO_2-eq. in 2016) showed significant increases in GHG-emissions released in the waste sector, with the selected Asian countries even clearly surpassing both the EU and North America in 2016. Figure 17 shows the GHG-emissions caused in the waste sectors of the observed larger regions in 1990 and 2016. In addition to the total values, Figure 17 shows the GHG-emissions converted to "per capita"-values for each one of the observed larger regions in 1990 and 2016.

By having huge populations, the observed Asian countries have with only approx. 69 kg CO_2-eq. cap.$^{-1}$ a^{-1} in 2016, much lower per-capita emissions than those of the other three larger regions. While Russia, Kazakhstan, Ukraine and Uzbekistan show the greatest amounts of released GHG-emssions per capita in the waste sector in 2016 (approx. 440 kg CO_2-eq. cap.$^{-1}$ a^{-1}), North America and the EU have similar amounts, both being around 330 kg CO_2-eq. cap.$^{-1}$ a^{-1}.

4. DISCUSSION

In a global context (Figures 16 and 17), the GHG-emissions caused through the disposal of waste on landfills and dumpsites clearly seem to be responsible for the largest amount of GHG-emissions released in the waste sector. This is not surprising, since the global warming factor of CH_4 related to CO_2 is 25 and even the best equipped landfills cannot catch all of the generated landfill gas.

In particular, the observed Annex I countries show different approaches and efforts on how to reduce the kinds of emissions from landfills and dumpsites. In Germany the disposal of waste containing biodegradable material on landfills was legally prohibited, which lead to considerably smaller amounts of biodegradable waste (which is a key factor for the amounts of generated landfill gas) ending up on German landfills (Gniffke and Strogies, 2018). Many other European Countries (e.g. Austria, Belgium, Czech Republic, Denmark, Netherlands, United Kingdom) charge landfill taxes for wastes containing biodegradable material

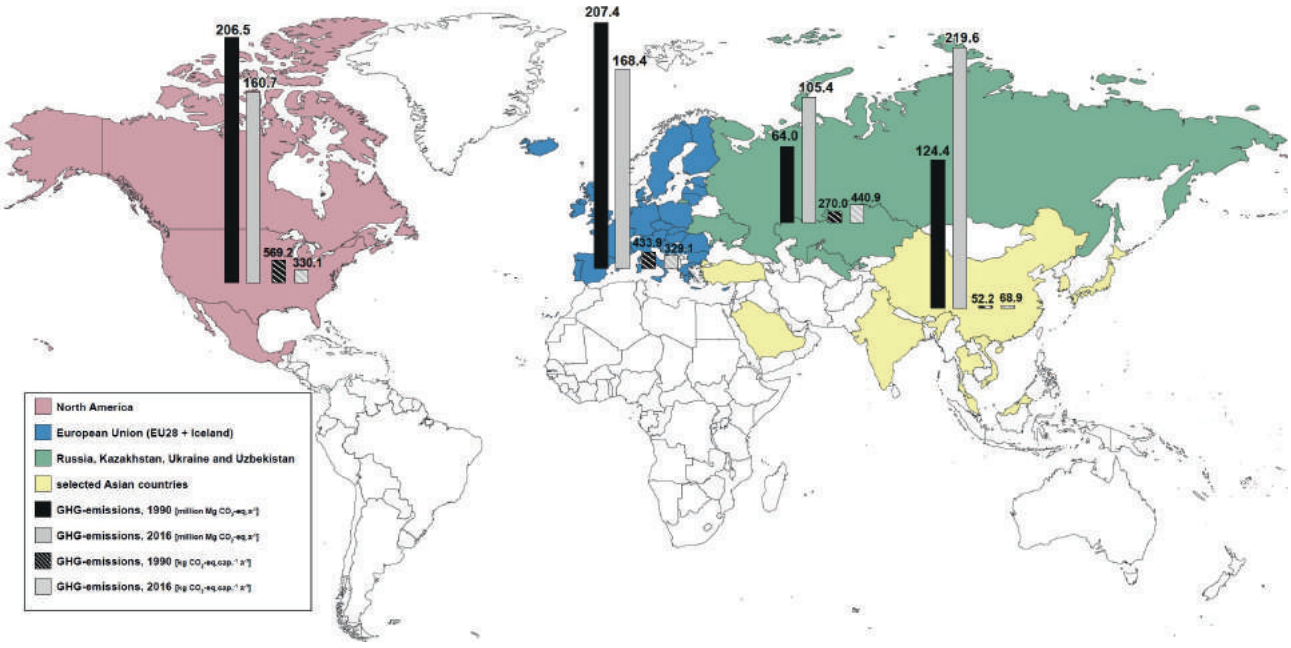

FIGURE 17: Greenhouse gas emissions released by the waste sector in the observed larger regions in 1990 and 2016 (own figure derived from UNFCCC, 2019).

to prevent the disposal of such waste on landfills (Paleari et al., 2012). Although disposing biodegradable material is prohibited (since 2005 in Germany) or strongly reduced by high landfill taxes (in some other European countries), those countries still report landfill-related GHG-emissions, since landfill gas is generated even many years after the deposition of biodegradable material.

Although the reduction of organic material being landfilled seems to be the most promising method to reduce GHG-emissions from landfills, many countries (especially developed ones) try to prevent methane emissions from reaching the atmosphere by installing landfill gas collection systems. Through the installation of horizontal or vertical wells, the generated gas is collected to a certain degree and can either be used to produce energy or just be flared to convert CH_4 to CO_2. However, in many cases (for example in the United States and Canada) only landfills of a certain size must be equipped with this kind of technology, while on smaller landfills without landfill gas collection systems, the generated gas continues to escape into the atmosphere (DOS, 2017) (ECCC, 2017). Meanwhile, in quite a few of the less developed countries, which are struggling with basic problems in their waste sectors (e.g. the non-existence of a nation-wide waste collecting system, often in rural parts of the country), huge amounts of waste are discarded on unorganized dumpsites with no serious efforts to prevent deposition of organic material and a general lack of state of the art technologies, such as landfill gas collection systems (IFC, 2017) (Vogt et al., 2015).

These observations can also be made in the progression of the waste-related GHG-emissions in the different observed countries. The GHG-emissions through landfilling in the United Stated decreased to a lesser extent than in Germany, as the focus in the USA is on collecting and using the generated landfill gas, while Germany prevents the disposal in the first place. On the other hand, emissions of the Russian Federation increased because there are many landfills and dumpsites which are not adequately equipped with state of the art technology.

Municipal solid waste in developed countries contains larger amounts of carbon, which is fixed in plastics, composite materials, textiles and papers, and in lesser amounts as easily bioavailable carbon in food waste. When this waste is disposed on well-managed landfills where the waste is kept relatively dry, bioactivity is reduced, and thus only small amounts of biogenic carbon are converted to landfill gas and larger amounts of carbon are sequestrated in the landfill. When in addition, large quantities of the generated landfill gas are collected and treated, relatively small amounts of GHG-emissions are released to atmosphere. As a result, the performance of well-managed and equipped landfills in terms of GHG-emissions released into the atmosphere can be better than that of the waste incineration process (Wünsch and Bilitewski, 2011). This is also demonstrated by the presented data. In the US, the majority of waste is landfilled and the specific GHG-emissions are around 0.48 Mg CO_2-eq./Mg generated waste for 2015 (126.3 million Mg CO_2-eq./a and 262.4 Mg/a generated (US EPA, 2018)). In Germany, significant amounts of waste are incinerated and the specific GHG-emissions are around 0.56 Mg CO_2-eq./Mg generated waste for 2015 (28,7 million Mg CO_2-eq./a and 51.6 Mg/a generated (BMU, 2018)). However, it must be emphasized that landfills are constructions with limited lifetimes. Someday the surface cover will break and water will penetrate the landfill body. Then the biodegradation of sequestrated organic carbon will immediately start, and landfill gas will be produced and emitted into atmosphere.

Even though the amount of GHG-emissions released through incineration of waste in a global context is still relatively small compared to that released by landfilling, incinceration became more and more popular over the last decades (especially in developed countries) and therefore was responsible for increasing amounts of released GHG-emissions. In Germany and Japan it even represents the disposal path with the largest amount of GHG-emissions. However, it should be noted, that GHG-emissions caused through landfilling and through waste incineration should not be evaluated the same way, since the incineration of waste has the key advantage of being able to use the energy content of not only the biological but also fossil bound carbon, while during landfilling only the biologically bound part of the carbon can be used (and that only if the necessary technology is available). In addition, landfilling comes with the disadvantage of only being able to produce energy from the amount of landfill gas that is effectively captured, while there is always a portion of non-collected gas which escapes into the atmosphere. This means that even if both disposal paths under certain circumstances are able to produce energy, in the end, incineration of waste proves to be the more effective and thus more sustainable method of waste treatment.

The increase of emissions from biological waste treatment is a result of more treated biodegradable waste and the implementation of more and more biogas plants for the anaerobic treatment of biowaste. GHG-emissions from biological waste treatment originate from fugitive CH_4 and N_2O. Small amounts of CH_4 are emitted when anaerobic conditions occur while the composting process takes place in open windrows without collecting and treating occurring emissions. CH_4 is also released during anerobic digestion; e. g. during the entry and exit of material in the digester or when the digestate is transferred from the digesters to the digestate storage. (Cuhls et al., 2015) N_2O can be emitted from biofilters (Jensen et al., 2017). Since the specific GHG-emissions per Mg of treated biodegradable material are relatively low, the total emissions are also low; even when considerable amounts of biodegradable waste are biologically treated.

Finally, it should be pointed out once more that the increase in GHG-emissions in non-Annex I states is also due to better quality and more well-registrated waste disposal sites (especially in rural areas), as well as the consideration of the corresponding emissions in recent reports.

5. CONCLUSIONS

The development of direct GHG-emissions among various contries and larger regions differs strongly dependening on national or regional economic status. Industrial countries and regions implement technical and organisational measures to reduce their GHG-emissions in the waste management sector, whereas developing and emerging countries generate more and more waste, which is in most cases simply dumped on dumpsites or on landfills equipped with inferior technology. However, the per capita GHG-emissions in particular show that there is still a wide range between approx. 500 kg CO_2-eq./a for developed contries/regions and much less than 100 kg CO_2-eq./a for developing and emerging countries.

Examples of developed states/regions show that a reduction of GHG-emissions in the waste sector is possible with the implementation of well-managed and equipped landfills, which keep the landfill body dry and collect and treat most of the generated landfill gas. The problem with this waste management practice is the sequestration of organic carbon and the resulting greenhouse gases generated and then emitted in the future when the landfill cover construction breaks, water penetrates in the landfill, and micro organisms start decomposing organic material. Similar or even better results can be gained when landfill bans or high landfill taxes for biodegradable materials are implemented, and more waste is incinerated or otherwise thermally treated.

A shift to separate collection and treatment of different waste types, especially biowaste, brings the best results in terms of GHG-emissions reduction in the waste sector.

Finally, it should be highlighted that by recovering energy (especially by thermal waste treatment) and secondary raw materials (through separate waste collection and treatment), significant amounts of GHG-emissions can be avoided (e.g. Wünsch and Simon, 2018; Bilitewski and Wünsch, 2017; Dehoust et al., 2010). This is due to the substitution of energy, which is usually at least partly generated out of fossil fuels, and the substitution of primary raw materials. Their extraction is usually much more energy extensive than the production of secondary raw materials from waste.

REFERENCES

Abu Qdais, H., Wünsch, C., Dornack, C., & Nassour, A. (2019). The Role of Solid Waste Composting in Mitigating Climate Change in Jordan. in Waste Management & Research, 1–10, June 2019, doi. org/10.1177/0734242X19855424

Bilitewski, B. & Wünsch, C. (2017). WTE, Greenhouse Gas Benefits. in Encyclopedia of Sustainability Science and Technology, Meyers, Robert A. (ed.), ISBN 978-1-4939-2493-6

BMU (2018) Waste Management in Germany 2018 - Facts, data, diagrams. Bundesministerium für Umwelt, Naturschutz und nukleare Sicherheit, Berlin, Germany

Cuhls, C., Mähl, B., & Clemens, J. (2015). Ermittlung der Emissionssituation bei der Verwertung von Bioabfällen, Texte 39/2015, Umweltbundesamtes, Dessau-Roßlau, Germany

Dehoust G., Schüler, D., Vogt, R., & Giegrich, J. (2010). Climate Protection Potential in the Waste Management Sector Examples: Municipal Waste and Waste Wood. Texte 61/2010, Umweltbundesamt, Dessau Roßlau, Germany

DOS (2017). United States Department of State (DOS). United States Climate Action Report 2014 (First Biennial Report and Sixth National Communication of the United States of America under the United Nations Framework Convention on Climate Change)

ECCC (2017). Canada's Seventh National Communication on Climate Change and Third Biennial Report – Actions to meet commitments under the United Nations Framework Convention on Climate Change. Evironment and Climate Change Canada (ECCC). Gatineau, ISBN 978-0-660-23785-5

EUROSTAT (2010). Using official statistics to calculate greenhouse gas emissions – A statistical guide. Baudouin, L., Fernandez, R., Gikas, A., Hass, J., Janowska A., Kitou, E., Moll, S., Mozes, C., Noreland, J., Piirto, J., Enescu, R., Nikolaos, R., Tavoularidis P. and Wieland, U. (eds.). ISBN 978-92-79-14487-5

Gniffke, P., & Strogies, M. (2018). National Inventory Report for the German Greenhouse Gas Inventory 1990 – 2016. Climate Change 12/2018, Umweltbundesamt, Dessau-Roßlau, Germany

IFC (2017). Municipal Solid Waste Management: Opportunities for Russia. International Finance Cooperation, World Bank Group. Moscow/Washington

IPCC (2006). 2006 IPCC Guidelines for National Greenhouse Gas Inventories, Prepared by the National Greenhouse Gas Inventories Programme, Eggleston H.S., Buendia L., Miwa K., Ngara T. and Tanabe K. (eds.). Published: IGES, Japan, ISBN 4-88788-032-4

IPCC (2007). Mitigation. Contribution of Working Group III to the Fourth Assessment Report of the Intergovernmental Panel on Climate Change. B. Metz, O.R. Davidson, P.R. Bosch, R. Dave, L.A. Meyer (eds.), Cambridge University Press

Jensen, M. T., Moeller, J., Moenster, J., & Scheutz, C. (2017). Quantification of greenhouse gas emissions from a biological waste treatment facility. Waste Management Volume 67,375-384. https//doi.org/10.1016/j.wasman.2017.05.033

Kanunnikova, T. (2016). Five incineration plants to be built in the Moscow region and Tatarstan by 2025. In Construction Russian online Journal

Kling, M., Baldauf, M., Böttger, S., & Nöh, C. (2018). Länderprofil zur Kreislauf- und Wasserwirtschaft in Brasilien. uve GmbH für Managementberatung in cooperation with German RETech Partnership and German Water Partnership (eds.). Berlin, Germany

Li, X., Zhang, C., Li, Y., Zhi, Q. (2016). The Status of Municipal Waste Incineration (MSWI) in China and its Clean Development. in Energy Procedia, Volume 104, 498-503. https://doi.org/10.1016/j.egypro.2016.12.084 Modak, P., Pariatamby, A., Saedon, J., Bhada-Tata, P., Borongan, G., Thawn, N., & Lim, B. (2017). ASIA Waste Management Outlook. United Nations Environment Programme, Economy Division, International Environmental Technology Centre

Nelles, M., Dorn, T., Wang, Y., Xu, A., & Morschek, G. (2015). State of waste management in the PR China. In Müll und Abfall Journal 4/2015, Berlin, Germany

Nojiri, Y., Hatanaka, E., Oda, T., Osako, A., Ito, H. Kosaka, N., Yanagawa, M., Hayashi, A., Tanaka, A., & Yoshinaga, H. (2018). National Greenhouse Gas Inventory Report of Japan 2018. National Institute for Environmental Studies. Tsubuka, Japan

Paleari, S., Fischer, C., Junker, H, Mazzanti, M., Wuttke, J., & Zoboli, R. (2012). Transboundary shipments of waste in the European Union. Reflections on data, environmental impacts and drivers

Skryhan, H., Shilova, I., Khandogina, O., Abashyna, K., & Chernikova, O. (2018). Waste Management in Post-Soviet Countries: How far from the EU?. in detritus – Multidisciplinary Journal for Waste, Resources & Residues, Volume 03 – 2018

UN (1992). United Nations Framework Convention on Climate Change. FCCC/INFORMAL/84. GE.05-62220 (E) 200705.

UNFCCC (2006). United Nations Framework Convention on Climate Change: Handbook. Produced by Intergovernmental and Legal Affairs, Climate Change Secretariat. Blobel, D., Meyer-Ohlendorf, N., Schlosser, C., Steel, P. (eds). ISBN: 92-9219-031-8, Bonn, Germany,

UNFCC (2014). Report of the Conference of the Parties on its nineteenth session - Addendum - Part two: Action taken by the Conference of the Parties at its nineteenth session

US EPA (2018) National Overview: Facts and Figures on Materials, Wastes and Recycling. https://www.epa.gov/facts-and-figures-about-materials-waste-and-recycling/national-overview-facts-and-figures-materials (accessed September 2019)

Vaccani A. & Asato S. (2014). Internationale Märkte für alternative Verfahren und Strategien der wichtigsten Marktteilnehmer. in Strategie, Planung, Umweltrecht, ISBN 978-3-944310-25-1, Neuruppin, Germany

Vehlow, J., Seifert H., & Eyssen R. (2015). Structural Changes in Japan's Waste Management. In Müll und Abfall Journal 5/2015Berlin, Germany

Vogt., R., Dehoust, G., Merz, C., Radde, C., Sieck, M., & Schwetje, A. (2015). Climate protection potential of waste management, Part 2 – India and Egypt. In Müll und Abfall Journal 6/2015, Berlin, Germany

WRI 2017. CAIT Climate Data Explorer. 2017. Washington, DC: World Resources Institute.

Wünsch, C. & Bilitewski B. (2011). Comparison of greenhouse galances between dumping, sanitary landfilling and incineration of resisual waste. in Proceedings SARDINIA 2011 Symposium: "XIII International Waste Management and Landfill Symposium", ISBN 9788862650007, S. Margherita di Pula (Cagliari), Italy

Wünsch, C., & Simon, F.-G. (2018). The Reduction of Greenhouse Gas Emissions Through the Source-Separated Collection of Household Waste in Germany. in The Handbook of Environmental Chemistry, Vol. 63, 269-290, ISBN 978-3-319-69071-1, Heidelberg, Germany

detritus | Multidisciplinary Journal for Waste Resources & Residues

CISA

FUGITIVE METHANE EMISSIONS FROM TWO EXPERIMENTAL BIOCOVERS CONSTRUCTED WITH TROPICAL RESIDUAL SOILS: FIELD STUDY USING A LARGE FLUX CHAMBER

Rafaela Franqueto [1], Alexandre R. Cabral [2], Marlon A. Capanema [3] and Waldir N. Schirmer [4,*]

[1] *Universidade Regional de Blumenau - FURB, Blumenau, Santa Catarina State, 89030-080, Brazil*
[2] *Université de Sherbrooke, Civil and Building Engineering, 2500, boul. de l'Université, Sherbrooke, J1K 2R1 Quebec, Canada*
[3] *Instituto Federal de Educação, Ciência e Tecnologia de Goiás, IF-GO, Goiânia, Goiás State, 74130-012, Brazil*
[4] *Universidade Estadual do Centro-oeste (UNICENTRO), Irati (Paraná State), 84500-000, Brazil*

Article Info:
Received:
17 January 2019
Revised:
6 June 2019
Accepted:
11 September 2019
Available online:
26 September 2019

Keywords:
Passive methane oxidation biocover
Flux chamber
Biogas
Landfill
Municipal solid waste

ABSTRACT

This study aimed at assessing the response of two experimental passive methane oxidation biocovers (PMOB) installed in a Brazilian landfill located in Guarapuava, State of Paraná. The PMOBs covered an area of 18 m² each, and were 0.70-m-thick. The first PMOB (control subarea) was constructed using the same soil used to cover closed landfill cells, i.e. a typical residual soil. The second PMOB (enriched subarea) was constructed with a mixture of the residual soil and mature compost, with a resulting organic matter content equal to 4.5%. CH_4 and CO_2 surface fluxes were measured in a relatively large (4.5 m²) static chamber. CH_4, CO_2 and O_2 concentrations were also measured at different depths (0.10, 0.20, 0.25 and 0.30 m) within PMOBs. The concentrations from the raw biogas were also measured. Methane oxidation efficiencies (Eff_{ox}) were estimated based on the CO_2/CH_4 ratio. The average CH_4 and CO_2 concentrations in the raw biogas (42% and 32%, respectively) for the 16 campaigns corroborated those typically found in Brazilian landfills. Lower CH_4 fluxes were obtained within the enriched subarea (average of 20 $g.m^{-2}.d^{-1}$), while the fluxes in the control subarea averaged 34 $g.m^{-2}.d^{-1}$. Eff_{ox} values averaged 42% for the control subarea and 80% for the enriched one. The results indicate that there is a great potential to reduce landfill gas (LFG) emissions by using passive methane oxidation biosystems composed of enriched substrates (with a higher content of organic matter).

1. INTRODUCTION

In Brazilian municipal solid waste (MSW) landfills, where there is no any biogas active recovery system in most of them, a common practice to reduce biogas emissions is to install a vertical drain – usually constructed with very coarse gravel – and flare it. These drains, which are often operated manually, are submitted to the large settlements that usually take place in landfills. Consequently, the integrity of the usually poorly maintained drains is negatively affected, reducing their capacity to drain landfill gas (LFG). In addition, Brazilian landfill covers are often constructed with readily available materials, which are placed in one single layer. Considering these premises, it can be expected that a significant proportion of the generated LFG migrates through the cover system in the form of fugitive emissions (Maciel and Jucá, 2011).

Several studies have shown that a passive biosystem (where the biogas passes through the cover naturally, without pumping it) installed in the cover system (interim or final) can be a very effective complement to active systems in reducing fugitive emissions of methane and odorous substances (Abichou et al., 2006a; Cabral et al., 2010a; Capanema et al., 2013; Capanema et al., 2014; Geck et al., 2016; Lucernoni et al., 2016; Roncato and Cabral, 2012; Sadasivam and Reddy, 2014; Scheutz et al., 2009). Most of these studies documented the performance of passive biosystems in temperate climates, while (to the authors' knowledge) no field-scale studies have been performed to document the performance of passive biosystems in Brazil (a tropical country) and employing residual soils. Such passive systems are in great need in developing countries due to the almost complete absence of active systems.

Documentation of methane, odorous substances and organic compound emissions has often relied on the use of flux chambers that cover surfaces lower than 1.0 m² (Abichou et al., 2006a,b; Gallego et al., 2014; Hudson and Ayoko, 2008; Scheutz et al., 2009; Trégourès et al., 1999). The low cost and simplicity of the static chamber

* Corresponding author:
Waldir Nagel Schirmer
email: wanasch@hotmail.com

https://doi.org/10.31025/2611-4135/2019.13844
© 2019 Cisa Publisher. Open access article under CC BY-NC-ND license

method resulted in its widespread use. However, given the fact that fugitive emissions are often concentrated in cracks that cover very small subareas (e.g. Geck et al., 2016; Rachor et al., 2011; Rachor et al., 2013), in addition to varying strongly in time, chances are that concentrated fluxes in these cracks will be missed during emissions assessments using small flux chambers. According to Geck et al. (2016), extrapolation of total emissions from measurements performed with small flux chambers can be questionable.

The present study documented the response of two experimental passive methane oxidation biosystems (PMOBs) installed in a Brazilian landfill where biogas is vented out passively. The landfill is located in the sub-tropical subarea of central Paraná, a southern state. The first PMOB (control) was constructed with the same residual soil that has been employed as both interim and final cover by the landfill operator. The other PMOB was constructed with this same soil after being enriched with organic-matter-rich compost. This study focused on the capacity of the two PMOBs to oxidize methane and on the magnitude of surface emissions. Oxidation efficiency was assessed by means of the CO_2 to CH_4 ratio along several gas profiles (Gebert et al., 2011a).

For this study, we designed and constructed a low-cost and easy-to-build large-scale chamber. Table 1 presents the characteristics of several flux chambers used in recently reported studies about landfill biogas emissions. Flux chambers with surfaces up to 17.7 m² and 880-L volume have been reported. Ideally, according to Rochette and Eriksen-Hamel (2008), the surface covered by the chamber and its volume should be proposed as a function of flux intensity (or biogas loading). Given the fact that the PMOBs were installed directly over the waste mass, and we did not have access to flux intensity data, our design was based on the largest possible chamber we could build and carry.

1.1 Abbreviations

AVG: Average
Eff_{ox}: Methane oxidation efficiencies
f: Biogas mass flux
FID: Flame ionization detector
GC: Gas chromatography
LFG: Landfill gas
MSW: Municipal solid waste
OM: Organic matter
PMOB: Passive methane oxidation biocover
STP: Standard temperature and pressure
TCD: Thermal conductivity detector
TOC: Total organic carbon

2. MATERIAL AND METHODS

2.1 Characterization of the study area and the cover soil

This study was carried out in a landfill located in Guarapuava, a city located in the south-central region of the State of Paraná (Brazil). This landfill has been used to dispose of non-hazardous municipal solid wastes (MSW). The authors selected a region within the landfill as flat as possible and as far away as possible from vertical drains, in order to avoid preferential pathways of the biogas to these drains, cracks on the surfaces and ensure that CH_4 was present in measurable concentrations at the surface. The cover in the selected area had been placed 4.5 years before beginning of our experiments. Chamber measurements were then performed to assess CH_4 emissions.

Within this area, two 18 m² subareas were delimited: one called the "control subarea" and the other "enriched subarea" (with compost), covered by a 0.70-m-thick residual soil layer. The spacing between each subarea was 1.0 m. The cover soil in the control subarea was the same as else-

TABLE 1: Shapes and sizes of flux chambers reported in the literature.

Shape of the chamber	Dimensions (m)		Surface (m²)	Volume (L)	Flux $g.m^{-2}.d^{-1}$	References
	Base	Height				
Rectangular	0.65	0.28	0.42	120	N.R.[1]	Chanton and Liptay (2000)
Rectangular	0.63	0.20	0.40	80	330 – 596 18.1– 117.5 Chanton et al. (2011) N.R[1]	Abichou et al. (2006b); Stern et al. (2007); Chanton et al. (2011)
Rectangular	1.80 (L) x 1.20 (W)	0.25	2.10	504	330-596 (maximum values) 18.1-117.5 (mean values) Chanton et al. (2011) N.R[1]	Capanema et al. (2013), Lakhouit et al. (2014)
Rectangular	1.22 (L) x 0.76 (W)	0.25	0.93	241	N.R.*	Capanema et al. (2014)
Quadratic	N.R.[1]	N.R.[1]	1.00	50	5.0 – 389.2	Araujo and Ritter (2016)
Quadratic	0.50 (L and W)	0.10	0.25	25	N.R.[1]	Lucernoni et al. (2016)
Quadratic	0.40 (L and W)	0.05	0.16	0.008	N.R.[1]	Monteiro et al. (2016)
Quadratic	4.2 (L and W)	0.50	17.7	880	0.98-6.69	Geck et al. (2016)
Rectangular	3.00 (L) x 1.5 (W)[2]	0.2	4.50	900		This study

[1] N.R.: not reported; [2] divided into 2 sections for ease of transportation. The sections are assembled on site.

where in the site (sandy clayey silt, 86.3% sieved through a 200-Mesh sieve); its average organic matter content is equal to 0.4%. In the enriched subarea, the uppermost 0.15 m of soil was substituted by a mixture of the mature compost (originally with 32% organic matter content) and the same natural soil, resulting in a substrate with 81.4% sieved through a 200-Mesh sieve and an organic matter content equal to 4.5%. The intention was to foster bacterial growth and assess addition of nutrients in order to improve passive methane oxidation. The pH of the soil (~6.6 for the control subarea; and 7.1 for the enriched subarea) varied very little throughout the study period. It can therefore be assumed that pH would not constitute a limiting parameter in this study. Moreover, it is known that methane-oxidizing bacteria perform better in pH near to neutrality (Delhomenie and Heitz, 2005).

The Atterberg limits determined for the control subarea were: Liquidity limit = 51%, Plasticity limit = 36%; and the Plasticity Index was 15%. The values found for the enriched subarea were: Liquidity limit = 51%, Plasticity limit = 36%; and the Plasticity Index was 16%. For the control subarea, the Standard Proctor's optimum moisture was 29.6% for a maximum dry density equal to 1.47 g/cm³, whereas the respective values for the enriched subarea were 35.6% and 1.39 g/cm³.

2.2 Characterization of raw biogas

Assessment of the characteristics of the raw biogas was performed by installing raw biogas pipes in each of the two subareas. Stainless steel pipes with a diameter of 10 mm were buried at a depth of 1.0 m in order to reach the interior of the waste mass. Once it was not possible to measure the loading rate or even the flow rate of biogas through the biocovers, the raw biogas concentration was the only parameter monitored, in order to determine the oxidation efficiency of the cover layer in both of the evaluated subareas.

The concentration of the main gases that compose the raw biogas was determined with the aid of a Columbus portable gas analyzer (Columbus Instruments Inc.) equipped with infrared sensors for detecting CO_2 and CH_4 in a range of 0-100 vol.%, and coupled to an electrochemical sensor for detecting O_2 between 0-21 vol.%. The measurement accuracy for methane and carbon dioxide is about 2% and 1% of the value read for oxygen. The biogas was sampled from the pipes using a 60-mL syringe and injected into the gas analyzer. N_2 concentrations were calculated by subtracting the sum of CO_2, CH_4 and O_2 concentrations from 100% (simplifying assumption).

2.3 Assessment of surface emissions using the large flux chamber

2.3.1 Flux chamber specifications

A flux chamber was built in a similar way to those used by Capanema et al. (2013) and Lakhouit et al. (2014); as shown in Figure 1a. It covers an area equal to 4.5 m² with a total internal volume equal to 0.9 m³.

A fishbone-shaped system with perforated copper piping was installed in the interior part of the flux chamber, in order to capture the gas from all points inside the chamber, directing them to the exit point (sampling point - Figure 1b). The frame (onto which the cover of the flux chamber rested) was inserted at 0.15 m depth and sealed with bentonite, as recommended by Capanema et al. (2014). The top of the frame had a groove where the water was poured to prevent the entry of atmospheric air during flux measurements. Each subarea had its own fixed frame.

Inside the chamber, two small battery-operated fans were installed to ensure homogenization of the emitted biogas, according to the field recommendations applied

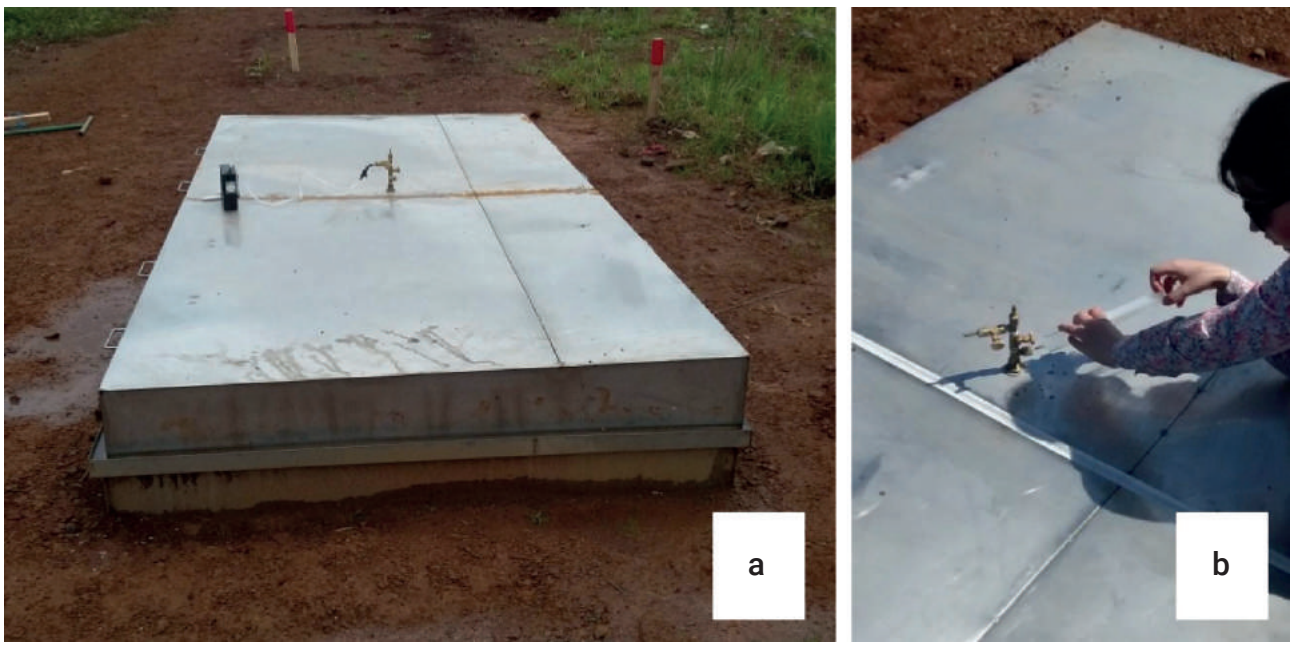

FIGURE 1: Biogas samplings: (a) flux chamber; (b) biogas sampling point.

by Abichou et al. (2006b), Scheutz et al. (2014) and Stern et al. (2007). A mercury thermometer was also installed to measure the temperature variation inside the chamber, and thus determine the biogas concentrations according to the standard temperature and pressure (STP).

Water content probes (ECH_2O CE-5 sensor, Decagon, Pullman, USA) were installed at 0.15 m below surface in both subareas to determine the soil water content. All samples were collected respecting at least two days between the last precipitation and the sampling campaign. However, there were intense rains in the days leading up to some campaigns, considerably increasing the soil moisture content. Precipitation and atmospheric pressure data were obtained from the Weather System of Parana State database, because site-specific data was not available.

2.3.2 Sampling and analysis of CH_4 and CO_2 emissions

Sixteen campaigns were carried out to determine CH_4 and CO_2 fluxes using the chamber. Emitted biogas samples were collected at 2-minute intervals using a 60 mL syringe (Figure 1b). All samples were collected within one hour, as suggested by the UK Environment Agency (2010).

The samples were inserted into 30 mL glass vials that had been previously placed under vacuum, and then sealed with a septum "crimp" (Du et al., 2006; Jantalia et al., 2008). They were subsequently analyzed by GC-flame ionization-thermal conductivity using a Shimadzu FID-TCD, equipped with a 5-m long Carboxen 1000 packed column (60/80 mesh). The main testing parameters are as follows: oven heating ramp: 40°C (6 min); heating rate: 20°C/min up to 220°C; carrier gas: argon. Gas chromatography analysis were only required for methane concentrations below 1% (below the Columbus detection limit).

2.3.3 Surface methane mass flux calculations

Biogas mass fluxes at the surface were calculated based on the results obtained using Equation 1 (according to Cabral et al., 2010a and Perera et al., 2002), corrected for the standard temperature and pressure (STP).

$$f=(V/A)\times(\Delta C/\Delta t)\times(273{,}15/(273{,}15+T_{int}))\times(P_{atm}/1013) \quad (1)$$

where: V = internal volume of the flux chamber (m^3); A = cover layer area of the chamber (m^2); $\Delta C/\Delta t$ = represents the slope of the plot relating the change in gas concentration to time ($mg.m^{-3}.s^{-1}$); T_{int} = internal temperature of the gas in the chamber (°C); P_{atm} = atmospheric pressure (mbar).

2.4 Vertical concentration profiles of biogas

2.4.1 Installation of the gas probes

Five nests of stainless steel gas probes were placed in each subarea, as shown in Figure 2. In each nest, the 10-mm (internal diameter) gas probes were inserted using a metal auger to desired position (0.10, 0.20, 0.25 and 0.30 m) below the surface, following the methodology described by Cabral et al. (2010a). After insertion, the upper ends were capped with a rubber septum.

2.4.2 Determining gas concentrations

Concomitantly with the 16 flux measurements, campaigns were also performed for determining the gas concentrations along the cover layer of the two evaluated subareas. First, each gas probe was purged of the volume of air initially contained therein using a 60 mL syringe. After one hour, a biogas sample was collected and analyzed in the portable gas analyzer "Columbus". Again, gas chromatography analysis were only required for methane concentrations below the Columbus detection limit (≅1%).

2.5 Estimation of methane oxidation efficiency (Eff_{ox}) based on gas profile data

The share of oxidized methane (x) at a certain depth was determined in both subareas, according to Equation 2 (Gebert et al., 2011b).

$$(CO_{2_{LFG}}+x)/(CH_{4_{LFG}}-x)=CO_{2\_i}/CH_{4\_i} \quad (2)$$

where x = share of oxidized CH_4 (vol.%), CH_{4-LFG} = CH_4 concentration of the landfill gas (vol.%), CO_{2-LFG} = CO_2 concentration of the landfill gas (vol.%), CH_{4-i} = CH_4 concentration at depth i (vol.%), CO_{2-i} = CO_2 concentration at depth "i" (vol.%).

The ratio between the percentage of oxidized methane at the depth of 0.10 m and the methane concentration in the raw biogas (CH_4_LFG) determines the methane oxidation efficiency (Eff_{ox}) in % according to Equation (3) (Gebert et al., 2011b). One important hypothesis associated with this method relates to soil respiration. The amount of CO_2 produced by soil respiration needs to be negligible compared to the CO_2 produced due to methane oxidation (Geck et al., 2016). It is assumed herein that respiration is negligible. We base this assumption on results presented by Gebert et al. (2011b), who found, in a batch experiment using soil with total organic carbon (TOC) 4.9%-7.5%, that

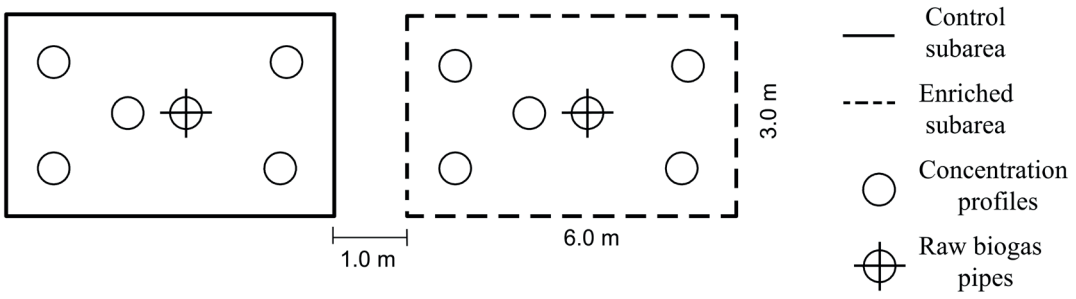

FIGURE 2: Concentration profiles of the subareas (enriched and control).

CO_2 respiration accounted for less than 2% of the observed CO_2 production. In the same study, the oxidation efficiency was only slightly overestimated when a soil with 6% organic matter was tested.

$$Eff_{ox} = (x/CH_{4_{LFG}})\ x\ 100 \quad (3)$$

where x = share of oxidized CH_4 (vol.%), CH_{4-LFG} = methane concentration in the landfill gas (vol.%).

3. RESULTS AND DISCUSSION

3.1 Raw biogas characterization

The concentration values of CH_4, CO_2 and O_2 in the raw biogas are shown in Figure 3. Raw biogas samples were collected at a depth of 1.0 m below the surface. The average (AVG) CH_4 concentration in the raw biogas for the 16 campaigns was 42% (with standard deviation, σ equal to ±4.49%). For CO_2, the AVG concentration was 32% (σ=±2.53). The concentration ranges in Figure 3 are typical of Brazilian landfills (Audibert and Fernandes, 2013; Candiani et al., 2011). The presence of O_2 in the waste is not a surprise. Despite near optimal conditions for accelerated waste degradation, cover systems in most landfills in Brazil (and in the developing world) are often composed of a single layer of soil; cracks can be formed during dry periods, thereby allowing penetration of atmospheric air. In fact, O_2 penetration has been documented for landfills in several subareas of the globe, including the UK (Barry et al., 2003), Iceland (Kjeld et al., 2014), Australia (Obersky et al., 2018) and Brazil (Audibert and Fernandes, 2013).

3.2 Evaluation of the surface emissions

Surface methane mass flux and soil temperatures (at 0.10 m depth) throughout the 16 campaigns and in each subarea are shown in Figure 4.

Methane fluxes in the control subarea ranged between 0 and 53 $g.m^{-2}.d^{-1}$ (AVG=34 $g.m^{-2}.d^{-1}$ and σ=±13.5), whereas methane fluxes in the enriched subarea varied between 0 and 49 $g.m^{-2}.d^{-1}$ (AVG=20 $g.m^{-2}.d^{-1}$ and σ=±15.3). On Feb 22nd, the soil was too wet and there was no noticeable

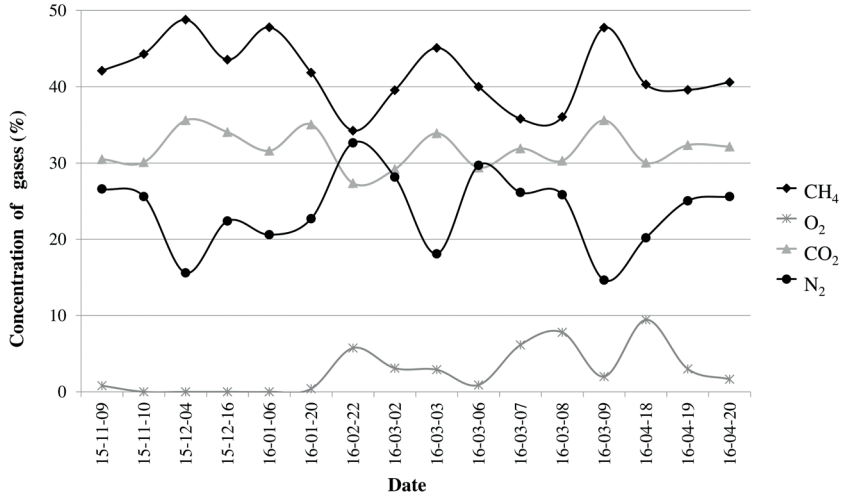

FIGURE 3: Average concentration of raw biogas throughout the 16 campaigns.

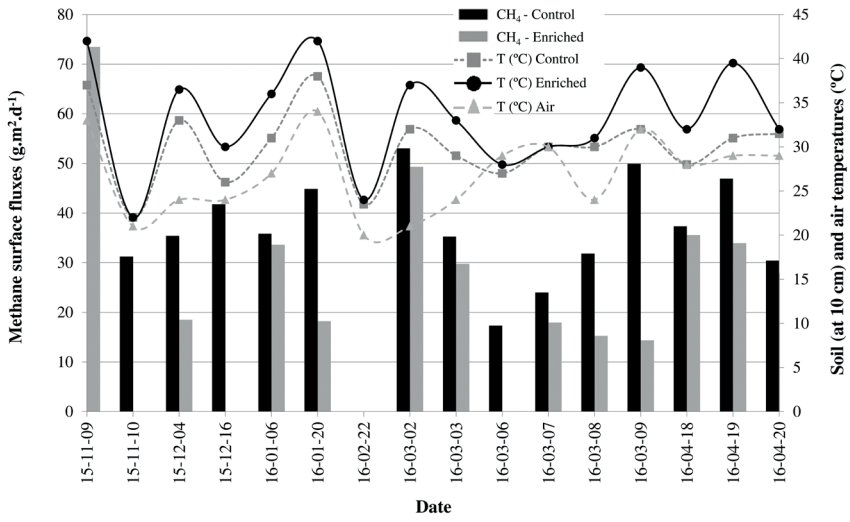

FIGURE 4: Surface methane mass fluxes ($g.m^{-2}.d^{-1}$), air and soil temperatures for both subareas.

increase in gas concentrations inside the flux chamber over several hours. Consequently, fluxes were considered equal to zero in both zones for this particular date. It is noteworthy that CH_4 fluxes in the enriched subarea were always lower or much lower than in the control subarea, with the exception of the first field campaign (on Nov. 9th, 2015) in the enriched subarea, when the microorganisms were probably acclimatizing and adapting to the environment.

Abichou et al. (2009) also compared an organic-rich biocover with an organic-poor cover and observed much lower CH_4 fluxes from the organic-rich biocover. The slightly lower average methane flux on the surface of the compost-enriched subarea may be associated with the greater organic matter content, which created better conditions for the development of ubiquitous methanotrophic bacteria (Humer and Lechner, 2001). An in-depth study using modern microbiology analysis tools could not be performed to confirm the preceding assertion.

The air temperature varied between 20 and 33°C during the 16 campaigns, while inside the interim cover soils temperatures varied between 22 and 38°C (control) and between 22 and 42°C (enriched), respectively. The higher soil temperatures within the enriched subarea (Figure 4) probably resulted from more intense microbial activity. Carbon dioxide mass fluxes are shown in Figure 5.

In the control subarea, CO_2 fluxes vary between 33 and 721 $g.m^{-2}.d^{-1}$ (AVG=251 $g.m^{-2}.d^{-1}$; σ=±168), while in the enriched subarea they vary between 0 and 794 $g.m^{-2}.d^{-1}$ (AVG=316 $g.m^{-2}.d^{-1}$; σ=±245). Fernandes (2009) reported CO_2 fluxes in Brazilians landfills between 0 and 388 $g.m^{-2}.d^{-1}$, and between 29 and 233 $g.m^{-2}.d^{-1}$ for conventional and enriched (soils), respectively.

The carbon dioxide surface flux is higher than the methane flux in the enriched area for most of the assays (e.g. data from January 20th and March 9th, 2016 in Figure 4 and Figure 5), highlighting the higher conversion of methane to carbon dioxide and water. A similar trend was reported by Christophersen et al. (2001), who found carbon dioxide emissions of 90 $g.m^{-2}.d^{-1}$, slightly higher than those found for methane (75 $g.m^{-2}.d^{-1}$). Scheutz et al. (2011) verified this increase in carbon dioxide emission in lysimeters with mature and stable compost.

Despite CH_4 emissions being considered equal to zero on Feb. 22nd, 2016, due to wet conditions, CO_2 concentration increases were measurable in the two zones for this same date. It can only be speculated that minimal soil respiration near the surface led to these non-zero values.

3.3 Vertical profiles of biogas

An average of the biogas composition for all set of gas probes along vertical profiles in the first 30 cm of the cover layer for both control (Figure 6a) and enriched (Figure 6b) subareas are presented.

The fact that the CH_4 and CO_2 curves cross at different depths (0.13 m for control subarea – Figure 6a - and 0.23 m for enriched subarea – Figure 6b) indicates a previous methane oxidation in the enriched subarea and, therefore, a highest capacity of oxidation of this substrate.

Figure 6 also shows that oxygen was present throughout the profile. The average percentage of oxygen remained between 12.4% (control subarea) and 13.9% (enriched subarea). According to Czepiel et al. (1996); Gebert et al. (2003); Jugnia et al. (2008), an oxygen concentration >3% is sufficient for the oxidation reaction. Therefore, oxygen was never a limiting parameter for methanotrophic activity. In addition, it can be observed that O_2 concentrations decreased in the profile due to soil retention and microbial methane oxidation.

The degrees of saturation were calculated using volumetric data of water content. The degree of saturation is between 71% (control area) and 80% (enriched area). According to Huber-Humer and Lechner (2003), the ideal degree of saturation for methanotrophic activity is between 40 and 80%. The degrees of saturation always remained lower than 85%, which approximately corresponds to the

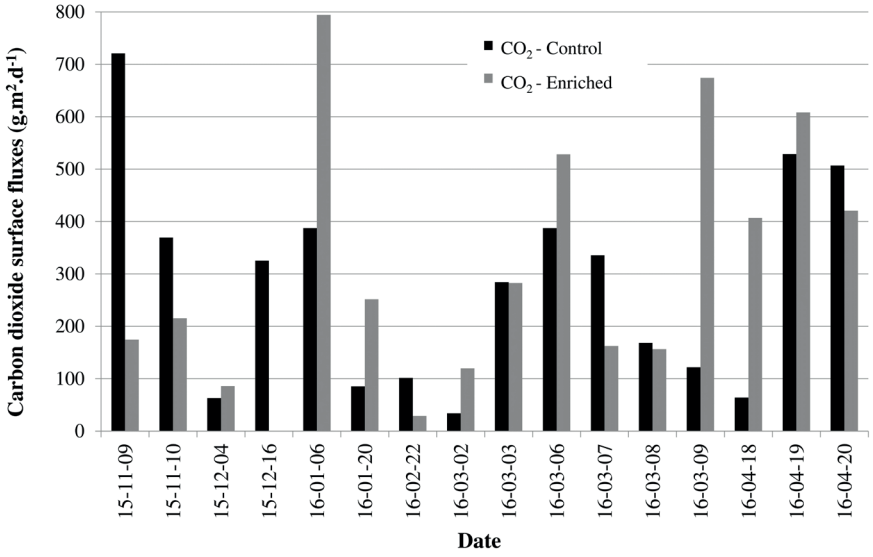

FIGURE 5: Surface carbon dioxide mass fluxes ($g.m^{-2}.d^{-1}$) for both subareas.

degree of saturation value beyond which air becomes occluded in the pores of fine grained soils (Nagaraj et al., 2006), such as the one used to construct the experimental covers. Consequently, with the exception of the near-zero CH_4 flow observed on Feb 22nd, no impedance to flow was observed. It is also worth pointing out that when soil moisture content increases (as observed on Feb 22nd), the upward flow of CH_4 and the downward flow of O_2 in the oxidation layer become limited to diffusion in the liquid phase, delaying the oxidation process (Cabral et al., 2010b).

3.4 Methane oxidation efficiencies

Figure 7 presents the average oxidation efficiencies of methane (Eff_{ox}) for the control and enriched subareas, calculated by Equation (3).

Figure 7 shows that the methane oxidation capacity varied over time and was affected by the type of material constituting the cover soil. Indeed, the methane oxidation efficiencies of the enriched subarea were always higher than in the control subarea. The mean efficiencies of methane oxidation at 0.10 m were 42% (±1.56%) and 80% (±1.88%) for the control and enriched subareas, respectively. The average CH_4 surface emissions were 34 and 20 $g.m^{-2}.d^{-1}$, respectively.

These results corroborate findings by several other studies. For example, Abichou et al. (2009) reported maximum methane efficiency equal to 63% for the control subarea in a landfill in Florida, while in the biocover it was 100%. Rose et al. (2012) obtained a maximum CH_4 oxidation efficiency of 67% for a conventional cover layer, while improving it with compost led to a maximum of 97%. Capanema et al. (2013) found a methane oxidation efficiency of 95.8% in a biocover whose O.M. content was similar to the top soil in the enriched subarea reported in the present study. Einola et al. (2008) observed that 96% of the methane was oxidized near the surface, where the topsoil was richer in organic matter.

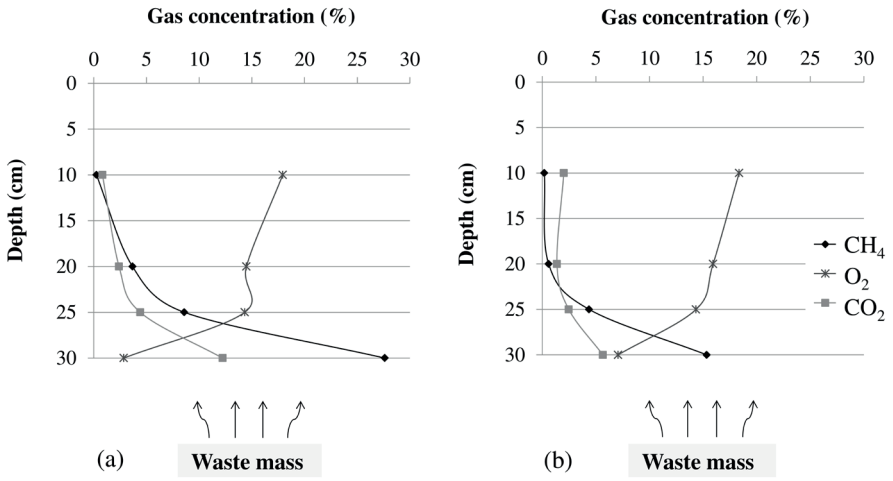

FIGURE 6: Vertical composition profiles of biogas for control (a) and enriched (b) subareas.

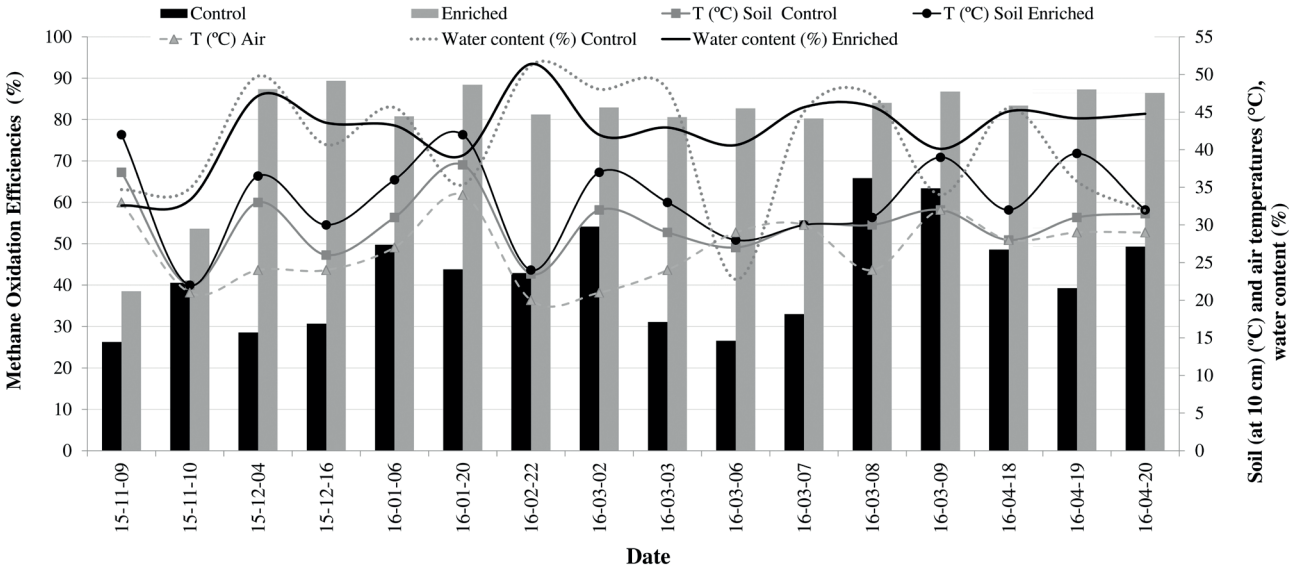

FIGURE 7: Methane oxidation efficiencies (Eff_{ox}) in the control and enriched subareas.

4. CONCLUSIONS

This study reported the capacity of two experimental passive methane oxidation biosystems (PMOBs) consisting of tropical soils typically found in developing nations. One of them was supplemented with organic-rich material (enriched subarea). In general, the average CH_4 and CO_2 concentrations in the raw biogas (42% and 32%, respectively) for the 16 campaigns corroborated those typically found in Brazilian landfills. The presence of oxygen in raw biogas resulted from atmospheric air penetration in the thin, single-layer cover, mainly through cracks.

The methane oxidation capacity was quite high for both subareas (control and enriched). Oxidation efficiencies (at a depth of 0.10 m) averaged 42% for the control subarea and 80% for the enriched area. CH_4 and CO_2 surface fluxes averaged 20 $g.m^{-2}.d^{-1}$ and 316 $g.m^{-2}.d^{-1}$ in the organic-matter-enriched subarea during the monitoring period, while those measured in the control subarea averaged 34 $g.m^{-2}.d^{-1}$ and 251 $g.m^{-2}.d^{-1}$, respectively. It is noteworthy that the surface fluxes were obtained using a custom-made 4.5-m² flux chamber, which allows for better representativeness of surface fluxes, because it allows inclusion of cracks and other imperfections that may affect measurements.

The lower CH_4 fluxes and higher oxidation efficiency in the enriched subarea can be associated with the greater organic matter content in the enriched subarea, which created more favourable conditions for the development of ubiquitous methanotrophic colonies (Humer and Lechner, 2001). Temperature conditions, which ranged from 20 to 42°C at the surface and within the first 10 cm of the cover, favoured methane oxidation.

The results obtained in this study point to the great potential in reducing residual LFG emissions by landfills located in developing nations using low-cost PMOBs constructed with typical tropical soils.

AKNOWLEDGEMENTS

Authors are thankful to “Fundação Coordenação de Aperfeiçoamento de Pessoal de Nível Superior” (CAPES, a Brazilian Agency, “Programa Ciência Sem Fronteiras – CsF”, Grant #88881.030497/2013-01) for the financial support.

REFERENCES

Abichou T, Chanton J, Powelson D, Fleiger J, Escoriaza S, Lei Y, Stern J (2006a) Methane flux and oxidation at two types of intermediate landfill covers. Waste Management, 26:1305-1312.

Abichou T, Powelson D, Chanton J, Escoriaza S, Stern J (2006b) Characterization of methane flux and oxidation at a solid waste landfill. Journal of Environmental Engineering, 132:220-228.

Abichou T, Mahieu K, Yuan L, Chanton J, Hater G (2009) Effects of compost biocovers on gas flow and methane oxidation in a landfill cover. Waste Management, 29:1595-1601.

Araujo TT, Ritter E (2016) Evaluation of biogas emissions from layers of a landfill cover. Perspectivas Online, 16:34-49 (in Portuguese).

Audibert JL, Fernandes F (2013) Preliminary qualitative and quantitative assessment of gases from biodigestion of solid wastes in the landfill of Londrina, Paraná State, Brazil. Acta Scientiarum Technology, 35:45-52.

Barry DL, Smith R, Gregory RG, Harries C (2003) Methane Production, Emission and Control during MSW Landfilling. In: Proceedings of the Ninth International Landfill Symposium, Cagliari, Sardinia, 6-10 October 2003.

Cabral AR, Moreira JFV, Jugnia L-B (2010a) Biocover Performance of Landfill Methane Oxidation: Experimental Results. Journal of Environmental Engineering, 136:785-793.

Cabral AR, Létourneau M, Yanful E, Song Q, McCartney JS, Parks J (2010b) Geotechnical issues in the design and construction of PMOBs. In: UNSAT 2010, Barcelona, pp. 1361-1367.

Candiani G, Silva ER, Moreira JML (2011) Methane balance in an experimental landfill cell. Avances en Energías Renovables y Medio Ambiente, 15:63-70 (in Portuguese).

Capanema MA, Ndanga E, Lakhouit A, Cabral AR (2013) Methane oxidation efficiencies of a 6-year-old experimental landfill biocover. In: Proceedings Sardinia, Fourteenth International Waste Management and Landfill Symposium, S. Margherita di Pula, Cagliari, Italy. 2013.

Capanema MA, Cabana H, Cabral AR (2014) Reduction of odours in pilot-scale landfill biocovers. Waste Management, 34:770-779.

Chanton JP, Liptay K (2000) Seasonal variation in methane oxidation in a landfill cover soil as determined by an in situ stable isotope technique. Global Biogeochemical Cycles, 14:51-60.

Chanton J, Abichou T, Langford C, Spokas K, Hater G, Green R, Goldsmith D, Barlaz MA (2011) Observations on the methane oxidation capacity of landfill soils. Waste Management, 31:914-925.

Christophersen M, Kjeldsen P, Holst H, Chanton J (2001) Lateral gas transport in soil adjacent to an old landfill: factors governing emissions and methane oxidation. Waste Management and Research, 19:595-612.

Czepiel PM, Mosher B, Crill PM, Harriss RC (1996) Quantifying the effect of oxidation on landfill methane emissions. Journal of Geophysical Research, 101:16721-16729.

Delhomenie MC, Heitz M (2005) Biofiltration of air: A review. Critical Reviews in Biotechnology, 25:53-72.

Du R, Lu D, Wang G (2006) Diurnal, seasonal, and inter-annual variations of N_2O fluxes from native semi-arid grassland soils of inner Mongolia. Soil Biology and Biochemistry, 38:3474-3482.

Einola JKM, Sormunen KM, Rintala JA (2008) Methane oxidation in a boreal climate in an experimental landfill cover composed from mechanically-biologically treated waste. Science of the Total Environment, 407:67-83.

Fernandes JG (2009) Evaluation of biogas emissions in an experimental landfill. Dissertação (Mestrado em Saneamento, Meio Ambiente e Recursos Hídricos) – Universidade Federal de Minas Gerais, Escola de Engenharia, 101p. (in Portuguese).

Gallego E, Perales JF, Roca FJ, Guardino X (2014) Surface emission determination of volatile organic compounds (VOC) from a closed industrial waste landfill using a self-designed static flux chamber. Science of the Total Environment, 470-471:587-599.

Gebert J, Groengroeft A, Pfeiffer E-M (2011a) Relevance of soil physical properties for the microbial oxidation of methane in landfill covers. Soil Biology and Biochemistry, 43:1759-1767.

Gebert J, Groengroeft A, Miehlich G (2003) Kinetics of microbial landfill methane oxidation in biofilters. Waste Management, 23:609–619.

Gebert J, Röwer IU, Scharff H, Roncato CDL, Cabral AR (2011b) Can soil gas profiles be used to assess microbial CH_4 oxidation in landfill covers? Waste Management, 31:987-994.

Geck C, Scharff H, Pfeiffer E-M, Gebert J (2016) Validation of a simple model to predict the performance of methane oxidation systems, using field data from a large scale biocover test field. Waste Management, 56:280-289.

Humer M, Lechner P (2001) Microbial methane oxidation for the reduction of landfill gas emissions. Journal of Solid Waste Technology and Management, 27:146-151.

Huber-Humer M, Lechner P (2003) Effect of methane oxidation on the water balance of the landfill cover and the vegetation layer. In: Proceedings Sardinia. Ninth International Waste Management and Landfill Symposium, Cagliari, Italy, 2003.

Hudson N, Ayoko GA (2008) Odour sampling. Comparison of physical and aerodynamic characteristics of sampling devices: a review. Bioresource Technology, 99:3993-4007.

Jantalia CP, Santos HP, Urquiaga S, Boddey RM, Alves BJR (2008) Fluxes of nitrous oxide from soil under different crop rotations and tillage systems in the South of Brazil. Nutrient Cycling in Agroecosystems, 82:161-173.

Jugnia L-B, Cabral AR, Greer CW (2008) Biotic methane oxidation within an instrumented experimental landfill cover. Ecological Engineering, 33:102-109.

Kjeld A, Cabral AR, Gústafsson LE, Andradóttir HO, Bjarnadóttir HJ (2014) Microbial Methane Oxidation at the Fíflholt landfill in Iceland. Verktækni, 30:31-36.

Lakhouit A, Schirmer WN, Johnson TR, Cabana H, Cabral AR (2014) Evaluation of the efficiency of an experimental biocover to reduce BTEX emissions from landfill biogas. Chemosphere, 97:98-101.

Lucernoni F, Rizzotto M, Tapparo F, Capelli L, Sironi S, Busini V (2016) Use of CFD for static sampling hood design: an example for methane flux assessment on landfill surfaces. Chemosphere, 163:259-269.

Maciel FJ, Jucá JFT (2011) Evaluation of landfill gas production and emissions in a MSW large-scale experimental cell in Brazil. Waste Management, 31:966-977.

Monteiro LS, Mota FSB, Silva WMB, Borges DA (2016) Emissions of gases through various types of materials used as cover layers of an experimental chamber filled with municipal solid wastes. Journal of Environmental Science and Water Resources, 05:24-31.

Nagaraj TS, Lutenegger AJ, Pandian NS, Manoj M (2006) Rapid estimation of compaction parameters for field control. Geotechnical Testing Journal, 29:497-506.

Obersky L, Rafiee R, Cabral AR, Golding SD, Clarke WP (2018). Methodology to determine the extent of anaerobic digestion, composting and CH_4 oxidation in a landfill environment. Waste Management, 76:364-373.

Perera MDN, Hettiaratchi JPA, Achari G (2002) A mathematical modeling approach to improve the point estimation of landfill gas surface emissions using the flux chamber technique. Journal of Environmental Engineering and Science, 1:451-463.

Rachor IM, Gebert J, Gröngröft A, Pfeiffer E-M (2011) Assessment of the methane oxidation capacity of compacted soils intended for use as landfill cover materials. Waste Management, 31:833-842.

Rachor IM, Gebert J, Gröngröft A, Pfeiffer E-M (2013) Variability of methane emissions from an old landfill over different time-scales, European Journal of Soil Science, 64:16-26.

Rochette P, Eriksen-Hamel NS (2008) Chamber measurements of soil nitrous oxide flux: are absolute values reliable? Soil Science Society of America Journal, 72:331-342.

Roncato CDL, Cabral AR (2012) Evaluation of methane oxidation efficiency of two biocovers: field and laboratory results. Journal of Environmental Engineering, 138:164-173.

Rose JL, Mahler CF, Izzo RLS (2012) Comparison of the methane oxidation rate in four media. Revista Brasileira de Ciência do Solo, 36:803-812.

Sadasivam BY, Reddy KR (2014) Landfill methane oxidation in soil and bio-based cover systems: a review. Reviews in Environmental Science and Bio/Technology, 13:79-107.

Scheutz C, Kjeldsen P, Bogner JE, De Visscher A, Gebert J, Hilger HA, Huber-Humer M, Spokas K (2009) Microbial methane oxidation processes and technologies for mitigation of landfill gas emissions. Waste Management and Research, 27:409-455.

Scheutz C, Pedicone A, Pedersen GB, Kjeldsen P (2011) Evaluation of respiration in compost landfill biocovers intended for methane oxidation. Waste Management, 31:895-902.

Scheutz C, Pedersen RB, Petersen PH, Jørgensen JHB, Ucendo IMB, Mønster JG, Samuelsson J, Kjeldsen P (2014) Mitigation of methane emission from an old unlined landfill in Klintholm, Denmark using a passive biocover system. Waste Management, 34:1179-1190.

Stern JC, Chanton J, Abichou T, Powelson D, Yuan L, Escoriza S, Bogner J (2007) Use of a biologically active cover to reduce landfill methane emissions and enhance methane oxidation. Waste Management, 27:1248-1258.

Trégourès A, Beneito A, Berne P, Gonze MA, Sabroux JC, Savanne D, Pokryszka Z, Tauziède C, Cellier P, Laville P, Milward R, Arnaud A, Levy F, Burkhalter R (1999) Comparison of seven methods for measuring methane flux at a municipal solid waste landfill site. Waste Management and Research, 17:453-458.

UK Environment Agency (2010) Guidance on monitoring landfill gas surface emissions, LFTGN07 v2, Bristol, UK, 66p.

detritus | Multidisciplinary Journal for Waste Resources & Residues

CISA

Techinal note

THE NATURALISTIC RECOVERY OF A OLD LANDFILL: THE CASE OF VIZZOLO PREDABISSI, MILAN, ITALY

Salvatore M. Colombo *

Nisi Parendo, via Palestrina 4, 20811 Cesano Maderno, Italy

Article Info:
Received:
25 June 2019
Revised:
31 August 2019
Accepted:
12 September 2019
Available online:
26 September 2019

Keywords:
Old landfill recovery
Waste architecture
Landfill capping
Forest landscape design

ABSTRACT
The naturalistic redevelopment of an old landfill appears to be one of the most interesting solutions for returning an area used over time for waste disposal to the environment. This choice, anyway, should already be considered during the design stage in order to avoid extremely artificial capping lining solutions that would not allow the growth of the desired phytocoenosis. On the Vizzolo Predabissi (Milan, Italy) landfill site, after an initial post-management phase, the environmental rehabilitation of the site was set through the elimination of the artificial superstructures and through a design of the forest landscape that allowed an evolution towards a naturalistic oasis with ecosystemic target. This article illustrates the techniques used, the challenges encountered and the management perspectives of the area, unfortunately still undefined by the public administration.

1. INTRODUCTION

Build a landfill, fill it, close it. This is the cycle that designers and administrators know well, and that is now well regulated and organized both from a technical and administrative / regulatory point of view.

However, if we try to investigate the last portion of the life of a landfill, we very often discover a stage that is not well defined, corresponding to the end of the so-called "post-closure" phase. Usually the final "destiny" of that portion of territory often wide and including the related service structures, on which the landfill rests, is left undetermined. In the best case scenario it is left to a stable meadow destination.

The target design of an environmental recovery with an ecosystem-naturalistic intent constitutes an interesting final destination perspective because it is "projected" into its future as well as it represents perhaps the best compensation to the land that hosted the landfill (Di Fidio, 1985). Today, our landscapes, often spoiled by an uncontrolled building sprawl and by a soil consumption that has reached alarming levels (Casa, 2017), have an absolute need for restoration with green areas that can become hubs of ecological networks and that could be able to mend and reconnect the remaining green areas, as well as redevelop from the landscape point of view, areas that nowadays are often characterized by negative and impacting elements.

In this context, the ecosystemic conversion of the surface of an old landfill is an interesting starting point for the enrichment of the local environment, as well as a point of possible peri-urban use for the inhabitants of the closest suburbs.

In order to achieve such a result this solution must be planned and studied already at the landfill design level, with an appropriate capping stratigraphy and with technical infrastructure choices made so that they are already compatible with future landscape function.

The experience conducted at the old Vizzolo Predabissi (Milan) landfill, whose environmental recovery was precisely guided by the criteria mentioned above, is presented below (Figure 1).

Today, the area presents an interesting ecosystem / landscape features that give it a particular and important role in the naturalistic context of the surroundings. Its 22 hectares extension and its morphology of the embankment (20 m above the countryside level) determine relevant ecosystem opportunities (Figure 2) in an area characterized historically by extensive agriculture and more recently by a wide industrial/logistic settlement, in addition to the construction of the new Milan Eastern Ring Road. Furthermore this highway presents here some of the most invasive and impacting features, such as the large railway and the Emilia road overpass (Figure 3).

2. LANDFILL DESCRIPTION

The landfill is located in the territory of Vizzolo Preda-

* Corresponding author:
Salvatore M. Colombo
email: salvatorecolombo20@gmail.com

https://doi.org/10.31025/2611-4135/2019.13848
© 2019 Cisa Publisher. Open access article under CC BY-NC-ND license

FIGURE 1: Current view of the former landfill from the North-West side.

FIGURE 2: The top of the closed landfill is now home to hundreds of tall trees.

FIGURE 3: The top of the closed landfill is now home to hundreds of tall trees.

bissi, in an area between the Lambro river and the current Milan-Rome high-speed railway line. The first deliveries of waste started in the late Seventies, on an area that was not waterproofed but which had a fair amount of natural protection thanks to a clay bench. In accordance with the first regional Lombardy law on the matter, the company Sacagica was authorized to cultivate a first portion of the landfill, subsequently expanded in 1987 by raising and waterproofing the old lots. The landfill has gradually become larger with successive lots up to a total area of 22 hectares. The last authorization, issued in 1996 by the Milan Delegated Commissioner for the waste emergency, brought the landfill to the current configuration, with an overall discharge estimated at around 4 million tons of urban waste. Disposals ended on the 30th of November 1999. The final testing of the closing works took place in December 2003 with the supervision of the Politecnico Geotechnical Lab.

The ownership of the landfill has always been held by the Municipality of Vizzolo, which - with subsequent resolutions - has entrusted the different phases of construction and management to private companies, starting precisely from Sacagica Srl, which later merged into the Waste Management Group. The post-closure phase was carried out by Vizzolo Ambiente Srl, a related company, with the support of Cofathec (later Cofely) for biogas management and energy recovery. The fifteen-year post-closure, penalized by a financial plan that had heavily underestimated the management costs, ended in 2015 with the withdrawal by the Municipality of the financial guarantees issued by the management Company, due to the lack of leachate removal and with the current management assigned to a local Consortium.

2.1 The capping

The number of subsequent construction activities over the years on the Vizzolo landfill has also produced some different choices in the final closing layers of the individual lots, which reflects the technical / construction knowledge of the related design time period. It isn't therefore possible to identify a unique typology of the closing stratigraphy, even if, from the legislative point of view, the common reference was the Delibera Comitato Interministeriale issued on July 27th, 1984. However, despite some differences, especially in regard to the thickness of the materials and the types of geotextiles used, it is possible to bring these variants back to a common denominator of components, i.e. (from top to bottom): topsoil ; drainage layer rain water; bentonite mattress (not everywhere); clay; biogas drainage layer; waste regularization layer (CTD, 1997).

For assessments on the suitability to install a naturalistic phytocoenosis, the thickness of the surface soil of the capping is clearly of vital importance, and it was indicated in the project documents ranging from 50 cm to one meter. In 2007, in anticipation of a new substantial tree planting activity, an extensive survey campaign was conducted to assess the actual thickness of the soil on the landfill capping. This survey has been carried out in order to assess both the areas where any settlement phenomena and / or surface erosion had reduced the thickness of the soil and to identify the areas where possible greater carryovers would have ensured the best conditions for the planting of trees and shrubs with greater need for substrate. The outcomes were particularly encouraging, since in all 27 surveys carried out a higher soil thickness than the designed one was found, with a minimum of 57 cm and a maximum of 137 cm, and with an average thickness of 84 cm (Figure 4). In all the surveys a good development in depth of the roots of the grassy turf was found, with the absence therefore of anoxia phenomena, biogas leaks or water stagnation.

2.2 First interventions

The testing of the closure of the Vizzolo landfill, carried out with the support of the Politecnico geotechnical laboratory, took place at the end of 2003. From 2007, after a period of management by the firm that carried out the works, the real post-management phase started, based on a naturalistic recovery criteria and an ecosystem / landscape target. A series of interventions were therefore set up with the goal to "lighten" the landfill from concrete structures and various infrastructures which, perhaps useful in the management phase, were now an obstacle to the full recovery and to the new management plan of the area. In particular, it was evaluated the actual need of the concrete wall, with a height varying from 50 cm to more than 2 meters, which bounded almost the entire perimeter of the landfill for over a kilometer. The wall had been built during the management of the active landfill in order to support the slopes in cultivation. In addition to the evident impact on the landscape, the presence of that low wall had led to a significant worsening of the drainage and external conveying capacity of rainwater, both from surface runoff and from those collected by the drainage layer existing in the capping between clay and soil. Considering the very large quantity of leachate produced and its evident dilution, there were therefore reasonable grounds for believing that a good part of the rain water - although drained and effectively collected by the apposed systems and infiltrated along the inner side of the wall at the end of their existing path - bypassed the waterproofing systems. Through the formation of a hydraulic head the water was flowing into the mass of waste, with the consequent abnormal production of leachate. This hypothesis has been verified through the performance of some tests that have shown how, even in a not particularly rainy period, a strong accumulation of water formed close to the inner side of the walls, evidently destined to infiltrate the landfill despite the presence of some drainage holes, which were completely insufficient for this purpose. A complete demolition (Figure 5) of the perimeter wall was then studied, replacing it with a permeable structure (Benini, 1990), consisting of stone cages (50 cm high and 1 meter deep), "moving" the edge of the landfill (i.e. modifying the slope) outside the anchoring of the bottom sheets of the landfill and resealing the area with a new clay fill, on which a draining mat and new cultivation ground have been placed (Figure 6).

After this work, the internal and superficial drainage

FIGURE 4: The layer of soil reported on the capping proved to be suitable for the growth of even tall trees.

FIGURE 5: Demolition of the perimetric concrete wall.

of the landfill has thus been much improved. The terminal part of the banks has been softened and the naturalistic appearance of the area has been strongly developed, thus starting it towards the final configuration, in line with the intended objectives.

3. DISCUSSION AND RESULTS

3.1 Reforestation Criteria

The last activity of the landfill closure, as planned in the original design, was the sowing of stable lawn and the planting of some patches of shrubs chosen simply on the basis of their strong chromatic impact during blooming season (broom and forsythia).

Instead, at the beginning of the new post-closure management phase, a naturalist, member of a local environmental association, had been involved. With his help, a list of native trees and shrubs that could constitute an interesting phytocoenosis was studied, as a premise for the transformation of the former landfill into a hub of the local ecosystem network (Figure 7).

The opportunity to foresee the planting on the capping not only of shrubs but also of trees has been evaluated in order to ensure over time a necessary and fundamental interpenetration between plant associations and waste bodies during the landfill mineralization phase, contrary to what it is often stated about the risks of "drilling" of the capping by the root apparatus. Even the possible risk of instability of the trees once grown, often cited as discouraging the planting of highly developed tree species, to date has never materialized, despite the presence of several hundred trees even at the top of the landfill, many of which are now over seven / eight meters high (Figure 8).

The absence of waterproof polyethylene sheets in the capping package, often designed to contain hypothetical excessive leachate production, was also found to be fundamental to ensuring the correct environmental recovery of the landfill in decades, allowing an important naturalistic requalification and also preventing phenomena of uneven surface layers, situation that never happened in Vizzolo despite the succession of periods of heavy rainfall over the years.

During several planting campaigns, which lasted from 2007 to 2013, approximately 9,000 specimens of trees and shrubs, belonging to native species and selected also on the basis of direct experience on the adaptability to the still difficult conditions of a landfill capping, were planted (Figure 9).

FIGURE 6: After the demolition of the wall, a permeable containment gabion is realized.

FIGURE 7: The side of the landfill sloping towards the Lambro river.

FIGURE 8: The absence of a waterproof sheet in the capping has allowed the growth of trees without compromising slope stability.

FIGURE 9: Phytocoenoses established on the landfill.

In particular, the resistance and growth capacity of the elm (*ulmus minor*) and of the field maple (*acer campestre*) have confirmed that these trees are extremely suitable for landfills recovery, while among the shrubs excellent results have been obtained with the hawthorn (*crataegus monogyna*) (Figure 10).

Therefore the usage of native species considered "pioneers" has been favored, deferring the enrichment with more demanding essences to subsequent management phases (Schiechtl & Stern, 1992). For the shrubs, the essences able to provide berries to the birds have been preferred (Figure 11). The essences planted during the different planting campaigns are indicated in Table 1.

For the planned planting activities, the use of small and medium-sized forest plants has been preferred, supplied in pots with a diameter variable from 9 to 15 cm. Their costs are truly paltry compared to the ones budgeted in some other landfill greening projects.

In fact, these dimensions guarantee a better rooting and recovery compared to specimens of greater development supplied with ground bead (Lassini, 1996). Even smaller dimensions, such as phytocell seedlings, although perhaps even more preferable from a strictly forestry and planting point of view, would have been too exposed to damage, considering however the strong presence of wild rabbits and also the need of performing periodicals mowing.

Plants such as those defined above still ensure a better survival rate compared to those in sod ("ready for effect") and grow in a regular and consistent manner. More developed plants, on the contrary, suffer from the disproportion between root system and branch apparatus, reacting with a stop or a strong slowing down of apical growth for the first years. Different choices have been made over the years on the protections to be applied to the planted trees, evaluated on the direct acquired experience. In a first phase, coconut fiber biodiscs were laid (small mats of 40-50 cm in width which should provide a good protection, maintaining humidity and preventing grass growth around the growing tree). Although the mats have been fixed to the ground with iron pegs, problems have been found essentially related to their instability in the face of intense winds and to their lifting by the grass still present under them. The solution

TABLE 1: Essences planted during the different planting campaigns.

Trees		**N°**
Ulmus minor	Elm tree	900
Acer campestre	Field maple	800
Carpinus betulus	White hornbeam	100
Quercus robur	Oak	100
Fraxinus excelsior	Ash tree	100
Prunus avium	Wild cherry	200
Shrubs		
Crataegus monogyna	Hawthorn	3200
Cornus mas	Dogwood	800
Prunus spinosa	Blackthorn	800
Rosa canina	Rosehip	800
Ramnus catarthica	Buckthorn	800

that gave the absolute best results – sometimes really surprising - was to prepare strips of mulching green polypropylene cloth (like the one used in agriculture), fixed to the ground with iron pegs, cross-cut to plant the seedlings. Each strip, with a width of 1.65 m and a length of 8, allowed for the staggered planting of seven trees, alternating trees and shrubs. The objective complexity of laying the sheets has been amply repaid by the results of protection from excessive soil drying and effective control of grass growth (Figure 12).

3.2 The Forest Landscape Design

The goal of recreating a natural environment has led to a careful evaluation of the design of the new plantings on the former landfill. It was therefore favored an irregular planting, without any geometric pattern, in order to mimic the natural configuration of the "patches of field", or spontaneous plant associations consisting of trees and shrubs (Lassini & Pandakovic, 1996) (Figure 13).

Even in the succession of laying the mulching sheets any straight line was deliberately avoided, favoring sinuous traces. The result was therefore a succession of wooded areas and clearings, i.e. the naturalistic configuration that

FIGURE 10: Hawthorn has proved to be an extremely resistant species with a great naturalistic and landscape value.

FIGURE 11: Field maple (left) and elm (right) have given excellent results resistance result and fast growth.

maximizes the ecosystem value of an area. It is in fact known that the wood-clearing transition bands are the richest from a naturalistic point of view, just as it has been demonstrated by an experimental thesis on the Lepidoptera population conducted on the former Vizzolo landfill by the Department of Ecology of the Territory of the University of Pavia.

The planting results, ten to twelve years later, testify the achievement of an interesting green cover on the former landfill (Figure 14).

The sequence of clearings and wooded areas proved its effectiveness in achieving an environment of great naturalistic richness: the area was immediately populated by wild rabbits, hares and foxes. Last spring (2018) a specimen of roe deer was also spotted, having arrived through the remaining protected areas of the nearby Parco Sud Milanese (Figure 15).

4. CONCLUSIONS

The future of the old Vizzolo landfill is today closely linked to the possible management choices of the local Consortium that is in charge of the area. It is advisable that the absurd hypothesis of a complete remaking of the capping with waterproof polyethylene sheets is dismissed definitely. This solution was proposed to contain as much as possible the production of leachate, but it would be devastating for what has been achieved so far and it is also contrary to the most recent indications for post-management of the landfills (Cossu, 2012).

Instead, all the interventions that can "lighten" the area from pre-existing structures that are no longer necessary and are completely incoherent with the naturalistic redevelopment in progress should be promoted. In particular, concrete slabs, premises and service sheds that are no longer needed, biogas substations and wells no longer in use should be removed. The current service tracks can be transformed into cycle paths, to be connected to the existing cycle path network of the Parco Sud Milanese, in collaboration with this park management (Toccolini, 2004) (Figure 16).

Furthermore, the system of future management of the area must be defined, in particular with respect to the ownership of the area, still held by the old management company, and to the possible collaboration between the territorial Authorities involved (Municipality, Metropolitan City of Milan, Consorzio Parco Sud Milanese). Recently contacts have been opened with an important national naturalistic association, which had publicly declared itself willing to start a project for the direct management

FIGURE 12: The mulching sheet used for the planting of trees and shrubs.

FIGURE 13: "Patch of field" forest design. In the foreground, heather bloom.

FIGURE 14: Alternation of lawn and wooded areas.

FIGURE 15: The roe deer sighted inside the former landfill.

FIGURE 16: The internal service tracks may constitute the future network of cycle paths connected to the South Milanese Park.

of the area. The subsequent choices recently made by the Municipality and the local Consortium have unfortunately momentarily stopped this collaboration opportunity, which will hopefully be recovered as soon as possible, with a specific aim at reestablishing an important part of the sought-after ecological network of the South Milan area and its local Park.

REFERENCES

Di Fidio, M., 1985. Architettura del paesaggio. Il Sole 24 Ore Pirola

Casa, M., Pileri, P.,2017. Il suolo sopra tutto. Altraeconomia

CTD - Comitato Tecnico Discariche, 1997. Linee guida per le discariche controllate di rifiuti solidi urbani. CISA

Benini, G., 1990. Sistemazioni idraulico-forestali. UTET

Schiechtl, H.M., Stern, R., 1992. Ingegneria Naturalistica, ed. Castoldi

Lassini, P., 1996. Aspetti tecnici ed economici connessi alla realizzazione di aree verdi e parchi periurbani. ANARF

Lassini, P., Pandakovic, D., 1996. Il disegno del paesaggio forestale. Il Verde Editoriale

Cossu, R., 2012. Anche le discariche possono essere sostenibili. Ambiente Rischio Comunicazione

Toccolini, A., 2004. Progettare i percorsi verdi. Maggioli

detritus | Multidisciplinary Journal for Waste Resources & Residues

CISA

PORTRAITS

Professor Dr. Rudolf Braun
born: 24th January 1920 in Lenzburg, Switzerland
died: 1999

Professor Dr. Rudolf Braun, the doyen and grand old man of Swiss waste management. He put special focus on promoting composting. The high density of composting plants in Switzerland in the 1970s is not least due to his activities.

Education

- Kantonsschule (Swiss high school) in Aarau, graduating in autumn 1939;
- Natural Sciences at ETH Zurich.

Academic career

His university teachers, Professors Gagman and Jaag, were able to fill him with enthusiasm for hydrobiology. At the age of 26 Rudolf Braun was granted a scholarship of the University of São Paulo to research the water resources of the Amazon River with regard to the settlement of Brazil. He analysed the research results of this travel between 1946 and 1948 in his dissertation on limnological studies of some lakes in the Amazonian region («Limnologische Untersuchungen an einigen Seen im Amazonasgebiet»), which earned him the Silver Medal of ETH Zurich.

In the years 1951/52 he went on extended botanical-hydrobiological study trips to Africa (Sahara, Nigeria, Chad, Cameroon).

In 1952 Rudolf Braun became head of the institute of qualitative water management and hydrobiology at the technical university of Karlsruhe, Germany. However, he rejected the professorship offered to him. In 1954 he returned to his home canton to establish one of the first cantonal water protection specialist units in Aarau in his role as hydrobiologist of Canton Aargau.

In 1955 Professor Jaag invited Rudolf Braun to EAWAG (the Swiss Federal Institute of Aquatic Science and Technology) and assigned him the task of establishing the section of «Waste research» at EAWAG, which later evolved into the department of «Management of solid waste». He headed it for 28 years. In this position he was active as researcher, teacher and adviser.

In 1970 Rudolf Braun became associate professor and in 1973 full professor of waste management at ETH Zurich. During this time he also was director of the institute of water protection and water technology for several years.

He retired in 1987.

His work was very multifaceted: new knowledge was acquired in research and applied in technical problem solutions. However, Rudolf Braun was not the kind of man who intended to curb the increasing flood of waste merely by technical means.

He was a pioneer of waste avoidance and recycling; «Waste is resources in the wrong location» – this phrase was coined by him and has often been quoted.

Rudolf Braun was a sought-after expert at home and abroad. He promoted international cooperation and his amiable and approachable character facilitated his contact to decision makers on all levels.

Between 1970 and 1985 Rudolf Braun was president of the Swiss association of water protection and air pollution control (VGL).

Since 1955 Rudolf Braun was scientific secretary of the «International working group of waste research» (today «International Solid Waste Association»). In this role he promoted the international cooperation between national organisations. He was also substantially involved in the organisation of the international congress on urban cleaning in Vienna in 1964 and the congress of the international working group of waste research (IAM) in Basel in 1969.

Rudolf Braun was a member of the Swiss federal commission of waste management («Eidg. Kommission für Abfallwirtschaft») and in 1972 became president of the European Federation for the Protection of Waters (FEG).

Managing editor:
Werner Bidlingmaier
email: werner.bidlingmaier@konsolan.de

Detritus / Volume 07 - 2019 / pages I-II
https://doi.org/10.31025/2611-4135/2019.13853
© 2019 Cisa Publisher

He was the first foreigner to be invited by the German government to join the German Advisory Council on the Environment. In this role Rudolf Braun also had great influence on the current EU legislation in the area of resource management.

Rudolf Braun advocated an environmentally sound waste management. He searched for solutions that were based on the natural cycle of elements and recognized early on the various possible uses of waste.

Source

Hans Wasmer, Ueli Bundi; Walter Obrist (Niederhasli); Jahresbericht der EAWAG 1999

detritus | Multidisciplinary Journal for Waste Resources & Residues

CISA

BOOKS REVIEW

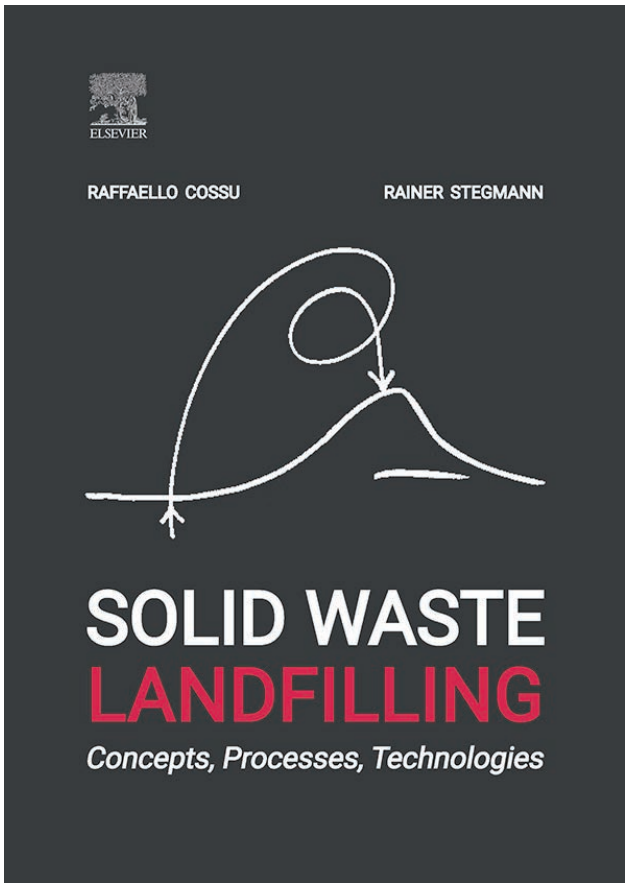

SOLID WASTE LANDFILLING. CONCEPTS, PROCESSES, TECHNOLOGIES

Edited by Raffaello Cossu and Rainer Stegmann

Material management, however efficient and cyclical it is, will generate waste. Even solid waste management, including recycling or energy recovery, generates waste that can no longer be recycled, re-used or exploited in any other way. To complete the waste management system we must have a way out of the cycle, so part of the system must take care of the "rejected" material flows. That is what we need a landfill for. Landfilling, despite tendencies to diminish its importance, is an inevitable element of any waste management system. A landfill is the society's liver helping to eliminate toxins or detoxify it. Knowledge, skills and experience in landfilling of waste must be maintained and transferred to coming generations to ensure safe and qualified landfill operations and to minimize risks to the environment and human health.

This book presents a comprehensive overview of all aspects of landfilling, including concepts, processes, technologies, planning, design, and the afterlife of a landfill when landfilling has ceased.

The introductory chapter describes general aspects of waste management strategies and the role of landfilling in them. It also covers issues related to global flows and fates of contaminants in the environment. The importance of raising awareness among politicians and society at large on waste avoidance, collection, reuse, and recycling is highlighted, and the need for a landfill as the final sink for materials (contaminants) is described and graphically illustrated. The generation, properties and categories of waste, as well as classification of landfills, are introduced, along with descriptions of legal frameworks of landfilling in various regions of the world.

The following chapters introduce the terminology, main concepts and design strategies for landfills; more deeply describe the biochemical and physico-chemical processes that occur in them, and highlight new challenges related to emerging contaminants in landfills. The chapters further cover the traditional areas of landfill technologies, such as: pre-treatment of waste prior to landfilling; geotechnical and hydraulic aspects of landfills; liner, drainage and cover systems; and management of emissions from landfills, including ways to trace, quantify and monitor uncontrolled emissions of landfill gases and leachates.

When more waste goes to energy recovery rather than directly to landfilling, new types of waste – incineration residues – are increasingly generated. Management of such waste requires additional knowledge and new strategies, which are presented in chapter 20.

Eventually, a landfill must be closed, and all active control measures should be safely removed. Thus, the book also describes approaches for aftercare of a closed landfill and describes several afteruse scenarios for landfills.

The book further describes methodologies for Environmental Impact and Life Cycle Assessment (LCA) of landfilling and exemplifies their applications by describing several case studies.

Even closed landfills require further investigation and remedial actions might be needed. Thus, the book provides a roadmap for investigating closed landfills, describes principles of their remediation and presents the concept of landfill mining.

The book concludes with an overview of the essential economic aspects of landfills and presents reference examples of case studies in various regions of the world.

The book covers decades of experience and worldwide expertise in landfilling of solid waste. It has potential to become a central piece of the library of any practitioner

Managing editor:
Roberto Raga
email: roberto.raga@unipd.it

Detritus / Volume 07 - 2019 / pages III-IV
https://doi.org/10.31025/2611-4135/2019.13852
© 2019 Cisa Publisher

in the waste management sector, as well as core teaching material for scholars worldwide.

Jurate Kumpiene
Luleå University of Technology, Sweden
e-mail: Jurate.kumpiene@ltu.se

ABOUT THE EDITORS

Raffaello Cossu

Innovator and visionary, outstanding scientist and leader, he contributed like no other to the development and dissemination of new concepts and to the end of well-established wrong ideas.
Full Professor of Solid Waste Management, he retired in September 2018 from the University of Padova, Italy, where he led the Research Center of Environmental Engineering for 20 years. Former President of the School of Environmental Engineering at the same University from 2000 to 2013.
Founding member and President of IWWG (International Waste Working Group) from 2004 until 2009, he is currently a member of the Managing Board.
From 2009 to 2017 he was Editor in Chief of Waste Management, the IWWG international scientific journal on waste management, published by Elsevier. From 2018 he is Editor in Chief of DETRITUS, the new IWWG international scientific journal for Waste Resources and Residues, CISA Publisher.
Invited and keynote speaker in conferences on Waste Management and landfilling throughout the world.
He is author of more than 200 scientific papers and five international books on waste management, published by Academic Press, Elsevier, EF and Spon.

Rainer Stegmann

Rainer Stegmann retired in 2008 as Professor. Head of the Institute of Waste Management at the Hamburg University of Technology, Germany.
His main research interest is waste management, biological waste treatment, sanitary landfilling and contaminated sites. He has been visiting professor at several international universities, was director of the research centre R3C at NTU in Singapore, and has coordinated several international and national research projects.
He was for more than 10 years a member of the environmental advisory board for Shanks, UK, chairman of IWWG (International Waste Working Group).
Dr. Stegmann is co-chairman of various international waste management conferences (e.g. "Sardinia", "Venice" and "Crete" Symposia). He has authored more than 300 papers and 5 international books on landfilling and contaminated sites.

Book Info:

Editors: Raffaello Cossu, Rainer Stegmann
Imprint: Elsevier
Year of publication: 2018
Page Count: 1190
Paperback ISBN: 9780128183366

detritus | Multidisciplinary Journal for Waste Resources & Residues

CISA

A PHOTO, A FACT, AN EMOTION

"A young girl scavenging amongst the garbage at the Demra dump in Dhaka in her struggle to survive. Myriads of flies swarm the area. The survival of many people living in dire poverty depends on garbage. The Demra dump, one of largest in Dhaka city, is a dangerous area polluted by noxious smells. On a daily basis numerous people gather to collect goods such as plastic bags, plastic bottles, old toys and metal items, at the end of the day selling the goods they have collected for a few coins and allow them to live to see another day."

"LIFE IN GARBAGE"

Dhaka, Bangladesh

Azim Khan Ronnie, Bangladesh

Managing editor:
Elena Cossu
email: studio@arcoplan.it

Detritus / Volume 07 - 2018 / pages V-VI
https://doi.org/10.31025/2611-4135/2019.13854
© 2019 Cisa Publisher

This photo was selected to participate in the third edition of Waste to Photo in 2019, the photo contest connected to the Sardinia Symposium, International Waste Management and Landfill Symposium organised by IWWG.

More than 100 photos were received to enter the third edition. The competition, open to all, aimed at recreating a scenario representing the global situation with regard to waste and landfill.

The panel of judges, which will include members of IWWG-MB and professional photographers, will choose the winning photo during the symposium week. The winner will be declared and price awarded during the symposium gala dinner.

In addition, the most significant shots were used to set up a photographic exhibition to illustrate the differences, the contradictions, the difficulties and progresses encountered by this complicated issue in a series of contexts throughout the world, ranging from the developing countries to the more industrialized nations.

Elena Cossu
Studio Arcoplan, Italy
email: studio@arcoplan.it

ABOUT THE AUTHOR

Azim Khan Ronnie

Azim Khan Ronnie was born in Dhaka and brought up in Bogra, Bangladesh. As a photographer with an overwhelming passion for photography, his main aim is to capture life moments, adding to their significance by fixing them in time. He loves to travel to new places, meet new people, and enjoy the experience afforded by photography to capture Earth's beautiful and awe-inspiring moments. He also loves to experiment with his photography.
He has taken part in many International Photography contests and has won a series of international photography awards, including the HIPA Merit Medal Award 2018, Won Andrei Stenin International Press Photo Contest 2019, SIENA International Photography Award 2019, Two awards from Drone photo contest 2019, Winner Agora images, BBC Wildlife Photo Contest winner 2017, and Grand prize winner from Chania Photo Festival, Greece etc. His photographs have been published in The Times, The Sun, The Guardian, The Telegraph, Daily Mail, New Atlas, BBC Wildlife Magazine, National Geographic Magazine, and the Smithsonian magazine, amongst others.

detritus | Multidisciplinary Journal for Waste Resources & Residues

CISA

DETRITUS & ART / A personal point of view on Environment and Art

by Rainer Stegmann

Artists seldom provide an interpretation of their own work; they leave this to the observer. Indeed, each of us will have our own individual view of a specific piece of art, seeing different contents and experiencing a range of feelings and emotions. Bearing this in mind, I created this page where you will find regularly a selected work of art from different epochs and I express my thoughts on what the work conveys to me personally. The interpretation should be related specifically to the environment and what kind of message I deduct from it: it may be to preserve the beauty and integrity of nature, to prevent destruction, issue warnings, etc.
I would also like to involve you, the reader of DETRITUS, to give your own interpretation of a work of art in max 8-10 lines. I will present the piece to be discussed in the next issue and I will publish your interpretation together with mine.
I look forward to a highly fruitful exchange of views and thoughts, and am convinced that art will open our eyes with regard to the specific work of art and its relationship with the environment.

MARC CHAGALL / PARADISE - 1961, Oil on Canvas, Chagall Museum, Nice, France

In this issue I will start by discussing "Paradise", a painting by Marc Chagall.

On first looking at this beautiful painting the clear bold colours overwhelmed me. You should also bear in mind the considerably large format (198 x 288 cm), which actually underpins the power of the colours. The painting shows a scene from the Bible depicting Adam and Eve on the left in Paradise, living in harmony. On the other side of the painting the snake, which has persuaded Eve to eat an apple from the forbidden tree: "If you eat the apple you become like God and will be able to discern between good and bad " the snake said. Eating an apple from this tree was the only thing God had expressly forbidden. Unfortunately, Eve ate the apple and gave it to Adam, who of

Managing editor:
Rainer Stegmann
email: stegmann@tuhh.de

Detritus / Volume 07 - 2019 / pages VII-VIII
https://doi.org/10.31025/2611-4135/2019.13858
© 2019 Cisa Publisher

course did the same. As stated in the Bible, God punished Adam and Eve by expelling them from Paradise: "The Fall of Man".

For me, this painting symbolises the "Second Fall of Man": humans have not succeeded in preserving the creation of our planet but have plundered its natural resources and exorbitantly polluted the elements water, air and soil.

The snake may represent a symbol of pure capitalism, suggesting that natural resources can be used unrestrictedly in order to further increase economic growth, and overlooking respect for the environment. People trusted the snake and still bit into, and continue to bite into the apple with the well-known consequences. Global pollution and climate change are making our living conditions more and more critical.

We are indeed in great danger of leaving our "Human Paradise" (different from the "Divine Paradise" that Adam and Eve left), with its beautiful nature, which is still intact in many places; I therefore interpret this wonderful painting as the "Second Fall of Man". In my opinion the beautiful expressive colours used in this work of art extol the beauty of nature.

However, in contrast to the first "Fall of Man" mankind has been given a chance to remedy his failings and stay in human paradise. To achieve this no efforts should be spared to preserve our environment. What would be the alternative? Hell.....?

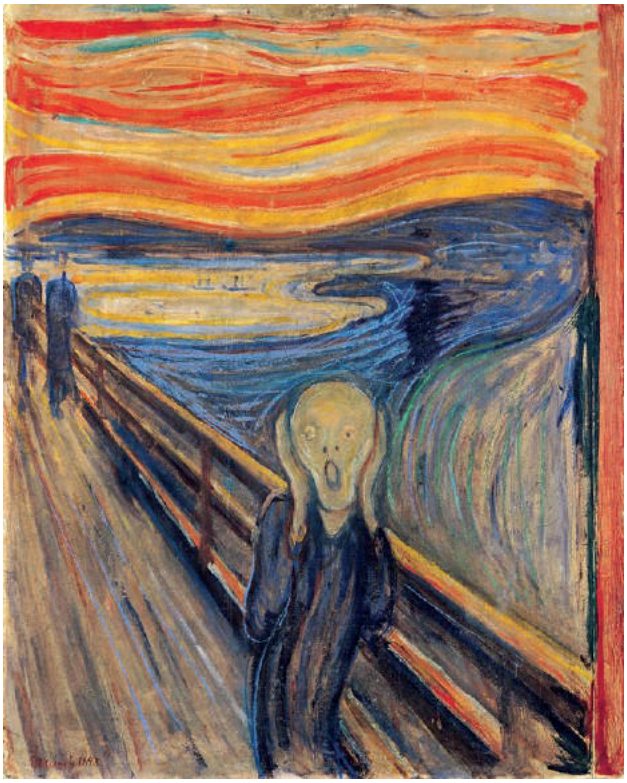

EDVARD MUNCH / THE SCREAM

In the next issue of DETRITUS I like to present "The Scream" created by Norwegian Expressionist Edvard Munch in 1893. There are several versions of this theme and I have selected this amazing coloured work of art. Please send your thoughts by 15th November to stegmann@tuhh.de.

detritus
Multidisciplinary Journal for Waste Resources & Residues

CISA

CONTENTS

VOLUME 07 / September 2019

ISSN 2611-4135 / ISBN 9788862650632